Trace metal effects on phytoplankton in subpolar seas with special emphasis on coccolithophores

Amy Harington

Thesis presented in fulfilment of the requirements for the Degree of

DOCTOR OF PHILOSOPHY

in the Department of Biological Sciences

UNIVERSITY OF CAPE TOWN

March 2017

Supervisors

Alex Poulton (National Oceanography Centre, University of Southampton, *al jp*01*@googlemail.com*)

Mike Lucas (University of Cape Town, *mikelucasuct@gmail.com*)

Coleen Moloney (University of Cape Town, *coleen.moloney@uct.ac.za*)

The financial assistance of the National Research Foundation (NRF) towards this research is hereby acknowledged. Opinions expressed and conclusions arrived are those of the author and not necessarily to be attributed to the NRF.

Abstract

Coccolithophores are a biogeochemically important phytoplankton group, fulfilling an important role in the global carbon cycle through primary production and the formation and export of calcium carbonate. Despite this biogeochemical importance, relatively little is known about their ecophysiology, for example their response to nutrient availability in terms of both macronutrient (nitrate, phosphate) and micronutrient (trace metal) or how this impacts on their competition with other phytoplankton groups (e.g. diatoms, *Synechococcus*). Hence, this study investigated the response of coccolithophores to trace metal (iron, zinc and cobalt) additions in the high latitude North Atlantic (Iceland and Irminger basins) and the Southern Ocean (Great Calcite Belt, Scotia Sea). The response of coccolithophores to environmental conditions was investigated by examining distribution patterns *in situ* and in targeted bioassays where natural communities were incubated with elevated levels of trace metal concentration. The wide range of initial conditions for these bioassays (e.g. temperature, macro- and micro-nutrient availability and phytoplankton community composition), provided valuable insights into coccolithophore responses to trace metal addition across a range of different biogeographic regions. These responses were investigated in terms of coccolithophore cell abundances, species composition, calcite production and growth rates, and were contrasted with responses of the total phytoplankton community (chlorophyll *a*) and abundances of diatoms and other phytoplankton groups (e.g *Synechococcus*). The major finding of this thesis is that iron addition positively enhances coccolithophore growth rates and calcite production in both the Northern and Southern subpolar oceans. Another significant finding was that zinc addition also positively enhanced growth rates of coccolithophores (and diatoms) in a number of bioassays across the Great Calcite Belt (Southern Ocean). Thus, the trace metals iron and zinc are important micronutrients to consider in regulating coccolithophore growth and calcite production. As climate change potentially altering the flux of such trace metals to the ocean it is therefore important to further investigate the role of these micronutrients in regulating coccolithophore communities and their biogeochemical impact.

Plagiarism Declaration

1. I know that plagiarism is wrong. Plagiarism is to use another's work and pretend that it is one's own.

2. I have used the Harvard Referencing system for citation and referencing. Each contribution to, and quotation in this thesis from the work(s) of other people has been attributed, and has been cited and referenced.

3. This thesis is my own work.

4. I have not allowed, and will not allow, anyone to copy my work with the intention of passing it off as his or her own work.

Signature _____

I hereby declare that this thesis is my own work and effort, both in concept and execution, with normal guidance and assistance from my supervisors.

A few comments are needed on the data used in this thesis:

Data for Chapter 2: "Iron stimulation of summer coccolithophore communities in the North Atlantic (Iceland and Irminger Basins, July - August, 2010)"

Data for this chapter was collected on board the *RRS Discovery.* Data from nutrient addition bioassay experiments was collected by Dr T. Ryan-Keogh, Dr A. Macey and Prof. M. Moore (University of Southampton, National Oceanography Centre (NOC), UK). Nutrient data was collected by Dr M. Stinchcombe (University of Southampton, NOC, UK), chlorophyll *a* by Prof. M. Moore and Dr A. Poulton (University of Southampton, NOC, UK). Dissolved Fe measurements were made by Prof. E. Achterberg. Primary production and calcite production were measured by Dr A. Poulton at sea and flow cytometry was conducted by Dr T. Ryan-Keogh and Prof M. Moore (University of Southampton, NOC, UK). SEM samples were run at the University of Cape Town (UCT), by M. Waldron (University of Cape Town, South Africa). Dr M. Lucas provided part of the data and assisted at sea. . SEM image analysis (identification and enumeration), collation of the primary and ancillary data and all statistical analyses were performed by myself.

Data for Chapter 3: "Coccolithophore responses to trace metal addition (Fe, Zn, Co) across the Atlantic and Indian sectors of the Southern Ocean's Great Calcite Belt"

Data for this chapter was collected on board the *R/V Melville* in 2011 and *R/V Revelle* in 2012. Data from trace metal addition bioassays was collected by Dr B. Twinning and Dr W. M. Balch/ Nutrient and chlorophyll *a* data was collected by Dr W. M. Balch. Measurements of initial trace metal concentrations were determined by P. Morton (Florida State University). SEM samples were run at the University of Cape Town (UCT), by M. Waldron (UCT, South Africa). SEM image analysis (identification and enumeration), collation of the primary and ancillary data and all statistical analyses were performed by myself.

Data for Chapter 4: "Effect of iron addition and pCO_2 manipulations on phytoplankton communities in the Scotia Sea"

Data for this chapter was collected on board the *RRS James Clark Ross*. Data from the +Fe and elevated pCO_2 bioassays was collected by Prof. M Moore, Dr S. Richier, Dr C. Daniels and Dr G. Fragoso. Measurements of macronutrient concentrations were conducted by Prof. R. Sanders and chlorophyll *a* were collected by Prof. M. Moore and Dr S. Richier. Primary production and calcite production were measured by Dr C. Daniels and Dr G.

Fragaso. Underway sampling was conducted by Dr J. Young, Prof. T. Tyrrell and Prof. E. Achterberg. Dissolved Fe measurements were made by Prof. E. Achterberg. *Emiliania huxleyi* enumeration were done by Dr J. Young. Collation of primary and ancillary data and all statistical analyses were performed by myself.

Acknowledgements

The words 'thank you' really feel ridiculously ineffective in the context of trying to express how incredibly grateful I am to all the people who have helped get me to this point. The proverb 'It takes a village' is perhaps an apt one in trying to describe the process of getting through an entire PhD with your sanity in tact. My 'village' has been spectacular.

Alex, your weekly skypes and calm, unflappable demeanour in the face of my barrage of questions and self doubt have been invaluable, I can honestly say that I would not have finished without your support, guidance and Star Wars wisdom. You have gone above and beyond in every possible way and I am truly, truly grateful. Mike, you've put up with me since third year of undergraduate BSc, I'm not sure why, but thank you all the same for opening that first door for me, for giving me the opportunity to start this journey. It has been a long one. Coleen, thank you for your advice on statistics and style and for coming on board last minute, your input has been most appreciated.

To my home away from home, the Institute of Marine Antarctic Studies and to all the people there, thank you for reading chapters, for the advice on statistics and for reminding me that I'm not the only person who's ever struggled through a PhD. Merel, Lavy, Delphi and everyone else, thanks for the chats and empathy. Special thanks go to Spoon for allowing me to pick his brain over and over again on statistics and for not laughing at my inane questions. To Emma, who I first encountered in a shared office at the National Oceanography Centre and who, somewhat serendipitously ended up on the other side of the world with me three years later just in time to read my entire thesis and encourage me through the last few weeks. Thank you so much.

To the non-technical team, Bex your peanut butter biscuits, enumerable cups of tea and near daily phone calls have over the last few years been more appreciated than I can say. Kace, thanks for being my unofficial therapist and always being available even with the 17 hour time difference. Amy, thank you for reading my introduction and giving it the benefit of your 'grammar junkie' skills.

To my wonderful family, who's torrent of support during this PhD and every other moment of my life have

sustained me and motivated me to keep going. I could never let you down so thank you for that. My future family-in-law, Lynne thanks for your interest and messages of support, Maarten thank you for your encouragement and interest over the years.

Finally, Tjaart, words fail me, you are incredible. You have read my entire thesis, you have fixed Latex when it decided to stop working, you have fixed me when I decided to stop working, you have fed me and brought me tea and wine and treats. You have believed in me when I did not believe in myself and your support and love have enabled me to work harder and better than I knew I was capable.

Funding Acknowledgements

The work for this PhD was made possible through funding provided by; the NRF Doctoral Innovation Scholarship and a Marine Biology Postgraduate Bursary (2016). Travel to the National Oceanography Centre, Southampton (UK) was made possible through a MA-Re BASIC Travel Award and through AEON's Iphakade program funded through the DST Global Change initiative.

Contents

List of Figures

List of Tables

"Gold Leader: *It's no good, I can't manoeuvrer!*

Gold Five: *Stay on target.*

Gold Leader: *We're too close!*

Gold Five: *Stay on target!*"

Star Wars: Episode IV - A New Hope

Chapter 1

General Introduction

1.1 Global Ocean and Phytoplankton

The oceans cover approximately 70% of the planet and play an integral role in many of the Earth's major processes, its role in regulating global biogeochemical cycles is of particular importance (**?**). Nearly 39 000 Gt of carbon are stored in the oceans (**?**). A continuous exchange of atmospheric carbon dioxide (CO_2) with oceanic CO_2 in the surface waters of the ocean results in approximately 90 Gt of carbon being exchanged between the atmosphere and ocean every year. The balance of this exchange results in slightly more carbon remaining in the ocean, such that the oceans act as a net carbon 'sink' (**?**). Phytoplankton in the modern ocean play a vital role in this global carbon cycle (Figure **??**). The carbon cycle is dependent on net primary productivity (NPP) which is defined as the rate at which an ecosystem accumulates biomass (fixed carbon) through photosynthesis, after subtracting respiration.

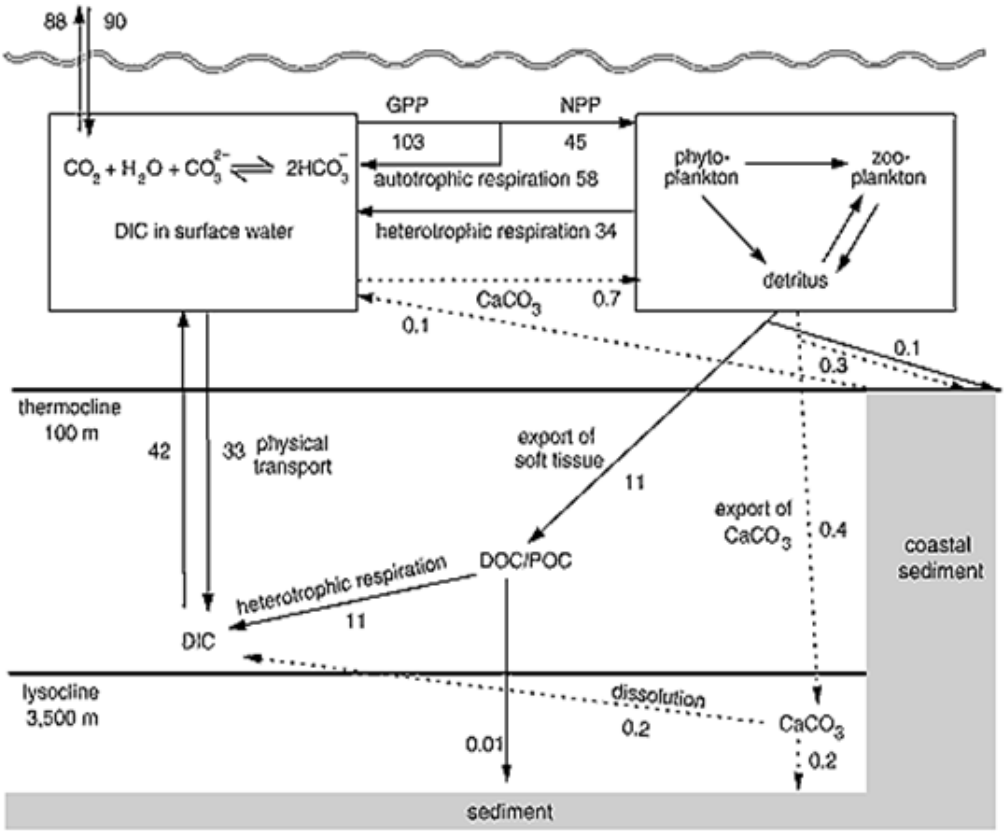

Figure 1.1: Illustration of the ocean's role in the global carbon cycle (taken from **?**). Numbers represent the flux of carbon ($\mathrm{Gt\,yr^{-1}}$).

Phytoplankton are microscopic ($< 200\,\mu$m), photosynthetic, unicellular organisms that form the base of the food web in the ocean and they account for approximately half of primary productivity generated by plants globally (**?**). Phytoplankton are found throughout the world's oceans in the photic zone (the sunlit, upper layers). There are nearly 20 000 different phytoplankton species, however only a few, key species control the cycling of carbon and other nutrients (**?**). There are several major groups of phytoplankton and these groups are often separated by size; microplankton ($> 20\,\mu$m) which includes large diatoms, dinoflagellates and microflagellates; nanoplankton ($2-20\,\mu$m) which includes coccolithophores and small diatoms, and picoplankton ($< 2\,\mu$m) which includes cyanobacteria. Through photosynthesis (Eq. **??**), phytoplankton are able to reduce the surface concentration of dissolved CO_2 and produce approximately 50% of the oxygen we breath (**?**).

$$6CO_2 + 6H_2O + \text{light} \rightarrow C_6H_{12}O_6 + 6O_2 \tag{1.1}$$

The wide variety in phytoplankton sizes and species means that phytoplankton biomass or carbon content also ranges widely, from $< 1\,\mathrm{pmol\,C\,cell^{-1}}$ (picoplankton) to $> 1\,\mu\mathrm{mol\,C\,cell^{-1}}$ (microplankton) and consequently,

understanding community structure of phytoplankton populations is integral in quantifying how the total phytoplankton community contributes to the ocean's ability to capture, store and potentially remove carbon from the surface to depth (export). Furthermore, the high diversity of phytoplankton in the ocean, both in terms of size and species, means that phytoplankton have a wide range of differing nutrient requirements.

1.2 Nutrients in the Ocean

Nutrient availability plays an incredibly important role in regulating a number of processes in the ocean, and in addition to light (**?**), is one of the key variables which control phytoplankton community structure and biomass (**?**). Phytoplankton growth can become limited by the availability of nutrients when other key variables, such as light and temperature are not limiting (**?**). Phytoplankton require carbon, nitrogen and phosphorus - as well as silicic acid for diatoms and calcium for coccolithophores - in addition, they also require a suite of micronutrients (such as iron, zinc (Zn) and cobalt (Co)) which are available in trace concentrations (**?**). Primary production (PP) (the rate at which organisms convert energy into organic compounds) by the different types of phytoplankton (e.g. coccolithophores and diatoms) can become limited by the availability of these macro- and micronutrients (**??**). Importantly, different phytoplankton groups are subject to different nutrient limitations, for example diatoms can often become limited by silicic acid availability which is required to build their frustules. Moreover, different phytoplankton size-fractions are known to have different nutrient requirements. Nano- and picoplankton ($< 5\,\mu$m) often have a competitive advantage over larger phytoplankton because they have a larger surface area to volume ratio and are therefore able to scavenge nutrients at low concentrations which would otherwise limit larger cells (**?**).

All phytoplankton require nitrogen and in over half the world's oceans, nitrogen in surface waters becomes depleted during summer, thereby limiting phytoplankton growth rates (Figure **??**) (**?**). In contrast, over 20% of the world's oceans are characterised by perennially high concentrations of macronutrients (nitrate, phosphate and silicate) (**?**). Despite abundant macronutrient concentrations in surface waters, productivity in these regions remains lower than expected (**????**). These areas, termed 'high nutrient, low chlorophyll' (HNLC) regions, occur in the subarctic Pacific, equatorial Pacific and most notably in the Southern Ocean (**????**). Such high residual macronutrient concentrations are thought to be due to the absence of iron (Fe) which compromises phytoplankton's ability to assimilate nitrate. This occurs partly because the ability of phytoplankton to use nitrate requires that it is reduced within the cells to nitrite and then to ammonium by the Fe-dependent enzymes nitrate and nitrite reductase, respectively (**???**). Various authors (e.g **??**) have demonstrated that Fe plays an integral role both in limiting

phytoplankton growth rates and in influencing the structure of the phytoplankton community across much of the worlds' oceans.

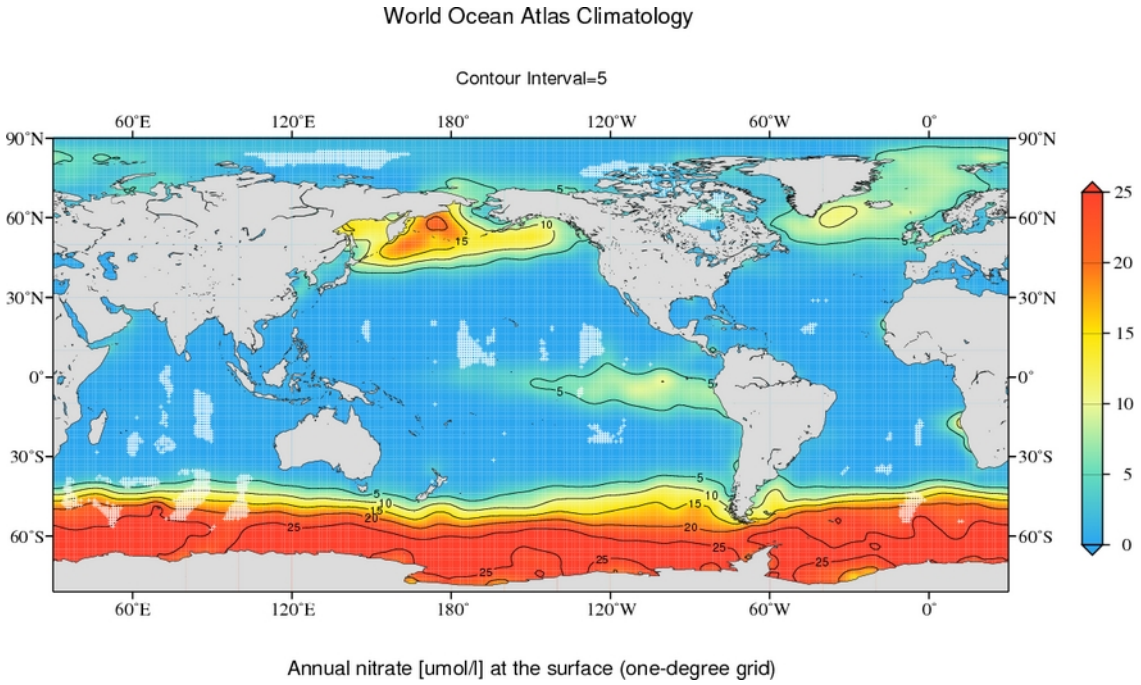

Figure 1.2: Image illustrating the surface concentrations of nitrate in the world's oceans (taken from **?**).

1.3 Iron

Iron is an essential micronutrient required by all organisms. While Fe may appear to be an unlikely contender for limiting biochemical processes - due to it being the fourth most abundant element in the earth's crust (**?**) - vast areas of the world's oceans are Fe limited. Small-scale (10-100 km^2), *in situ* Fe enrichment experiments, where Fe and the conservative tracer SF_6 are added to HNLC surface waters (**?**), have shown that the availability of Fe in the ocean limits primary productivity in one-third of the world's oceans (**?**). In the past thirty years, our understanding of this micronutrient has grown exponentially. Primary production, community structure and sinking carbon flux (transport of carbon down through the water column) are all sensitive to the availability of Fe, and this is especially true in HNLC areas. Iron is required for a number of biochemical processes such as nitrogen utilization, photosynthesis and respiration (**???**). It is utilised in a variety of enzyme systems, most notably in those that facilitate photosynthesis, respiration, nitrate reduction and nitrogen fixation (**?**). Phytoplankton's ability to 'fix' nitrogen (the process whereby atmospheric nitrogen is assimilated into organic compounds) in particular, through the reduction of inorganic nitrogen species (**??**), is strongly influenced by the deposition of atmospheric Fe, as exemplified in the sub-tropical gyre of the North Atlantic (**?**). Indeed, phytoplankton biological requirements for

Fe associated with photosynthesis, has been estimated to represent up to 80% of their total Fe requirement (**?**). Thus, Fe deficiency limits PP in many areas of the ocean (**??**). Additionally, it has been linked to phytoplankton biomass, growth rates and species composition (**?**). However, due to the vast differences in cellular Fe requirements between phytoplankton species, any changes in Fe concentrations will also influence the composition of the phytoplankton community (**?**). It is also important to note that not all chemical forms of Fe found in seawater are directly available to phytoplankton (**??**).

In the geological past, before the evolution of oxygenic photosynthesis, the ocean was anoxic (depleted of dissolved oxygen) and Fe was present in very high concentrations (**?**). However, as oxygen concentrations increased, soluble Fe was oxidised and precipitated out of the surface seawater (**?**), to form the characteristic banded Fe concentrations of insoluble ferric Fe, typical of many sediment deposits. For example, iron-induced productivity contributed to approximately 30% of the 80 ppm drawdown of atmospheric CO_2 observed during the last glacial maxima (**?**). In the modern ocean, bioavailable (soluble) Fe concentrations on average do not exceed a few nanomolar (**?**) and Fe limitation in the modern ocean is prevalent where there are no inputs such as the remote Southern Ocean.

Iron is supplied to the ocean in a number of ways (Figure **??**). Aeolian dust transport from the major continents is the main source of Fe in the ocean (**??**). Consequently, remote areas, like the Southern Ocean, are for the most part, Fe deficient (**?**) with the exception of coastal seas that surround Fe-rich sub-Antarctic Islands (**?**). Another major source of Fe to the oceans is via an extensive global transport system, mainly through rivers as suspended sediments (**??**). However, Fe supplied via rivers and fluvial deposits tends to only supply coastal systems (**?**). Evidence suggests that, generally, coastal regions and shallow waters experience less Fe limitation than open ocean environments, with a trend of decreasing Fe with distance from land as identified by numerous authors (**??**). Other sources of Fe to the ocean include hydrothermal vents (**??**), volcanic eruptions (**?**), sea ice (**??**), anthropogenic and extra-terrestrial sources (**?**) (Figure)**??**). However, aeolian dust remains the main source of Fe to the open ocean (**?**).

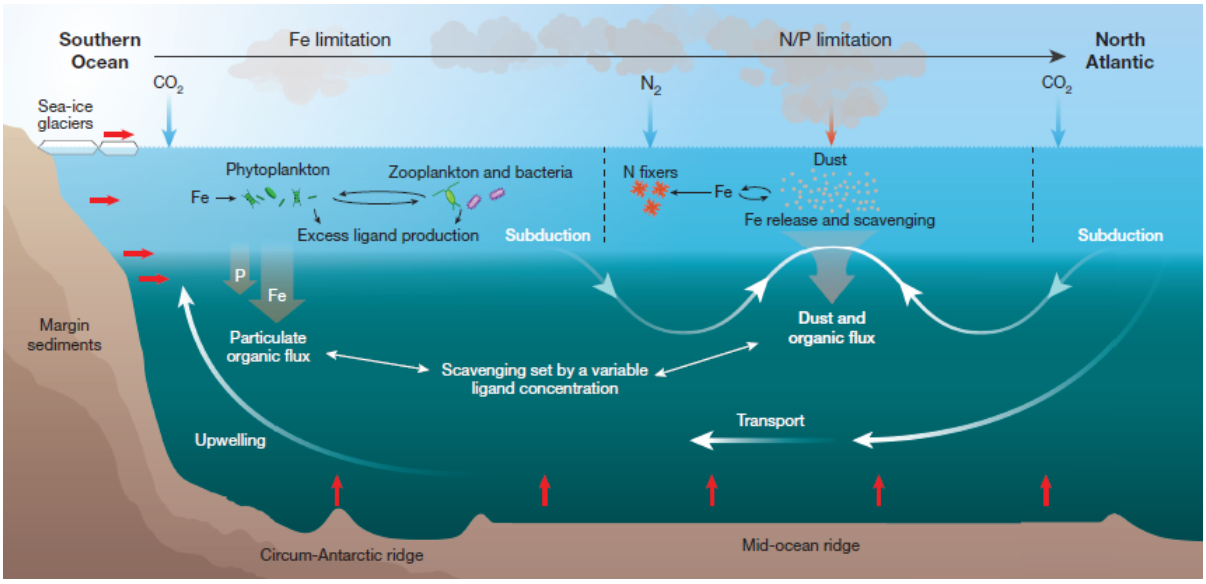

Figure 1.3: Illustration of the processes governing the global iron cycle including sources of iron to the ocean from erosion of continental shelf sediments, upwelling from hydrothermal vents and deposition of aeolian dust (taken from **?**).

Climatic factors affect the production, transport and deposition of dust to the oceans (**?**). In the last glaciation, dust fluxes were between 2 and 20 times higher than is currently the case due to increased winds that prevailed at the time, compounded by lowered sea level, reduced precipitation and changes in vegetation cover (**?**). Contrary to some predictions of increased Fe supply to the oceans due to desertification, though other predictions conclude that with increased global warming, important sources of dust to the oceans such as the Sahel and southern Sahara could 'green' because of locally increased rainfall, which would lower global dust production from this region (**?**).

1.4 Other Trace Metals

In addition to changes in Fe availability as a result of climate change, it is likely that the availability of other trace metals such as Zn and Co, which play an important role in phytoplankton physiological processes (**??**), could be similarly affected. The rates of Fe and Zn deposition in the modern ocean are up to ten times lower than in glacial times (**????**), thus it is possible that modern phytoplankton will be subject to trace metal limitation. Globally, dissolved Zn concentrations range from 0.1 to 10 nM (**?**) and it displays a nutrient-like vertical profile in the water column with concentrations increasing with depth (**?**). Zinc has been shown to play an important role in the phytoplankton community, playing a role in a variety of enzymatic systems (**?**). Specifically, Zn serves as a co-factor in extracellular phosphatase which is required by microorganisms in order to acquire phosphorus from organic P compounds (**?**). However, there is little information on the responses of phytoplankton to Zn (and to Co),

with the majority of studies focussing on diatoms in HNLC areas. For example, Zn has been shown to limit the growth of the diatom *Thallassiosira weissflogi* (**?**) The response of other important taxa such as coccolithophores is relatively unknown, however there is evidence that the haptophyte *Phaeocystis antarctica* is co-limited by Zn and Co (**?**).

1.5 Phytoplankton Diversity

Bloom forming phytoplankton such as siliceous diatoms and calcifying coccolithophores play a disproportionately large role in the modern ocean. Approximately one-fifth of total photosynthesis globally (land and sea) is carried out by diatoms (**?**), whereas coccolithophores account for from <1 to ~40% of PP regionally (**??**). The word 'diatom' is derived from the Greek *diatomos* which means 'cut in half', which refers to their two-part cell walls (or frustules) composed of silica. They are among the most diverse group of phytoplankton, with cell sizes covering several orders of magnitude from a few micrometers to a few millimetres, and can exist as individual cells or form chains (**?**). Perhaps as a result of their wide diversity, diatoms often dominate phytoplankton communities across a wide range of biogeochemical regions.

Traditionally, phytoplankton blooms are thought to progress in terms of community composition through succession of different types (Figure **??**), where as nutrients become depleted the dominant phytoplankton are replaced by others that are better adapted to the new conditions (**??**). Spring blooms are typically dominated by fast growing diatoms, which are able to outcompete other slower growing phytoplankton types. Diatoms are generally highly productive when conditions are conducive to growth (i.e. optimal light and macro- and micronutrients (e.g. nitrate, silicic acid and Fe) availability). Due to their large sizes and high density, which imparts fast sinking rates, diatoms are able to sequester atmospheric CO_2 into the deep ocean by sinking out of the euphotic zone, which may be mediated by mesozooplankton grazing and faecal pellet production. However, once silicic acid becomes depleted (at around $\sim 1-2\,\mu$M), seasonal community succession occurs where diatoms are replaced by non-siliceous types such as phytoflagellates and/or coccolithophores (e.g. **?**). Despite this traditional view of different phytoplankton groups succeeding each other in bloom conditions, several studies recently have challenged this viewpoint (**?**). For example, a comparison of particulate inorganic carbon (PIC), produced by coccolithophores during calcification, and chlorophyll *a* peak dates using satellite images provided evidence that in many open ocean regions, coccolithophores and other phytoplankton (diatoms) often co-occur in blooms (**?**).

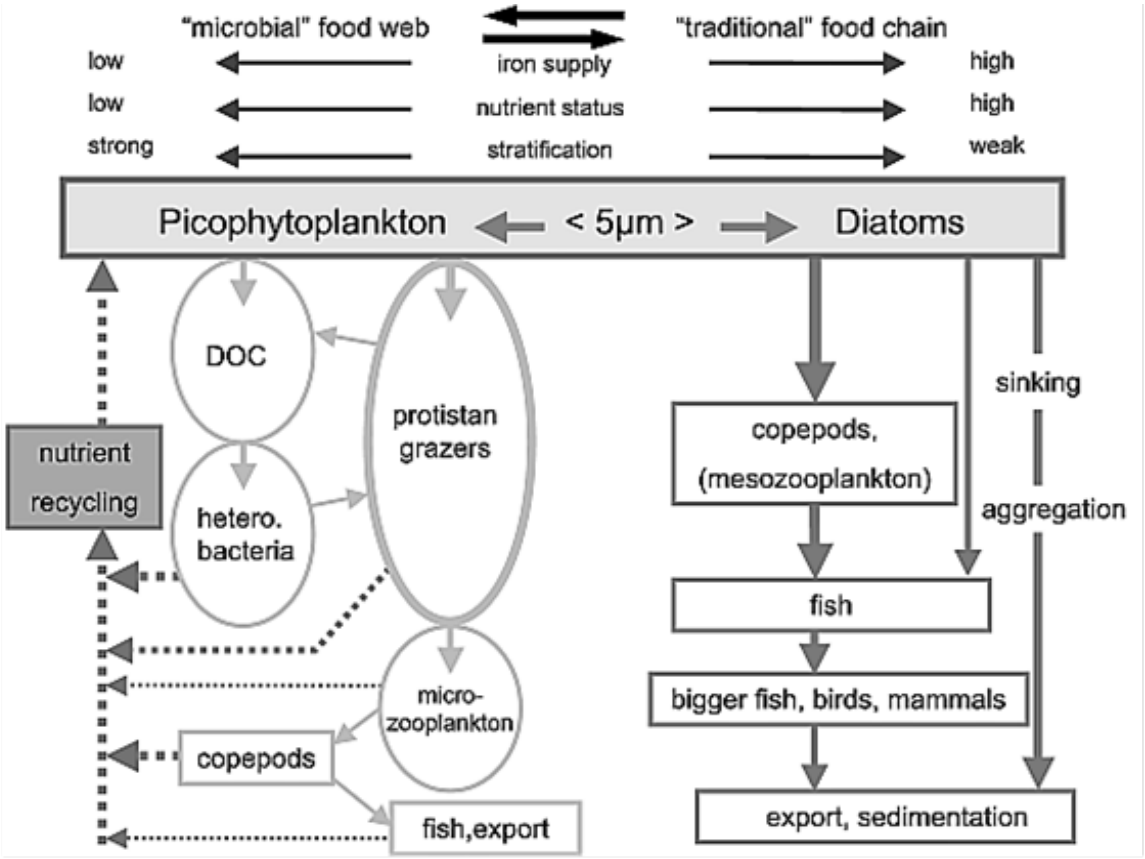

Figure 1.4: Conventional view of a two-state oceanic food web illustrating succession (**?**).

Coccolithophore blooms are generally thought to follow from diatom blooms once surface waters have become seasonally depleted in inorganic macronutrients (nitrate, silicic acid) and have become more stratified (and stable) with the development of a seasonal thermocline (a formation of a marked temperature gradient, where surface seawater layers are separated by a distinct temperature change with deeper layers) (**????**). Coccolithophore blooms have been linked with high mixed layer irradiances (**?**) and seasonally shallow mixed layers and high temperatures (**??**). The coccolithophore species *Emiliania huxleyi* generally dominates coccolithophore blooms, however other coccolithophore species such as *Coccolithus pelagicus* as well as other phytoplankton (e.g. small diatoms) are frequently present (**??**). In contrast, large diatoms are usually dominant in turbulent, low-stratified waters and are frequently the first group to bloom during spring. Additionally, in conditions where the supply of nutrients is fluctuating, diatoms are also more likely to dominate due to their higher capacity for luxury nutrient consumption (when organisms acquire an excess of non-limiting resources (**?**)) when compared with coccolithophores (**??**).

Primary production by coccolithophores represents a much smaller sink of CO_2 than PP by non-calcifying phytoplankton (**?**). This is due to their impact on the partial pressure of CO_2 during calcification, which leads

to the production of CO_2 during calcification and coccolith formation. A decrease in the opal:carbonate ratio recorded since the early 1980s could indicate that there has been an increase in the abundance and productivity of coccolithophores relative to diatoms (**?**), which would act to weaken the biological carbon pump. Coccolithophore production of calcium carbonate ($CaCO_3$) exoskeletons, along with their sinking below the euphotic zone when they die, directly affects the exchange of CO_2 between the atmosphere and sea surface (**?**). Over long-time scales, coccolithophores play an important role in influencing the 'rain ratio', which is the relative rates of export of $CaCO_3$ and particulate organic carbon (POC) from the surface ocean to the deep ocean (**?**). Coupled ocean-sediment models have shown that a mean global reduction of 40% in the $CaCO_3$:POC export ratio, could result in a drawdown of between 70 and 90 ppm of atmospheric CO_2 (**?**). Changes in the rain ratio could be caused by simple shifts in ecosystem composition, specifically a change in the relative contribution of coccolithophores to net primary production (**?**).

Grazer control is another factor that affects the seasonal succession of the major phytoplankton groups. While the silicic acid frustules of diatoms appear to deter grazing (**?**), the role of coccolithophores is presently unclear although grazing defence has recently been supported through ecological modelling (**?**). Mesozooplankton grazing control typically only occurs late in the seasonal cycle as a result of the relatively slow development of copepods and other predators. This may account for the timing of *E. huxleyi* blooms, which usually only occur late spring/summer (**?**).

1.6 Coccolithophores

Coccolithophores are thought to be the most productive calcifying organisms on earth (**?**) and contribute to both the biological and carbonate pumps (**?**), contributing up to 20% of the total PP in selected areas of the ocean (e.g. in subtropical gyres in non-bloom conditions) (**??**) as well as dominating pelagic (open ocean) calcification through the production of coccoliths (**?**). Additionally, coccolithophores can act as important agents for the transfer of organic carbon from the surface of the ocean to the deep ocean through their 'ballast effect'(**?**). **?** distinguished three forms of mineral ballast: calcium carbonate, opal and lithogenic material. Transfer efficiency – the fraction of exported organic matter that reaches the deep ocean – has been positively linked to deep ocean calcite recovered from sediment traps (**?**), which implies that ballasting by calcium carbonate ($CaCO_3$) could play an important role in regulating the transfer efficiency (**??**). Thus, understanding the effect of changing ocean conditions on processes such as calcification and coccolithophore growth is integral to being able to make predictions about the future of our oceans. Coccolithophores are particularly sensitive to processes such as climate change and ocean acidification

(**?**) and, while the predicted decrease in ocean pH has been expected to have a negative effect on calcifying organisms in cultures and field studies, this is not always the case, with numerous studies producing conflicting results; some report a decrease in calcification in response to elevated pCO_2 (**??**) while others have reported increases in calcification (**?**). A meta-analysis by **?** which examined all existing data regarding responses of coccolithophores to ocean acidification indicated that, generally, calcification decreases while growth and photosynthesis will increase or stay the same under elevated pCO_2 conditions. However, responses are very species dependent with the two most prolific coccolithophore species, *E. huxleyi* and *Gephyrocapsa oceanica* being negatively affected with respect to calcification and the cellular PIC/POC ratio, whereas a more heavily calcified species, *Coccolithus braarudii* did not show a clear response to elevated pCO_2 (**?**). Moreover, it appears that the increases (or decreases) in calcification may be dependent on the strain/morphotype of *E. huxleyi* used in addition to there being differences in response patterns between coccolithophore species (**?**). It appears that the sensitivity of *E. huxleyi's* calcifying ability and organic carbon fixation to increased concentrations of CO_2 depends on the nutrient status and light availability (**?**). Much attention has been paid to the effect of decreasing ocean pH on calcifying phytoplankton such as coccolithophores, with numerous studies examining coccolithophores (e.g. *E. huxleyi*) under various nutrient limitations (**?**) as well as various CO_2 levels (**?**), although few data exist on the effect of Fe addition on coccolithophore calcification and growth. In the modern ocean, coccolithophores are one of the most prominent groups of phytoplankton, with *E. huxleyi* being the most important of the calcifying plankton numerically (**??**). Additionally, *E. huxleyi* is an extremely cosmopolitan coccolithophore species (**?**), occurring in nearly every ocean except the Arctic Ocean and the high latitude Southern Ocean (**??**). In studies conducted in the 1980s and 1990s, *E. huxleyi* was only found in very small numbers or was completely absent south of 60º in the Southern Ocean. However, between 2002 and 2006 it was found consistently in quantities of approximately $100\,\text{cells}\,\text{mL}^{-1}$ of seawater between 60ºS and 65ºS (**?**). A north-south shift in *E. huxleyi* calcification morphotypes in the southern hemisphere mimicked the north-south decline in the calcite saturation state (see Figure **??**), with this trend in decreasing calcification of *E. huxleyi* in the Southern Ocean reflecting a change in dominance between one ecotype and the next (**?**).

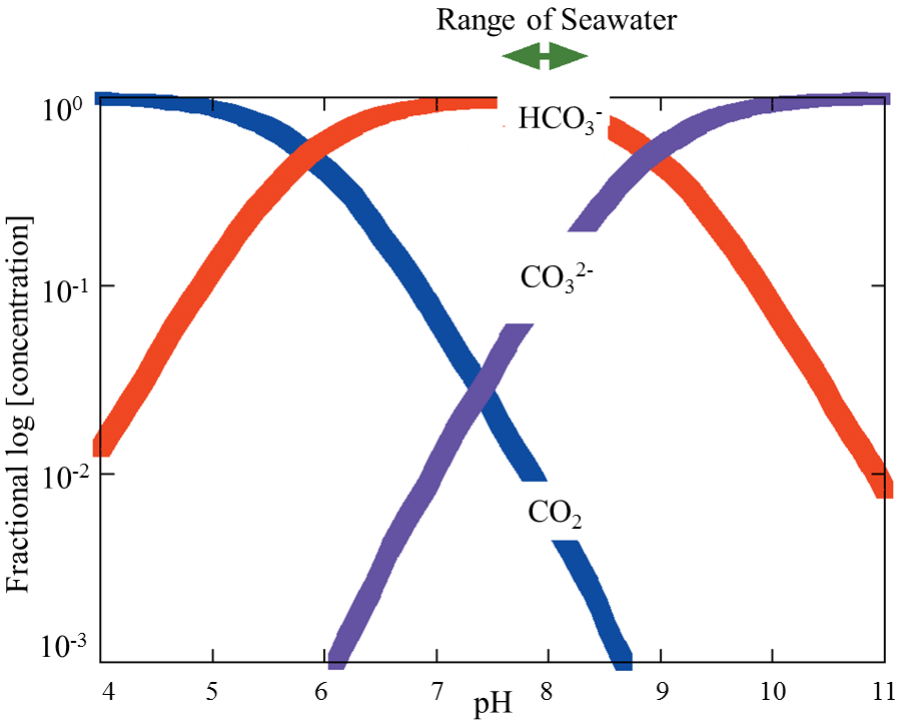

Figure 1.5: Illustration of the relative proportions of the three inorganic forms that CO_2 takes on when dissolved in seawater (bicarbonate ions (HCO_3^-), carbonate ions (CO_3^{2-}) and aqueous/dissolved CO_2). The green arrow indicates the narrow range of pH (7.5-8.5) that is likely to be found in the oceans now and in the future. Y-axis is plotted logarithmically (taken from **?**).

Emiliania huxleyi is a species that displays significant genetic diversity, molecular phylogenetic studies have shown that there are at least two mitochondrial sequence groups; a cool-water group (located in the subarctic North Atlantic and Pacific) and a warm water group (located in the subtropical Atlantic and Pacific and the Mediterranean Sea) **?**. There are several different morphotypes of *E. huxleyi* currently recognised in the literature. The morphotypes are termed A, B, B/C and R (**???**), and each forms slightly different coccolith morphotypes (**?**). No studies have linked morphotype, based on PIC content, with genotype (**?**). Natural populations of *E. huxleyi* often consist of a mix of the different morphotypes and thus one might observe variations in coccolith size as well as degree of calcification (**?**). Morphotype A is typically found in warm (>10ºC), nutrient-poor (0.1-10 µmol nitrate kg^{-1}) waters with higher calcite saturation states (>4.5) (**?**). Morphotype B is distinctly less calcified than type A (**?**) (Figure **??**), while morphotype B/C is dominant in the cold waters of the Southern Ocean and is commonly found in the Atlantic, Indian and Pacific sectors of the Southern Ocean (**???**). Type B/C coccoliths are lightly calcified relative to types A and B, with this morphotype typically found in cold (<10ºC), nutrient rich ($>$ 10 µmol nitrate kg^{-1}) waters with calcite saturation states of ~3.5 (**?**). The majority of laboratory studies have been on morphotypes A and B (**?**), however strains of B/C from the Southern ocean are now also being studied (**???**).

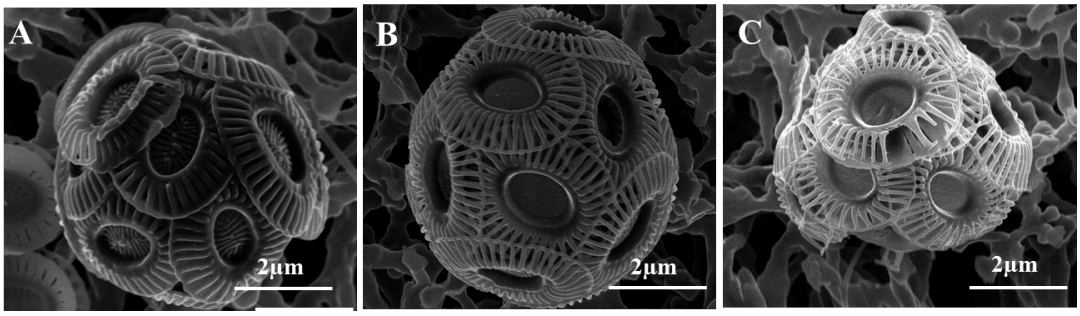

Figure 1.6: SEM images of *Emiliania huxleyi* morphotypes A) A type, B) B/C type and C) damaged B/C type. (SEM images from the Southern Ocean, run at University of Cape Town by Miranda Waldron).

A lot of the information on calcification and coccolithophore physiology comes from work done on *E. huxleyi* as a result of its suitability for use in cultures. However, it is important to note that coccoliths of different species all contain differing amounts of $CaCO_3$ (**??**) and that so-called 'heavy' species tend to calcify at a faster (mass) rate than 'light' species. For example, the calcification of *E. huxleyi* is <1 pmol C cell^{-1}d^{-1} (**?**), while other species such as *Calcidiscus leptoporus* and *Coccolithus pelagicus* can calcify at much higher rates of 8 and 18 pmol C cell^{-1}d^{-1} respectively (**???**). The process of calcification is strongly dependent on irradiance and can be stimulated by nutrient stress (**?**). The cellular process of photosynthesis relies on the use of CO_2 and $HCO^-{}_3$, whereas, calcification is thought to use just $HCO^-{}_3$ as its main source of carbon (**??**). The rate of photosynthesis has been observed to decrease as CO_2 concentrations decrease, despite a concurrent increase in the rate of calcification (**???**).

Due to the relative ease of identification and low cost, acidic Lugols is often the preferred method of phytoplankton identification and enumeration. However, this method largely precludes mineralising nanoplankton such as coccolithophores, foraminifera and *Tetraparma* species (**?**) and thus, many studies on the effects of Fe and other trace metals on phytoplankton have focussed on diatoms. However, experimental observations by **?** in the North Atlantic indicated a positive response by coccolithophores with respect to cell numbers (and thus likely an increase in growth rates) to Fe addition, despite Fe not being generally regarded as one of the factors controlling coccolithophore calcification or growth rates (**?**). Additionally, **?** found that coccolithophore abundance and calcification rates did not correlate with any of the environmental factors currently associated with coccolithophore blooms (i.e. irradiance, mixed layer depth, nitrate and phosphate) and suggested that Fe may be an important factor in regulating cellular calcification and net growth rates.

1.7 Thesis Aims and Outline

The aim of this thesis is to further understanding the effect Fe and other trace metals (Zn and Co) have on coccolithophores growth and calcification, as well as species composition. A secondary aim is to also investigate how changing CO_2 conditions in the ocean may affect coccolithophore responses to trace metal availability. A large proportion of the global ocean is Fe limited (**??**) and coccolithophores are important drivers of the global carbon cycle (**?**). Ocean acidification and climate change will directly affect both the carbonate system and future dust deposition. Understanding how coccolithophores respond to trace metals and changing CO_2 conditions, and contrasting this response with other phytoplankton groups (e.g. diatoms) will allow predictions of future change.

The main hypotheses of this thesis are:

1. That coccolithophores will respond positively to +Fe addition through increased calcite production, increased growth rates, and changes in species composition to faster-growing species;

2. That coccolithophores will respond positively to +Zn addition, calcite production, increased growth rates, and changes in species composition to faster-growing species;

3. That coccolithophores will respond positively to +Fe addition with increased growth rates and calcite production under ambient pCO_2 conditions, but negatively under elevated pCO_2 conditions (in contrast, the phytoplankton community will only respond positively to increased pCO_2 conditions when dFe is non-limiting).

Responses of coccolithophores to Fe addition experiments performed in the Iceland and Irminger Basins in the North Atlantic in 2010 are examined in this context. This research focuses on changes in coccolithophore abundance, community composition and calcification rates in response to +Fe addition as well as to other macronutrient (nitrate (+N) and Fe and nitrate (+FeN)) additions. The coccolithophores are also compared and contrasted to diatoms and small-celled phytoplankton. Similar experiments performed in the Atlantic (2011) and Indian (2012) sectors of the Southern Ocean's Great Calcite Belt examine coccolithophore responses to the trace metals Fe, Zn and Co, as well as comparing and contrasting this response with that of the diatom community. The response of phytoplankton to +Fe addition and elevated pCO_2 is examined using bioassay experiments in the Scotia Sea, with additional data from underway sampling and depth profiles. Finally, *in situ* data from both the North Atlantic and Southern Ocean are compared in order to examine the role of Fe and other environmental factors in controlling coccolithophore abundance, community composition, and to investigate whether any of these factors can be used to predict how phytoplankton communities might respond to future changes in trace metal availability and decreasing pH.

This thesis has four results chapters:

Chapter 2: Iron stimulation of summer coccolithophore communities in the North Atlantic (Iceland and Irminger Basins, July - August, 2010);

Chapter 3: Coccolithophore responses to trace metal addition (Fe, Zn, Co) across the Atlantic and Indian sectors of the Southern Ocean's Great Calcite Belt;

Chapter 4: Effect of iron addition and pCO_2 manipulations on phytoplankton communities in the Scotia Sea;

Chapter 5: General Synthesis.

Chapter 2

Iron stimulation of summer coccolithophore communities in the North Atlantic (Iceland and Irminger Basins, July - August, 2010)

Abstract

The North Atlantic is a region known globally for summer coccolithophore blooms, numerically dominated by the coccolithophore *Emiliania huxleyi*. Recent research has highlighted the potential role of dissolved iron (dFe) in limiting post-spring and summer phytoplankton communities in the North Atlantic. The aim of this study was to investigate the growth response of coccolithophores (*E. huxleyi*) to iron (Fe) addition through seven +Fe addition bioassays in the Iceland and Irminger Basins, examining the response of the coccolithophore community in terms of species composition, calcite production (CP) and growth rates. The response of coccolithophores were also contrasted with that of the wider phytoplankton community. Bioassay design included +Fe addition (+Fe; 2 nM), nitrate addition (+N; 2μM) and +Fe plus nitrate additions (+FeN; 2 nM and 2μM, respectively). Coccolithophores responded positively to Fe amendment in a number of ways: growth rates and CP all responded positively to Fe, but it is unclear to what extent initial Fe availability affected the species composition of the coccolithophore community. Diatoms followed a similar pattern of response to coccolithophores between bioassays, although generally cell abundance and community diversity were higher in the diatom population than in the coccolithophore population. Responses varied between the Iceland and Irminger Basins. Phytoplankton in the Iceland Basin, where phytoplankton were Fe and nitrate limited, responded strongly to +FeN and/or +N treatments, whereas

phytoplankton in the Irminger Basin, where macronutrients were not limiting but initial dFe concentrations were low (<0.01 nM and 0.28 nM), displayed a strong response in +Fe treatments. Within the Iceland and Irminger Basins, phytoplankton community responses were very much dependent on the initial community composition and physiochemical conditions rather than on the nutrient manipulations. This chapter demonstrates that Fe can be a strong limiting factor to coccolithophore communities, however initial species composition is a strong determinant of how the community responds in terms of species composition, CP and growth rates.

2.1 Introduction

The North Atlantic is a key region globally for coccolithophore blooms, often mesoscale (>100-250 $\times 10^3\,km^2$) in size (**?**). Calcite production (CP) and coccolithophore abundances in such blooms can be very high (>2 $mmol\,C\,m^{-2}d^{-1}$ and >1000 $cells\,mL^{-1}$, respectively) (**???**) relative to levels seen in other environments (e.g. global mean CP $\sim 1\,mmol\,C\,m^{-2}d^{-1}$ (**?**)). These blooms are predominantly numerically dominated by *Emiliania huxleyi* (**?**), though other more heavily calcified species are present at much lower cell densities, such as *Coccolithus pelagicus,* and can be more important in terms of CP (e.g. **?**) and export of material to depth (**?**). Seasonally, coccolithophore blooms peak during early summer, decreasing gradually during autumn and winter (**?**). Coccolithophores are also present during earlier spring blooms (**?**) and relatively abundant ($100-200\,cells\,mL^{-1}$) coccolithophore communities often persist throughout the summer (**?**). Coccolithophore blooms, most often dominated by *E. huxleyi*, in the North Atlantic have been shown to be associated with relatively slow rates of photosynthesis and low chlorophyll *a* concentrations (**?**), due to the small size of the cells (approximately 5 μm in diameter) (**??**). Additionally, *E. huxleyi* blooms can have significant impacts on the environment through deep fluxes of calcium carbonate out of surface waters and changes in carbonate chemistry through the process of calcification (**?**), as well as the production of the climatically active gas dimethyl-sulphide (DMS) (**?**).

Coccolithophores occur in all oceans except the Arctic and high latitude Southern Ocean, south of the polar front ($\sim$ 60ºS), (where they either are not present or occur in very low numbers) (**?**) and blooms contribute significantly to the global production (**??**). Despite the importance of coccolithophores and the vast array of data that has been collected from laboratory, mesocosm and field experiments (most commonly from *E. huxleyi*), relatively little is known about the factors that initiate bloom formation (**?**). Coccolithophore blooms (*E. huxleyi*) are generally believed to follow on seasonally from diatom blooms once macronutrient concentrations have become limiting (e.g. silicic acid) (**?**). Other factors that have been linked to bloom formation are high mixed layer irradiances (**??**), water column stability and relatively low concentrations of macronutrients (such as phosphate) (**?**). However, in the

Patagonian Shelf, an *E. huxleyi* bloom which occurred in December 2008 was associated with high macronutrient concentrations, cold water temperatures and low irradiance (**?**). **?** suggested that this bloom may have been linked to iron (Fe) availability due to high concentrations of residual nitrate. However, in contrast to the established theory of sequential changes in phytoplankton taxa (from diatoms to coccolithophores as macronutrient concentrations decline), observations of both diatom and non-diatom communities co-existing highlight how, instead of undergoing succession, phytoplankton instead are able to grow concurrently, indeed **?** is an influential paper in this regard. A comparison of particulate inorganic carbon (PIC) and chlorophyll *a* 'peaks' shows that, in several open ocean regions, blooms of coccolithophores and other phytoplankton co-occur (**?**). It has been suggested that, in areas where phytoplankton co-exist, limited availability of resources such as silicic acid and Fe may enable coccolithophores - with their lack of or lower requirement of these resources (**?**) - to establish themselves (**?**).

Recently, it has been proposed that summer coccolithophore communities are limited by the availability of the micronutrient Fe (**??**). Iron is known to limit phytoplankton communities in high nutrient, low chlorophyll (HNLC) conditions of the Southern Ocean, Equatorial Pacific and North Pacific (**????**), although the limitation of coccolithophores specifically by Fe remains unclear. Iron plays a strong role in influencing a number of surface biogeochemical processes such as nitrate uptake, nitrogen fixation and photosynthesis.. Iron performs an important role in photosynthetic electron transfer between photosystems and may be involved in chlorophyll synthesis (**?**). Thus, Fe is crucial for the optimal functioning of all phytoplankton including coccolithophores. Despite the universal role of Fe, several studies have shown no limitation by Fe of coccolithophore growth (e.g. **??**) whereas others have observed a positive response to Fe (e.g. **??**). It is important to note that the haploid form of *E. huxleyi* (naked cells) would be counted as flagellates or possibly nano-flagellates, thus a response in this group to Fe could include a response from the naked *E. huxleyi*, whereas the diploid forms (calcified cells) would not respond and therefore one would potentially not see a response in *E. huxleyi* abundance or calcification rates (**?**). Additionally, because the haploid form is photosynthetic and would have similar requirements for Fe and other trace metals it could, hypothetically, show a response to dFe addition. Because of the importance of coccolithophore CP in terms of air-sea fluxes of CO_2 (**??**) and the export of carbon to the deep-sea (e.g. **??**), potential Fe limitation of coccolithophore activity in the North Atlantic is significant.

Despite conflicting results in previous studies as to the response of coccolithophores to Fe addition, the universal physiological requirements of Fe by phytoplankton cells leads to a hypothesis that coccolithophores will respond to increased Fe availability similarly to diatoms: increased growth rates and a shift in species composition to faster-growing species, able to take advantage of increased Fe and residual ambient macronutrient concentrations.

However, because there is no known role for Fe in calcification it is unclear whether calcification rates will also increase. Coccolithophores grown under low Fe conditions were found to have decreased growth rates as well as concurrently decreasing cellular calcification rates, however there was no significant reduction in the cellular calcite content (**?**). Calcite production (the sum of all cells and species' individual calcification rates), could potentially increase, however, it is unclear whether cell-specific CP would increase as the production of new coccoliths is linked to cell division, such that cells can only divide once they have the requisite number of coccoliths required to cover a new daughter cell.

The high-latitude North East Atlantic is an important region globally because of its role in global ocean circulation and biogeochemistry (**?**). The North East Atlantic is not a classic HNLC region and Fe is certainly present in non-limiting quantities, such that the highly productive, annual, diatom-dominated, spring bloom is sustained (**?**). Following the annual spring bloom the high-latitude North East Atlantic exhibits low concentrations of residual nitrate ($2-5\,\mu$M), dissolved Fe (0.01 - 0.2 nM) and chlorophyll *a* ($0.2-0.4\,\mu$gL^{-1}) (**???**). The diatom-dominated spring bloom in the North East Atlantic is succeeded by one of the most extensive coccolithophore blooms on earth (**????**). Typically, between 10 and 30% (but as much as 70%, **?**) of primary production (PP) is exported to depth through sinking in this region (**??**).

The aims of this chapter were to: (1) determine the response of coccolithophores to Fe addition in terms of growth rates, community composition and CP; and (2) compare and contrast this response with that of the wider phytoplankton community. Seven small-scale bioassays were performed during a summer 2010 cruise to the Iceland and Irminger Basins in the North Atlantic, with trace metal (dFe) and macronutrient (nitrate, N) additions and sampling to examine the response of the phytoplankton community and coccolithophore population. It is hypothesised that coccolithophores will respond positively to Fe addition through (1) increased calcite production, (2) increased growth rates, and (3) changes in species composition to faster-growing species.

2.2 Materials and Methods

2.2.1 Sampling

Bioassays were conducted in the Iceland and Irminger Basins during the summer of 2010 (Figure **??**) onboard the *RRS Discovery* (D354), which departed from Avonmouth, UK on the 4th of July, 2010 and docked in Birkenhead, UK on the 11th of August 2010. Bioassay sampling occurred at night – usually between 02h00-03h00 (local time) to avoid light shock of the phytoplankton communities. Seawater for the bioassays was collected using a trace

metal clean "Achterberg" tow fish (towed body) from a depth of >4 m. The towed fish was only used when the ship was steaming at a minimum of 5 knots, either towards a fixed position or along a track around a fixed position, in order to avoid contamination from the ship. Seawater from the towed fish was pumped directly into a trace metal clean chemistry container located on the aft deck using a Teflon pump system through acid-washed PVC tubing. Seawater was collected directly into randomly ordered, acid-washed 4.5L polycarbonate (NalgeneTM) bottles. The locations of the sampling for the bioassays are shown in Figure **??**.

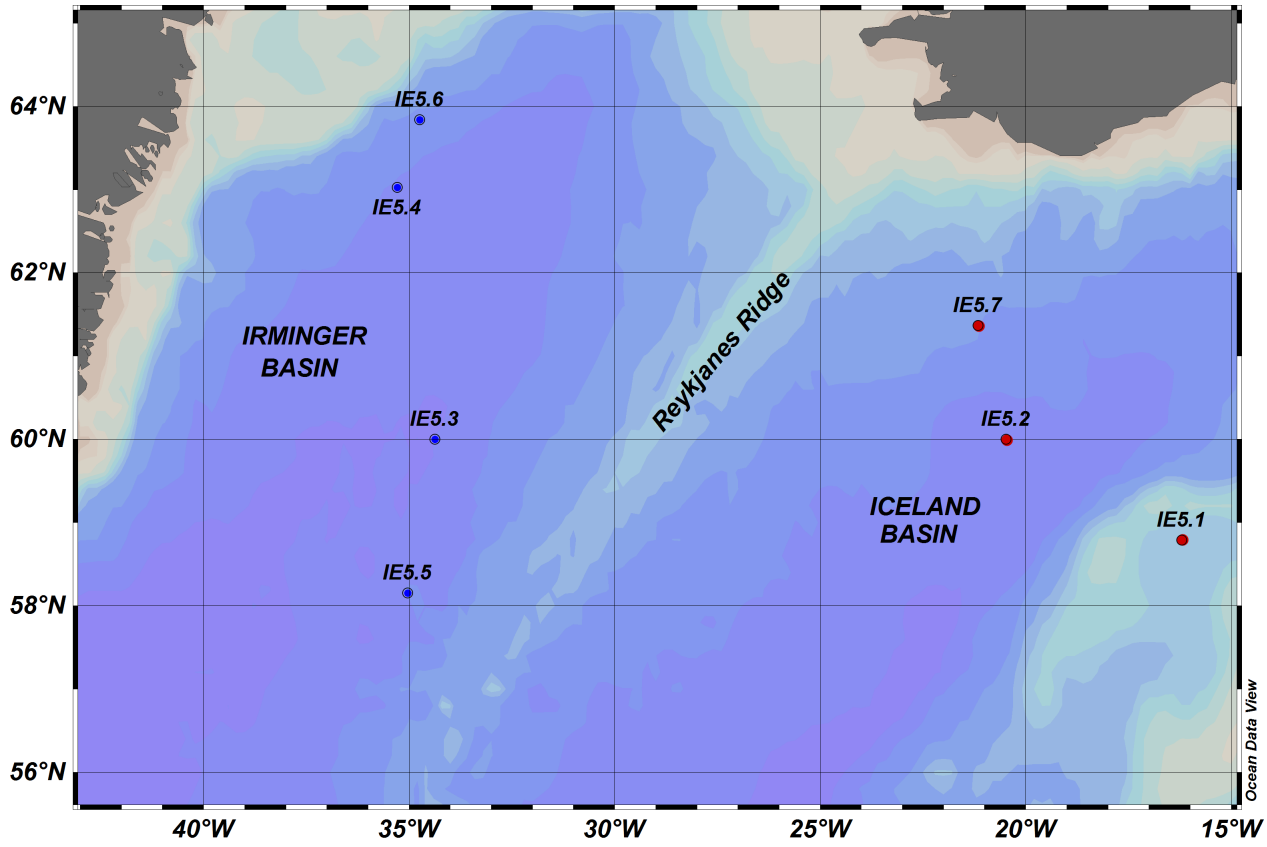

Figure 2.1: Map of the Iceland (IE5.1, 2 and 7, indicated by red dots) and Irminger (IE5.3, 4, 5 and 6, indicated by blue dots) Basins in the North Atlantic showing the locations of each of the bioassay sampling sites. The eastern Iceland Basin is separated from the western Irminger Basin by the Reykjanes Ridge (**?**).

2.2.2 Bioassays

Seven nutrient addition bioassays were performed in order to determine the effect of macro- and micronutrient (+Fe, +N and +FeN) addition on phytoplankton physiology, growth and nutrient drawdown over different timescales (**?**). The experimental design allowed bioassays to be sampled at various time points (T48, T72 and T120) through the

use of sacrificial incubation bottles with identical treatments and parallel incubations to avoid contamination.

Bioassays were conducted in 2.1L and 4.5L polycarbonate bottles, which had been thoroughly trace-metal cleaned by soaking in 50% HCl for one week, followed by rinsing and storage with acidified MilliQ water prior to the cruise. All experimental work setting up the bioassays and sub-sampling were performed within a dedicated Class-100 air-filtered trace metal-clean container.

Initial samples (T0) were taken directly from the underway system during filling of the bioassay bottles. One T0 sample was collected at the start of the bottle filling, one when half the incubation bottles were filled and one when all the bottles had been filled. This sampling protocol allowed the determination of the degree to which initial conditions varied during bioassay set-up. The time between the primary initial sampling and the final initial sampling was 30-40 minutes, which is equivalent to the distance travelled of ~2.5 nm (or 4.6 km). Once the incubation bottles had been filled and treated with macronutrient and/or trace metal addition (or no addition), they were sealed using parafilm, double bagged and then incubated on deck at sea surface temperature. Running seawater was used to maintain incubation temperatures and 'Blue lagoon' light filters (LEE filters) were used to recreate light levels corresponding to ~35-40% of surface irradiance. Experimental light levels were slightly higher than in situ average mixed layer irradiance which ranged between 20-40% (**?**).

The bioassay treatments were either conducted using eighteen 4.5L bottles, with four sets of replicates, or sixteen 4.5L bottles, with two sets of replicates (see Table **??**). For the eighteen bottle experiments the treatments were: control (6 replicate bottles); 2 nM dFe addition (6 replicates); 2μM nitrate addition (3 replicates); 2 nM dFe and 2μM nitrate additions (3 replicates). For the sixteen bottle experiments the treatments were: control (8 replicate bottles) and 2 nM dFe addition (8 replicates). The eighteen 4.5L bottle bioassays were sampled at 48-hours (T48) and/or 72-hours (T72), while the sixteen 4.5L bottle bioassays were sampled at 72-hours (T72) and 120-hours (T120) (see Table **??**). For measurements of PP and CP a separate set of 1.2L polycarbonate bottles was used, with these bottles treated identically to the larger 4.5L bottles (see Section **??**).

2.2.3 Determination of Phytoplankton Community Composition: Enumeration and Identification

Phytoplankton community composition and abundance were examined using scanning electron microscopy (SEM) of filtered bioassay seawater samples. Between 250 and 500mL of seawater from the bioassays was gently vacuum-filtered onto 25 mm Whatman 0.8μm pore-size polycarbonate filters. These were then rinsed with trace ammonia solution (pH 9-10) in order to prevent salt crystals forming, which would interfere with producing clear SEM images. Filters were placed into Millipore Petri slides and dried overnight at 30ºC before being stored at room

temperature for later analysis.

Back in the laboratory ashore (University of Cape Town), a small portion (~0.5×0.5 cm) of the filters was mounted onto a 12 mm aluminium pin stub with carbon glue and sputter coated with 20 nm of gold. SEM images were obtained using a LEO1450 microscope, operated with a tungsten filament at 10kV and a spot size of 500pA. A secondary detector was used and the images were taken at 1200 × magnification. For cell counts, a 16 × 15 frame grid of individual fields of view was imaged and archived according to a tailored macro. This ensured SEM images were recorded in the same pattern for all of samples.

Each coccolithophore or diatom cell in the ~240 fields of view (FOV) per filter was identified and counted, a total of 10,320 SEM images were counted.. FOVs that were blurred or obscured were discounted from the final 'cells mL^{-1}' calculations. Species identification followed **?** for coccolithophores and **?** and **?** for diatoms.

Cells were identified down to species level where possible. However, due to some poorer quality images, this was not always possible. For example, individual *Syracosphaera* coccolithophore species were grouped together in the final abundance calculations, as well as the diatoms *Chaetoceros, Nitzschia and Pseudonitzschia*.

Cell abundances (cells mL^{-1} of seawater) were calculated as:

$$\text{Cell Abundance} = \frac{(\text{CxR})}{\text{V}} \tag{2.1}$$

where C is the number of cells counted, R is a ratio of the total filtration area to the counted area (as detailed in equation **??**, below) and V is the volume of water filtered (mL).

$$\text{R} = \frac{\text{A}}{\text{A}_{\text{FOV}} \times \text{N}_{\text{FOV}}} \tag{2.2}$$

A is the filtration area (mm^2), A_{FOV} is the area of one FOV and N_{FOV} is the total number of FOVs counted.

Standard errors (S.E.) for SEM count data per bioassay treatment (in cases where only one SEM was counted per treatment) were estimated following **?**, assuming a normal distribution, by taking the square root of the counted cells (C) divided by the equivalent volume of the sample investigated ($\text{A} \times (\frac{\text{V}}{\text{F}})$) (see **?**);

$$\text{S.E.} = \sqrt{\left(\frac{\text{C}}{\text{A} \times \left(\frac{\text{V}}{\text{F}}\right)}\right)}$$

where A is the area investigated (mm^2), F is the total filter area investigated (mm^2) (which is determined by the

area of the FOV multiplied by the number of FOVs counted) and V is the volume filtered (mL).

For the determination of the abundance of pico- and nanoplankton, flow cytometry counts of seawater samples from the bioassays was also performed. Seawater samples (1.8mL) were fixed in 1% paraformaldahyde and incubated at 4ºC for 24-hours before being flash frozen in liquid nitrogen and stored at -80ºC . Phytoplankton enumeration was performed using a Becton Dickinson FacsortTM flow cytometer (Becton Dickinson Biosciences, Oxford, UK) on slowly thawed samples, with a reference bead stock added to all samples at a known concentration using syringe pumped flow cytometry (**?**).

2.2.4 Ancillary Measurements

Seawater samples were also taken from the bioassays for analysis of the concentration of macronutrients, total chlorophyll *a* and size-fractionated chlorophyll *a* (see Table**??**).

Table 2.1: Treatments applied to bioassays at each sampling station, number of repetitions/bottles for each treatment and the sampling and sub-sampling procedure for the individual bioassays, indicating at which time points (hours) samples were taken for measurements of nutrients, chlorophyll *a*, Scanning Electron Microscopy (SEM), Primary Production (PP), Calcite Production (CP) and Flow Cytometry. *one bottle missing.

Location	Bioassay	Treatment (no. of bottles)	Nutrients	Chlorophyll	SEM	PP	CP	Flow Cytometry
Iceland	IE5.1	Control (3), +Fe (3), +FeN (3), +N (3)	T0, T48	T0, T48	T0, T48	T0, T24	T0, T24	nd
Iceland	IE5.2	Control (6), +Fe (6), +FeN (3), +N (3)	T0, T24, T48	T0, T24, T48	T0, T48	nd	nd	T0, T24, T48
Irminger	IE5.3	Control (8), +Fe (8)	T0, T24, T72, T120	T0, T24, T72, T120	T0, T120	nd	nd	T0, T24, T72, T120
Irminger	IE5.4	Control (8), +Fe (8)	T0, T24, T72, T120	T0, T24, T72, T120	T0, T120	T0, T24	T0, T24	T0, T24, T72, T120
Irminger	IE5.5	Control (5*), +Fe (6), +FeN (3), +N (3)	T0, T24, T72	T0, T24, T72	T0, T72	nd	nd	T0, T24, T72
Irminger	IE5.6	Control (8), +Fe (8)	T0, T24, T72, T120	T0, T24, T72, T120	T0, T120	T0, T24	T0, T24	T0, T24, T72, T120
Iceland	IE5.7	Control (6), +Fe (6), +FeN (3), +N (3)	T0, T24, T48T72	T0, T24, T48T72	T0, T72	nd	nd	T0, T24, T48T72

Seawater samples (40mL) for macronutrient analysis were drawn into diluvials and stored at 4ºC until analysis (~12-hours). Macronutrient concentrations (nitrate+nitrite (NO_x) and dissolved silicic acid) were determined using a Skalar San Plus autoanalyser following the methods of **?**. The detection limits for the macronutrient measurements were $\pm 0.1\,\mu$M for NO_x and $\pm 0.1\,\mu$M for silicic acid. The changes in NO_x and silicic acid concentrations ($\triangle NO_x$ and $\triangle SiO_4$) were calculated by subtracting the initial nutrient measurement from the final nutrient measurement in order to determine nutrient drawdown.

Seawater samples (250mL) for total chlorophyll *a* determination were filtered onto 25 mm Whatman GFF filters (approximately $0.7\,\mu$m pore-size) and chlorophyll *a* were extracted in 10mL of 90% acetone (HPLC grade) at 4ºC for 18 to 24-hours in the dark. For the $> 5\,\mu$m fraction water samples (250mL) were filtered onto 25 mm diameter $5\,\mu$m pore-size polycarbonate membrane (MilliporeTM) filters and then treated as with total chlorophyll

a measurements. Measurements of chlorophyll *a* were quantified using a Turner Designs TD-700 Fluorometer equipped with **?** filters and calibrated using a pure chlorophyll *a* standard. The chlorophyll *a* contribution of the $< 5\,\mu$m fraction was determined by subtracting the $> 5\,\mu$m chlorophyll *a* fraction from the total (GFF).

2.2.5 Primary Production and Calcite Production

Daily rates (dawn-to-dawn, 24-hour) of PP and CP were measured in three bioassays (IE5.1, IE5.4 and IE5.6), with parallel on-deck incubations of the 4.5L bottles in 1.2L polycarbonate bottles spiked with $100\,\mu$Ci of ^{14}C-labelled sodium bicarbonate at the end time of sampling of the total bioassay (i.e. T72 or T120).

Incubations were run for a further 24-hours (dawn to dawn) and then each 1.2L bottle was divided into six 200mL replicates, three of which were used to measure PP and CP using the micro-diffusion technique (Figure **??**) and three of which were used to determine the $> 5\,\mu$m PP (data not shown here).

Daily rates (dawn to dawn) of PP and CP were determined following **?** and **?** from on deck post-incubation by filtering water samples through 25 mm $0.2\,\mu$m polycarbonate filters, using fresh, filtered seawater to rinse off any residual ^{14}C-sodium bicarbonate not incorporated during the incubation.

Filters were then placed into the bottom of glass vials and sealed with a gas-tight septum and small bucket containing a Whatman GFA filter soaked in phenylethylamine (PEA) (Figure **??**). The glass vials then had phosphoric acid (1mL, 1%) injected through the septum into the bottom of the vial to convert ^{14}C-particulate inorganic carbon (calcite) into ^{14}C-CO_2. This effectively allows one to differentiate organic carbon production by photosynthesis from CP, which represents calcification. The GFA filters were removed after approximately 24-hours and placed in a new glass vial, with 10-15mL liquid scintillation cocktail (Optima Gold, Perking Elmer) added to both. One vial contained the polycarbonate filter (non-acid labile; i.e. PP) and the other contained the GFA filter (acid-labile; i.e. CP). Finally, a Beckman liquid scintillation counter was used to determine isotope activity on both of the filters and disintegrations per minute (DPM) counts were converted into uptake rates using standard methods (e.g. **??**).

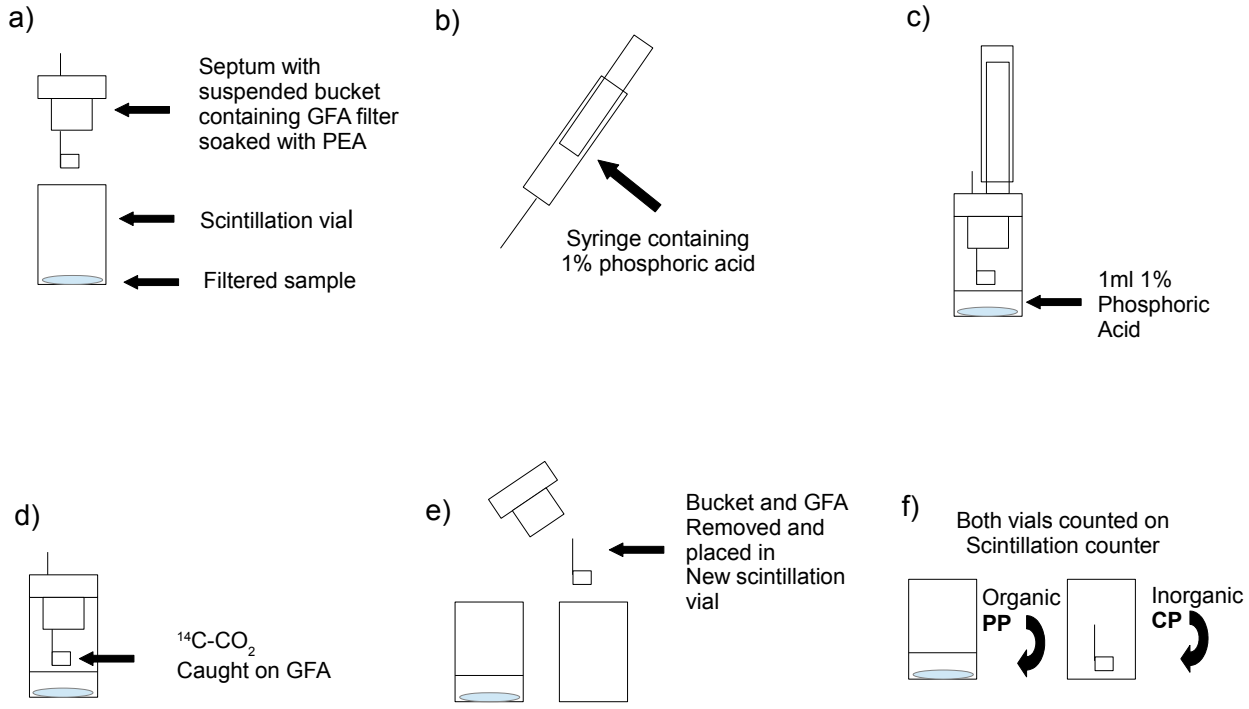

Figure 2.2: Diagram illustrating the micro-diffusion technique (MDT), adapted from **?** and **?**.

2.2.6 Data Analysis

The statistical analysis of environmental variables and of PP and CP was performed using R (**?**). One-way ANOVA tests were used to determine if there were significant differences between treatment responses in each bioassay experiment. Significant results obtained from ANOVA tests were further investigated using a *post hoc*, Tukey HSD (Honestly Significantly Different) test ($p < 0.05$) to determine which specific treatments were significantly different.

Multivariate statistical analysis of phytoplankton counts (cells mL^{-1}) was conducted using the multivariate programme E-PRIMER (Plymouth Routines In Multivariate Ecological Research, version 6.16) (**?**). Coccolithophore and diatom abundance data were treated similarly, with the exception of coccolithophore abundance data being transformed using a square root transformation, while diatom abundance data were transformed using a fourth root transformation. This was due to the differences in overall abundance; coccolithophore abundance ranged between 0 and a few hundred cells mL^{-1}, whereas maximum diatom abundances were on average much higher (a

few thousand cells mL^{-1}). Between-station statistical differences in species composition were calculated using all species present, irrespective of their contribution to total abundance, as rare species can also respond to iron and/or macronutrient additions.

A Bray-Curtis similarity matrix was calculated before applying hierarchical cluster analysis and ordination via non-metric Multi-Dimensional Scaling (nMDS) to determine (dis-)similarities in species composition between treatments. Factors were created for 'treatment', 'bioassay', 'length' and 'basin' to better explore regional patterns in the coccolithophore and diatom community composition. Labelling of nMDS ordinations and cluster diagrams using these factors allowed for better visual representation of how they might influence coccolithophore and diatom community structure.

Analysis of similarity (ANOSIM) tests were used to examine whether these pre-determined factors created statistically significant groups (**?**). Similarity percentages (SIMPER) tests were used to identify which species are primarily providing the basis for discrimination between the observed sample clusters, using the rectangular data matrix with the added 'factors' (**?**). SIMPER generates a list of species that differentiate the different groups.

Diversity indices were also calculated using the initial abundance data in order to look at differences between treatments, bioassays and basins. The number of species (S) and Pielou's evenness (J') index were determined for both coccolithophore and diatom abundance data. Pielou's evenness is an indication of how evenly cell abundance is distributed among the different species present, without accounting for species richness. Pielou's evenness ranges between 0 and 1, with low values indicative that the population is not evenly distributed among the different species, with one or a few species dominating.

2.3 Results

2.3.1 General Oceanography

Three bioassays (IE5.1, IE5.2 and IE5.7) were performed in the Iceland Basin, whereas four bioassays (IE5.3, IE5.4, IE5.5 and IE5.6) were performed in the Irminger Basin (Figure **??**).

Initial mean ($\pm$S.E) total chlorophyll *a* concentrations (total phytoplankton biomass) varied among the seven bioassays (Figure **??**), ranging from a low of $0.70 \pm 0.58\,\mu gL^{-1}$ in IE5.1 in the Iceland Basin to a maximum of $2.32 \pm 0.20\,\mu gL^{-1}$ in IE5.3 in the Irminger Basin, with the rest of the bioassays averaging $1.41 \pm 0.31\,\mu gL^{-1}$. The mean ($\pm$S.E) $> 5\mu$m chlorophyll *a* concentrations ranged from a minimum of $0.31 \pm 0.01\,\mu gL^{-1}$ in IE5.7 in the Iceland Basin to a maximum of $1.33 \pm 0.19\,\mu gL^{-1}$ in IE5.3 in the Irminger Basin. Expressed as a percentage of

total chlorophyll *a*, the contribution of the $> 5\,\mu$m size-fraction to total chlorophyll *a* concentrations ranged from 27% to 67% (IE5.6 and IE5.1, respectively), with bioassays IE5.1, IE5.3 and IE5.5 having >50% of their total chlorophyll *a* concentrations comprised of $> 5\,\mu$m chlorophyll *a* initially. On average, the $> 5\,\mu$m chlorophyll *a* represented below half (44%) of chlorophyll *a* in the initial samples, indicating a large proportion of the total phytoplankton biomass was derived from small-celled phytoplankton such as picoeukaryotes and *Synechococcus*. Generally, initial total chlorophyll *a* concentrations were on average significantly lower ($t(19) = -2.63$, $p < 0.05$) in the Iceland Basin ($1.11 \pm 0.47\,\mu\text{gL}^{-1}$) than in the Irminger Basin ($1.69 \pm 0.48\,\mu\text{gL}^{-1}$).

In terms of initial mean ($\pm$S.E) macronutrient concentrations there was a clear split between the Iceland and Irminger basins for both NO_x and silicic acid. Initial NO_x concentrations ranged from a maximum of $5.24 \pm 0.35\,\mu$M in bioassay IE5.6 in the Iceland Basin to a minimum of $0.29 \pm 0.24\,\mu$M in bioassay IE5.2 in the Irminger Basin. Overall, initial NO_x concentrations were relatively high ($> 3.5\,\mu$M) in the Irminger Basin (see Figures **??**, **??**, **??** and **??**) and low ($< 1.0\,\mu$M) in the Iceland Basin.

Initial silicic acid concentrations were variable between the different bioassays, although as with NO_x, there was a clear distinction between the two basins. Concentrations ranged from $0.42 \pm 0.03\,\mu$M (IE5.7, Iceland Basin) to $2.00 \pm 0.02\,\mu$M (IE5.5, Irminger Basin), with the Iceland Basin bioassays having initial concentrations of $< 1\,\mu$M, whereas, Irminger Basin bioassays were generally $> 1\,\mu$M (although, there were a few exceptions; for example, bioassay IE5.6 had a low initial silicic acid concentration ($0.44 \pm 0.07\,\mu$M) relative to the other of the Irminger Basin bioassays, which had $1.84 \pm 0.11 - 2.00 \pm 0.02\,\mu$M of silicic acid present initially).

Table 2.2: Locations and initial conditions of Iceland Basin (IE5.1, IE5.2, and IE5.7) and Irminger (IE5.3, IE5.4, IE5.5, and IE5.6) bioassays. Initial mean ($\pm$S.E) total and size-fractionated chlorophyll and macronutrient (nitrate+nitrite (NO_x) and silicic acid (SiO_4)) concentrations and initial phytoplankton (coccolithophore, diatom, picoeukaryotes and *Synechococcus*) abundance. Picoeukaryote and *Synnechococcus* abundance was not determined (nd) in bioassay IE5.1.

Bioassay	**Lat** (ºN)	**Lon** (ºE)	**Total Chl a** (μgL^{-1})	**$< 5\,\mu$mChl a** (μgL^{-1})	**NOx** (μM)	**SiO_4** (μM)	**Coccolithophores** (cells mL^{-1})	**Diatoms** (cells mL^{-1})	**Picoeukaryotes** (cells mL^{-1})	***Synechococcus*** (cells mL^{-1})
IE5.1	8.790	-16.201	0.70 ± 0.34	0.47 ± 0.07	0.71 ± 0.27	0.69 ± 0.07	50.12 ± 5.09	564.37 ± 17.08	nd	nd
IE5.2	60.000	-20.475	1.63 ± 0.21	0.65 ± 0.04	0.29 ± 0.14	0.84 ± 0.06	6.05 ± 3.50	289.54 ± 26.50	$17.89 \times 10^3 \pm 2.85 \times 10^3$	$136.23 \times 10^3 \pm 5.22 \times 10^3$
IE5.3	60.002	-34.377	2.32 ± 0.12	1.33 ± 0.19	3.78 ± 0.17	1.84 ± 0.06	560.87 ± 27.49	622.81 ± 18.62	$110.93 \times 10^3 \pm 122.19 \times 10^3$	$46.42 \times 10^3 \pm 9.18 \times 10^3$
IE5.4	63.027	-35.289	1.18 ± 0.01	0.41 ± 0.05	4.64 ± 0.17	1.96 ± 0.01	372.41 ± 13.99	1512.58 ± 28.20	$7.58 \times 10^3 \pm 3.91 \times 10^3$	$20.80 \times 10^3 \pm 12.52 \times 10^3$
IE5.5	58.155	-35.032	1.75 ± 0.04	0.91 ± 0.09	4.27 ± 0.03	2.00 ± 0.01	57.26 ± 10.91	976.83 ± 23.05	$9.08 \times 10^3 \pm 0.70 \times 10^3$	$22.42 \times 10^3 \pm 2.67 \times 10^3$
IE5.6	63.840	-34.738	1.50 ± 0.00	0.40 ± 0.02	5.24 ± 0.20	0.44 ± 0.02	4.30 ± 1.69	611.63 ± 18.40	$11.53 \times 10^3 \pm 1.96 \times 10^3$	$18.15 \times 10^3 \pm 3.52 \times 10^3$
IE5.7	61.368	-21.158	0.99 ± 0.03	0.31 ± 0.01	0.62 ± 0.36	0.42 ± 0.02	1.29 ± 0.50	86.49 ± 42.00	$7.62 \times 10^3 \pm 1.23 \times 10^3$	$95.15 \times 10^3 \pm 10.23 \times 10^3$

Due to the obvious geographical separation of bioassays, based on initial conditions (total chlorophyll *a* and macronutrients), the bioassays were grouped by sampling location in the following sections.

2.3.2 Iceland Basin Bioassays

The bioassays from the Iceland Basin consisted of two short-term experiments (IE5.1 and IE5.2), which lasted 48-hours, and one mid-length experiment lasting 72-hours (IE5.7). An analysis of variance (ANOVA) ($p < 0.05$) indicated that in all three Iceland Basin bioassays, total and size-fractionated chlorophyll *a* concentrations as well as NO_x drawdown showed significant variation among the treatments, whereas there was no significant change in silicic acid drawdown (see full list of ANOVA and Tukey HSD results in Appendix **??**).

Post hoc, Tukey HSD tests revealed that the total mean ($\pm$S.E) chlorophyll *a* concentrations increased significantly in response to +FeN additions relative to the control in all three (IE5.1, IE5.2 and IE5.7) bioassays ($p = 0.00$) (Figures **??**, **??** and **??**). Additionally, there were significant differences between the +N treatment and the control in IE5.2 ($p = 0.03$). However, there was no evidence that total chlorophyll *a* concentrations in the +Fe treatments were significantly different from the control in IE5.1 and IE5.2 ($p = 0.53$ and $p = 0.85$, respectively). In the 72-hour bioassay total chlorophyll *a* concentrations increased significantly in the +Fe treatment relative to the control ($p = 0.00$). In contrast, $> 5\mu$m chlorophyll *a* concentrations did not respond to treatments, with no change in concentrations relative to the control in IE5.1 (Figure **??**). Whereas, in IE5.2 the $> 5\mu$m chlorophyll *a* size-fraction exhibited increased concentrations relative to the control in both the +FeN and +N treatments ($p = 0.00$ and $p = 0.04$, respectively) (Figure **??**), $> 5\mu$m chlorophyll *a* concentrations followed a similar pattern of response to that of the total chlorophyll *a* (Figure **??**).

Changes in macronutrient concentrations between initial and end points were calculated in terms of nutrient drawdown ($\triangle NO_x$ and $\triangle SiO_4$). NO_x utilization was significantly increased in +FeN and +N treatments relative to the control ($p = 0.00$), with no evidence of change observed in the +Fe treatments ($p = 1.00$, 1.00 and 0.87, respectively) (Figures **??**, **??** and **??**).

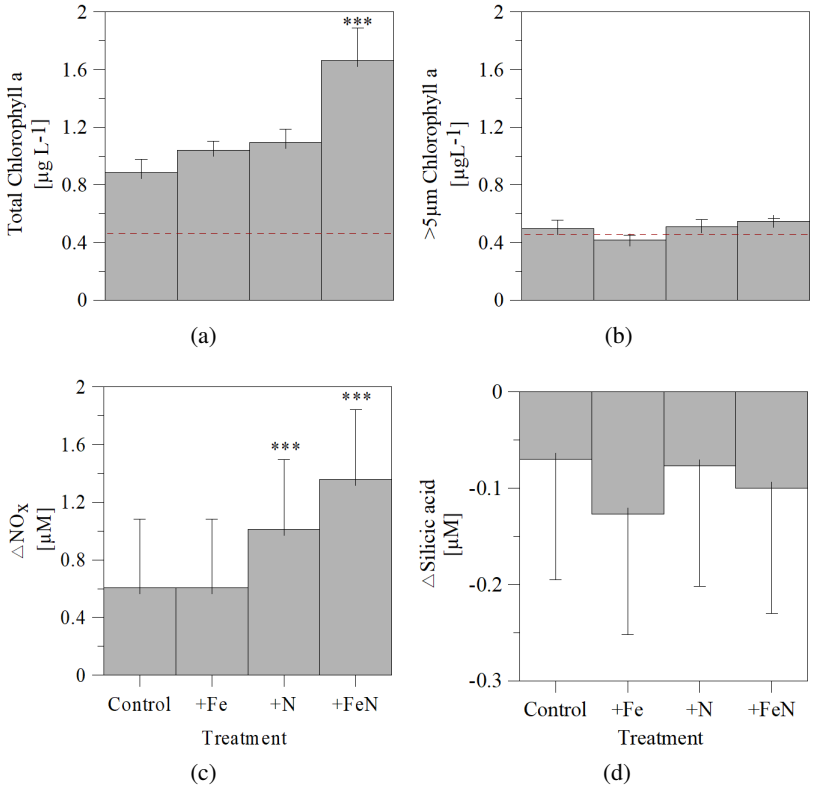

Figure 2.3: Bar graphs for bioassay IE5.1 showing the a) mean total chlorophyll *a* concentrations (μgL^{-1}, b) mean >5μm size-fractionated chlorophyll *a* concentrations (μgL^{-1}), c) mean change in nitrate+nitrite (NO_x) concentrations (μM), and the d) mean change in silicic acid (SiO_4) concentrations (μM) over the course of the 48-hour bioassay. Error bars indicate standard errors. Dashed red lines indicate initial conditions. Asterisks indicate only significant results from Tukey HSD test for multiple pair-wise comparisons of significant ANOVA results between the control and treatments: * $p < 0.05$, ** $p < 0.01$, *** $p < 0.005$. n=3 for all bioassays.

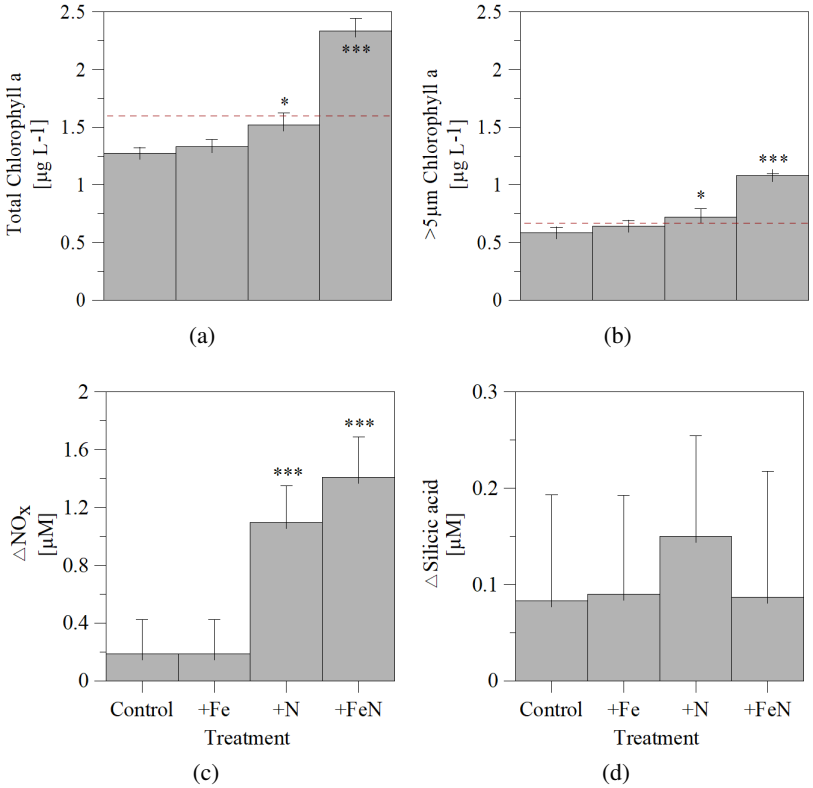

Figure 2.4: Bar graphs for bioassay IE5.2 showing the a) mean total chlorophyll *a* concentrations (μgL^{-1}, b) mean >5μm size-fractionated chlorophyll *a* concentrations (μgL^{-1}), c) mean change in nitrate+nitrite (NO_x) concentrations (μM), and the d) mean change in silicic acid (SiO_4) concentrations (μM) over the course of the 48-hour bioassay. Error bars indicate standard errors. Dashed red lines indicate initial conditions. Asterisks indicate only significant results from Tukey HSD test for multiple pair-wise comparisons of significant ANOVA results between the control and treatments: * $p < 0.05$, ** $p < 0.01$, *** $p < 0.005$. n=3 for all bioassays.

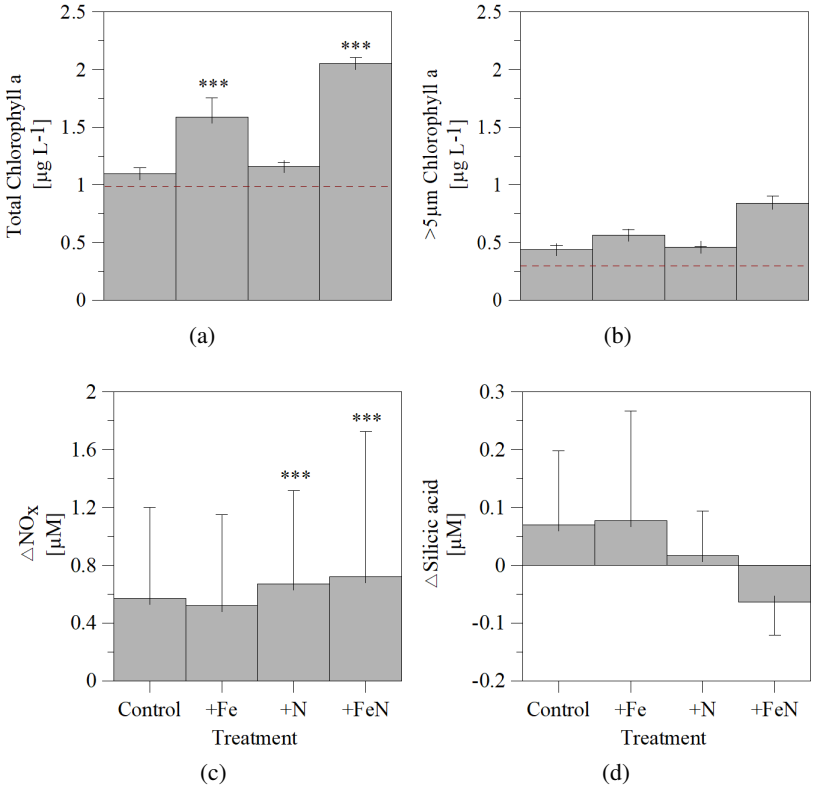

Figure 2.5: Bar graphs for bioassay IE5.7 showing the a) mean total chlorophyll *a* concentrations (μgL^{-1}, b) mean >5μm size-fractionated chlorophyll *a* concentrations (μgL^{-1}), c) mean change in nitrate+nitrite (NO_x) concentrations (μM), and the d) mean change in silicic acid (SiO_4) concentrations (μM) over the course of the 72-hour bioassay. Error bars indicate standard errors. Dashed red lines indicate initial conditions. Asterisks indicate only significant results from Tukey HSD test for multiple pair-wise comparisons of significant ANOVA results between the control and treatments: * $p < 0.05$, ** $p < 0.01$, *** $p < 0.005$. n=3 for all bioassays.

The initial phytoplankton community in the Iceland Basin was composed of low abundances of coccolithophores ($< 50\,\text{cells}\,\text{mL}^{-1}$), relatively high diatom abundances ($>250\,\text{cells}\,\text{mL}^{-1}$) (Figures **??** and **??**), with the exception of initial diatom abundances in IE5.7, see Figure **??**) and high abundances of picoeukaryotes ($>7 \times 10^3\,cells\,mL^{-1}$) and *Synechococcus* ($>95 \times 10^3\,\text{cells}\,\text{mL}^{-1}$). In bioassay IE5.1 there was a decrease in cell abundance across all treatments, with very little difference between treatments (Figure **??**). In contrast, in bioassays IE5.2 and IE5.7, coccolithophore abundance increased, with the highest abundance recorded in the +FeN and +N treatments ($47.1\,\text{cells}\,\text{mL}^{-1}$ and $47.2\,\text{cells}\,\text{mL}^{-1}$, respectively) in IE5.2 and in the +Fe treatment ($82.0\,\text{cells}\,\text{mL}^{-1}$) in IE5.7 (Figures **??** and **??**).

In IE5.1, initial mean ($\pm$S.E.) diatom abundance was relatively high ($564.4 \pm 17.1\,\text{cells}\,\text{mL}^{-1}$) and decreased over the course of the bioassay in all treatments (Figure **??**). In IE5.2, although both total coccolithophore and diatom abundances increased, there were no visible differences between final abundances in the different treatments. In contrast, in IE5.7, there was a much greater increase in both coccolithophore ($81.2 \pm 6.7\,\text{cells}\,\text{mL}^{-1}$)

and diatom ($3685.3 \pm 42.6\,\text{cells}\,\text{mL}^{-1}$) abundances in the +Fe treatment when compared with the control, +N and +FeN treatments (Figure **??**).

The small-size fraction of phytoplankton (*Synechococcus* and picoeukaryotes) represented a much larger percentage of the community numerically. Initial *Synechococcus* mean (±S.E.) abundance was lowest in IE5.7 ($95.2 \times 10^3 \pm 10.2 \times 10^3$ $\text{cells}\,\text{mL}^{-1}$) (Figure **??**) and highest in IE5.2 ($136.2 \times 10^3 \pm 5.2 \times 10^3$ $\text{cells}\,\text{mL}^{-1}$) (Figure **??**), reaching a maximum of $285.4 \times 10^3 \pm 31.4 \times 10^3$ $\text{cells}\,\text{mL}^{-1}$ in the +FeN treatment of IE5.2.

An analysis of variance (ANOVA) ($p < 0.05$) indicated that in IE5.2 and IE5.7, picoeukaryote abundance showed significant variation among the treatments ($F(3,8) = 63,42$ and 5.2, $p < 0.05$, respectively) and that *Synechococcus* abundance showed significant variation in IE5.2 ($F(3,8) = 5.93$, $p < 0.05$), but that there was no change in IE5.7 among treatment conditions ($F(3,8) = 0.98$, $p > 0.05$) (see full list of ANOVA and Tukey HSD results in Appendix **??**).

In IE5.2 and IE5.7, Tukey HSD tests showed that there was no difference between picoeukaryote abundance in the control and +Fe treatments ($p = 0.30$ and 0.89, respectively). In contrast, picoeukaryote abundance in IE5.2 showed significant increases in the +FeN and +N treatments relative to the control ($p = 0.00$) and in IE5.7 there was weak evidence of a significant decrease in abundance in the +FeN treatment relative to the control ($p = 0.04$) only. *Synechococcus* abundance in IE5.2 was significantly different between the +Fe and +FeN treatments ($p = 0.02$). Initial mean (±S.E) picoeukaryote abundances were lowest in IE5.7 ($7.6\text{x}10^3$ $\text{cells}\,\text{mL}^{-1}$) (Figure **??**) and highest in IE5.2 ($17.9 \times 10^3 \pm 2.8 \times 10^3$ $\text{cells}\,\text{mL}^{-1}$), reaching a maximum of $43.2 \times 10^3 \pm 1.6 \times 10^3$ $\text{cells}\,\text{mL}^{-1}$ in the control treatment of IE5.2 (Figure **??**). In IE5.2, picoeukaryote abundance increased in all treatments apart from the +N treatment, with cell abundances nearly doubling in both the control and +Fe treatments. There was a more modest increase in picoeukaryote abundance in the +FeN treatment compared with the +Fe treatment. *Synechococcus* abundance increased across all treatments in IE5.2, with the smallest increase in the +Fe treatment (Figure **??**). In IE5.7, total *Synechococcus* abundance decreased across all treatments and there were no differences in abundance between the treatments. Picoeukaryote abundance decreased slightly in the control, +Fe and +N treatments relative to initial abundance. In IE5.7 there was a comparatively large increase in abundance in the +FeN treatment (from $7.6 \times 10^3 \pm 1.2 \times 10^3$ to $11.6 \times 10^3 \pm 3.7 \times 10^3$ $\text{cells}\,\text{mL}^{-1}$) .

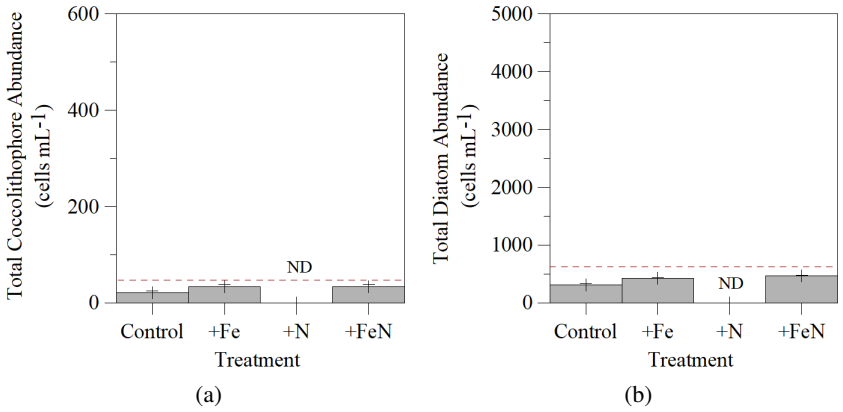

Figure 2.6: Bar graphs for bioassay IE5.1 showing a) total coccolithophore abundances (cells mL^{-1}) and b) total diatom abundance (cells mL^{-1}). Error bars indicate standard errors. Dashed red lines indicate initial conditions.

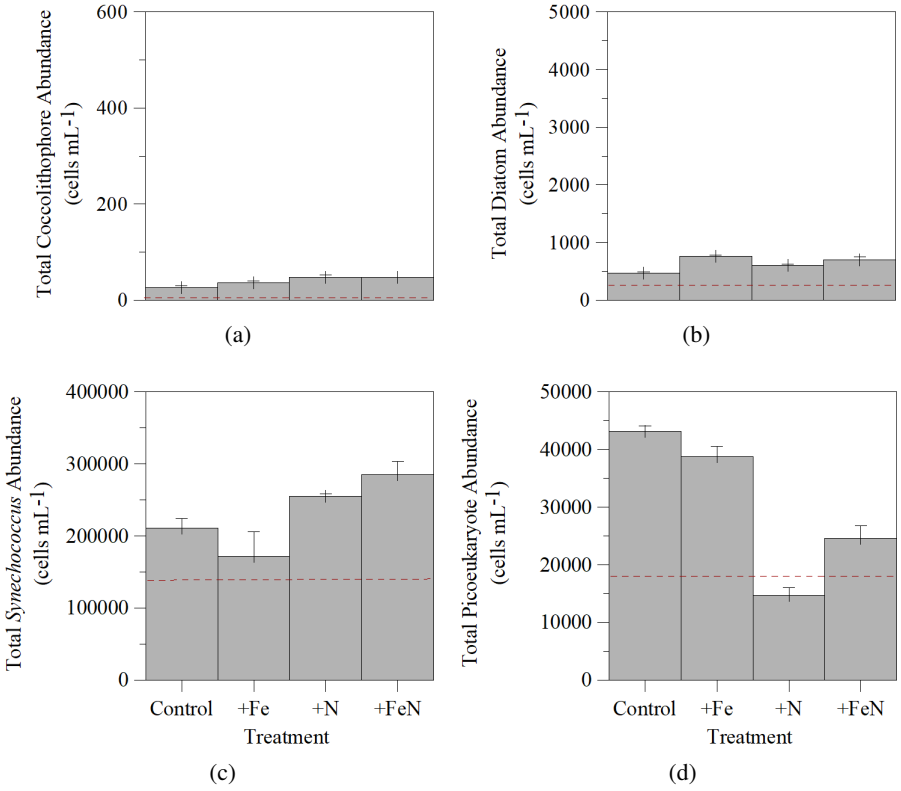

Figure 2.7: Bar graphs for bioassay IE5.2 showing a) total coccolithophore abundances (cells mL^{-1}) b) total diatom abundance (cells mL^{-1}), c) total *Synechococcus* abundance (cells mL^{-1}) and d) total picoeukaryote abundance (cells mL^{-1}). Error bars indicate standard errors. Dashed red lines indicate initial conditions.

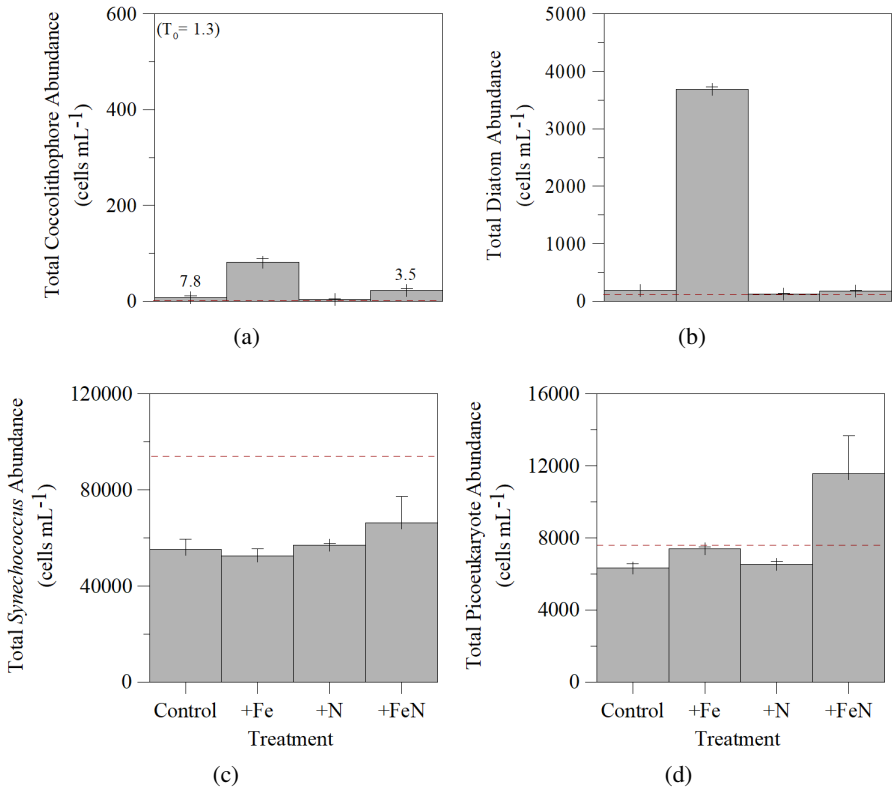

Figure 2.8: Bar graphs for bioassay IE5.7 showing a) total coccolithophore abundances (cells mL^{-1}) b) total diatom abundance (cells mL^{-1}), c) total *Synechococcus* abundance (cells mL^{-1}) and d) total picoeukaryote abundance (cells mL^{-1}). Dashed red lines indicate initial conditions.

2.3.3 Irminger Basin Bioassays

Irminger Basin bioassays were incubated for longer time periods than those in the Iceland Basin (72-hour (IE5.5) to 120-hour (IE5.3, IE5.4, IE5.6; Figures **??**, **??**, **??** and **??**), this was based on initial responses of the Iceland Basin bioassays. These longer term bioassays showed marked differences compared with the shorter ones from the Iceland Basin, with statistically significant ($p < 0.05$) responses to +Fe addition across all of the measured variables (total and $> 5\mu$m chlorophyll *a* concentrations, NO_x, and silicic acid drawdown) in all four of the Irminger Basin bioassays.

For example, in the 72-hour bioassay (IE5.5) significant responses to +Fe addition were shown for both total chlorophyll *a* and $> 5\mu$m chlorophyll *a* as well as in both NO_x and silicic acid drawdown ($p = 0.00$, $p < 0.05$) (Figure **??**). There was a more varied response to both +N and to +FeN in the Irminger Basin however, where NO_x drawdown responded to both treatments, whereas there were contrary responses in silicic acid drawdown, total chlorophyll *a* and $> 5\mu$m chlorophyll *a* concentrations. In contrast, there was no significant response to +N for either silicic acid or total chlorophyll *a* ($p = 0.94$ and $p = 1.00$, $p < 0.05$, respectively), although there

was a significant increase in the $> 5\,\mu$m chlorophyll *a* concentration in the +N treatment (p = 0.00, p < 0.05). This is in contrast with the response to +FeN addition, where NO_x, silicic acid drawdown and total chlorophyll *a* concentrations all showed significant responses (p = 0.00, p < 0.05), while the $> 5\,\mu$m chlorophyll *a* size-fraction showed no response to +FeN addition (p = 1.00, p < 0.05).

There was a clear, significant response to +Fe addition, in nearly all parameters measured (with the exception of silicic acid concentrations in IE5.3 (see figure **??**)), in all four Irminger Basin bioassays. The 120-hour bioassays (Figures **??**, **??** and **??**) showed pronounced responses to +Fe with respect to total and size-fractionated chlorophyll *a* concentrations and macronutrient drawdown (p < 0.05). In bioassay IE5.3 (Figure **??**) total chlorophyll *a* concentrations doubled (from 2.3 ± 0.2 to $5.8 \pm 0.2\,\mu gL^{-1}$). This pattern was mirrored in the NO_x drawdown response to treatments, where there was a significant response in NO_x drawdown to +Fe addition (F(1,8) = 62.60, p < 0.05) (Figure **??**).

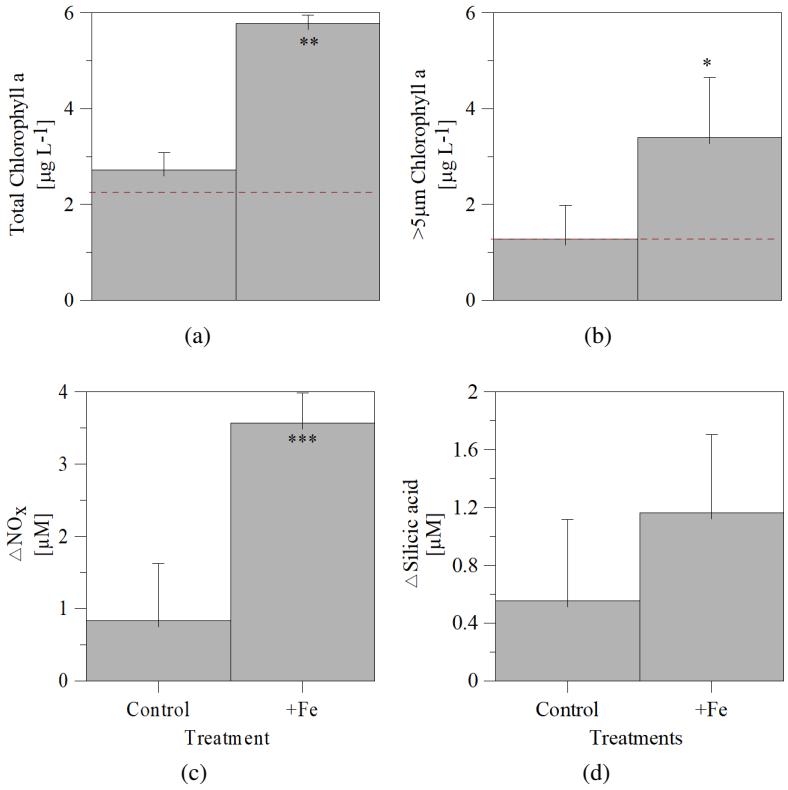

Figure 2.9: Bar graphs for bioassay IE5.3 showing the a) mean total chlorophyll *a* concentrations (μgL^{-1}, b) mean >5μm size-fractionated chlorophyll *a* concentrations (μgL^{-1}), c) mean change in nitrate+nitrite (NO_x) concentrations (μM), and d) the mean change in silicic acid (SiO_4) concentrations (μM) over the course of the 120-hour bioassay. Error bars indicate standard errors. Dashed red lines indicate initial conditions. Asterisks indicate only significant results from Tukey HSD test for multiple pair-wise comparisons of significant ANOVA results between the control and treatments: * p < 0.05, ** p < 0.01, *** p < 0.005. n=3 for all bioassays.

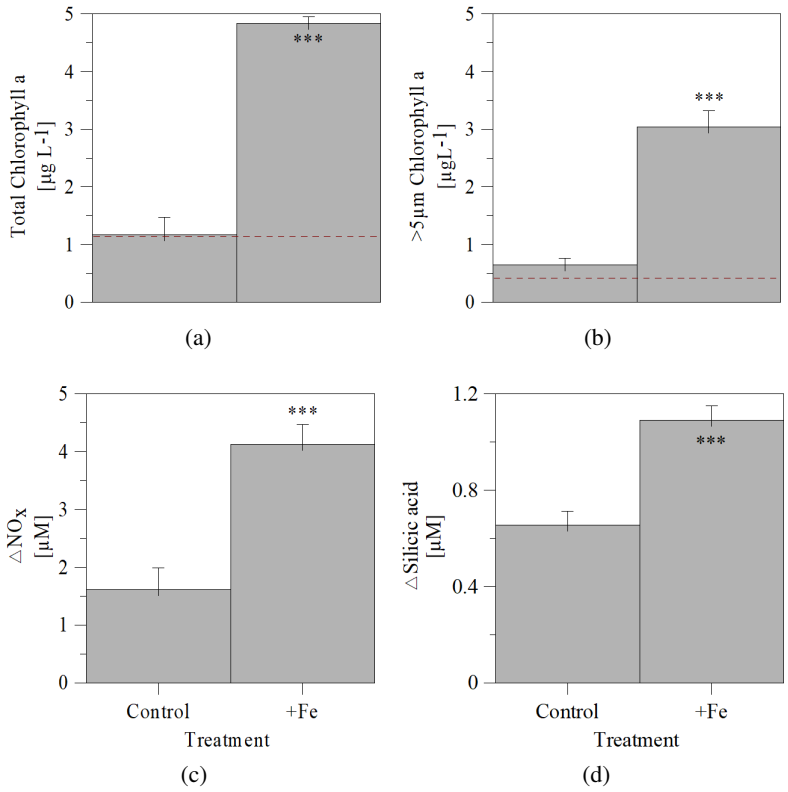

Figure 2.10: Bar graphs for bioassay IE5.4 showing the a) mean total chlorophyll *a* concentrations (μgL^{-1}, b) mean >5μm size-fractionated chlorophyll *a* concentrations (μgL^{-1}), c) mean change in nitrate+nitrite (NO_x) concentrations (μM), and d) the mean change in silicic acid (SiO_4) concentrations (μM) over the course of the 120-hour bioassay. Error bars indicate standard errors. Dashed red lines indicate initial conditions. Asterisks indicate only significant results from Tukey HSD test for multiple pair-wise comparisons of significant ANOVA results between the control and treatments: * $p < 0.05$, ** $p < 0.01$, *** $p < 0.005$. n=3 for all bioassays.

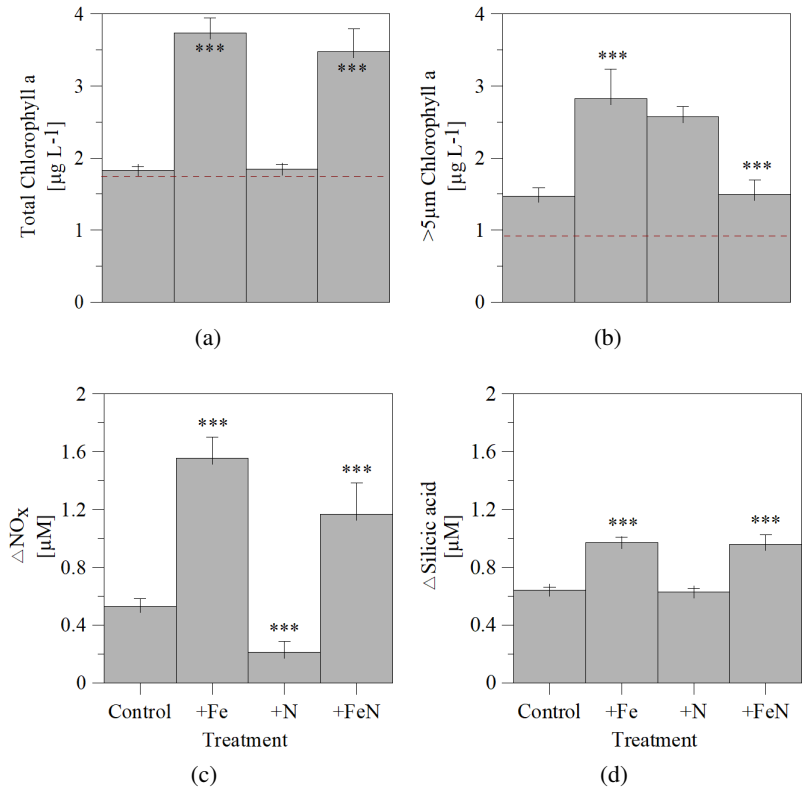

Figure 2.11: Bar graphs for bioassay IE5.5 showing the a) mean total chlorophyll *a* concentrations (μgL^{-1}), b) mean >5μm size-fractionated chlorophyll *a* concentrations (μgL^{-1}), c) mean change in nitrate+nitrite (NO_x) concentrations (μM), and d) the mean change in silicic acid (SiO_4) concentrations (μM) over the course of the 72-hour bioassay. Error bars indicate standard errors. Dashed red lines indicate initial conditions. Asterisks indicate only significant results from Tukey HSD test for multiple pair-wise comparisons of significant ANOVA results between the control and treatments: * $p < 0.05$, ** $p < 0.01$, *** $p < 0.005$. n=3 for all bioassays.

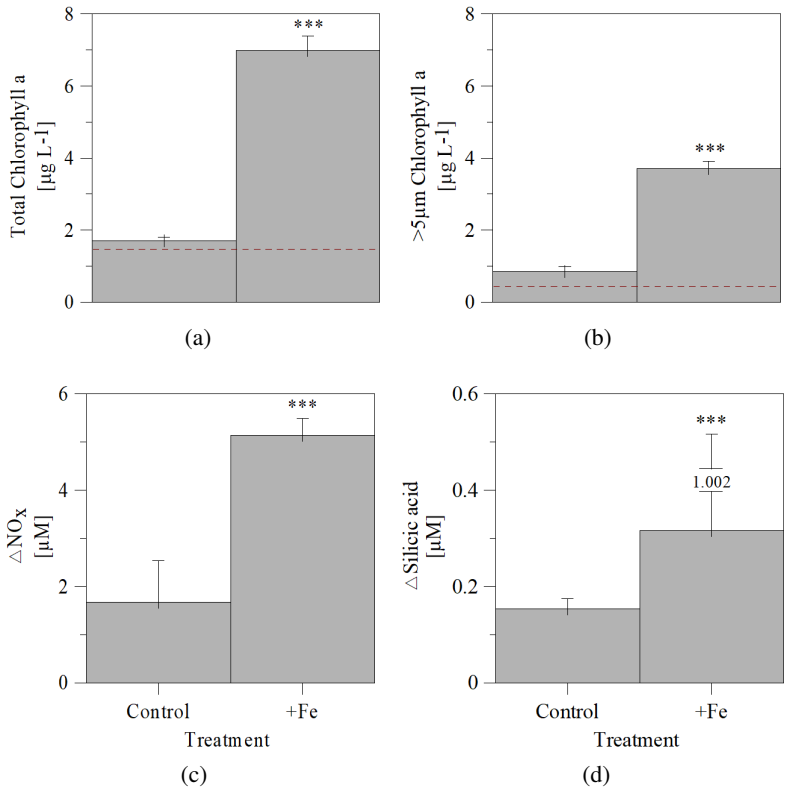

Figure 2.12: Bar graphs for bioassay IE5.6 showing the a) mean total chlorophyll *a* concentrations (μgL^{-1}, b) mean >5μm size-fractionated chlorophyll *a* concentrations (μgL^{-1}), c) mean change in nitrate+nitrite (NO_x) concentrations (μM), and d) the mean change in silicic acid (SiO_4) concentrations (μM) over the course of the 120-hour bioassay. Error bars indicate standard errors. Dashed red lines indicate initial conditions. +Fe treatment error bar amended so that it fits on the page. Asterisks indicate only significant results from Tukey HSD test for multiple pair-wise comparisons of significant ANOVA results between the control and treatments: * $p < 0.05$, ** $p < 0.01$, *** $p < 0.005$. n=3 for all bioassays.

Irminger Basin bioassays displayed quite varied phytoplankton abundances, with initial abundances of coccolithophores ranging between 4.3±1.2 (IE5.6) and 560.9±26.8 (IE5.3) cells mL^{-1} (Figures **??** and **??**, respectively) and for diatoms, between 611.6±12.6 (IE5.6) and 1512.6±27.2 (IE5.4) cells mL^{-1} (Figures **??** and **??**). Initial *Synechococcus* abundance ranged between $18.1 \times 10^3 \pm 3.5 \times 10^3$ (IE5.6) and $46.4 \times 10^3 \pm 9.2 \times 10^3$ (IE5.3) cells mL^{-1} (Figures **??** and **??**). Total initial picoeukaryote abundance also displayed a large range, from $7.6 \times 10^3 \pm 3.9 \times 10^3$ (IE5.4) to $110.9 \times 10^3 \pm 122.2 \times 10^3$ cells mL^{-1} (IE5.3) (Figures **??** and **??**). Both picoeukaryote and *Synechococcus* abundance peaked in the +Fe treatment of IE5.3 ($72.2 \times 10^3 \pm 76.4 \times 10^3$ cells mL^{-1} and $127.9 \times 10^3 \pm 148 \times 10^3$ cells mL^{-1}, respectively)..

The response of coccolithophores and diatoms to +Fe addition was clear in all Irminger Basin bioassays (Figures **??**, **??**, **??**, **??**, **??**, **??**, **??** and **??**). In IE5.3, coccolithophore abundances decreased to near 'zero' in the control but only dropped by approximately 50% in the +Fe treatment (Figure **??**). However, the total diatom

abundance in this bioassay increased dramatically in the +Fe treatment (from $622.8 \pm 18.6\,\text{cells}\,\text{mL}^{-1}$ initially, to $3334.3 \pm 41.7\,\text{cells}\,\text{mL}^{-1}$), while the control population stayed roughly similar to initial values ($522.1 \pm 17.4\,\text{cells}\,\text{mL}^{-1}$) (Figure **??**). In IE5.4, both total coccolithophore and diatom abundances increased (from $372.4 \pm 14.0\,\text{cells}\,\text{mL}^{-1}$ to $500.9 \pm 16.3\,\text{cells}\,\text{mL}^{-1}$, and from $1512.6 \pm 28.2\,\text{cells}\,\text{mL}^{-1}$ to $3811.8 \pm 45.0\,\text{cells}\,\text{mL}^{-1}$, respectively) over the course of the bioassay in the +Fe treatment (Figures **??** and **??**). The 72-hour Irminger Basin bioassay (IE5.5) had low coccolithophore abundance overall ($< 100\,\text{cells}\,\text{mL}^{-1}$), with total coccolithophore abundances decreasing in all but the +Fe treatment (Figure **??**). Total diatom abundances were much higher ($> 900\,\text{cells}\,\text{mL}^{-1}$) and showed a similar response pattern to the coccolithophores, with the greatest increase in abundance relative to the control ($2499.8 \pm 37.2\,\text{cells}\,\text{mL}^{-1}$) shown in the +Fe treatment ($3944.2 \pm 45.9\,\text{cells}\,\text{mL}^{-1}$) and the smallest response evident in the +N treatment ($1104.0 \pm 24.6\,\text{cells}\,\text{mL}^{-1}$) (Figure **??**). Total coccolithophore abundance in IE5.6 was comparatively low ($< 100\,\text{cells}\,\text{mL}^{-1}$), although there was still a clear response by the coccolithophore community to +Fe (Figure **??**). Diatom abundance in this bioassay was much higher, with diatom abundance in the +Fe treatment nearly 5 times higher than in the control treatment (Figure **??**).

In IE5.3, there was no significant difference in response to Fe in either *Synechococcus* or picoeukaryote abundance ($F(1,4) = 1.20$ and $F(3,2) = 1.33$, $p > 0.05$, respectively) (Figures **??** and **??**). Both *Synechococcus* ($F(1,4) = 27.72$, $p < 0.05$) and picoeukaryote ($F(1,4) = 82.07$, $p < 0.05$) abundances both increased significantly in response to +Fe in IE5.4 (from $20.8 \times 10^3 \pm 12.5 \times 10^3\,\text{cells}\,\text{mL}^{-1}$ to $48.9 \times 10^3 \pm 5.0 \times 10^3\,\text{cells}\,\text{mL}^{-1}$, and from $7.6 \times 10^3 \pm 3.9 \times 10^3\,\text{cells}\,\text{mL}^{-1}$ to $32.7 \times 10^3 \pm 2.6 \times 10^3\,\text{cells}\,\text{mL}^{-1}$, respectively) (Figures **??** and **??**). Although both *Synechococcus* and picoeukaryote abundances increased in all treatments in IE5.5, there was no significant difference in abundances among treatments. *Synechococcus* abundance in IE5.6 did not change significantly between treatments ($F(1,4) = 3.99$, $p > 0.05$) (Figure **??**) and picoeukaryote abundance was significantly higher in the +Fe treatment than in the control ($F(1,4) = 41.3$ $p < 0.05$) (Figure **??**).

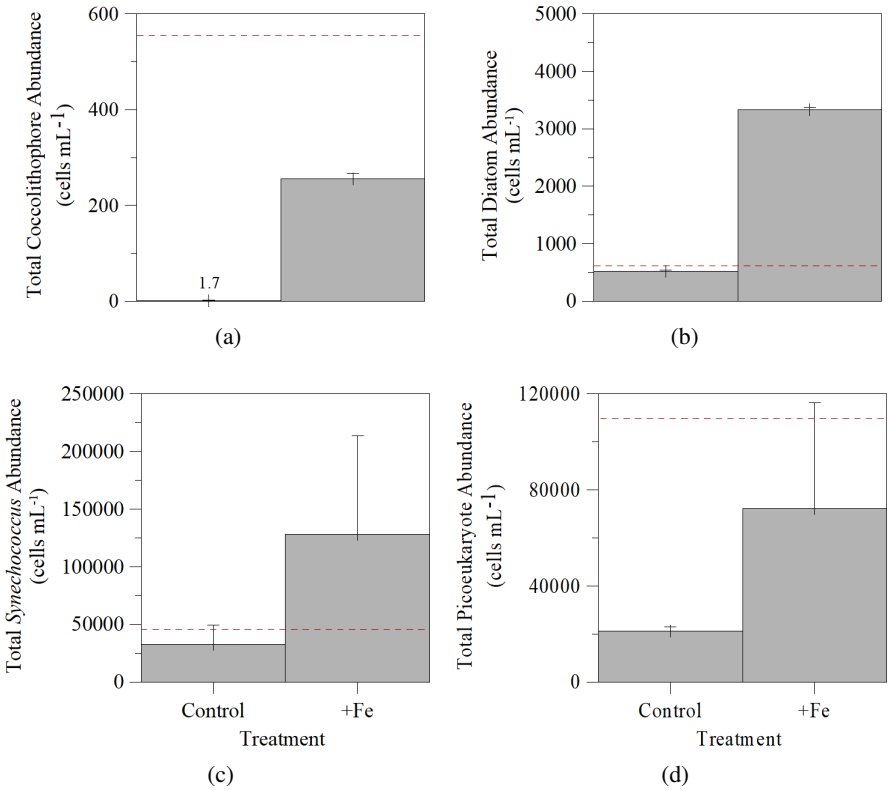

Figure 2.13: Bar graphs for bioassay IE5.3 showing a) total coccolithophore abundances (cells mL^{-1}) b) total diatom abundance (cells mL^{-1}), c) total *Synechococcus* abundance (cells mL^{-1}) and d) total picoeukaryote abundance (cells mL^{-1}). Error bars indicate standard errors. Dashed red lines indicate initial conditions.

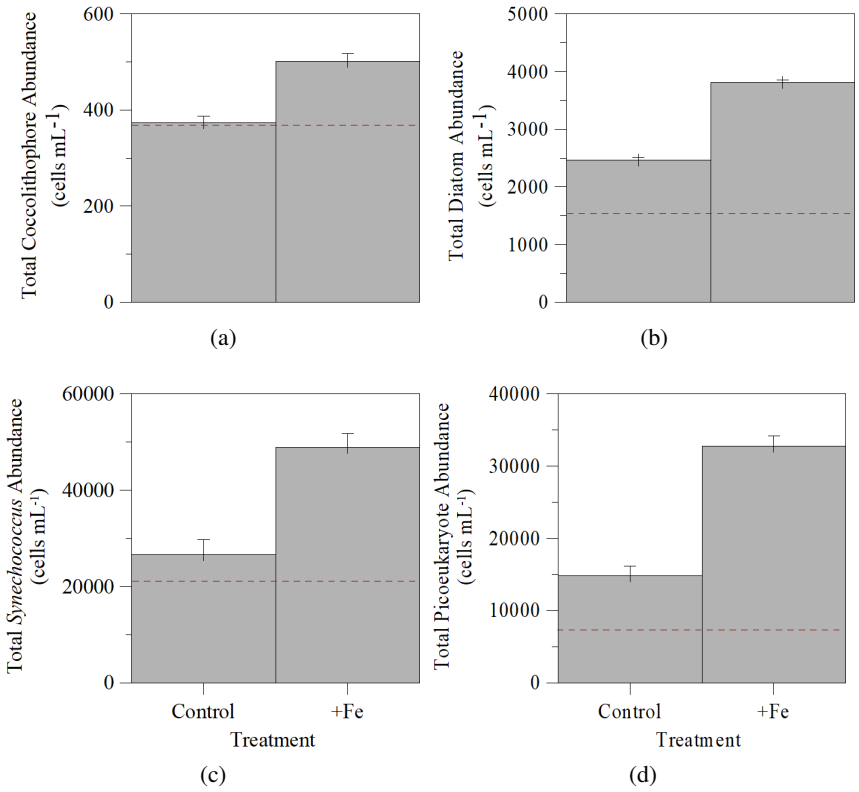

Figure 2.14: Bar graphs for bioassay IE5.4 showing a) total coccolithophore abundances (cells mL^{-1}), b) total diatom abundance (cells mL^{-1}), c) total *Synechococcus* abundance (cells mL^{-1}) and d) total picoeukaryote abundance (cells mL^{-1}). Error bars indicate standard errors. Dashed red lines indicate initial conditions.

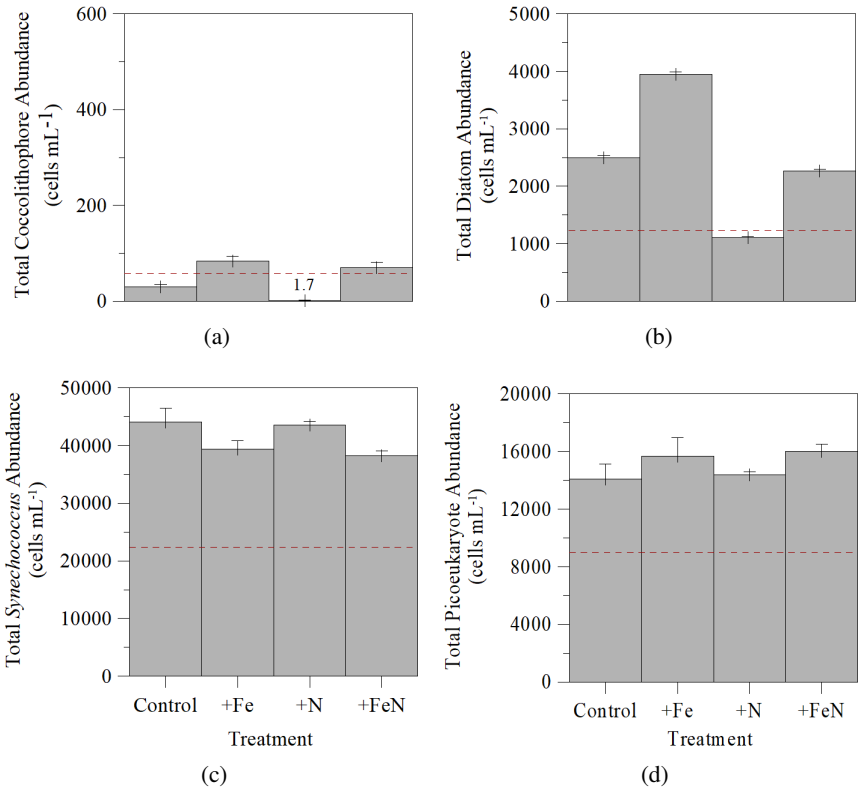

Figure 2.15: Bar graphs for bioassay IE5.5 showing a) total coccolithophore abundances (cells mL^{-1}) b) total diatom abundance (cells mL^{-1}), c) total *Synechococcus* abundance (cells mL^{-1}) and d) total picoeukaryote abundance (cells mL^{-1}). Error bars indicate standard errors. Dashed red lines indicate initial conditions.

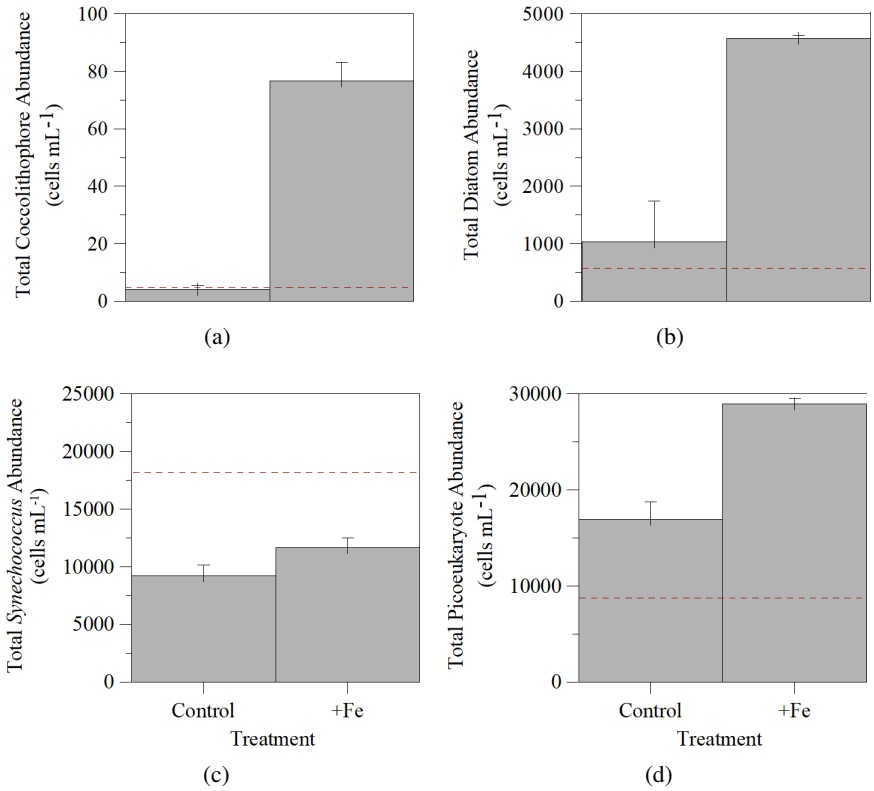

Figure 2.16: Bar graphs for bioassay IE5.6 showing a) total coccolithophore abundances (cells mL^{-1}), b) total diatom abundance (cells mL^{-1}), c) total *Synechococcus* abundance (cells mL^{-1}) and d) total picoeukaryote abundance (cells mL^{-1}). Error bars indicate standard errors. Dashed red lines indicate initial conditions.

2.3.4 Primary Production and Calcite Production

An analysis of variance (ANOVA) ($p < 0.05$) indicated that there were no significant treatment effects in either PP ($F(3,8) = 2.31$, $p > 0.05$) or CP ($F(3,8) = 2.77$, $p > 0.05$) in bioassay IE5.1 (Figure**??**). Only two of the longer bioassays (IE5.4 and IE5.6) collected from the Irminger Basin had PP and CP measured (Figures **??**, **??**, **??** and **??**). Primary production increased significantly compared with the control in the +Fe treatment in both bioassays ($F(1,8) = 43.14$ and 158.30, $p < 0.05$, respectively). Although, initial PP was fairly similar in the two bioassays (1.18 ± 0.19 and 1.01 ± 0.06 mmol C $m^{-3}d^{-1}$, respectively), PP in the +Fe treatment for IE5.6 was nearly twice that measured in the same treatment in IE5.4 (4.67 ± 0.37 and 2.8 ± 0.67 mmol C $m^{-3}d^{-1}$, respectively). There was only weak evidence of a response in CP to +Fe when compared with the control in IE5.4 $F(1,8) = 9.03$, $p < 0.05$) (Figure **??**), although there was a more convincing response in IE5.6, with CP increasing in the +Fe treatment ($F(1,8) = 33.34$, $p < 0.05$) (Figure **??**). Generally, CP followed a similar pattern of response to that observed in the PP measurements, with similar initial CP values followed by a near doubling of CP in the +Fe treatment of IE5.6 (131.21 ± 18.13 μmol C $m^{-3}d^{-1}$) compared with the same treatment in IE5.4 (77.48 ± 10.62 μmol C $m^{-3}d^{-1}$).

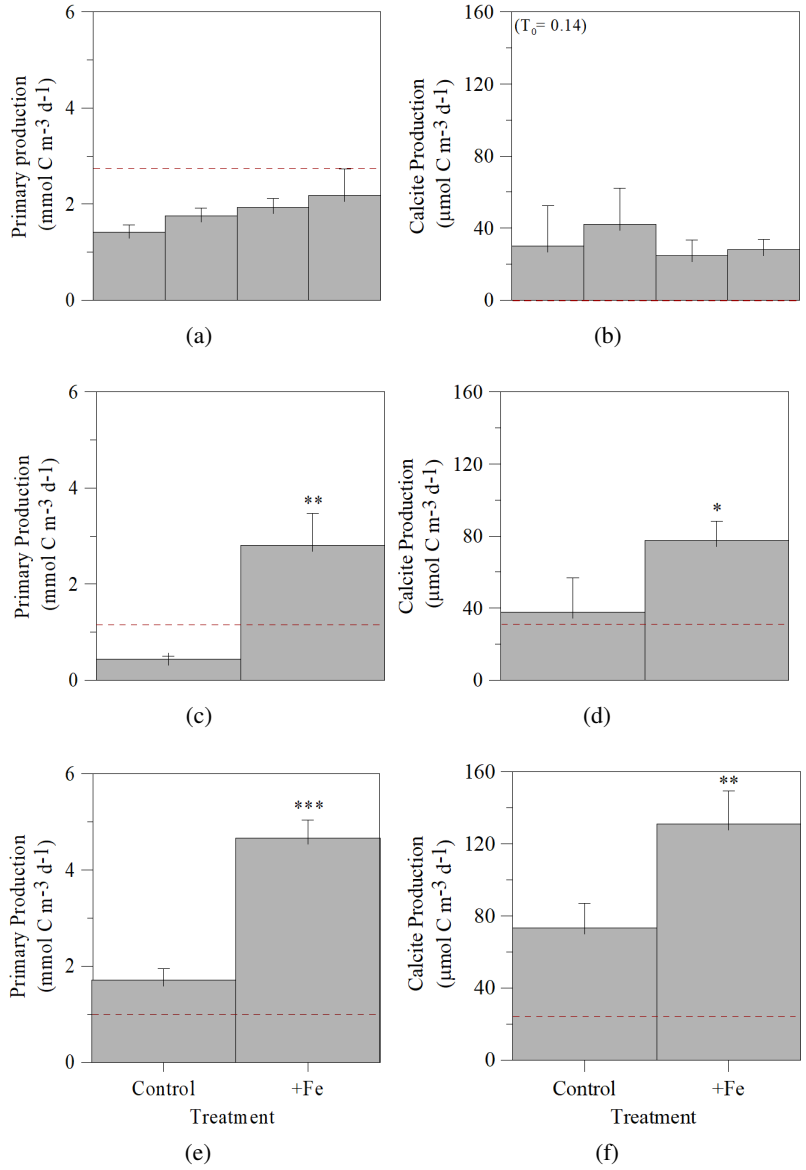

Figure 2.17: Bar graphs showing primary production (mmol C $m^{-3} d^{-1}$) and calcite production (μmol C $m^{-3} d^{-1}$) at T_{end} for each bioassay treatment, a) IE5.1, b) IE5.1, c) IE5.4, d) IE5.4, e) IE5.6, f) IE5.6. Error bars indicate standard errors. Dashed red lines indicate initial conditions. Asterisks indicate only significant results from Tukey HSD test for multiple pair-wise comparisons of significant ANOVA results between the control and treatments: * $p < 0.05$, ** $p < 0.01$, *** $p < 0.005$. n=3 for all bioassays.

2.3.5 Statistical Analysis of Community Composition

An nMDS analysis of phytoplankton (coccolithophore and diatom) community abundance based on a priori factors showed distinct patterns in community abundance for three of the predetermined factors: 'basin', 'length' and 'bioassay', while 'treatment' appeared to show little in the way of a distinct pattern in either coccolithophore or diatom abundance (Figures **??** and **??**).

Bioassays from the Irminger Basin were more widely dispersed in the nMDS ordination than those in the Iceland Basin (Figure **??** and **??**). With respect to experimental length, the shorter bioassays (48-hour) were more tightly clustered than either of the two longer bioassays (72- and 120-hour) in the Iceland Basin, with this distinction more evident in diatom than coccolithophore species composition (Figures **??**, **??**, **??** and **??**). It is noteworthy that the individual bioassays tended to cluster together in terms of experimental treatments for both diatom and coccolithophore species composition.

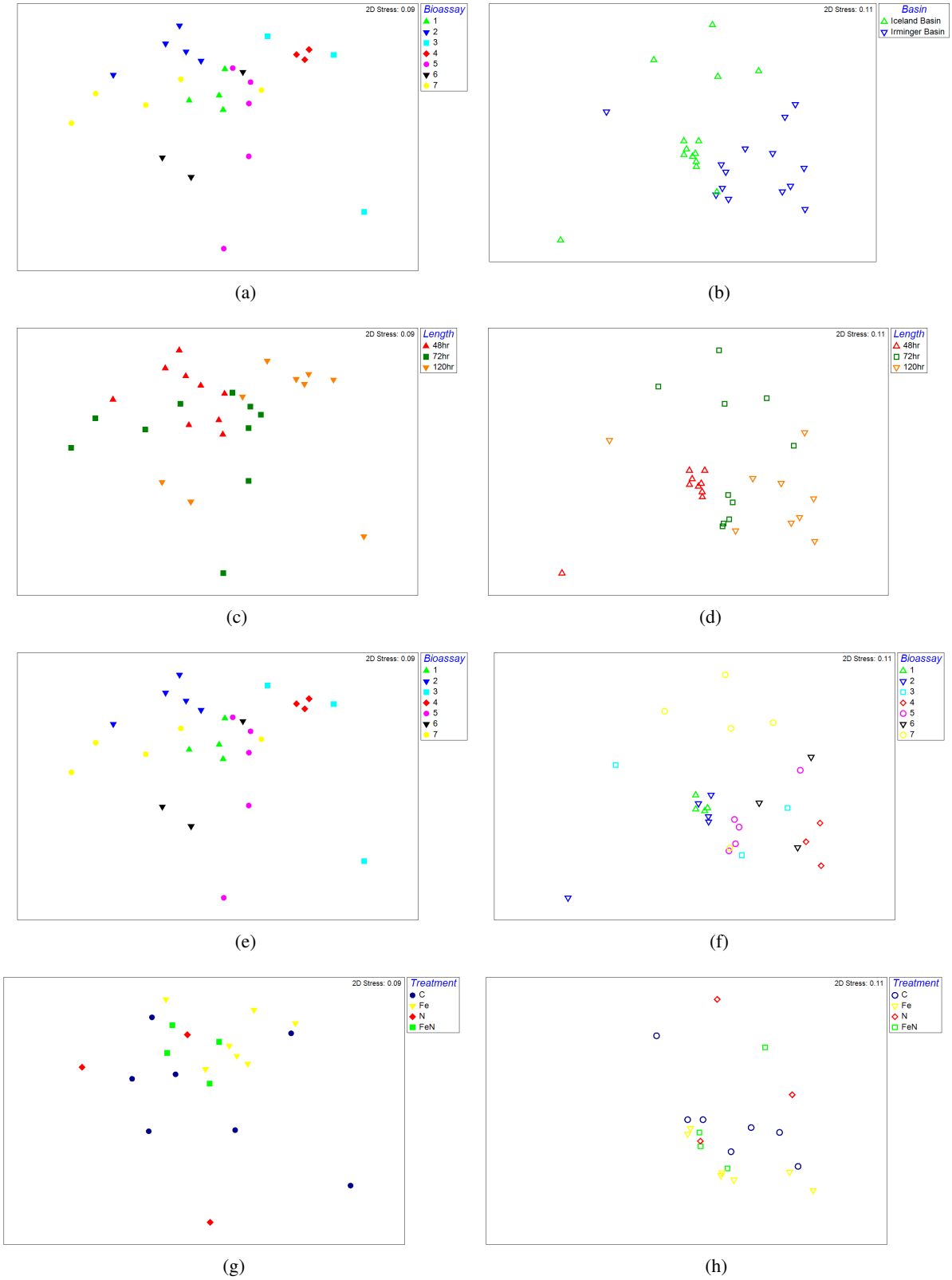

Figure 2.18: Non-metric multidimensional scaling (nMDS) ordination of coccolithophore (a, c, e, g) and diatom (b, d, f, h) community composition in different (a, b) basins, (c, d) length of incubations, (c, f) bioassays and (g, h) treatments (excluding initial conditions) based on Bray-Curtis similarity. Closed symbols represent coccolithophores and open symbols represent diatoms.

Results of the ANOSIM test confirmed the significance of the a-priori selected factors 'bioassay', 'basin' and 'length' ($p < 0.05$) (see Table **??**). R-values scale between +1 and -1, with high R-values indicating a high separation between levels of the factor, whereas an R-value close to 0 indicates no separation between levels of the factor. Analysis of R-values indicate that, though the factors 'basin' and 'length' led to significantly different compositions, these factors were not as important to coccolithophore and diatom community structure as the factor 'bioassay' (R = 0.401 and 0.323, p = 0.001, respectively). Indeed, the duration of the bioassay had less of an effect on coccolithophore community structure (R = 0.203, p = 0.002) than on diatom community structure (R = 0.267, p = 0.001). SIMPER analysis showed which coccolithophore and diatom species were primarily driving the average dissimilarity between the two basins and the different sample clusters. The Iceland and Irminger Basins were on average 61% dissimilar in terms of coccolithophore composition, with differences in *Syracosphaera* spp. abundance contributing 43% to the total dissimilarity (Table **??**). *Syracosphaera* spp., on average were more abundant in the Irminger Basin than in the Iceland Basin (averages 8.4 and 1.8 cells mL^{-1}, respectively) while *Emiliania huxleyi* was on average almost equally abundant in both basins (4.3 and 4.5 cells mL^{-1}, respectively).

Table 2.3: ANOSIM test results for coccolithophore and diatom groups identified in the cluster analyses presented in Figure **??** showing R values and corresponding probability (p-values) that there is no effect of the factors.

	Coccolithophores				**Diatoms**			
Factor	Treatment	**Bioassay**	**Basin**	**Length**	Treatment	**Bioassay**	**Basin**	**Length**
R-value	0.126	0.401	0.287	0.203	0.021	0.323	0.276	0.267
P-value	0.089	**0.001**	**0.001**	**0.002**	0.377	**0.001**	**0.001**	**0.001**

Diatom community composition between the two basins had a much lower degree of dissimilarity (33%), with a number of different diatom species contributing to this dissimilarity (> 6 species). Notably, small *Fragilariopsis* species accounted for 13% of the differences between the two basins, whereas diatoms were generally more abundant in the Irminger Basin than in the Iceland Basin (see Table **??**). Generally, coccolithophore community diversity was much lower than that of the diatom community, with a total of six coccolithophore species identified compared with a total of fifteen diatom species (see Table **??**). Consequently, the dominant species of diatom varied far more than the dominant species of coccolithophore, and in general, the dominant coccolithophore species made up a much greater percentage of the total coccolithophore community present than the dominant diatom species of the diatom community. For example, in IE5.2 the dominant coccolithophore in each treatment made up more than 90% of the total abundance, whereas the dominant diatom species comprises less than 30% of the total abundance.

Table 2.4: SIMPER results showing the contribution of coccolithophore and diatom species responsible for ~60% of the differences between basins.

Iceland vs. Irminger Basins	**Average Abundance** (cells mL^{-1})		**Contribution to total dissimilarity (%)**
Coccolithophores, average dissimilarity = 61.2%	Iceland Basin	Irminger Basin	
Syracosphaera spp.	1.78	8.38	43.2
Emiliania huxleyi	4.29	4.52	28.1
			= 71.3%
Diatoms, average dissimilarity = 33.2%			
Fragilariopsis sp. (small)	2.75	4.88	13.14
Pseudonitzschia sp.	3.12	4.06	11.90
Nitzschia sp.	1.41	2.64	10.97
Thallassiosira sp.	2.31	3.32	6.99
Thalassionema nitschoides	1.45	1.46	6.71
Proboscia sp.	1.69	0.81	6.63
			= 62.3%

Clearly there were strong differences between bioassays located in the Iceland versus the Irminger Basin and hence it is also appropriate to examine the differences in species composition between communities in the Iceland Basin and the Irminger Basin. The Irminger Basin bioassays were largely dominated by *Syracosphaera* spp., while the majority of the Iceland Basin bioassay treatments were dominated by *E. huxleyi* (Table **??**). *Syracosphaera* spp. also showed up as an abundant coccolithophore species in the Iceland Basin, although Iceland Basin bioassays where *Syracosphaera* spp. were abundant tended to be associated with higher J' values, indicating a more diverse community in general. In the Irminger Basin, there was more variability in the dominant species of coccolithophore, with *Syracosphaera* spp., *Rhabdosphaera* sp. and *Coccolithus pelagicus* all appearing as dominant species in the various bioassays in addition to *E. huxleyi*. In contrast, the diatom community was dominated by *Pseudonitzschia* spp. in 43% of the Irminger Basin bioassays and 57% of the Iceland Basin bioassays. Small *Fragilariopsis* spp. were dominant in 43% of the Irminger Basin treatments, while other notable diatom genera included *Corethron* (28% in IE5.2 Initial), medium-sized *Chaetoceros* (27% in IE5.2 +FeN and 26% in IE5.7 +FeN) in the Iceland Basin, and *Thalassionema nitschoides* (35% in IE5.3 Initial) and *Nitzschia* species (51% in IE5.6 +Fe) in the Irminger Basin. Generally, bioassays in the Irminger Basin had more diverse coccolithophore communities than in the Iceland Basin, while the pattern was opposite for diatoms between the two basins.

Table 2.5: Summary of phytoplankton community diversity. Coccolithophore and diatom abundance (cells mL^{-1}), number of species (S), Pielou's evenness (J') and dominant species (contribution to total abundance in brackets). Dominant coccolithophore abbreviations, *Syracosphaera* spp. (*Syraco*), *Emiliania huxleyi* (*E. hux*), *Rhabdosphaera* sp. (*Rhabdo*). Dominant diatom abbreviations, *Pseudonitzschia* sp. (*Pseudo*), *Fragilariopsis* sp. (*Frag*), *Chaetoceros* sp. (*Chaet*).

Bioassay	**Coccolithophore Abundance**	**Community diversity**		**Dominant Coccolithophore Taxa**	**Diatom Abundance**	**Community diversity**		**Dominant Diatom Taxa**
	(cells mL^{-1})	S	J'		(cells mL^{-1})	S	J'	
Iceland Basin								
IE5.1 T0	50	3	0.71	*Syraco* (50%)	564	14	0.74	*Pseudo* (41%)
IE5.1 Cont	21	3	0.42	*E. hux* (88%)	314	15	0.76	*Pseudo* (41%)
IE5.1 Fe	34	4	0.66	*E. hux* (61%)	421	15	0.77	*Pseudo* (28%)
IE5.1 FeN	34	5	0.73	*Syraco* (44%)	462	14	0.74	*Pseudo* (32%)
IE5.2 T0	6	1	***	*E. hux* (100%)	289	10	0.81	*Corethron* (28%)
IE5.2 Cont	26	1	***	*E. hux* (100%)	472	13	0.82	*Frag* (sml) (24%)
IE5.2 Fe	37	2	0.28	*E. hux* (95%)	760	13	0.75	*Pseudo* (29%)
IE5.2 FeN	47	2	0.13	*E. hux* (98%)	703	14	0.75	*Chaet* (med) (27%)
IE5.2 N	47	2	0.40	*E. hux* (92%)	609	14	0.74	*Pseudo* (29%)
IE5.7 T0	1	1	***	*E. hux* (100%)	87	11	0.85	*Pseudo* (24%)
IE5.7 Cont	8	2	0.50	*E. hux* (89%)	189	9	0.64	*Frag* (sml) (58%)
IE5.7 Fe	82	4	0.75	*Syraco* (49%)	3685	13	0.40	*Pseudo* (70%)
IE5.7FeN	23	2	0.39	*E. hux* (92%)	179	8	0.82	*Chaet* (med) (26%)
IE5.7 N	3	1	***	*E. hux* (100%)	128	8	0.69	*Frag* (sml) (47%)
Irminger Basin								
IE5.3 T0	561	6	0.47	*Syraco* (69%)	623	12	0.69	*T. nitschoides* (35%)
IE5.3 Cont	27	2	0.92	*Rhabdo* (67%)	522	9	0.68	*Pseudo* (42%)
IE5.3 Fe	229	2	0.71	*Syraco* (81%)	3334	12	0.57	*Pseudo* (55%)
IE5.4 T0	362	4	0.34	*Syraco* (87%)	1512	8	0.43	*Frag* (sml) (76%)
IE5.4 Cont	375	5	0.41	*Syraco* (76%)	2466	9	0.42	*Frag* (sml) (77%)
IE5.4 Fe	502	4	0.50	*Syraco* (71%)	3812	8	0.65	*Frag* (sml) (48%)
IE5.5 T0	61	3	0.98	*Syraco* (43%)	977	12	0.65	*Pseudo* (42%)
IE5.5 Cont	26	3	0.81	*C. pelagicus* (47%)	2500	12	0.41	*Peusdo* (72%)
IE5.5 Fe	79	3	0.85	*E. hux* (47%)	3944	13	0.39	*Peusdo* (73%)
IE5.5 FeN	63	2	0.90	*Syraco* (69%)	2262	12	0.47	*Pseudo* (66%)
IE5.5 N	3	2	0.92	*Syraco* (67%)	1104	8	0.44	*Frag* (sml) (74%)
IE5.6 T0	5	3	0.91	*Syraco* (54%)	612	8	0.39	*Frag* (sml) (78%)
IE5.6 Cont	4	3	0.93	*E. hux* (53%)	1030	12	0.54	*Frag* (sml) (43%)
IE5.6 Fe	77	3	0.70	*E. hux* (57%)	4576	10	0.46	*Nitzschia* (51%)

2.4 Discussion

2.4.1 Phytoplankton Responses to Iron Addition in the North East Atlantic

While not traditionally thought of as an Fe limited system, the high latitude North East Atlantic receives very low dust input and thus Fe availability could be considered to be comparable to that in the HNLC north Pacific (**?**). Indeed, both **?** and **?** measured low to limiting ($< 0.01 - 0.2$ nM) concentrations of Fe in the Iceland Basin during the summer months (July - August). However, the phytoplankton in the Iceland Basin bioassays in this study showed far less of a response to +Fe than those in the Irminger Basin, and responded much more strongly to +N and +FeN treatments. These results, coupled with low initial NO_x concentrations (average of $0.54 \pm 0.22\,\mu$M), suggest that phytoplankton were either co-limited by both Fe and nitrate or limited by nitrate alone in the Iceland Basin in 2010. Silicic acid concentrations were similarly relatively low initially (average of $0.65 \pm 0.21\mu$M), and initial chlorophyll *a* concentrations were on average lower than those measured in the Irminger Basin. In contrast, the Irminger Basin community displayed a strong response to Fe addition and had comparatively much higher starting concentrations of both NO_x and silicic acid (average initial concentrations of $4.48 \pm 0.62\,\mu$M and $1.56 \pm 0.75\,\mu$M, respectively), which suggests that phytoplankton were Fe limited in the Irminger Basin. However, an important observation across the different bioassays was the importance of the starting population composition in the overall response of the community. Generally, coccolithophore and diatom abundance in the Iceland Basin ($29.9 \pm 22.4\,\text{cells}\,\text{mL}^{-1}$ and $633.0 \pm 903.7\,\text{cells}\,\text{mL}^{-1}$, respectively) was lower than in the Irminger Basin ($169.6 \pm 198.0\,\text{cells}\,\text{mL}^{-1}$ and $2091.0 \pm 1384.9\,\text{cells}\,\text{mL}^{-1}$, respectively), which can be attributed to the limiting initial concentrations of NO_x (and silicic acid).

Total chlorophyll *a* concentrations were initially elevated ($1.69 \pm 0.48\,\mu\text{g}\text{L}^{-1}$ in the Irminger Basin versus $1.11 \pm 0.21\,\mu\text{g}\text{L}^{-1}$ in the Iceland Basin), but generally showed more variation than the initial nutrient measurements. Total chlorophyll *a* concentrations in the Iceland basin increased significantly in the +FeN treatment, with less than half (on average 43.3%) of the chlorophyll *a* biomass in all treatments composed of the $> 5\,\mu$m size-fraction, suggesting PP was dominated by small-celled phytoplankton like picoeukaryotes and *Synechococcus*. In contrast, in the Irminger Basin, where total chlorophyll *a* concentrations increased significantly in the +Fe treatments, generally more than half (on average 63.8%) of the chlorophyll *a* biomass was dominated by the $> 5\,\mu$m size-fraction after +Fe addition. This suggests that PP was dominated by larger phytoplankton, such as coccolithophores and diatoms. Further support for diatom dominance can be seen by the presence of silicic acid in non-limiting concentrations (e.g. $> 2\,\mu$M of silicic acid) (**?**) in the Irminger Basin, hence supporting the growth of

diatoms over coccolithophores. Furthermore, **?** showed that the proportion of PP produced by diatoms is controlled by the availability of silicic acid while **?** suggested that the competition between coccolithophores and diatoms was strongly influenced by the relative availability of silicic acid versus nitrate (see also **?**). In this study, the phytoplankton community in the Irminger Basin was heavily dominated by diatoms and the diatom community in this Basin, where silicic acid concentrations were on average nearly twice that found in the Iceland Basin (see Table **??**), was far more abundant (see Table **??**).

Iron availability, or lack thereof, has been shown many times to provide a fundamental role in photosynthesis and in phytoplankton productivity in many oceanic systems. Though the North East Atlantic is typically not considered an Fe limited system, areas such as the central Iceland Basin have been shown to display some of the characteristics of a HNLC system. These characteristics include low surface concentrations of dissolved Fe ($< 0.01 - 0.2\,\mathrm{nM}$) coupled with the presence of residual nitrate ($2 - 5\,\mu\mathrm{M}$) and low chlorophyll *a* concentrations ($0.2 - 0.4\,\mu\mathrm{gL}^{-1}$) (**?**). However, the Iceland Basin during our study in 2010 was characterised by low NO_x concentrations ($< 1\,\mu\mathrm{M}$) coupled with elevated total chlorophyll *a* concentrations ($> 2\,\mu\mathrm{gL}^{-1}$). Typically, surface waters of the Iceland Basin have dissolved Fe in concentrations of approximately 0.2-0.6 nM (**?**), whereas initial Fe concentrations at experimental locations in the central Iceland Basin during our study ranged between <0.01 nM and 0.28 nM (**?**). The average concentration (S.E.) of dFe in the Irminger and Iceland Basins during this study were $0.08 \pm 0.24\,\mathrm{nM}$ and $0.06 \pm 0.06\,\mathrm{nM}$, respectively (**?**). Iron addition experiments performed in 2007 indicated increased productivity as well as increased growth rates for a number of different phytoplankton taxa, including coccolithophores (**?**). However, in our study the Iceland Basin bioassays were shown to be nitrogen limited, responding to both +N and the +FeN treatments rather than to +Fe addition alone.

In the past, satellite data from the Irminger Basin have typically described a short and intense diatom-dominated spring bloom followed by a summer minimum in chlorophyll *a* concentrations (**?**). **?** found that the Irminger basin region had low residual surface concentrations of Fe (0.0151 - 0.037 nM) at the time of our study in 2010. These low Fe concentrations, coupled with the high initial NO_x (3.78 ± 0.17 - $5.24 \pm 0.20\,\mu\mathrm{M}$) concentrations in Irminger Basin bioassays, would suggest that the phytoplankton community is Fe stressed and likely to display strong growth responses in +Fe treatments. This was confirmed in our study (Figures **??**, **??**, **??**, **??** and **??**), with Irminger Basin bioassays showing significant responses to +Fe addition in all four bioassays. It is important to note that in the spring of 2010 the Icelandic volcano – Eyjafjallajökull – erupted, and satellite imagery showed that the ash plume containing Fe was advected southwards by equatorward air streams that deposited ash over most of the North East Atlantic. This resulted in significant dissolved Fe inputs into the Iceland Basin and comparison of *in situ* nitrate

concentrations with historical data indicated that ash deposition resulted in enhanced macronutrient drawdown (**?**). Additionally, during the winter of 2009/2010 the North Atlantic Oscillation (NAO) became extremely negative, causing in an influx of freshwater, which spread through the basin resulting in anomalous nutrient (the N:Si drawdown ratio in spring to summer 2010 was 3:1 as opposed to the usual 1:1) and mixed layer depth (unusually shallow) conditions (**?**). Hence, although 2010 was an anomalous year in terms of atmospheric and volcanic sources of Fe to the Iceland and Irminger Basins, summer phytoplankton communities did experience Fe limitation, although at the time of our sampling this was constrained to the Irminger Basin.

2.4.2 Coccolithophore Response to Iron Addition

Iron limitation is more typically associated with traditional HNLC regions like the Southern Ocean, Equatorial Pacific and North Pacific (**????**) and there is plenty of evidence as to its effect on diatoms in these regions. In the Southern Ocean, *E. huxleyi* typically dominates coccolithophore assemblages in the Atlantic and Indian sectors (**??????**). In the past, *E. huxleyi* blooms have been associated with relatively high nitrate and low phosphate concentrations (**?**), and the Fe requirement of *E. huxleyi* and other oceanic coccolithophores is thought to be low relative to coastal diatoms (**??**), which suggests that coccolithophores should flourish in parts of the ocean where diatoms are limited by Fe. Indeed, in this study coccolithophores displayed clearly enhanced abundances in +Fe treatments relative to the control in both the Iceland and Irminger Basins (Table **??**), regardless of initial Fe concentrations. Though coccolithophore blooms are not customarily linked to Fe and are traditionally associated with parameters such as irradiance, mixed layer depth, nitrate, phosphate or calcite saturation, these parameters were shown to have no clear correlation with community cellular calcification by **?** in the Iceland Basin. **?** hypothesized that other factors, such as Fe availability and grazing, could instead be influencing the coccolithophore community in the central Iceland Basin in summer. **?** (on the same research cruise as **?**) showed that the growth rates of a number of different phytoplankton taxa, including coccolithophores, all increased following Fe addition in the North Atlantic. Furthermore, Fe has been invoked as a potential factor in the formation of the Patagonian Shelf (South Atlantic) coccolithophore bloom, which occurs in high nitrate low silicate waters (**??**).

Coccolithophore blooms ($> 1000\,\text{cells}\,\text{mL}^{-1}$) in the Iceland Basin occur frequently (**?**) and are often associated with significant amounts of CP (**?**). However, in our study coccolithophore abundances at the start of the seven bioassays were generally low in the Iceland ($< 50\,\text{cells}\,\text{mL}^{-1}$) and Irminger ($< 600\,\text{cells}\,\text{mL}^{-1}$) Basins. **?** found similar low coccolithophore abundance ($< 1\text{x}10^{3}$ $\text{cells}\,\text{mL}^{-1}$) in the Iceland Basin between July and August of 2007. Furthermore, overall coccolithophore community diversity was low in both the Iceland and Irminger Basin

bioassays (between one and six different coccolithophore species present in bioassays), with coccolithophore community diversity in the Iceland Basin generally lower than that in the Irminger Basin (Table **??**). The species *E. huxleyi* was more numerically dominant in Iceland Basin bioassays (Table **??**), where NO_x and silicic acid limited diatom growth and Fe was in non-limiting concentrations, rather than in the Irminger Basin bioassays, where macronutrient concentrations were not limiting and diatoms were more prevalent. These Irminger Basin bioassays showed more diversity in terms of the coccolithophore community composition (Table **??**), with little dominance by *E. huxleyi*. Despite low cell abundances and low community diversity, it is clear that coccolithophores respond positively to Fe amendment in many of the bioassays undertaken in the summer of 2010.

Using the cell numbers at the starting point of the bioassays and those at the sampling times allows calculation of (net) growth rates and comparison between treatments (following **?**). These reaffirm the different responses to +Fe addition between the two basins, with growth rates for the coccolithophores in the +Fe treatments of the two short-term Iceland Basin bioassays of $-0.19\,d^{-1}$ and $0.89\,d^{-1}$, respectively, which equates to a % increase relative to the control of 56% and 22%, respectively (Table **??**). However, in the 72-hour treatment, coccolithophore growth rates were significantly higher ($1.38\,d^{-1}$) relative to the control ($0.00\,d^{-1}$), possibly highlighting the importance of ensuring bioassays are run for a sufficient length of time. For example in an Fe fertilization experiment performed in the eastern equatorial Pacific (IronEx II), it was shown that, while all phytoplankton taxa responded to Fe with increased growth rates, the different groups differed in the timing of their response (**?**). In the present study, the duration of the bioassay was found to be a factor affecting coccolithophore (and diatom) community composition (Table **??**). Coccolithophores in the Irminger Basin, where initial Fe concentrations were low, also showed strong increases in growth rates in response to +Fe addition (Table **??**). Coccolithophore growth rates of $1.44\,d^{-1}$ were measured in the +Fe treatment of IE5.6, and were the highest recorded for any of the phytoplankton taxa in any of the bioassays. Coccolithophores in the Irminger Basin +Fe treatments exhibited markedly higher growth rates relative to the control than those in the Iceland Basin, with the % increase relative to the control ranging from 85% (IE5.3) to 6461% (IE5.7) (Table **??**). More than half of the coccolithophore population in this bioassay was dominated by *E. huxleyi* (57%), with *Syracosphaera* spp. (41%) making up most of the rest.

Table 2.6: Growth rates (d^{-1}) and the % change in growth rates relative to the control determined for mean total chlorophyll *a*, coccolithophores, diatoms, picoeukaryotes and *Synechococcus*. In bioassay IE5.1, 'nd' refers to 'not determined'. Bioassays where there was no change in the control could not have a % change calculated as any change is infinite relative to the control, these have been marked 'na'.

Bioassay	Treatment	Mean Chl (d^{-1})	% Change	Coccolithophores (d^{-1})	% Change	Diatoms (d^{-1})	% Change	Picoeukaryotes (d^{-1})	% Change	*Synechococcus* (d^{-1})	% Change
Iceland Basin											
IE5.1 (48hr)	Control	0.12	-	-0.44	-	-0.29	-	nd	-	nd	-
	+Fe	0.20	68%	-0.19	56%	-0.15	50%	nd	nd	nd	nd
	+N	0.23	89%	nd	nd	nd	nd	nd	nd	nd	nd
	+FeN	0.43	263%	-0.20	55%	-0.10	66%	nd	nd	nd	nd
IE5.2 (48hr)	Control	-0.12	-	0.73	-	0.24	-	0.44	-	0.22	-
	+Fe	-0.10	17%	0.89	22%	0.48	98%	0.39	-12%	0.12	-48%
	+N	-0.03	72%	1.03	41%	0.37	53%	-0.10	-123%	0.31	43%
	+FeN	0.18	-248	1.03	41%	0.44	82%	0.16	-64%	0.37	69%
IE5.7 (72hr)	Control	0.05	-	0.00	-	0.26	-	-0.04	-	-0.11	-
	+Fe	0.23	378%	1.38	na	1.25	379%	-0.01	-86%	-0.12	-10%
	+N	0.08	55%	0.33	na	0.13	-50%	-0.03	-17%	-0.10	5%
	+FeN	0.36	641%	0.95	na	0.24	-7%	0.08	325%	-0.07	33%
Irminger Basin											
IE5.3 (120hr)	Control	0.08	-	-2.87	-	-0.09	-	-0.82	-	-0.17	-
	+Fe	0.46	487%	-0.39	86%	0.84	1051%	-0.21	74%	0.51	390%
IE5.4 (120hr)	Control	0.00	-	0.00	-	0.24	-	0.13	-	0.05	-
	+Fe	0.71	na	0.15	na	0.46	89%	0.29	119%	0.17	248%
IE5.5 (72hr)	Control	0.02	-	-0.34	-	0.47	-	0.15	-	0.23	-
	+Fe	0.38	1637%	0.19	157%	0.70	49%	0.18	25%	0.19	-16%
	+N	0.03	19%	-1.75	-421%	0.06	-87%	0.15	0%	0.22	-3%
	+FeN	0.34	1475%	0.10	129%	0.42	-11%	0.19	29%	0.18	-21%
IE5.6 (120hr)	Control	0.06	-	-0.02	-	0.26	-	0.13	-	-0.23	-
	+Fe	**0.77**	1090%	1.44	6461%	1.01	286%	0.31	137%	-0.15	36%

? found that *E. huxleyi* exhibited growth rates in laboratory cultures of between $0.5\,d^{-1}$ and $0.9\,d^{-1}$ and that *E. huxleyi* and *C. pelagicus* could grow at similar rates ($0.7\,d^{-1}$) when grown under identical light and temperature conditions. In this study, net growth rates of *E. huxleyi* and *C. pelagicus* ranged from $-0.2\,d^{-1}$ to $2\,d^{-1}$ and from $-0.6\,d^{-1}$ to $0.3\,d^{-1}$, respectively, and *Syracosphaera* spp. net growth rates ranged between $-1.3\,d^{-1}$ to $1.1\,d^{-1}$, with the highest net growth rate for all three species occurring in the +Fe treatments (Table **??**). This disparity in

growth rates between different coccolithophore taxa clearly demonstrates the importance of looking at species-level information when considering community response to nutrient addition. The +Fe treatment of IE5.6 consistently exhibited the highest net growth rates overall, and *E. huxleyi* tended to have the highest net growth rates within treatments (relative to *Syracosphaera* spp. and *C. pelagicus*, with the exception of IE5.1).

Table 2.7: Comparative coccolithophore growth rates. **Emiliania huxleyi, Syracosphaera* spp. and *C. pelagicus* were highlighted due to the fact that they are present in every bioassay and treatment where PIC was measured.

	Growth rate based on total cell numbers	**Growth rate based on cell PIC changes**	**Growth rates based on cell numbers***		
	(d^{-1})	(d^{-1})	*E. huxleyi*	*Syracosphaera* spp.	*C. pelagicus*
IE5.1					
Control	-0.4	0.2	-0.1	-1.3	0
+Fe	-0.1	0.5	0	-0.4	0.3
+FeN	-0.1	0.2	-0.2	-0.2	0
IE5.4					
Control	-0.01	-0.2	0.35	-0.06	-0.55
+Fe	0.2	-0.1	0.6	0.1	-0.5
IE5.6					
Control	0.0	0.3	0.4	-0.3	0.3
+Fe	1.3	0.5	2	1.1	0

The response of coccolithophores to experimental manipulation can also be assessed by examining the cellular levels of CP (**??**). The Iceland Basin bioassay (IE5.1, Figure **??**) CP showed no significant response to +Fe addition, although coccolithophore abundance in this bioassay was very low ($\lesssim 50\,\text{cells}\,\text{mL}^{-1}$) and this, coupled with initial higher ambient Fe concentrations compared with Irminger Basin stations, may shed light on the lack of response to Fe in this particular bioassay. In contrast, there was a significant response to +Fe addition in both Irminger Basin bioassays measured, with CP increasing in all treatments (Figures **??** and **??**). However, bulk measures of CP, and indeed cell-specific calcification (Cell-CF) (**?**), are often difficult to interpret without delving into the exact species composition and their relative contributions to community calcite and CP (**??**). To do this, the percentage of total calcite associated with each species present in the community was calculated as:

$$\%\,\text{Total Calcite} = \left(\frac{\text{C}_{\text{sp}}}{\text{Community Calcite}}\right) \times 100$$

where, C_{sp} is the cellular calcite content of a specific species and Community Calcite is the sum of all the

species' C_{sp}. C_{sp} values for cellular calcite for the coccolithophore species present in each bioassay (IE5.1, IE5.4 and IE5.6) were obtained from the following papers; **?** and **?** for *E. huxleyi*, **?** for *C. pelagicus*, **?** for *Syracosphaera* spp., **?** for *Calcidiscus leptoporus and Helicosphaera carteri*, and **?** and **?** for *Rhabdosphaera* sp.*Coccolithus*, *Calcidiscus, Rhabdosphaera* and *Helicosphaera* are among some of the largest and/or heaviest calcified modern coccolithophore species and thus, despite only making up between 1 and 28% of the total coccolithophore abundance in these three bioassays (with *E. huxleyi* and *Syracosphaera* spp. dominating the coccolithophore community numerically), their contribution to total community calcite is disproportionately high (Table **??**).

The relative proportions that different coccolithophore species contribute to the overall community abundance, and how those proportions change in response to Fe amendment, significantly changes the dominant source of CP in the community (see Table **??**). In this study, the numerically dominant coccolithophore species in bioassays changed between *E. huxleyi* and *Syracosphaera* spp.. However, these species are small and have low relative cellular calcite contents when compared with larger and more heavily calcified species such as, *C. pelagicus*, *C. leptoporus*, *H. carteri* and *Rhabdosphaera* sp., which were present in over half of the bioassays in relatively low abundances.

Due to the high cellular calcite content of these four species relative to *E. huxleyi,* or the similarly calcified *Syracosphaera* spp., their effect on bulk CP measurements is disproportionately high. Thus, both increases and decreases in these species' abundance in response to Fe amendment significantly alters the community calcite content and CP (Table **??**). Additionally, a decline in these species abundance may mask a positive responses of *E. huxleyi* and *Syracosphaera* spp. to +Fe addition, as occurred in IE5.6 where there was a large and significant *increase* in community calcite content, but a decline in cell-specific calcification due to a significant drop in *C. pelagicus* abundance (see Table **??**). These results in terms of the dominance of community calcite content by *C. pelagicus* are supported by studies from the Iceland Basin and the Arctic Ocean (**?**). Due to the variability in the occurrence of *C. lepotoporus*, *H. carteri* and *Rhabdosphaera* sp. (i.e they were not present in every treatment of each bioassay, or in every bioassay), their response to +Fe is unclear. *C. pelagicus* abundance decreased in the +Fe treatments in the Irminger Basin where Fe concentrations were low initially. However, in the Iceland Basin, *C. pelagicus* abundance increased slightly in the +Fe treatment. Additionally, *C. pelagicus'* contribution to the total community calcite decreased in the Irminger Basin +Fe treatments and increased slightly in the Iceland Basin treatment. *E. huxleyi* abundance increased in the +Fe treatments in both the Iceland and Irminger Basins, while *Syracosphaera* spp. abundance decreased (Table **??**).

These results show the importance of understanding the subtleties involved in coccolithophore responses to Fe.

Table 2.8: Breakdown of the coccolithophore community calcification. Cellular calcite; *E. huxleyi* (**??**), *C. pelagicus* (**?**), *Syracosphaera* spp. (**?**), *C. leptoporus* (**?**), *H. carteri* (**?**), *Rhabdosphaera* sp. (**??**).

	Bulk CP	**Cell-specific calcification**	**% of total coccolithophore abundance made up of**						**% of total Calcite**					
	(μmolCm^{-3}d^{-1})	(pmolCcell^{-1}d^{-1})	*E. huxleyi*	*C. pelagicus*	*Syracosphaera*	*C. leptoporus*	*H. carteri*	*Rhabdosphaera*	*E. huxleyi*	*C. pelagicus*	*Syracosphaera*	*C. leptoporus*	*H. carteri*	*Rhabdosphaera*
IE5.1														
Initial	0.14	0.003	48	0	50	2	0	0	24	0	58	43	0	0
Control	29.94	1.43	88	4	8	0	0	0	27	70	3	0	0	0
+Fe	42.12	1.24	61	5	32	3	0	0	12	74	11	22	0	0
+FeN	27.89	0.83	41	3	44	5	8	0	5	59	24	25	48	0
IE5.4														
Initial	31.58	0.08	10	3	87	0	0	2	2	56	40	0	0	34
Control	37.86	0.10	21	1	76	0	0	1	8	30	58	0	0	34
+Fe	77.48	0.15	27	1	71	0	0	1	11	24	59	0	0	26
IE5.6														
Initial	25.50	5.93	17	17	54	0	0	0	2	90	9	0	0	0
Control	73.47	17.87	36	28	24	0	0	0	2	95	3	0	0	0
+Fe	131.21	1.71	57	1	41	0	0	0	33	36	32	0	0	0

The initial composition of the coccolithophore community as well as the initial, differing biogeochemistry of the North Atlantic regions investigated (i.e. Iceland Basin, low initial macronutrient concentrations and higher initial Fe concentrations; Irminger Basin, non-limiting concentrations of macronutrients coupled with limiting concentrations of Fe), all contribute to the subsequent response of different coccolithophore species in these different regions. In the Iceland Basin, where the small ($< 5\,\mu$m) phytoplankton made up the majority of the chlorophyll *a* biomass and the coccolithophore community was heavily dominated by *E. huxleyi*, diatoms were less abundant (relative to the Irminger Basin), potentially due to limiting macronutrient concentrations despite higher Fe availability. In the Irminger Basin conditions were different (high macronutrient concentrations and low Fe concentrations), the coccolithophore community was more abundant and more diverse (with the concurrent increase in abundance and diversity of the diatom community). Species such as *C. pelagicus*, though not numerically dominant, can play a disproportionately large role in the community CP response to +Fe addition. Overall, Fe addition positively enhances coccolithophore growth rates and calcite production, but that response is heavily influenced by initial conditions, additionally coccolithophore composition does not change radically in responds to dFe addition..

2.4.3 Contrasting Responses to Iron Addition by Different Phytoplankton Groups

In a review of various +Fe addition experiments, it has been shown that, while all phytoplankton groups showed positive responses to +Fe addition, only diatoms bloomed, which was due to their ability to escape grazing pressure (**?**). Diatom abundance in the Irminger and Iceland Basins during our study were highly variable ($87 - 4576\,\text{cells}\,\text{mL}^{-1}$), though generally more abundant than coccolithophores ($< 1 - 561\,\text{cells}\,\text{mL}^{-1}$). Diatoms strongly responded to to +Fe and +FeN in the Iceland Basin (Figure **??**, **??** and **??**), where NO_x and silicic acid were in limiting concentrations. Previous +Fe addition experiments (e.g. FeXs) have shown that, when diatoms are relieved from Fe stress, their silica requirements are reduced (**?**). In the Irminger Basin, diatom cell abundances were much higher than in the Iceland Basin ($522 - 4576\,\text{cells}\,\text{mL}^{-1}$), with notable increases (see Table **??**) in response to +Fe addition. The diatom community was strongly dominated by *Pseudonitzschia* spp. and small *Fragilariopsis* spp. in most bioassays and treatments, though the community was more evenly distributed in the Iceland Basin than in the Irminger Basin. In a comparison of eight different Fe fertilisation experiments from the Northwest Pacific Ocean to the Pacific sector of the Southern Ocean, **?** found that the species of *Pseudonitzschia* universally dominated the diatom community after Fe fertilization. This trend of small, lightly silicified diatom species dominating the response to +Fe addition appears to also occur in the Iceland and Irminger Basins.

The success of one phytoplankton group over another has been hypothesised to be dependent on a mix of

factors, including the bottom-up supply of nutrients or top-down grazing (**?**). Models have predicted that when silicic acid concentrations reach a critical, low state, non-silicious phytoplankton such as coccolithophores may dominate (**?**). **?** found that in the Southern Ocean, a concurrent upwelling of Fe combined with elevated nitrate relative to silicic acid (high residual nitrate) - as was seen in the current study in the Irminger Basin - created optimal conditions for the increased abundance of non-silicious phytoplankton relative to diatoms. Hence, the level of residual nitrate present in an environment may predict whether coccolithophores respond to +Fe addition. Diatoms generally require nitrate and silicic acid in equal proportions (**?**), and growth in the open-ocean may be limited by silicic acid availability. In our study, residual nitrate (calculated by subtracting total nitrate from silicic acid (**?**)) showed that initially, in the Iceland Basin, NO_x and silicic acid are found in roughly equal proportions and that by the end of the three Iceland Basin bioassays (control and +Fe treatments), nitrate had become limiting. However, in the Irminger Basin, both nitrate and silicic acid were found in relatively high concentrations with high concentrations of residual nitrate ($1.94 - 4.80\,\mu$M). In IE5.6, both NO_x and silicic acid were drawn down to near zero concentrations in the +Fe treatment with a concurrent large increase in the diatom population (Figures **??** and **??**).

In contrast to the coccolithophores and diatoms, the small size class of phytoplankton (*Synechococcus* and picoeukaryotes) showed no obvious response to +Fe addition. *Synechococcus* abundance was not significantly different between treatments in either the Iceland or Irminger Basin bioassays (Figures **??**, **??**, **??**, **??**, **??** and **??**). Picoeukaryote abundance in the Iceland and Irminger Basins exhibited a positive response to +Fe addition, with increased growth rates relative to the control in all bioassays (Table **??**). Thus, it is possible picoeukaryotes are able to take advantage of lower concentrations of Fe due to their high surface area to volume ratio.

Cell size of the different phytoplankton taxa may explain why diatoms respond more obviously and impressively to +Fe addition. In IRONEX (iron experiment), it was shown that, although both large and small phytoplankton size classes responded to +Fe addition, the small phytoplankton were not able to form high biomass due to a concurrent increase in the grazing microzooplankton population (**?**). Coccolithophores are thought to have lower Fe requirements than coastal diatoms, which may explain *E. huxleyi's* success in areas where low Fe concentrations limit diatom growth (**??**). It is commonly thought that, under limiting Fe conditions, small phytoplankton ($< 5\,\mu$m) are more successful due to their ability to utilise Fe at low concentrations (**?**). However, by virtue of their small size they are also far more vulnerable to predation. **?** hypothesised that instantaneous grazing and Fe limitation could account for less than optimal growth rates of small phytoplankton taxa despite ideal growth conditions. Diatoms are generally grazed on by large mesozooplankton (>200 -500 μm), whereas the dominant grazers on coccolithophores

are likely to be microzooplankton ($< 200\mu$m). Though suppression of microzooplankton grazing has been suggested to be involved in the formation of coccolithophore blooms (**?**), there is currently very little information on grazing losses from coccolithophore communities from microzooplankton in non-bloom conditions.

Cell size differences and differential growth rates between different phytoplankton groups, as well as their differing nutrient requirements, provide significant insight into phytoplankton responses to +Fe addition and limitation. The small phytoplankton (such as picoeukaryotes and *Synechococcus*) may be less likely to show significant responses to +Fe addition, as their smaller size means they may not be limited to the same degree as the large phytoplankton such as diatoms and coccolithophores. However, interestingly, though the response of *Synechococcus* was less clear cut, picoeukaryote growth rates in the North Atlantic did show a positive response to +Fe addition relative the control which may reflect differing nutrient requirements. Under conditions where Fe may be a limiting factor, both coccolithophores and diatoms respond positively to +Fe addition by increasing their growth rates significantly, although the level of residual nitrate has a strong influence on whether diatoms dominated the response or if coccolithophores could successfully compete with them. Moreover, faster growing coccolithophore species (such as *E. huxleyi*) may be able to outcompete slower growing coccolithophores (e.g. *Syracosphaera* spp.), becoming more numerically dominant within the coccolithophore community after +Fe addition even if they are not the dominant coccolithophore species in the assemblage.

2.5 Conclusions and Wider Implications

This study expanded on initial findings by **?**, which suggested that the North Atlantic phytoplankton community as a whole was limited by the availability of dFe in summer and which also found circumstantial evidence of a positive response by *E. huxleyi,* and by **?** that found that dFe concentrations were likely an important control on CP and on coccolithophores. The results of this study clearly show that coccolithophores do indeed respond to dFe addition experimentally with enhanced growth rates and CP.

Responses of bioassays in the North Atlantic to Fe and nutrient amendment were markedly different depending on a number of factors. The location of the bioassay - the Iceland or the Irminger Basin - was very important in determining the community's response to any subsequent nutrient or Fe amendment. Another aspect of this 'location' effect was the importance of the individual bioassays' initial conditions in determining community responses to nutrient addition. Additionally, the length of the bioassay affected the community response. In this study, bioassays were run for 48-, 72- and 120-hours. The short-term bioassays (two 48-hour and one 72-hour experiments) were conducted in the Iceland Basin, where there was little response to Fe from the coccolithophore community within

the 48-hour incubations. However, in the 72-hour incubation there was a notable increase in both coccolithophore and diatom abundance, suggesting that 48-hours is an insufficient length of time for the phytoplankton to respond. **?** showed that incubations of less than 48-hours were of an insufficient length in order to observe a phytoplankton response to Fe in terms of cell numbers, although increased NO_3 uptake was observed in this time frame. Interestingly, the 'treatment effect' was not significant with respect to coccolithophore or diatom community structure. However, other measured parameters such as chlorophyll *a*, NO_x and silicic acid concentrations, were all significantly different between treatments, with the Iceland Basin bioassays tending to show significant positive responses to +N and +FeN treatments and the Irminger Basin bioassays responding strongly to +Fe amendments. In future studies involving +Fe addition incubations, it is important to ensure adequate time, at least 72-hours, is allowed for incubations such that the phytoplankton community (and its different constituents) have enough time to respond to Fe amendment. In this study it is unclear if the lack of response to Fe by the phytoplankton community in the Iceland Basin is in part due to the shorter length of the bioassays. Additionally, due to the poor spatial resolution of this study, large-scale implications of potential iron-limitation in the Iceland and Irminger Basins are difficult to assess.

The contrasting initial nutrient and coccolithophore community conditions measured in the Iceland and Irminger Basins at the start of the bioassays and their responses to +Fe addition may give may help researchers to predict how coccolithophore communities might respond to Fe by taking into account different initial conditions. For example, knowledge of factors such as the initial composition of the coccolithophore communities (which does not change significantly in response to dFe addition), as well as initial nitrate to silicic acid ratios (which is an indication of which phytoplankton taxa will dominate community composition) allow insight into how the carbonate and counter-carbonate pumps may be affected by Fe availability. These results highlight the importance of clearly elucidating the composition of the coccolithophore community when it comes to interpreting responses to +Fe addition in terms of calcite production. Additionally, Fe is one trace metal among a number required by phytoplankton for growth and metabolism (**???**). Several laboratory studies have shown that *E. huxleyi* requires trace metals such as iron, zinc and cobalt for its metabolism (**??**). Indeed, zinc availability has been shown to limit coccolithophore growth in the Subpolar North Pacific (**?**). Rates of atmospheric deposition of both Fe and zinc have been estimated to be ten times lower today than glacial times (**?**) and the supply of trace metals to the open ocean through aeolian dust may be affected by changes (**?**). Hence, there is a need for a wider perspective on trace metal limitation of coccolithophore communities than just Fe limitation.

Acknowledgements

Thanks go to the Master, the officers and crew, and participating scientists onboard the *RRS Discovery* during this study.

Work from this chapter was made possible through funding by the National Environmental Research Council (NERC) Postdoctoral Fellowship to Dr Alex J Poulton, grant no. NE/F015054/1; NERC standard grant to Prof. Eric Achterberg and Prof. Mark Moore for cruise, grant no. NE/E006833/1.

Chapter 3

Coccolithophore responses to trace metal addition (Fe, Zn, Co) across the Atlantic and Indian sectors of the Southern Ocean's Great Calcite Belt

Abstract

The Great Calcite Belt (GCB) is a large band of elevated particulate inorganic carbon (PIC) water across the Southern Ocean, resulting from elevated coccolithophore concentrations. It covers approximately 16% of the global ocean (**?**) and is an important region for the global calcite budget. Despite the fact that large swathes of the Southern Ocean are iron (Fe) limited and are characterised by high residual macronutrient concentrations, the GCB develops in an area of seasonal nutrient drawdown. The success of one phytoplankton group over another in the GCB is potentially related to the bottom-up supply of nutrients, despite relatively low Fe requirements for coccolithophores (relative to other phytoplankton groups) there is evidence of their being limited by Fe availability in the North Atlantic (**??** and Chapter 2). There is also evidence of zinc (Zn) limiting coccolithophore growth in the north-eastern subarctic Pacific (**?**). Thus, there is the potential that coccolithophores are limited by trace metal availability. The aim of this chapter is to examine coccolithophore responses to trace metal addition (iron, zinc and cobalt (Co)) across the GCB. During two cruises, one to the South Atlantic (2011) and the other to the South Indian (2012) sectors of the Southern Ocean, six bioassay experiments (two in the South Atlantic and four in the South

Indian Ocean) were conducted to test the response of coccolithophores to trace metal additions whilst contrasting their response with that of the diatom community. Results show increased growth rates of coccolithophores in response to Fe addition in three of the six bioassays and also that coccolithophores responded positively to Zn in three of the six bioassays. Diatom growth rates increased in three of the six bioassays in response to Fe and increased dramatically in response to Zn in one bioassay. Coccolithophore and diatom community composition did not show significant variation between treatments ($p = 0.989$ and 984, respectively), however, the location of each bioassay (South Atlantic or South Indian Ocean) was a significant factor in determining responses in community composition ($p = 0.001$). Nitrate drawdown was significantly increased in the Fe treatments in three bioassays and in the Zn treatments in two bioassays ($p < 0.05$). This study confirms Fe limitation in coccolithophores and diatoms in the Southern Ocean, and is the first study from the Southern Ocean showing positive coccolithophore responses to Zn addition, highlighting a strong potential for Zn limitation of coccolithophore growth and pelagic calcite production. In contrast, there was little response to Co addition across the South Atlantic and South Indian Oceans, with the exception of a single bioassay (RV1) where coccolithophore and diatom abundance increased relative to the control. The lack of response to Co was potentially due to non-limiting concentrations or to substitution of Zn for Co in limiting conditions. Results of this chapter suggest further studies are needed to examine at Zn limitation of coccolithophores in the Southern Ocean and other oceanic regions.

3.1 Introduction

Trace metals such as iron (Fe), zinc (Zn) and cobalt (Co) are involved in a wide range of catalytic and redox functions in phytoplankton cells (**?**); as co-factors for a number of common proteins, such as ferredoxin (Fe), involved in photosynthesis; nitrate reductase (Fe) and alkaline phosphatase (Zn) involved in nutrient uptake; carbonic anhydrase (Zn) involved in carbon acquisition; and vitamin B_{12} (Co) (**??**). Hence, trace metals are essential for phytoplankton growth and their availability influences algal physiology, ocean productivity and biogeochemical cycles (**?**). The role of Fe in limiting phytoplankton growth in the Southern ocean is now well established (e.g. **?**), however the potential for trace metals such as Zn and Co to limit phytoplankton growth or photosynthesis is not well documented. Evidence of Zn and Co limitation of growth of certain open ocean phytoplankton species has been shown: for example Zn has been shown to limit growth of the diatom *Thallassiosira weissflogii* (**?**), Co may limit the cyanobacteria *Prochlorococcus* (**?**), and the haptophyte *Phaeocystis antarctica* has been shown to be co-limited by both Zn and Co, (**?**).

Trace metals are supplied to the ocean in a number of ways, through coastal erosion, hydrothermal inputs and

glacial sediments (**?**), coastal areas can be supplied from rivers as suspended sediments, similarly glacial input can be an important source of trace metals to coastal and near-coastal areas (**?**). However, the dominant external source of trace metals to the open oceans is via transport of aeolian dust (**?**). Atmospheric trace metal dust deposition has varied substantially over geological time (**?**), with the rates of Fe and Zn deposition in the modern ocean up to ten times lower than in glacial times (**????**). This suggests that modern phytoplankton may experience more Fe and/or Zn limitation than those in the geological record. The role of Fe in promoting primary production (PP) by phytoplankton is also well documented, especially in high nutrient, low chlorophyll (HNLC) areas such as the Southern Ocean, where limiting concentrations of Fe (<0.2 nM) are well documented (e.g. **?**). However, although there is limited evidence of Zn availability influencing phytoplankton growth (particularly coccolithophores (**??**), no consensus yet exists on the significance of such open ocean Zn limitation in terms of pelagic calcite production (**?**). In fact, diatoms in HNLC areas exhibit increased nitrogen utilization, as well as increased biomass production, in response to Fe or combined Fe and Zn addition (**??**). In contrast, evidence concerning phytoplankton limitation by Co is even more patchy, though there is evidence from two studies conducted using different phytoplankton culture strains of Co limitation of the cyanobacteria, *Prochlorococcus* (**?**), and Zn-Co co-limitation of *Phaeocystis antarctica* (**?**).

An important role of Zn in phytoplankton is as a co-factor in carbonic anhydrase (CA), which enhances the rate of dehydration of bicarbonate ions (HCO_3^-) to free CO_2 (**?**). Zinc may also play a role in silicification (frustule formation) by diatoms (**??**), although this has been debated with **?** demonstrating that only 1 to 3% of Zn in diatom cells is actually part of the frustule. Previous studies have also indicated that phytoplankton have adapted to the modern ocean's lower Zn concentrations by decreasing their cellular Zn requirements. For example, some phytoplankton (e.g. the diatom *Thalassiosira weissflogii*) are able to replace Zn with similar metals such as Co (**?**). Surface water concentrations of Zn in the Pacific and Atlantic oceans are comparable to that of Fe (~ 1 nM) (**????**) and Zn typically occurs in surface waters at concentrations of ≤ 0.1 nM (**?**). Concentrations of Zn and Co in the open-ocean exhibit a nutrient-like depth profile similar to those of major nutrients (N, Si and P) (**??**), with depleted surface concentrations that increase with depth as remineralisation and macronutrient release occurs (**?**). The percentage of usable Zn available to phytoplankton (as with Fe) is also reduced by the presence of organic ligands which bind to the free Zn ions [Zn^{2+}], and the remaining small fraction of 'free' Zn (~ 0.01 - 0.1 nM, **?**) is thought to be low enough to limit phytoplankton growth (**??**). In spite of these relatively low Zn concentrations, a number of studies have shown that open ocean species of phytoplankton grow at or near maximum rates at low Zn concentrations (0.001 - 0.01 nM) (**??**). Moreover, as Zn can be replaced by Co (**??**) studies which found

phytoplankton growing optimally under limiting Zn conditions often had saturating Co concentrations which may indicate that phytoplankton were utilising Co instead of Zn. Utilisation of Co is minimal in the metabolism of higher organisms (**?**) but is thought to be integral to the algal formation of vitamin B_{12}, which is required for the synthesis of several vital enzymes (**??**). Furthermore, the formation of B_{12} was shown to double in Co amended experiments performed in low-dissolved Co waters ($\sim 20\,\mathrm{p\,mol\,L^{-1}}$) in the North Atlantic (**?**). With Co concentrations in the open ocean $\sim 25\,\mathrm{p\,mol\,L^{-1}}$, and the concentrations of free [Co^{2+}] at $< 5\,\mathrm{f\,mol\,L^{-1}}$, Co also has the potential to be a limiting factor for phytoplankton (**?**).

Though there is emerging evidence that Fe availability influences coccolithophore growth (**?** and Chapter 2 of this thesis), relatively little is known of the roles of Zn or Co in coccolithophores. *Emiliania huxleyi* requires trace metals for its metabolism and it has been shown that *E. huxleyi* is able to replace Zn with Co (**?**). Zinc requirements of *E. huxleyi* are comparatively low relative to other phytoplankton species (**??**) which may be attributed to the fact that in *E. huxleyi*, carbonic anhydrase is thought to have no essential function in inorganic carbon acquisition (**?**) and Zn can be fully substituted with Co by *E. huxleyi* (**?**). Under Fe limitation, both growth and calcification rates decrease, whereas under Zn limitation cellular growth rates and calcification become decoupled in *E. huxleyi*, which causes a build up of cellular calcite as calcification continues (**?**). Observations of Zn limitation of coccolithophores are varied, for example in the subpolar North Pacific coccolithophore growth has been shown to be limited by Zn availability (**?**) whereas in the Tasman Sea (east of Australia) the growth rate of *E. huxleyi* was unaffected by low Zn concentrations (**?**). It is important to note, however, that Zn limitation is thought to primarily affect the growth of organisms that use carbonic anhydrase dependent HCO^{-} transport system, whereas coccolithophores exhibit very little or no carbonic anhydrase activity as they are thought to be able to use CO_2 formed from HCO_3^- during calcification (**?**). In fact, all coccolithophores appear to use HCO_3^- as their main source of carbon for calcification (**??**).

The GCB is a band of elevated particulate inorganic carbon (PIC) water in the Southern Ocean observable from space during each austral spring and summer (**?**), which covers an area of approximately $88 \times 10^6\,\mathrm{km^2}$, from south of the ~ 30ºS parallel and extends southward to ~ 60ºS (**?**). The elevated PIC levels in the GCB are a result of elevated concentrations of coccolithophores, though their relative abundance to other phytoplankton groups is currently unclear. The PIC found in the GCB is thought to contribute up to 26% of PIC globally despite the GCB only making up approximately 16% of the global ocean by surface area (**?**).

In situ investigations of the GCB in 2011 and 2012 showed an extensive area of relatively high coccolithophore abundance (cells and detached coccoliths) in the GCB, which exists in an area of seasonal dissolved silicic acid

drawdown suggesting the presence of diatoms (i.e. the seasonal high nutrient (nitrate), low silicate part of HNLC). Previously, phytoplankton blooms were thought to consist of a series of sequential blooms dominated by individual phytoplankton types, however, remotely sensed particulate inorganic carbon (PIC) and chlorophyll data have shown that in many open ocean regions, coccolithophore blooms can co-exist with those of other phytoplankton taxa (**???**). **?** have also shown that in regions where phytoplankton taxa co-exist, such as the Southern Ocean (and parts of the North Pacific and North Atlantic), dFe is a major limiting nutrient. Furthermore, **?** found a correlation between regions where phytoplankton succession occurred and regions of high dFe availability, with regions where phytoplankton co-exist associated with low Fe availability.

As different groups of phytoplankton have differing trace metal requirements (**??**), the effect of the availability of these trace metals on the phytoplankton community as a whole needs to be dissected by examining the response of the different taxa individually. In light of evidence that coccolithophores respond to Fe addition (**??** and Chapter 2 of this thesis), and limited evidence of a response to Zn addition (**?**), the aims of this chapter were to: (1) investigate the response of coccolithophores to trace metal (Fe, Zn and Co) additions in terms of growth rates and community composition; and (2) compare and contrast this response with that of the diatom community. It is hypothesised that coccolithophores will (1) respond positively to Fe and Zn addition, with increased growth rates, but that (2) coccolithophores will not respond to Co and (3) that diatoms are expected to respond more quickly to trace metal addition. Six on-deck incubation experiments were performed during two cruises to the South Atlantic (2011) and South Indian (2012) oceans. Incubations were amended with Fe, Zn or Co and sampled to examine the response of the coccolithophore and diatom community.

3.2 Methods

3.2.1 Sampling

Data was collected from two cruises in the GCB in 2011 and 2012. The first cruise sampled the South Atlantic Ocean sector of the GCB and ran from January to February of 2011 (MV1101). The ship sampled between Punta Arenas, Chile and Cape Town, South Africa. The second cruise took place in the South Indian Ocean sector and ran from February to March of 2012 (RV1202). The second cruise sampled between Durban, South Africa and Fremantle, Australia. Sampling occurred between 38ºS and 60ºS at two to three day intervals, covering a wide range of oceanic regions and features. Letters 'MV' for MV1101 and 'RV' for RV1202 have been used in text to differentiate between the two cruises' station numbers based on the use of the ship is *R/V Melville* in 2011 and

R/V Revelle in 2012 (Figure **??**). Dissolved Fe (dFe), dissolved Zn (dZn) and dissolved Co (dCo) concentrations were determined by Peter Morton following the methods of **?**, with the data provided for this study by Florida State University.

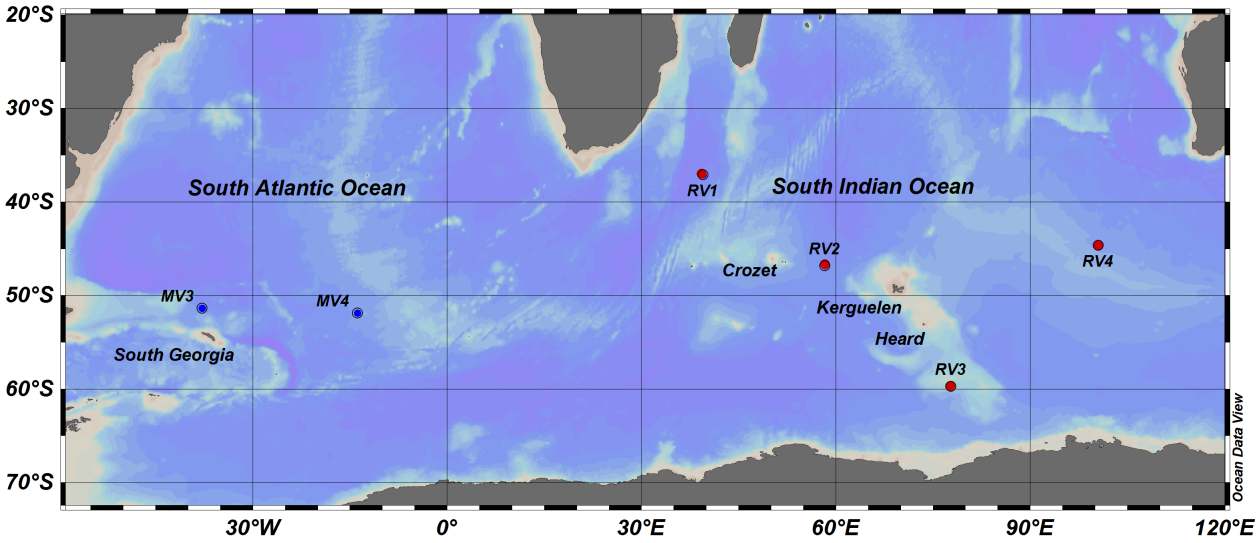

Figure 3.1: Map of the Great Calcite Belt, Southern Ocean showing the location of each of the bioassay sampling sites in the South Atlantic ('MV' stations from the 2011 cruise, indicated by blue dots) and South Indian ('RV' stations from the 2012 cruise, indicated by red dots) sectors of the Southern Ocean (**?**).

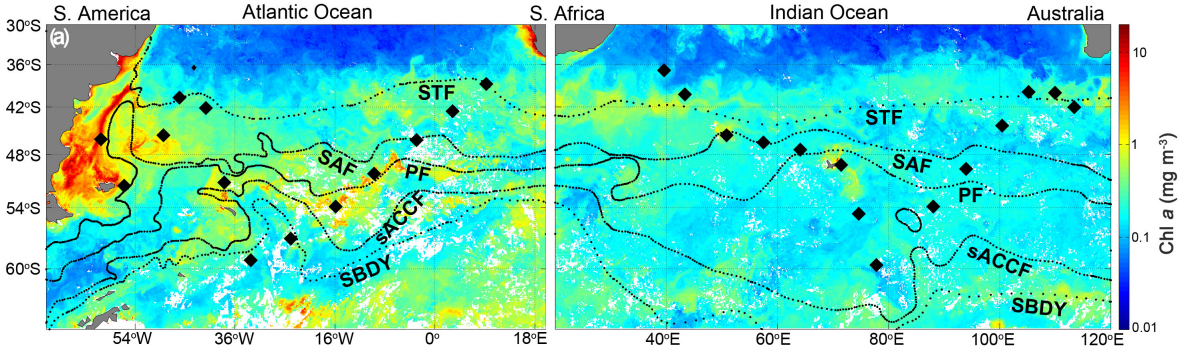

Figure 3.2: Rolling 32-day composite taken from MODIS-Aqua showing chlorophyll a (μgL^{-1}) for the South Atlantic (17th January to 17th February, 2011) and the South Indian sector (18th February to 20th March, 2012) and the averaged positions of fronts as defined by **?**; Sub-Tropical front (STF), Sub Antarctic front (SAF), Polar Front (PF), Southern Antarctic Circumpolar Front (SACCF) and Southern Boundary (SBDY) (taken from **?**).

3.2.2 Bioassays

Seawater for all the incubation experiments was collected from a depth of 20 m using a 30L GO-Flo bottle deployed on a non-metal wire (1.4" Aracom Mini-Line). Bottles were then transported into a positive-pressure clean van and water was gently dispensed into 10L low-density polyethylene cubitainers. A 200μm mesh was utilised, in-line,

to remove larger micro- and mesozooplankton grazers. All bottles and plasticware were acid-cleaned prior to use and trace metal clean techniques (**?**) were utilized at each step. Bottles and plasticware were first soaked in a 1% Micro detergent for several days and then rinsed using ultrapure >18.2MΩ water and soaked in 1 M reagent HCl for several more days before being rinsed once more and air dried before use.

Seawater for incubations was decanted into four Low-density polyethylene cubitainers and were then spiked with either, Fe, Zn, Co or left unamended as a control. Trace metal solutions were made up from AAS (Atomic Absorption Spectroscopy) standards diluted to 0.01 M Optima HCl.

Bioassays MV3 and MV4s were treated with Fe, Zn and Co in concentrations of 2.0, 2.0 and 0.4 nM respectively, they also had approximately 4μM of nitrate added to the Fe and Zn treatments due to the high level of AAS standard solution needed. Incubations MV3 and MV4 were conducted in nitrate-replete waters ($>$ 15μM nitrate), thus, these additions are unlikely to have affected the experimental results. During the 2012 cruise, stock solutions of higher concentrations were used and Fe, Zn and Co additions were made of 2.0, 2.0 and 0.5 nM respectively, each addition involved the addition of negligible nitrate through the use of a different AAS solution.

Sample seawater was decanted into triplicate 2.5L polycarbonate bottles. Bottles were filled to the top in order to minimize head space, and were then sealed with Parafilm and vinyl tape, and placed in incubators at 50% surface irradiance and allowed to incubate for between ~73- and 102-hours in the first cruise and for between ~120- and 160-hours during the second cruise. Experiment durations were determined based on observed chlorophyll *a* changes and macronutrient drawdown as well as changing surface seawater temperatures during MV1101.

During the 2011 cruise, incubator temperatures were maintained using surface seawater circulated through the ship's through-hull system. In some instances, surface seawater temperatures varied - such as during north or south transits - which led to changing temperatures relative to initial conditions. During the 2012 cruise, incubator temperatures were maintained using a deck-board heater/chiller unit which allowed temperatures to remain constant when the ship transited across oceanographic temperature gradients. Temperatures were recorded daily to ensure that correct temperatures were maintained during incubations. However, incubation RV3 started in 1ºC water, and temperatures gradually warmed to 4ºC over the course of the 6-day incubation, whilst sea surface temperatures increased to 9ºC during this period.

3.2.3 Determination of Phytoplankton Community Composition: Enumeration and Identification

Phytoplankton community composition and abundance were examined using scanning electron microscopy (SEM) analysis of the filtered bioassay seawater samples. Between 250 and 500mL of water from the bioassays was

gently vacuum-filtered onto 25 mm Whatman 0.8μm pore-size polycarbonate filters. These were then rinsed in trace ammonium solution (pH 9-10) in order to prevent salt crystals forming, which could interfere with producing clear SEM images. Filters were then placed into Millipore Petri dishes and dried overnight at 30ºC before being stored at room temperature for later analysis.

Back in the laboratory ashore, a small portion ($\sim 0.5 \times 0.5$ cm) of the filters were mounted onto a 12 mm aluminium pin stub with carbon glue and sputter coated with 20 nm of gold. SEM images were obtained using a LEO1450 microscope, operated with a tungsten filament at 10 kV, spot size 500 pA. A secondary detector was used and the images were taken at 1200 $\times$ magnification. For cell counts, a 16×15 frame grid of individual fields of view was imaged and archived according to a tailored macro. This ensured SEM images were recorded in the same pattern for all of the samples.

Each coccolithophore or diatom cell in the ~240 fields of view (FOV) per filter were identified and counted, a total of 6,298 SEM images were counted. FOVs which were blurred or obscured were discounted from the final 'cells mL^{-1}' calculations. Species identification followed **?** for the coccolithophores and **?** and **?** for the diatoms. In bioassays where cells were abundant (> 300 cells mL^{-1}), 50 images were counted. Cells were identified down to species level where possible, however, due to some poorer quality images this was not always possible.

Cell abundances (cells mL^{-1} of seawater) were calculated as:

$$\text{Cell Abundance} = \frac{(\text{CxR})}{\text{V}} \tag{3.1}$$

where C is the number of cells counted, R is a ratio of the total filtration area to the counted area (as detailed in equation **??**, below) and V is the volume of water filtered (mL).

$$\text{R} = \frac{\text{A}}{\text{A}_{\text{FOV}} \times \text{N}_{\text{FOV}}} \tag{3.2}$$

A is the filtration area (mm^2), A_{FOV} is the area of one FOV and N_{FOV} is the total number of FOVs counted.

Standard errors (S.E.) for SEM count data per bioassay treatment (in cases where only one SEM was counted per treatment) were estimated following **?**, assuming normal distribution, by taking the square root of the counted cells (C) divided by the equivalent volume of the sample investigated ($\text{A} \times (\frac{\text{V}}{\text{F}})$) (see **?**);

$$\text{S.E.} = \sqrt{\left(\frac{\text{C}}{\text{Ax}\left(\frac{\text{V}}{\text{F}}\right)}\right)} \tag{3.3}$$

where, A is the area investigated (mm^2), F is the total filter area investigated (mm^2) (which is determined by the area of the FOV multiplied by the number of FOVs counted) and V is the volume filtered (mL).

3.2.4 Ancillary Measurements

Incubation bottles were sampled two to three times over the course of each incubation for total chlorophyll *a* and macronutrients (nitrate+nitrite and silicic acid). During the Atlantic sector incubations, bottles were sampled at approximately 48-hours and 72-hours or 96-hours. During the Indian sector, bottles were sampled at three time points between days 2 and 6.

Seawater samples (200mL) were also collected for nitrate+nitrite (NO_x) and silicic acid measurements, which were filtered through 0.4μm 25 mm PCTE filters then dried at 60ºC before storage. Samples were digested in 0.2 M NaOH (**?**). Dissolved nutrients were analysed by an ODF (Oceanographic Data Facility) technician on board. Detection limits were 0.02μM and 0.5μM for NO_x and silicic acid, respectively.

Seawater samples (100mL) were collected for chlorophyll *a* measurements, which were filtered through 0.4μm 25 mm Millipore HA filters and frozen. Samples were then extracted using a 90% solution of acetone and run on the fluorometer (following methods in **?**).

3.2.5 Data Analysis

Statistical analysis of biotic and abiotic data was undertaken whereby one-way ANOVA tests were used to determine if there were significant differences between treatment responses in each bioassay experiment. Significant results obtained from ANOVA tests were further investigated using a *post hoc*, Tukey HSD (Honestly Significantly Different) test ($p < 0.05$) to determine which specific treatments were significantly different. ANOVAs were performed for total chlorophyll *a* concentrations, NO_x and silicic acid concentrations. Statistical tests were performed using R (**?**).

Phytoplankton counts (cells mL^{-1}) were analysed using the multivariate programme E-PRIMER (Plymouth Routines In Multivariate Ecological Research, version 6.16) (**?**). Bioassay treatments where less than one coccolithophore was present were removed from the analysis in order to prevent the results from being heavily skewed.

Coccolithophore and diatom abundance data were treated similarly, with both being transformed using a fourth root transformation in order to account for the wide range of abundance recorded. Both coccolithophore and diatom multivariate analysis followed the same routine. Between station differences were calculated using all species present, irrespective of their contribution to total abundance due to the importance of rare species' responses to trace metals.

A Bray-Curtis similarity matrix was calculated before applying hierarchical Cluster analysis and ordination via non-metric Multi-Dimensional Scaling (nMDS) in order to determine (dis-)similarities in species composition between treatments. Cluster analysis created a dendogram, which provides a measure of similarity of the different samples based on species composition. Factors were created for 'treatment', 'bioassay', 'length' and 'location' in order to better explore patterns in the coccolithophore and diatom community composition. Labelling of nMDS ordinations and Cluster diagrams using these factors allowed for better visual representation of how they may influence coccolithophore and diatom community structure.

Analysis of Similarity (ANOSIM) tests were then used to examine whether these pre-determined factors created statistically significant groups. Similarity Percentages (SIMPER) tests were used to identify which species were primarily providing the basis for discrimination between the observed sample clusters, using the rectangular data matrix with the added 'factors'. SIMPER generates a list of species that differentiate the different groups.

Finally, diversity indices were calculated based on the initial, untransformed abundance data in order to examine the observed differences between the previously determined significant groups. The number of species (S) and Pielou's evenness (J') were determined for both coccolithophore and diatom abundance data. Pielou's evenness is an indication of how evenly the biomass is distributed among the different species, without accounting for species richness. Pielou's evenness ranges between 0 and 1, with a low value indicating that the population is not evenly distributed amongst the different species with perhaps one or two species dominating.

3.3 Results

3.3.1 General Oceanography

Bioassays were collected across different environmental conditions (Table **??**) associated with changes in latitude and the Antarctic Circumpolar Current (ACC) front (see Figure **??**). Sea surface temperatures (SST) in the South Atlantic Ocean were fairly consistent with temperatures averaging 5.6 ± 0.4ºC. Temperatures in the second cruise decreased with latitude, from 21ºC in the first bioassay to 1.1ºC in the third bioassay, as the cruise track moved

north again, temperatures increased to 13ºC in the final bioassay (Table **??**).

Table 3.1: Locations and initial conditions of South Atlantic (MV) and South Indian (RV) Ocean bioassays. Sea surface temperature (SST), initial trace metal concentrations (dissolved iron (dFe), dissolved zinc (dZn), dissolved cobalt (dCo)), initial mean (±S.E) macronutrient concentrations (nitrate+nitrite (NO_x), silicic acid (SiO_4)) and initial coccolithophore and diatom abundance. Initial macronutrient measurements in the South Indian Ocean were single measurements.

	Lat (ºN)	**Lon** (ºE)	**SST** (ºC)	**dFe** (nM)	**dZn** (nM)	**dCo** (pM)	**Chl *a*** ($\mu g L^{-1}$)	**NO_x** (μM)	**SiO_4** (μM)	**Coccolithophores** (cells mL^{-1})	**Diatoms** (cells mL^{-1})
MV3	-51.362	-37.842	5.9	0.74	nd	nd	0.85	17.46 ± 0.05	2 ± 0.14	1579.39 ± 7.83	250.23 ± 3.11
MV4	-51.862	-13.868	5.3	0.73	1.32	45	0.71	23.1 ± 0.39	1.48 ± 0.05	< 0.88	437.71 ± 15.17
RV1	-37.074	39.492	21	0.25	29.75	26	0.16	0.06	1.30	94.53 ± 7.14	3.48 ± 1.37
RV2	-46.828	58.277	8.7	0.14	0.72	35	0.22	18.45	1.70	364.26 ± 14.32	127.96 ± 8.49
RV3	-59.712	77.458	1.1	0.24	3.57	62	0.26	27.74	40.10	0.95 ± 0.67	1636.02 ± 27.69
RV4	-44.617	100.499	13	0.38	0.28	16	0.32	6.38	0.50	187.24 ± 17.03	148.74 ± 8.92

The two South Atlantic bioassays were sampled from similar latitudes, however, MV3 was collected offshore of South Georgia and MV4 was sampled from the open ocean (Figure **??**). Initial conditions were fairly uniform between these two bioassays with respect to initial total chlorophyll *a* (0.85 and $0.71 \mu gl^{-1}$, respectively) and dFe (0.74 nM and 0.73 nM, respectively) concentrations. Initial silicic acid concentrations in MV3 were similar to MV4 ($2.0 \pm 0.1 \mu M$ and $1.5 \pm 0.1 \mu M$, respectively) ($p > 0.05$), while initial NO_x concentrations were significantly higher in MV4 than in MV3 ($23.1 \pm 0.4 \mu M$ and $17.5 \pm 0.1 \mu M$, respectively) ($p < 0.05$). Initial dZn and dCo measurements were not determined for bioassay MV3, while in MV4 initial dZn and dCo concentrations were 1.32 nM and 45 pM, respectively. Initial coccolithophore abundances were 1579.4 ± 7.8 cells mL^{-1} in MV3 and < 0.9 cells mL^{-1} in MV4, which reflected coccolithophore bloom conditions around South Georgia in MV4. In contrast, initial diatom abundances were relatively high and more similar: 250.2 ± 3.1 cells mL^{-1} in MV3 and 437.7 ± 15.2 cells mL^{-1} in MV4.

Bioassays collected from the southern Indian Ocean exhibited highly variable initial macronutrient and chlorophyll *a* conditions (Table **??**) which are reflective of the varying sample locations (Figure **??**). NO_x concentrations ranged from as low as $0.6 \mu M$ (RV1) to as high as $27.74 \mu M$ (RV3). Similarly, silicic acid concentrations ranged from a minimum of $0.5 \mu M$ to a maximum of $40.1 \mu M$ (RV4 and RV3, respectively). Initial total chlorophyll *a* concentrations were relatively low compared to the South Atlantic Ocean, only ranging from $0.16 \mu gL^{-1}$ in RV1 to $0.32 \mu gL^{-1}$in RV4. Initial dFe was generally low (<4 nM) in the South Indian Ocean bioassays, ranging from 0.14 nM to 0.38 nM (RV2 and RV4, respectively). However, both initial dZn and dCo concentrations were more

variable, with initial dZn concentrations ranging between a minimum of 0.28 nM in RV4 to a maximum of 29.75 nM in RV1 and initial dCo concentrations ranging between 16 pM in RV4 and 62 pM in RV3. Initial phytoplankton abundance was also highly variable across the four bioassays, though generally lower than MV3 in the Atlantic sector, with coccolithophore community abundance ranging from 1.0±0.7 to $364.3 \pm 14.32\,\text{cells}\,\text{mL}^{-1}$ (RV3 and RV2, respectively), and initial diatom abundance ranging from 3.5 ± 1.4 to $1636.0 \pm 27.7\,\text{cells}\,\text{mL}^{-1}$ (RV1 and RV3, respectively).

3.3.2 Bioassay Results: South Atlantic (2011)

The two bioassays from the South Atlantic were run for 102 and 73-hours, respectively. An analysis of variance (ANOVA) ($p < 0.05$) indicated that in the South Atlantic bioassays, there was no evidence of a response to trace metal addition with respect to changes in total chlorophyll *a* concentrations ($F(3,8) = 0.84$ and 1.41, $p > 0.05$, respectively) (Figures **??** and **??**). However, NO_x drawdown showed significant variation among the treatments ($F(3,8) = 1185.00$ and 73.34, $p < 0.05$) and although there was no change in silicic acid drawdown in bioassay MV3 ($F(3,8) = 2.80$, $p > 0.05$) there was evidence of a response to treatments in MV4 ($F(3,8) = 5.46$, $p < 0.05$) (see full list of ANOVA and Tukey HSD results in Appendix **??**).

Changes in nutrient drawdown ($\triangle NO_x$ and $\triangle SiO_4$) were assessed by determining the difference between initial and final macronutrient concentrations. *Post hoc*, Tukey HSD tests revealed that there was a significant change ($p < 0.05$) in NO_x concentrations between each of the different treatments in bioassay MV3 ($p = 0.00$) (Figure **??**), and that the greatest drawdown of NO_x occurred in the +Fe treatment ($1.47 \pm 0.03\,\mu$M). There was a significant increase in NO_x utilization in both the +Fe and +Zn treatments relative to the control, however NO_x utilisation in the +Co treatment was significantly less than in the control. There was a significant change in NO_x drawdown in MV4 in both the +Fe and +Zn treatments relative to the control ($p = 0.00$), with both treatments exhibiting significantly greater NO_x drawdown than in either the control or +Co treatments. NO_x utilization in both the control and +Co treatments were similar in magnitude ($0.61 \pm 0.08\,\mu$M and $0.76 \pm 0.05\,\mu$M, respectively). Although there was no significant change in silicic acid drawdown between any of the treatments in MV3 (Figure **??**), there was a significant increase in silicic acid drawdown in the +Co addition in MV4 ($p = 0.03$) when compared with the control (Figure **??**).

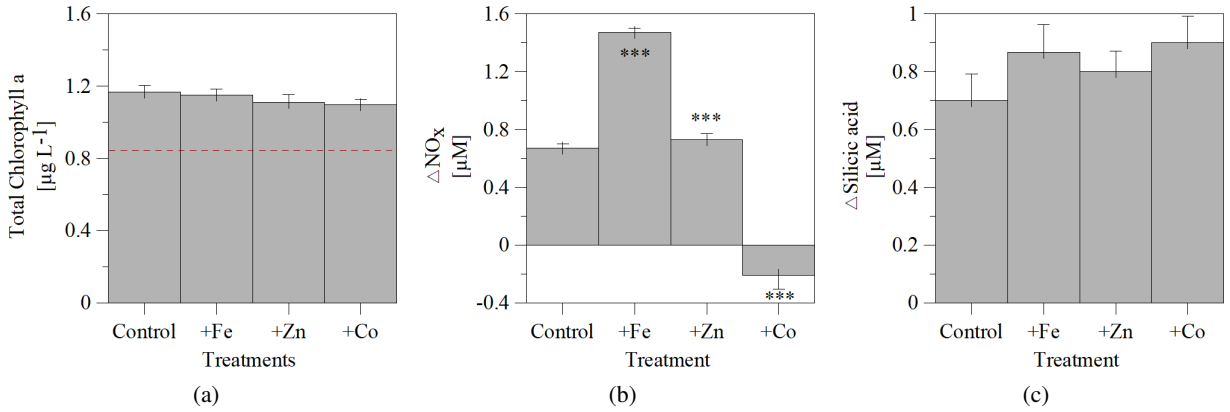

Figure 3.3: Bar graphs for bioassay MV3 showing a) total chlorophyll *a* concentrations (μgL^{-1}), b) the change in nitrate+nitrite (NO_x) concentrations (μM), and d) the change in silicic acid (SiO_4) concentrations (μM) over the course of the 102-hour bioassay. Error bars indicate standard errors. Dashed red lines indicate initial conditions. Asterisks indicate only significant results from Tukey HSD test for multiple pair-wise comparisons of significant ANOVA results between the control and treatments: * $p < 0.05$, ** $p < 0.01$, *** $p < 0.005$. n=3 for all bioassays.

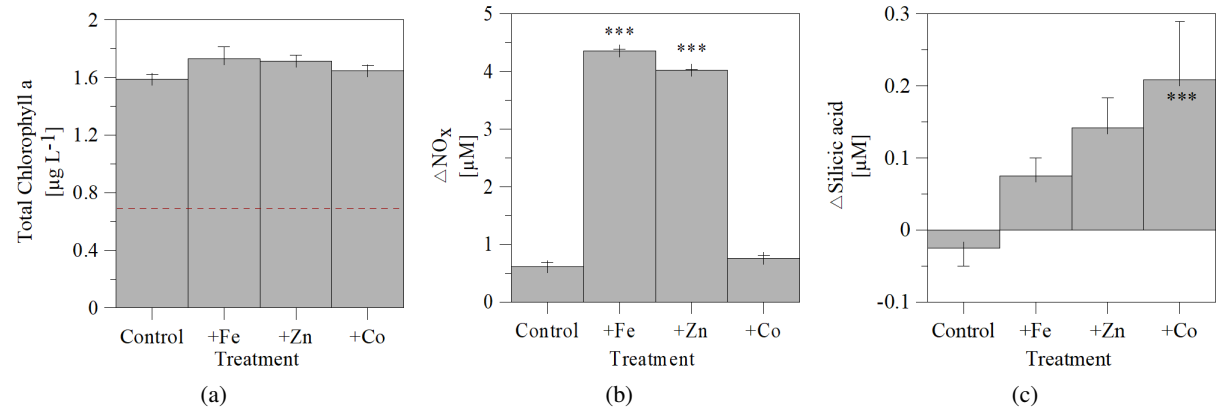

Figure 3.4: Bar graphs for bioassay MV4 showing a) total chlorophyll *a* concentrations (μgL^{-1}), b) the change in nitrate+nitrite (NO_x) concentrations (μM), and d) the change in silicic acid (SiO_4) concentrations (μM) over the course of the 73-hour bioassay. Error bars indicate standard errors. Dashed red lines indicate initial conditions. Asterisks indicate only significant results from Tukey HSD test for multiple pair-wise comparisons of significant ANOVA results between the control and treatments: * $p < 0.05$, ** $p < 0.01$, *** $p < 0.005$. n=3 for all bioassays.

Coccolithophore and diatom community abundance in MV3 and MV4 were completely contrasting, with high coccolithophore abundance in MV3 ($> 700\,\text{cells}\,\text{mL}^{-1}$) (Figure **??**) and very low abundance in MV4 ($< 150\,\text{cells}\,\text{mL}^{-1}$) (Figure **??**). Similarly, diatom abundance was low in MV3 ($< 420\,\text{cells}\,\text{mL}^{-1}$) (Figure **??**), but significantly higher in almost all treatments in MV4 ($> 1400\,\text{cells}\,\text{mL}^{-1}$) (Figure **??**) with the exception of the +Zn treatment in both MV3 and MV4, which both had lower diatom abundances of approximately $400\,\text{cells}\,\text{mL}^{-1}$. Overall, coccolithophore abundance decreased over the course of the longer (102-hour) bioassay (MV3), with the highest final abundance recorded in the +Zn treatment ($1093.3 \pm 5.2\,\text{cells}\,\text{mL}^{-1}$) and the lowest abundance recorded in the +Fe

treatment ($746.9 \pm 4.6\,\text{cells}\,\text{mL}^{-1}$). Coccolithophore abundance in MV4 increased over the course of the bioassay, with the highest final abundance, also measured in the +Zn treatment ($142.3 \pm 8.8\,\text{cells}\,\text{mL}^{-1}$). The lowest abundance was recorded in the control and +Co treatment ($25.2 \pm 4.0\,\text{cells}\,\text{mL}^{-1}$ and $28.6 \pm 4.2\,\text{cells}\,\text{mL}^{-1}$, respectively) (Figure **??**). Diatom abundance increased overall (from T0) in both South Atlantic bioassays, with the greatest increase in abundance in MV3 in the +Zn treatment ($413.6 \pm 2.8\,\text{cells}\,\text{mL}^{-1}$), whereas the greatest increase in MV4 occurred in the +Fe treatment ($1873.6 \pm 30.4\,\text{cells}\,\text{mL}^{-1}$) and little change in abundance occurred in the +Zn treatment from T0. The final diatom abundances in the control and +Co treatments were highly similar to each other in both bioassays ($\sim 300\,\text{cells}\,\text{mL}^{-1}$ in MV3 and $\sim 1400\,\text{cells}\,\text{mL} - 1$ in MV4).

Thus, neither of the South Atlantic bioassays showed any significant response to trace metal additions with respect to overall changes in biomass (chlorophyll *a*) or macronutrient drawdown, but did show numerical responses by the diatom and coccolithophore communities. With respect to coccolithophore abundance, the +Zn treatments consistently had the highest abundance at the end of both bioassays (Figures **??** and **??**) compared with the control and other trace metal treatments. Diatom abundance in MV3 (Figure **??**) was also greatest in the +Zn treatment, however, in MV4 (Figure **??**) diatom abundance was greatest in the +Fe and +Co treatments respectively.

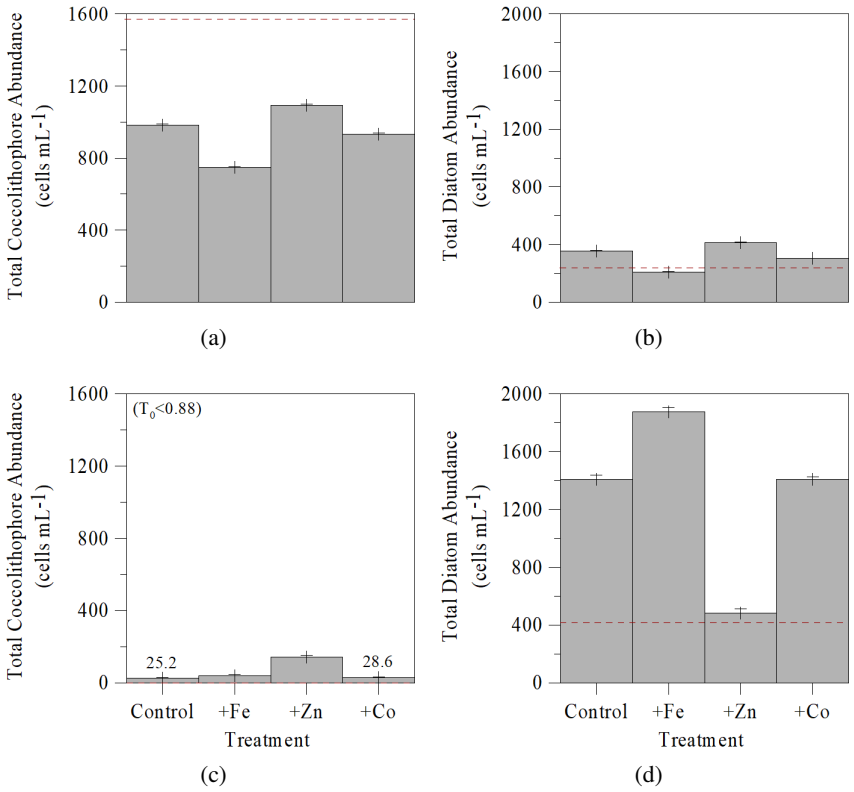

Figure 3.5: Bar graphs for South Atlantic bioassays, MV3 and MV4 showing total coccolithophore (a) MV3, c) MV4) and diatom abundance (b) MV3, d) MV4) (cells mL^{-1}). Error bars indicate standard errors. Red dashed line indicate initial abundances. Initial coccolithophore abundance in MV4 was below the detection limit of 0.88 cells mL^{-1}.

3.3.3 Bioassay Results: South Indian Ocean (2012)

The four bioassays conducted on the second cruise in the South Indian Ocean were run for longer than the South Atlantic bioassays ranging from 121 (RV1) to ~160-hours (RV2). The South Indian Ocean bioassays also displayed quite varied responses to trace metal additions. An analysis of variance (ANOVA) ($p < 0.05$) showed that there was no change in total chlorophyll *a* (Figure **??**), NO_x (Figure **??**) and silicic acid (Figure **??**) concentrations in bioassay RV1 ($F(3,8) = 0.78$, 0.20 and 0.67, $p > 0.05$, respectively). However, this may be an artefact of the lack of replicates (n=1) for the final trace metal nutrient measurements.

In contrast, in all three remaining bioassays (RV2, RV3 and R4), there were significant responses ($p < 0.05$) to trace metal addition with respect to total chlorophyll *a* concentrations as well as to NO_x drawdown. Total chlorophyll *a* concentrations in all three remaining bioassays showed significant increases ($p = 0.00$) relative to the control in response +Fe addition (Figures **??**, **??** and **??**), with the +Fe treatment response significantly different from both the +Zn and +Co treatments. Chlorophyll *a* concentrations were highest in the +Fe treatments, with

the greatest recorded final chlorophyll *a* concentration occurring in RV2 ($1.9 \pm 0.06 \mu gL^{-1}$, Figure **??**). There was a significant response in chlorophyll *a* to all trace metal treatments in RV2 relative to the control (Figure **??**). However, in RV3 and RV4, there was no significant response in the +Co treatment (Figures **??** and **??**), with a weak response to Zn in RV4 and no significant change in RV3.

NO_x utilization was significantly enhanced in the presence of +Fe relative to the control in RV2 and RV4 (p = 0.00). Additionally, in RV2 and RV3, there were significant differences in drawdown between the +Fe and +Zn (p = 0.00) and +Fe and +Co treatments (p = 0.00) (Figure**??** and **??**, see Appendix **??**), whereas in RV4 there were significant differences between all trace metal treatments (p = 0.00). Thus, with respect to NO_x utilization in the South Indian Ocean, drawdown increased in all treatments, with the greatest increases evident in the +Fe treatments. Responses in the +Zn and +Co treatments were more variable between the individual bioassays. Changes in silicic acid concentrations, were highly variable with no significant changes in silicic acid concentrations in response to any of the trace metal additions (p > 0.05).

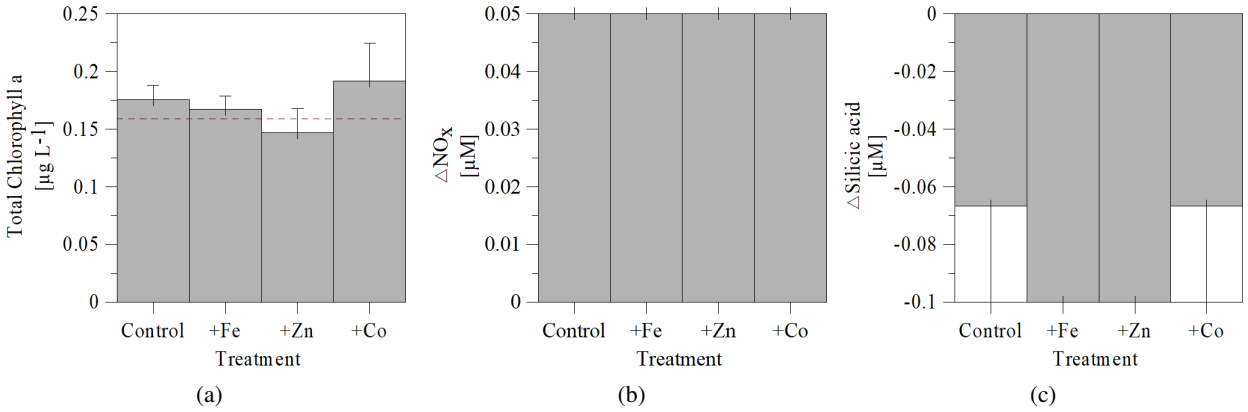

Figure 3.6: Bar graphs for bioassay RV1 showing a) total chlorophyll *a* concentrations (μgL^{-1}), b) the change in nitrate+nitrite (NO_x) concentrations (μM), and d) the change in silicic acid (SiO_4) concentrations (μM) over the course of each bioassay treatment. Error bars indicate standard errors. Dashed red lines indicate initial conditions. Asterisks indicate only significant results from Tukey HSD test for multiple pair-wise comparisons of significant ANOVA results between the control and treatments: * $p < 0.05$, ** $p < 0.01$, *** $p < 0.005$. n=3 for all bioassays.

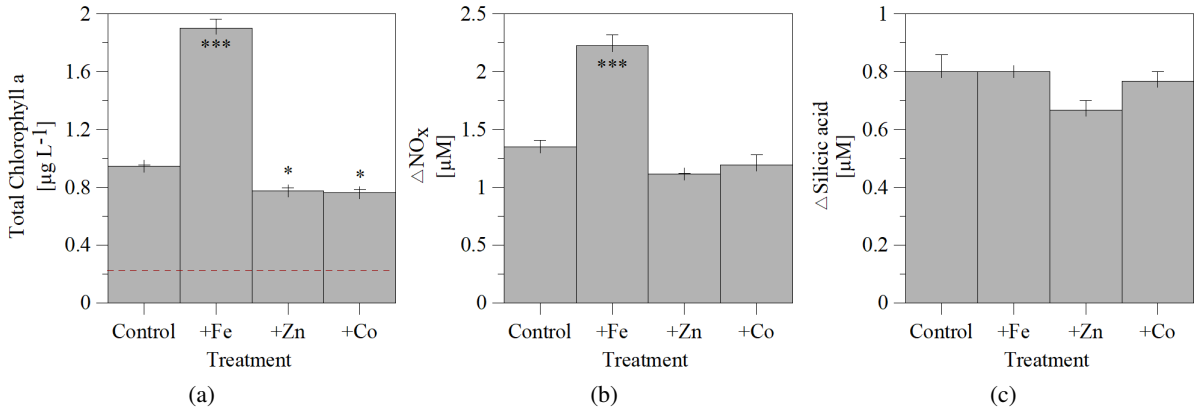

Figure 3.7: Bar graphs for bioassay RV2 showing a) total chlorophyll *a* concentrations (μgL^{-1}), b) the change in nitrate+nitrite (NO_x) concentrations (μM), and d) the change in silicic acid (SiO_4) concentrations (μM) over the course of each bioassay treatment. Error bars indicate standard errors. Dashed red lines indicate initial conditions. Asterisks indicate only significant results from Tukey HSD test for multiple pair-wise comparisons of significant ANOVA results between the control and treatments: * $p < 0.05$, ** $p < 0.01$, *** $p < 0.005$. n=3 for all bioassays.

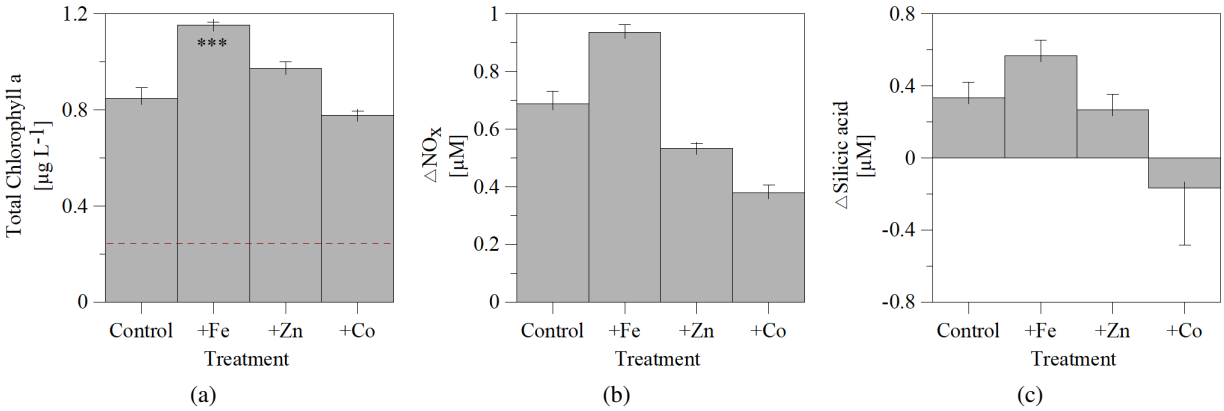

Figure 3.8: Bar graphs for bioassay RV3 showing a) total chlorophyll *a* concentrations (μgL^{-1}), b) the change in nitrate+nitrite (NO_x) concentrations (μM), and d) the change in silicic acid (SiO_4) concentrations (μM) over the course of each bioassay treatment. Error bars indicate standard errors. Dashed red lines indicate initial conditions. Asterisks indicate only significant results from Tukey HSD test for multiple pair-wise comparisons of significant ANOVA results between the control and treatments: * $p < 0.05$, ** $p < 0.01$, *** $p < 0.005$. n=3 for all bioassays.

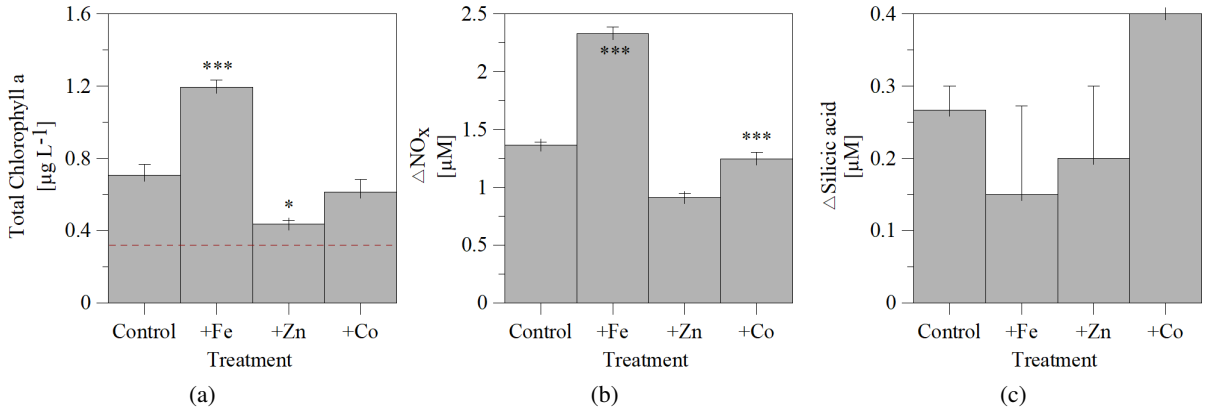

Figure 3.9: Bar graphs for bioassay RV4 showing a) total chlorophyll *a* concentrations (μgL^{-1}), b) the change in nitrate+nitrite (NO_x) concentrations (μM), and d) the change in silicic acid (SiO_4) concentrations (μM) over the course of each bioassay treatment. Error bars indicate standard errors. Dashed red lines indicate initial conditions. Asterisks indicate only significant results from Tukey HSD test for multiple pair-wise comparisons of significant ANOVA results between the control and treatments: * $p < 0.05$, ** $p < 0.01$, *** $p < 0.005$. n=3 for all bioassays.

The relative abundances of the coccolithophore and diatom communities sampled in the four South Indian Ocean bioassays were highly variable. In the case of RV1, the coccolithophore population (Figure **??**) far outnumbered the diatom population (Figure **??**) with both groups reaching their maximum abundance in the +Fe treatment (373.6 ± 14.5 and 153.6 ± 9.3 cells mL^{-1}, respectively). The highest coccolithophore abundance measured during this cruise was in bioassay RV2 (Figure **??**), where abundances in all treatments doubled during the course of the bioassay (from ~ 300 cells mL^{-1} to ~ 600 cells mL^{-1}). However there was little difference between treatments. In contrast, though the initial diatom population was less than half as abundant as that of the initial coccolithophore population, diatom abundance increased dramatically with the greatest abundance recorded in the +Fe treatment (968.1 ± 24.0 cells mL^{-1}, Figure **??**). The bioassay with the lowest recorded total coccolithophore abundance was RV3 (ranging from 10.8 ± 2.3 cells mL^{-1} (+Co) to 47.5 ± 5.0 cells mL^{-1} (+Fe)), this was coupled with the highest diatom abundance recorded in the South Indian Ocean bioassays (ranging from 1789.5 ± 32.1 cells mL^{-1} (+Zn) to 2597.4 ± 37.1 cellsmL^{-1} (+Fe)). The highest abundance for both coccolithophores and diatoms in this bioassay was again measured in the +Fe treatment (Figures **??** and **??**). Bioassay RV4 showed completely different patterns in coccolithophore abundance compared with previous bioassays with an increase in abundance in both the control and +Zn treatment. Coccolithophore abundance in the control and +Zn in RV4 was relatively high (360.5 ± 13.9 cells mL^{-1} and 585.9 ± 18.2 cells mL^{-1}, respectively), but in the +Fe and +Co treatments coccolithophore abundances decreased dramatically to < 1.74 cells mL^{-1} (Figure **??**). In contrast, diatom abundances increased in all treatments with the highest abundances recorded in the +Fe and +Co treatments

($855.4 \pm 21.6\,\text{cells}\,\text{mL}^{-1}$ and $674.3 \pm 19.1\,\text{cells}\,\text{mL}^{-1}$, respectively) (Figure **??**).

There was no trace metal treatment response in RV1 in terms of either total chlorophyll *a* concentrations, or NO_x and silicic acid drawdown. The highest coccolithophore and diatom abundances were both measured in the +Fe treatment ($373.6 \pm 14.5\,\text{cells}\,\text{mL}^{-1}$ and $153.6 \pm 9.3\,\text{cells}\,\text{mL}^{-1}$, respectively) of RV1, and were dramatically higher than the control (increases of 173% and 1700%, respectively, relative to the control). RV2, RV3 and RV4 all exhibited similar responses to trace metal additions. Total chlorophyll *a* concentrations were highest in the +Fe treatments, these also showed a significantly higher chlorophyll *a* concentration relative to the control, +Zn and +Co treatments. Additionally, all three showed significantly increased drawdown of NO_x in the +Fe treatment relative to the control. There was no significant change in silicic acid drawdown in any of the treatments. Diatom abundance was also consistently highest in the +Fe treatments (in all South Indian Ocean bioassays). In contrast, there was less of a consistent response to trace metals in in terms of changes in coccolithophore abundance. In RV1 and RV3, maximum coccolithophore abundance occurred in the +Fe treatment, however in RV2 the maximum abundance was recorded in the +Co treatment ($699.7 \pm 21.0\,\text{cells}\,\text{mL}^{-1}$), although coccolithophore abundances were roughly similar between treatments ($\sim 600\,\text{cells}\,\text{mL}^{-1}$). In RV4, maximum coccolithophore abundance occurred in the +Zn treatment ($585.9 \pm 18.2\,\text{cells}\,\text{mL}^{-1}$), with abundance in both the +Fe and +Co treatments less than $1.74\,\text{cells}\,\text{mL}^{-1}$.

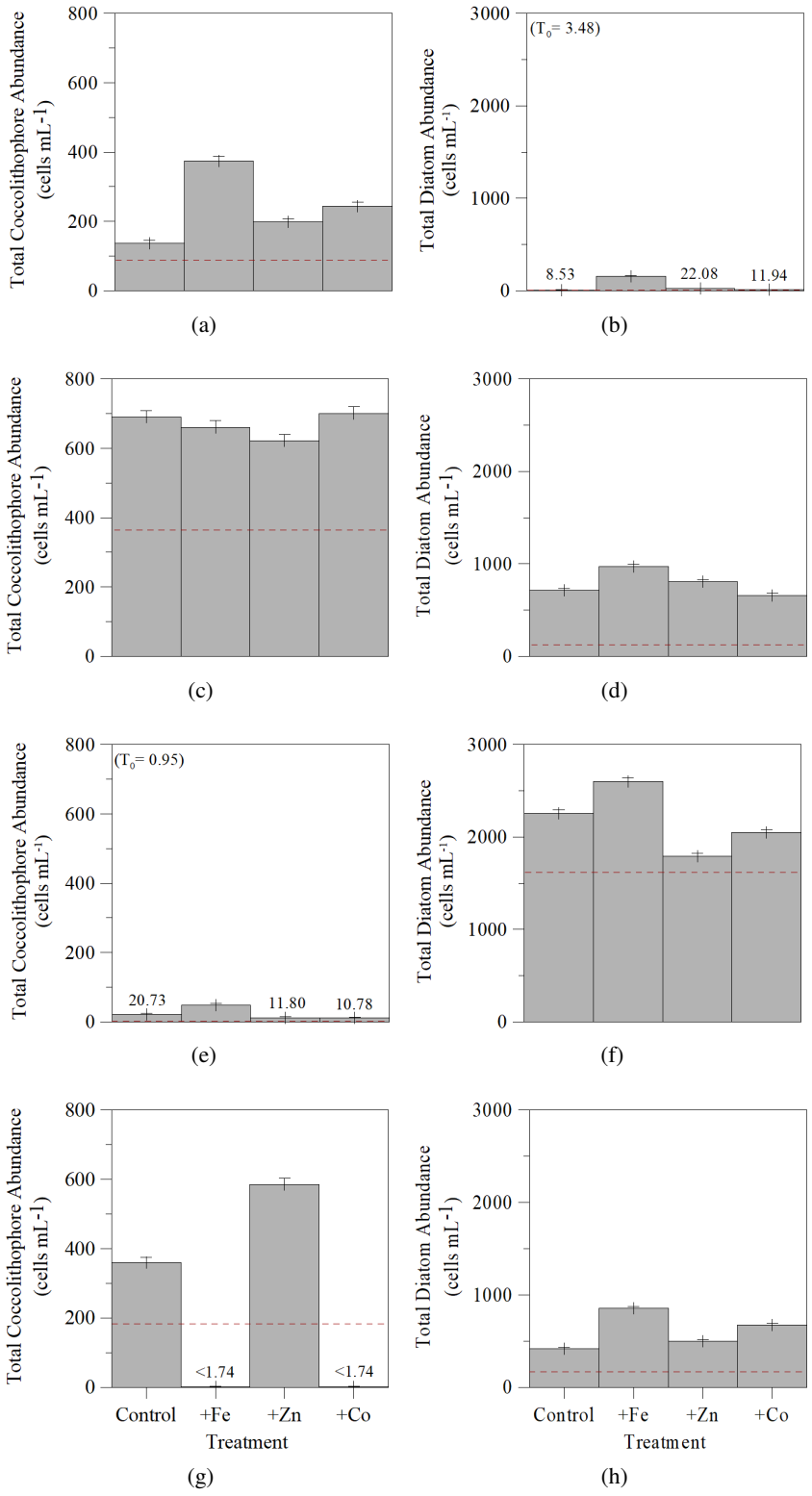

Figure 3.10: Bar graphs for South Indian bioassays, RV1-RV4 showing total coccolithophore (a, c, e, g) and diatom abundance (b, d, f, h) (cells mL^{-1}). Error bars indicate standard errors. Red dashed line indicate initial abundances. Coccolithophore abundance in RV4 for the +Fe and +Zn treatments was below the detection limit of 1.74 cells mL^{-1}.

Though bioassays in the South Indian Ocean varied considerably with respect to their initial conditions, the responses to trace metals were slightly more consistent across bioassays. Diatom abundance increased in all +Fe treatments relative to the control, while coccolithophore abundance in +Fe treatments increased in RV1 and RV3, and decreased in RV2 and RV4. Responses to +Zn treatments were less consistent than in the South Atlantic Ocean, with positive responses in RV1 and RV4 for both coccolithophores and diatoms. Cobalt amended treatments in RV1 had increased coccolithophore and diatom abundances, whereas only diatom abundances increased in RV2 and RV4 in the +Co treatments. With respect to changes in biomass (total chlorophyll *a*) and NO_X drawdown, RV2, RV3 and RV4 all responded positively to +Fe.

3.3.4 Growth Rates

Net growth rates for total chlorophyll *a,* as well as for the total coccolithophore and diatom communities, were calculated using the chlorophyll *a* concentrations and cell numbers at T0 and those at T_{end} (following **?**). Total chlorophyll *a* growth rates in the South Atlantic were similar within the individual bioassays, with growth rates in bioassay MV4 higher than those in bioassay MV3. Coccolithophore growth rates in MV3 were negative, with the highest growth rate measured in the +Zn treatment ($-0.18\,d^{-1}$). Diatom growth rates were similarly highest in the +Zn treatment ($0.25\,d^{-1}$) in this bioassay. In MV4, the highest coccolithophore growth rates were measured in the +Zn treatment ($2.54\,d^{-1}$), whereas the highest diatom growth rates were in the +Fe treatment ($0.73\,d^{-1}$) (Table **??**). Total chlorophyll *a* growth rates in the first South Indian Ocean bioassay (RV1) were all extremely low ($< 0.1\,d^{-1}$). Comparatively, both coccolithophore and diatom growth rates were higher with maximum growth rates for coccolithophores and diatoms measured in the +Fe treatment ($0.69\,d^{-1}$ and $1.89\,d^{-1}$, respectively). In RV2, RV3 and RV4 maximum chlorophyll *a* growth rates were in the +Fe treatment ($1.08\,d^{-1}$, $0.74\,d^{-1}$ and $0.65\,d^{-1}$, respectively). There was little difference in coccolithophore and diatom growth rates between treatments and the control in bioassay RV2 (see Table **??**). Maximal coccolithophore and diatom growth rates in RV3 were measured in the +Fe treatment ($2.95\,d^{-1}$ and $0.23\,d^{-1}$, respectively). In RV4, maximum growth rates of diatoms were measured in the +Fe treatment ($0.87\,d^{-1}$), whereas maximal coccolithophore growth rates were measured in the +Zn treatment ($0.57\,d^{-1}$) (Table **??**). Although diatom growth rates were generally greater than coccolithophore growth rates in the same treatments, coccolithophore growth rates were higher than diatom growth rates in bioassays MV4 and RV3, with the average (S.E.) coccolithophore growth rate in trace metal treatments in MV3 $2.06 \pm 0.21\,d^{-1}$ versus $0.46 \pm 0.18\,d^{-1}$ for the diatoms in the same treatments, similarly in MV4 the average coccolithophore growth rates were $1.47 \pm 0.21\,d^{-1}$ and the average diatom growth rates were $0.13 \pm 0.05\,d^{-1}$. Generally, phytoplankton growth

rates were enhanced in several of the trace metal treatments relative to the control, though growth rates in the control and +Co treatments were often more similar (MV4, RV2 and RV3, see Table **??**).

Table 3.2: Growth rates (d^{-1}) for chlorophyll *a*, coccolithophores and diatoms.

Bioassay	**Treatment**	**Chlorophyll *a***	**% Change**	**Coccolithophores**	**% Change**	**Diatoms**	**% Change**
		(d^{-1})		(d^{-1})		(d^{-1})	
South Atlantic							
MV3	Control	0.16		-0.24		0.18	
	+Fe	0.15	-4%	-0.37	58%	-0.09	-152%
	+Zn	0.13	-15%	-0.18	-22%	0.25	42%
	+Co	0.13	-19%	-0.26	11%	0.10	-46%
MV4	Control	0.40		1.68		0.58	
	+Fe	0.45	10%	1.91	14%	0.73	24%
	+Zn	0.44	9%	2.54	52%	0.05	-92%
	+Co	0.42	4%	1.74	4%	0.59	0.2%
South Indian							
RV1	Control	0.05		0.18		0.45	
	+Fe	0.02	-51%	0.69	274%	1.89	323%
	+Zn	-0.04	-186%	0.37	102%	0.92	106%
	+Co	0.09	91%	0.47	158%	0.62	38%
RV2	Control	0.74		0.32		0.86	
	+Fe	1.08	47%	0.30	-7%	1.01	18%
	+Zn	0.64	-14%	0.27	-16%	0.92	7%
	+Co	0.63	-15%	0.33	2%	0.82	-5%
RV3	Control	0.58		1.54		0.16	
	+Fe	0.74	26%	1.95	27%	0.23	44%
	+Zn	0.65	12%	1.26	-18%	0.04	-72%
	+Co	0.54	-8%	1.21	-21%	0.11	-30%
RV4	Control	0.39		0.33		0.52	
	+Fe	0.65	67%	-2.34	-814%	0.87	69%
	+Zn	0.15	-62%	0.57	74%	0.60	17%
	+Co	0.32	-18%	-2.34	-814%	0.76	46%

3.3.5 Statistical Analysis of Community Composition

Coccolithophore community abundance in surface waters was highly variable across the two cruises in the GCB. A maximum of $1579.4 \pm 7.8 \text{cells}\,\text{mL}^{-1}$ were counted at the start of MV3 and a minimum of $< 0.9\,\text{cells}\,\text{mL}^{-1}$ at the start of MV4. In the South Indian Ocean, a maximum of $699.7 \pm 21.0\,\text{cells}\,\text{mL}^{-1}$ were counted in the +Co treatment of RV2 and a minimum of $< 1.0 \pm 0.7\,\text{cells}\,\text{mL}^{-1}$ at the start of RV3.

Figure 3.11: Non-metric multidimensional scaling (nMDS) ordination of coccolithophore (a, c, e, g) and diatom (b, d, f, h) abundance based on Bray-Curtis similarity. Closed symbols represent coccolithophores and open symbols represent diatoms.

nMDS analysis of the phytoplankton (coccolithophore and diatom) community composition in bioassays sampled from across the GCB revealed distinct differences in distribution patterns between the coccolithophore and

diatom community composition. Coccolithophore communities generally appeared more widely distributed in the nMDS (Figure **??**, **??**, **??** and **??**), whereas the diatom communities tended to cluster more tightly (Figures **??**, **??**, **??** and **??**) indicating that bioassays were more similar to each other with respect to diatom community composition than to coccolithophore community composition. It is also clear from the nMDS ordination plots that the diatom community composition in RV1 was quite distinct in terms of composition in all four factors represented. An ANOSIM test confirmed the significance of the predetermined factors 'bioassay' and 'length' in influencing coccolithophore community composition and factors 'bioassay', 'location' and 'length' which affected the diatom community composition. Interestingly, there was no significant difference in the coccolithophore community composition sampled between treatments (R = -0.159, p = 0.989), nor was there a significant difference between the coccolithophore community composition sampled from the South Indian Ocean compared with that sampled from the South Atlantic Ocean (R = 0.002, p = 0.431). Furthermore, in contrast to the diatom community, there was a significant difference between coccolithophore communities (p = 0.02) based on the duration of the bioassay (based on a low R-value, R = 0.164), with this factor interpreted as only having a small effect on community composition. However, there was a strong and significant difference between coccolithophore community composition in the individual bioassays (R = 0.898, p = 0.001). With respect to the diatom community, during the initial analysis it became clear that bioassay RV1 was an outlier, skewing the interpretation of the composition of the diatom community (see Figures **??**, **??**, **??** and **??**). When this bioassay was removed from the analysis a much clearer pattern emerged. As with the coccolithophore community, there was no significant difference in diatom community structure between the different treatments (R = -0.159, p = 0.984). However, for all three remaining factors (bioassay, location and length) there was a strong significant result (p = 0.001) with accompanying high R-values indicating a high degree of separation (Table **??**).

Table 3.3: ANOSIM test results for coccolithophore and diatom groups identified in the cluster analyses presented in Figure **??**. *Diatom analysis performed without the outlier RV1.

	Coccolithophores				**Diatoms***			
Factors	Treatment	**Bioassay**	Location	**Length**	Treatment	**Bioassay**	**Location**	**Length**
R-value	-0.159	0.898	0.002	0.164	-0.159	0.738	0.616	0.712
P-value	0.989	**0.001**	0.431	**0.02**	0.984	**0.001**	**0.001**	**0.001**

SIMPER analysis showed which coccolithophore and diatom species were primarily driving the average dissimilarity between the two oceans and the different sample clusters. There was a high degree of similarity within bioassay groups with the average similarity within bioassays ranging from 69 to 92% for the coccolithophore com-

munity (Table **??**). Similarly, the diatom community displayed a high degree of similarity within bioassay groups (65 - 87%), with the exception of RV1 which was only 36% similar on average. With respect to community composition within trace metal treatments, generally there was a high degree of similarity (56% - 93%) between the treatment coccolithophore populations and the control population (Table **??**). This was echoed in the diatom community composition, with the exception of RV1 where trace metal treatments displayed a much lower degree of similarity compared with the control (23% - 47%).

Table 3.4: SIMPER and Bray-Curtis bioassay results showing the average similarity (%) of the different treatments and the similarity of the individual trace metal treatments to the control.

Bioassay	**Coccolithophores**				**Diatoms**			
	Av. similarity (%)	**Similarity to Control (%)**			**Av. similarity (%)**	**Similarity to Control (%)**		
		+Fe	**+Zn**	**+Co**		**+Fe**	**+Zn**	**+Co**
MV3	91.5	85.4	87.6	88.1	68.4	78	75.5	68.2
MV4	84	92.3	69.6	98.1	65.2	75.6	41.8	84.6
RV1	73.5	79.9	61.7	87.1	36.5	23.2	37.2	46.9
RV2	70.2	69.6	66.5	55.5	78.6	84.1	82	80.8
RV3	79.6	89.7	93	91.8	87.63	91.7	86.5	91.3
RV4	69	na	71.8	na	76.1	77	81.3	77.4

With respect to 'location', coccolithophores sampled from bioassays in the South Atlantic were on average 62% similar compared with only 49% similar in the South Indian Ocean (data not shown). *E. huxleyi* were on average more abundant in the Atlantic ($4.2\,\text{cells}\,\text{mL}^{-1}$) than in the Indian ($3.5\,\text{cells}\,\text{mL}^{-1}$) ocean, contributing 32% to the total dissimilarity between the two ocean basins. *Syracosphaera* spp. was roughly equally abundant (1.22 versus $1.1\,\text{cells}\,\text{mL}^{-1}$) in the South Atlantic and South Indian ocean bioassays. However, the 'location' factor was found to not be a significant driver of differences in coccolithophore community composition (Figure **??**). Diatom community structure however, was far more similar within ocean basins, with the South Atlantic bioassays exhibiting diatom species which were on average 61% similar and in the South Indian bioassays, the diatom community was on average 70% similar (data not shown).

Table 3.5: SIMPER results showing the contribution of both coccolithophore and diatom species responsible for ~60% of the differences between the South Atlantic and South Indian Ocean bioassays. RV1 has been excluded from this analysis.

South Atlantic vs. South Indian	**Average Abundance** (cells mL^{-1})		**Contribution to total dissimilarity (%)**
Coccolithophores, average dissimilarity = 50.4%	Atlantic	Indian	
Emiliania huxleyi	4.24	3.50	31.7
Syracosphaera spp.	1.22	1.12	20.5
Palusphaera sp.	0	0.96	10.68
			= 62.9%
*Diatoms, average dissimilarity = 45.2%			
small *Fragilariopsis* sp.	3.47	3.33	8.5
Chaetoceros sp. (10-20μm)	1.78	3.54	7.4
Cylindrotheca sp.	0.09	1.83	7.4
Chaetoceros sp. (<10μm)	0.85	2.32	7
Pseudonitzschia sp.	2.82	3.83	6.7
Rhizosolenia sp.	1.69	0.98	6.6
large *Fragilariopsis* sp.	1.98	2.07	6.2
Proboscia sp.	0.71	1.70	6.1
Thallassiosira sp.	2.71	1.47	6
			= 61.8%

A total of seven different coccolithophore species were identified in the six bioassays; only three taxa were present in the South Atlantic (*E. huxleyi, Syracosphaera* spp. and *Calcidiscus leptoporus*), whereas all seven (*Gephyrocapsa oceanica., Umbellosphaera* sp*., Acanthoica* sp. and *Dicosphaera tubifera*) were present in the South Indian Ocean. Coccolithophore abundance was heavily dominated by *E. huxleyi*, which contributed between 21 to 100% towards the total abundance (Table **??**). *Syracosphaera* spp. also contributed significantly (50-76%) to the total coccolithophore abundance in a few of the bioassays in the South Atlantic Ocean (MV4, control, +Fe, +Zn and +Co). Pielou's evenness (J') was low (<0.4) overall indicating a community heavily dominated by a small number of species (i.e. *E. huxleyi* and *Syracosphaera* spp.). In contrast, the diatom community was far more diverse with a total of 17 different species identified across the GCB. Twelve diatom species were present in surface waters of the South Atlantic Ocean and between two and 17 different species were identified in the South Indian Ocean, diatom species composition was on average 55% similar between the two Oceans, with most diatom species more abundant in the Indian Ocean (Table **??**). The dominant diatom species in the South Indian Ocean bioassays was

small *Fragilariopsis* sp., and in the South Atlantic bioassays there was more variation with small *Fragilariopsis*, *Pseudonitzschia* and *Chaetoceros* species all contributing significantly to total diatom biomass. In bioassay MV3, which was sampled close to South Georgia (see Figure **??**), the coccolithophore community was exclusively composed of *E. huxleyi* ($> 99\%$ of the coccolithophore community), whereas in MV4 the coccolithophore community was more diverse (two to three coccolithophore taxa present) and *Syracosphaera* spp. was dominant ($\gtrsim 50$ of cell numbers) (Table **??**). The South Indian Ocean bioassays in comparison were far more diverse with respect to the coccolithophore community (with the exception of RV3, which again comprised solely of *E. huxleyi*) with, on average, four species of coccolithophore present in the different bioassays, although *E. huxleyi* was the dominant coccolithophore in every treatment. There was no change in coccolithophore species composition, or shifts in species dominance, between the different trace metal treatments.

Table 3.6: Summary of phytoplankton community diversity. Coccolithophore and diatom abundance (cells mL^{-1}), number of species (S), Pielou's evenness (J') and dominant species (contribution to total abundance in brackets). Medium - 10-20 μm, small $< 10\mu$m. Dominant coccolithophore abbreviations, *Syracosphaera* spp. (*Syraco*), *Emiliania huxleyi* (*E. hux*), *Rhabdosphaera* sp. (*Rhabdo*). Dominant diatom abbreviations, *Pseudonitzschia* sp. (*Pseudo*), *Fragilariopsis* sp. (*Frag*), *Chaetoceros* sp. (*Chaet*).

Bioassay	**Coccolithophore Abundance**	**Community diversity**		**Dominant Coccolithophore Taxa**	**Diatom Abundance**	**Community diversity**		**Dominant Diatom Taxa**
	(cells mL^{-1})	S	J'		(cells mL^{-1})	S	J'	
MV3 T0	1579	1	****	*E. hux* (100%)	250	7	0.58	*Frag* (sml) (61%)
MV3 Cont	983	2	0.04	*E. hux* (99%)	356	11	0.75	*Frag* (sml) (60%)
MV3 Fe	747	1	****	*E. hux* (100%)	209	9	0.84	*Frag* (sml) (62%)
MV3 Zn	1093	1	****	*E. hux* (100%)	414	12	0.80	*Frag* (53%)
MV3 Co	934	1	****	*E. hux* (100%)	303	9	0.72	*Frag* (sml) (58%)
MV4 T0	<0.88	nd	nd	-	438	9	0.62	*Frag* (sml) (50%)
MV4 Cont	50	3	0.59	*Syraco* (76%)	1407	10	0.47	*Frag* (sml) (65%)
MV4 Fe	80	3	0.68	*Syraco* (50%)	1874	10	0.51	*Pseudo* (44%)
MV4 Zn	285	2	1.00	*E. hux* (50%) *Syraco* (50%)	483	9	0.48	*Frag* (70%)
MV4 Co	57	3	0.64	*Syraco* (70%)	1410	7	0.60	*Frag* (sml) (57%)
RV1 T0	95	7	0.52	*E. hux* (58%)	3	5	0.97	*F. kergulensis* (25%) *Pseudo* (25%) *Thallassiosira* (25%)
RV1 Cont	136	7	0.64	*E. hux* (64%)	9	2	0.97	*Frag* (sml) (60%)

RV1 Fe	374	6	0.32	*E. hux* (86%)	154	13	0.79	*Pseudo* (40%)
RV1 Zn	199	3	0.62	*E. hux* (73%)	22	3	0.55	*Pseudo* (82%)
RV1 Co	244	7	0.55	*E. hux* (53%)	12	2	0.59	*Pseudo* (86%)
RV2 T0	364	4	0.36	*E. hux* (87%)	128	16	0.87	*Pseudo* (19%) *Chaet* (med) (19%)
RV2 Cont	689	1	****	*E. hux* (100%)	714	14	0.72	*Chaet* (med) (42%)
RV2 Fe	660	3	0.25	*E. hux* (94%)	968	15	0.62	*Pseudo* (51%)
RV2 Zn	624	6	0.19	*E. hux* (93%)	805	15	0.60	*Chaet* (med) (40%)
RV2 Co	700	4	0.16	*E. hux* (95%)	659	13	0.61	*Chaet (med) (42%)*
RV3 T0	1	1	****	*E. hux* (100%)	1636	15	0.51	*Frag* (sml) (60%)
RV3 Cont	21	1	****	*E. hux* (100%)	2256	17	0.55	*Frag* (sml) (57%)
RV3 Fe	47	1	****	*E. hux* (100%)	2597	17	0.62	*Frag* (sml) (53%)
RV3 Zn	12	1	****	*E. hux* (100%)	1790	16	0.54	*Frag* (sml) (59%)
RV3 Co	11	1	****	*E. hux* (100%)	2049	15	0.56	*Frag* (sml) (51%)
RV4 T0	191	6	0.52	*E. hux* (73%)	149	13	0.66	*Pseudo* (49%)
RV4 Cont	362	5	0.41	*E. hux* (78%)	418	10	0.46	*Pseudo* (73%)
RV4 Fe	<1.74	nd	nd	-	855	13	0.42	*Pseudo* (74%)
RV4 Zn	596	7	0.26	*E. hux* (89%)	499	11	0.47	*Pseudo* (70%)
RV4 Co	<1.74	nd	nd	-	674	14	0.56	*Pseudo* (58%)

Overall, community composition did not change significantly in response to trace metal additions for either the coccolithophore or diatom populations. The coccolithophore population across both the South Atlantic and South Indian Ocean bioassays was highly similar and heavily dominated by *E. huxleyi* cells. There was no apparent change in composition or species dominance in response to trace metal treatments in the coccolithophores. The diatom community structure was more diverse, though bioassays were still mostly dominated by only a few species (small *Fragilariopsis, Chaetoceros* and *Pseudonitzschia*), although there was no apparent shift in species dominance in response to trace metal addition.

Table 3.8: Summary of significance of changes (ANOVA and Tukey HSD test results) in chlorophyll *a*, NO_x and SiO_4 concentrations to trace metal additions in bioassays. Blue indicates that there was no significant change, dark green indicates a significant increase relative to the control/treatment in each row, and dark red indicates a significant decrease relative to the control/treatment in each row in chlorophyll *a*, NO_x or SiO_4 concentrations between treatments. Similarly, changes in phytoplankton abundance in treatments relative to the control/treatments indicated in each row are indicated by light green (increase) or light red (decrease) and treatments where abundance was similar are indicated by light blue. Due to a sample size of n=1 in the SEM data, significance of changes in abundance could not be determined.

Bioassay	Treatment	Chl a			NO_x			SiO_4			Coccolithophore abundance			Diatom abundance		
		+Fe	+Zn	+Co	+Fe	+Zn	+Co	+Fe	+Zn	+Co	+Fe	+Zn	+Co	+Fe	+Zn	+Co
MV3	Control															
	+Fe															
	+Zn															
	+Co															
MV4	Control															
	+Fe															
	+Zn															
	+Co															
RV1	Control															
	+Fe															
	+Zn															
	+Co															
RV2	Control															
	+Fe															
	+Zn															
	+Co															
RV3	Control															
	+Fe															
	+Zn															
	+Co															
RV4	Control															
	+Fe															
	+Zn															
	+Co															

3.4 Discussion

3.4.1 Differences in phytoplankton communities between the South Atlantic and South Indian Sectors of the Southern Ocean

Bioassays sampled from the South Atlantic and South Indian Oceans across the GCB in 2011 and 2012 were highly diverse in terms of SSTs, dissolved trace metal concentrations, initial chlorophyll *a*, NO_x and silicic acid concentrations as well as exhibiting a wide range of initial coccolithophore and diatom abundances (Table **??**). The wide range of initial conditions likely contributed to the subsequent varied responses to trace metal additions (Table **??**). Responses to trace metal additions (Fe, Zn and Co) varied with no significant change in biomass (as inferred from bulk chlorophyll *a* concentrations) in either of the South Atlantic bioassays, nor in the first South Indian Ocean bioassay (RV1) (Table **??**). In contrast, in the remaining South Indian Ocean bioassays there were significant changes in chlorophyll *a* biomass in response to trace metal additions (Table **??**). There was no significant difference between coccolithophore community structure in the bioassays sampled in the South Atlantic compared with bioassays sampled in the South Indian Ocean, suggesting that the composition of the coccolithophore community was fairly uniform across the GCB, despite quite dramatic variations in sea surface temperature and silicic acid concentrations, which is has been shown to be the two most influential factors known to influence coccolithophore biogeography in the Southern Ocean (**?**). In contrast, diatom species composition was generally more varied across the South Indian Ocean (Table **??**). Although there was no significant difference in community structure with respect to the different treatments (Table **??**), in a number of the bioassays, both coccolithophore and diatom growth rates were enhanced in the trace metal treatments relative to the control (Table **??**). Diatom growth rates were consistently highest in the +Fe treatments (with the exception of bioassay MV3, where diatoms responded to +Zn) and coccolithophore growth rates responded positively to both +Fe (MV4, RV1 and RV3) and +Zn (MV3, MV4, RV1 and RV4) additions (Table **??**).

3.4.2 Phytoplankton responses to trace metal addition

The general phytoplankton responses (total chlorophyll *a*, diatom and coccolithophore abundance) to the +Co treatments were far less consistent across the different bioassays. Frequently growth rates of coccolithophores in the control and +Co treatment were quite similar (MV3, MV4 and RV2). Exceptions to this occurred in bioassay RV1 where coccolithophore growth rates in the +Co treatment were high relative to the control ($0.47\,d^{-1}$ compared with $0.18\,d^{-1}$), and in RV4 where coccolithophore growth rates were dramatically lower in the +Co than in the

control ($-2.34\,d^{-1}$ compared with $0.33\,d^{-1}$) (Table **??**). Initial dCo in these treatments were 26 pM and 16 pM, respectively. Increases in coccolithophore abundance in the +Co treatment of RV1 suggest that +Co addition relieved *in situ* Co limitation in this bioassay. However, negative responses in RV4, where initial dCo were even lower can not be explained in the same way. In bioassays where there was no change in coccolithophore abundance in response to +Co, initial dCo was considerably higher (35-62 pM). Unfortunately, there is very little information on the Co requirements in different phytoplankton groups, with most studies investigating the substitution of Zn with Co (**??**). In RV2, initial dZn concentrations were the lowest measured across the GCB (0.28 nM) thus, it is possible that the negative response in +Co treatments (where initial dCo was also the lowest measured across the GCB) is due to coccolithophores requiring both Zn and Co in non-limiting concentrations in much the same way that diatoms can be co-limited by the availability of both nitrate and silicic acid. Initial dZn concentrations in RV1, were very high (29.75 nM) so it appears that when Co concentrations increased in the +Co treatment, coccolithophores were no longer co-limited and were able to respond. Other explanations could lie in differences in coccolithophore community structure between RV1 and RV4, grazing pressure or competition with diatoms.

Despite no change in total biomass or macronutrient concentrations in RV1, both coccolithophores and diatoms responded to +Fe, +Zn and +Co addition with quite dramatic increases in abundance. Diatom abundance increased most dramatically, with all (nine) species responding to +Fe addition and *Pseudonitzschia* and small *Fragilariopsis* dominating the assemblage (40% and 21%, respectively). Whereas, in the +Zn and +Co treatments, species diversity (three and two species present, respectively) dropped and *Pseudonitzschia* dominated the diatom assemblage (82% and 86%, respectively). *Pseudonitzschia* is most often reported as the dominant diatom responding to +Fe addition in Fe experiments (**?**), however in this bioassay, while *Pseudonitzschia* abundance increased significantly in in the +Fe treatment, small *Fragilariopsis* also contributed significantly to the total biomass (~20%).

The response of phytoplankton to +Fe treatments was the most consistent of the trace metal responses observed across the different GCB bioassays. Bioassays RV2, RV3 and RV4 all exhibited significant increases in total chlorophyll *a* concentrations and NO_x drawdown increased in MV3, MV4, RV2 and RV4 over the course of the bioassays (relative to the control) (Figures **??**, **??** and **??**). In contrast, there was no significant response to +Fe addition with respect to silicic acid drawdown in any of the bioassays despite the changes in diatom cell abundance. Total diatom abundance also increased in all +Fe treatments when compared with the control, apart from MV3, while coccolithophore responses in +Fe treatments were more varied. In the +Fe treatments of bioassays MV3, RV2 and RV4 coccolithophore abundances decreased (Figures **??**, **??** and **??**), whereas in MV4, RV1 and RV3 cell abundances increased (Figures **??**, **??** and **??**).

Studies documenting phytoplankton responses to the trace metal Fe are perhaps the most well represented of the three trace metals tested in this study. Mesoscale studies investigating the effects of +Fe addition experiments have decisively shown that Fe availability limits PP in approximately 30% of the world's oceans where surface macronutrient concentrations are high (**?**). The Southern Ocean is one example of such an area where Fe is available in limiting concentrations. It appears that the majority of the South Indian Ocean bioassays, where variables increased in response to +Fe addition, were sampled from Fe limited waters (RV2, RV3 and RV4). However bioassays from the South Atlantic Ocean, where there were no significant increases in biomass (as inferred from total chlorophyll *a* concentrations) in response to +Fe treatments, do not appear to have been sampled from Fe limited waters. In support of this, initial dFe measurements in the South Atlantic were high relative to those in the South Indian Ocean (>0.7 nM versus <0.4 nM, respectively, see Table **??**).

In bioassay MV3, which was sampled north of South Georgia (see Figure **??**), neither coccolithophore or diatom abundance increased in response to +Fe, suggesting Fe was not a limiting factor initially. Several studies have reported enhanced Fe availability supporting blooms around island systems such as South Georgia (**?**) and the Crozet Plateau (**??**). Initial coccolithophore abundance in MV3 was the highest initial coccolithophore abundance ($1579.4 \pm 7.8\,\text{cells}\,\text{mL}^{-1}$) enumerated across the entire GCB, while diatoms only made up between 13 and 27% of the total cell abundance. Furthermore, both coccolithophore and diatom abundance exhibited the greatest decrease in the +Fe treatment compared with the control (decreasing by 24 and 41%, respectively (Table **??**)). This further supports the notion that phytoplankton in this bioassay were not limited by Fe. Despite much of the Southern Ocean being Fe limited, the waters surrounding South Georgia consistently support large and long-lasting phytoplankton blooms, characteristic of those found in Fe replete environments (**?**). Indeed, initial dissolved Fe concentrations in this bioassay were among the highest recorded for the GCB (0.74 nM, Table **??**). Moreover, while initial concentrations of NO_x were also high ($17.46 \pm 0.05\,\mu$M), initial concentrations of silicic acid were potentially limiting for diatoms ($2.00 \pm 0.14\,\mu$M, (**?**)). Though *E. huxleyi* blooms frequently coincide with relatively high nitrate concentrations (**?**), previous blooms around South Georgia have been found to be heavily dominated by large phytoplankton and diatoms typically accounted for the majority of abundance (**?**). In contrast, in this study bioassay MV3 was dominated by *E. huxleyi* and the relatively rare diatom population was dominated by small *Fragilariopsis* species (>50%).

In MV4, despite there being no significant change in total chlorophyll *a* concentrations in response to +Fe addition, and the fact that initial dissolved Fe concentrations in this bioassay were relatively high (0.73 nM, Table **??**) (Figure **??**), both coccolithophore and diatom abundance increased relative to the control in response to +Fe

(59% and 33%, respectively (Table **??**)). Diatom abundance was generally high ($> 1400\,\text{cells}\,\text{mL}^{-1}$) (with the exception of the +Zn treatment) and diatoms comprised >75% of the total counted cell abundance in this case. Coccolithophore abundance was low overall, contributing only ~2% of the total counted phytoplankton abundance (again, with the exception of the +Zn treatment). High initial diatom abundance coupled with low concentrations of silicic acid suggests that this bioassay was sampled towards the end of a growth cycle where diatoms had already depleted *in situ* silicic acid and their population was in decline, thus an injection of additional Fe only had a small positive effect. The response by coccolithophores in this bioassay to +Zn addition was, however, quite striking with an increase in abundance of 465% relative to the control. With initial dZn concentrations of 1.32 nM, it appears that coccolithophore growth was limited by Zn availability in this bioassay.

Interestingly, in RV1 where initial dissolved Fe concentrations were relatively low (0.25 nM, Table **??**), and there was no significant response to any trace metal with respect to chlorophyll *a* concentrations (Figure **??**), both coccolithophore and diatom abundance exhibited large increases in abundance in the +Fe treatment relative to the control (173% and 1700%, respectively (Table **??**)). This suggests that the majority of the biomass represented by total chlorophyll *a* concentrations in this bioassay was made up of small-celled or naked phytoplankton which do not show up in SEM images. These small phytoplankton are also less likely to respond to +Fe addition as they are better adapted to take advantage of low nutrient concentrations by virtue of their large surface area to volume ratio and may be heavily grazed by small grazers (**?**).

Although there was no significant change in total chlorophyll *a* concentrations in response to +Zn addition relative to the control in the majority of bioassays (MV3, MV4, RV3 and RV4) there was a significant increase in chlorophyll *a* concentrations in RV2 relative to the control. In several bioassays, both coccolithophore and diatom abundance increased in the +Zn treatment relative to the control, for example in the South Atlantic Ocean both coccolithophore and diatom abundance increased in the +Zn treatment. In MV4 (Figures **??** and **??**), while diatom abundance decreased by 66% in the +Zn treatment, coccolithophore abundance increased dramatically in the same treatment (a 465% increase) (Table **??**). In fact, coccolithophore abundance increased in nearly every +Zn treatment relative to the control across the GCB, with the exceptions of RV3 (where abundance decreased by 43%) and in RV2 (where coccolithophore abundance did not change) (Table **??**). Notably, initial dZn concentrations in RV3 were high (3.57 nM) relative to the other bioassays (Table **??**). With respect to overall diatom abundance, +Zn treatments exhibited increased abundance relative to the control in only MV3 (16% increase) and in RV1 (159%) (Table **??**). Thus, +Zn addition treatments typically displayed increased coccolithophore abundance relative to the control (with the exception of bioassays RV2 and RV3), and in some instances significantly enhanced growth rates

relative the control, +Fe and +Co treatments (MV4 and RV4) (Table **??**). A similar result was found by **?** in the north-eastern subarctic Pacific, where the abundance of small diatoms and coccolithophores was found to be higher in Zn amended incubations relative to the control. In the Southern Ocean, concentrations of biologically available Zn have been thought to be relatively high ($> 2\,\mathrm{nM}$; (**?**)) and unlikely to be limiting, although several of the bioassays in the GCB had Zn less than 2 nM (Table **??**). Hence, the results presented here indicate that Zn does appear to limit the activity of coccolithophores, and to a lesser degree diatoms, across the GCB.

In general, Co amended bioassays across the GCB showed the least change overall, and in some cases (RV2) chlorophyll *a* concentrations actually decreased significantly relative to the control (Figure **??**). There was no significant change in total chlorophyll *a* concentrations, silicic acid or NO_x drawdown in any of the other +Co bioassays. With respect to changes in coccolithophore and diatom abundance, the effect of +Co additions were negligible in the majority of the bioassays. Coccolithophore abundance generally decreased in response to +Co treatments when compared with the control, though in bioassays MV4 and RV1 +Co addition resulted in increases in coccolithophore abundance of 13% and 79%, respectively, relative to the control (Table **??**). Diatom abundance in the +Co treatment of MV4 did not change relative to the control, but in RV1 diatom abundance increased by 40% relative to the control and in RV2 diatom abundance increased by 12% in the +Co treatment (Table **??**). Thus, with the exception of bioassay RV1 (Figure **??**), +Co treatments resulted in little meaningful increases or decreases in diatom abundance relative to the control. Coccolithophores appeared to respond more to +Co addition, with relatively greater increases and decreases in abundance compared with the control population. Despite a significant decrease in total chlorophyll *a* concentrations in the +Co treatment of RV2 (Figure **??**), this was not reflected in either the coccolithophore or diatom community abundance, with coccolithophore abundance staying the same in all treatments whereas diatom abundance increased by only 13% in the +Co treatment (Table **??**). Once again, as with the +Fe treatments in RV1, this suggests that the majority of the biomass represented by total chlorophyll *a* concentrations in this bioassay is made up of small-celled phytoplankton which did not show up in SEM images.

Table 3.9: Percentage change in coccolithophore and diatom abundance in trace metal treatments relative to the control

Bioassay	Phytoplankton	Iron	Zinc	Cobalt
MV3	Coccolithophore	-24%	11%	-5%
	Diatom	-41%	16%	-15%
MV4	Coccolithophore	59%	465%	13%
	Diatom	33%	-66%	0.22%
RV1	Coccolithophore	174%	46%	79%
	Diatom	1700%	159%	40%
RV2	Coccolithophore	-4%	1%	-10%
	Diatom	36%	-8%	13%
RV3	Coccolithophore	129%	-43%	-48%
	Diatom	15%	-21%	-9%
RV4	Coccolithophore	-100%	63%	-100%
	Diatom	105%	19%	61%

As seen in Table **??**, responses to trace metal additions were highly variable between experiments and between parameters measured. However, closer examination of changes in coccolithophore and diatom abundance in the trace metal treatments relative to the control suggests that despite there being no significant change in total community biomass (as inferred from total chlorophyll *a* concentrations) in a number of bioassays and treatments, individual taxa appear to experience large increases in abundance in some of the trace metal treatments (Table **??**). For example, despite no significant change in total chlorophyll *a* concentrations in any of the trace metal treatments in bioassay RV1, both coccolithophore and diatom abundance increased in response to Fe (by 173% and 1700%, respectively) (Table **??**). Similarly, in MV4 coccolithophore abundance increases by 465% in response to the +Zn treatment relative to the control, whereas total chlorophyll *a* concentrations increased significantly in response to +Fe. In contrast, in RV2 total chlorophyll *a* in both the +Zn and +Co treatments decreased significantly whereas there was very little change in overall coccolithophore and diatom abundance (Table **??**). These results suggest that changes in total chlorophyll *a* concentrations (community biomass) are not necessarily representative of the response of coccolithophores and diatoms to trace metal additions. As small-celled and non-biomineralised phytoplankton do not show up in SEM preparations, where these small phytoplankton dominated the community they are likely to dominate the chlorophyll *a* response. A similar trend was seen in Chapter 2, where *Synechococcus* and picoeukaryote abundance, though high, showed no significant response to +Fe addition.

Initial macronutrient conditions, rather than trace elements, across the GCB bioassays may have also played an important role in limiting phytoplankton growth. Diatoms typically require silicic acid and NO_x in roughly equal amounts (**?**), however, there was a great disparity in initial concentrations of NO_x and silicic acid across the GCB, with NO_x typically found in high (non-limiting) concentrations of more than $17\,\mu$M (MV3, MV4, RV2 and RV3) and silicic acid frequently found in near limiting concentrations of less than $2\,\mu$M (MV4, RV1, RV2 and RV4) (**?**). Thus, it is highly likely that at the majority of bioassay locations diatoms were already limited by silicic acid availability, in addition to potential trace metal limitations. For example, diatoms in bioassay RV1 were likely to be co-limited by NO_x and silicic acid availability (initial concentrations of $0.06\,\mu$M and $1.30\,\mu$M, respectively) and this is reflected in the low initial diatom abundances ($3.5 \pm 1.4\,\text{cells}\,\text{mL}^{-1}$) (Table **??**). In RV1 coccolithophores also numerically dominated (>70%) and are generally able to grow faster under low nutrient conditions (**?**). However, in the +Fe treatment, despite low macronutrient concentrations, both coccolithophores and diatoms did exhibit large increases in their growth rates (from $0.18\,\text{d}^{-1}$ to $0.69\,\text{d}^{-1}$ and from $0.45\,\text{d}^{-1}$ to $1.89\,\text{d}^{-1}$, respectively (Table **??**)). Similarly, both +Zn and +Co treatments exhibited increased growth rates relative to the control, whereas, in bioassay RV3, which was characterised by extremely high initial concentrations of both NO_x and silicic acid ($27.74\,\mu$M and $40.10\,\mu$M, respectively), diatom abundance was initially high ($1636.0 \pm 27.7\,\text{cells}\,\text{mL}^{-1}$) and coccolithophore abundance negligible ($1.0 \pm 0.7\,\text{cells}\,\text{mL}^{-1}$). While both taxa responded to +Fe addition with higher growth rates over the course of the experiment ($1.54\,\text{d}^{-1}$ to $1.95\,\text{d}^{-1}$ and from $0.16\,\text{d}^{-1}$ to $0.23\,\text{d}^{-1}$, respectively, see Table **??**), coccolithophore abundance increased by 129% relative to the control, whereas diatom abundance increased by only 15%. This indicates that despite lower overall growth rates, coccolithophores exhibited a greater response to +Fe addition relative to the control compared with diatoms. This suggests that despite the phytoplankton community initially being heavily dominated by diatoms, coccolithophores were still able to take advantage of the increased Fe availability via elevated growth rates. This directly contradicts the results of **?**, where initial low cell numbers of *E. huxleyi* further decreased in response to Fe fertilisation. In bioassays where no response by phytoplankton to trace metals was evident, it is possible that increases in abundance could be masked by zooplankton grazing effectively removing any new biomass. Moreover, negative responses could be due to negative effects on cellular metabolism or increased competition between taxa. Generally, these results support other evidence that different taxa co-exist (rather than replace each other through succession) through differences in net population growth rates and that competition between groups is affected by variability in macro- and micronutrient uptake rates and shifts in grazer dominance.

3.4.3 Coccolithophore response to trace metals

Previous studies, including Chapter 2, have also demonstrated that coccolithophores respond positively to Fe (**??**), while several studies have shown that *E. huxleyi* requires metals such as Fe (**??**), Zn and Co (**???**) for its metabolism. Coccolithophore growth in the subpolar North Pacific has also been found to be limited by Zn availability (**?**), while *E. huxleyi* requirements for Zn are low in comparison to other phytoplankton species (**??**) and Co can be substituted for Zn by *E. huxleyi* (**?**). Hence, although +Fe treatments appeared to show the most consistent response across the majority of GCB bioassays, in a subset of the bioassays (i.e. MV3, MV4, RV1, and RV4) +Zn treatments coccolithophore abundance exhibited similar positive results. In fact, coccolithophores more typically responded positively to +Zn treatments (Table **??**) than +Fe treatments. Therefore, Zn limitation of coccolithophore growth can be expanded from the sole observations of Crawford et al. (2003) in the subpolar North Pacific to include sections of the South Atlantic and South Indian Oceans. In contrast, the response to +Co addition was much more complex, with measured parameters either remaining similar to the control or decreasing slightly, apart from in the bioassays that had low initial Co concentrations (RV1 and RV4, 26 and 16 pM, respectively). To conclude, the response to trace metals by coccolithophores and diatoms is related to the initial nutrient availability, including both macro- and micronutrients, and initial community dynamics, although most communities in the GCB responded positively to Fe, coccolithophores often exhibited strong responses to +Zn addition, while little overall response was seen for Co additions.

3.5 Conclusions and Wider Implications

It is clear from this study that coccolithophores respond positively to Fe with increased abundance relative to unamended bioassays. Moreover, it appears that coccolithophores will respond positively to +Fe additions even when initial dFe concentrations are relatively high, as was seen in the South Atlantic bioassay (MV4). Interestingly, in some bioassays both coccolithophores and diatoms responded positively to Zn amendment though this did not appear to necessarily correlate with low initial dZn concentrations. Though there were isolated instances of coccolithophore and diatoms responding to Co, generally Co amended bioassays did not show significant changes in abundance, macronutrient utilisation or total chlorophyll *a* concentrations. The location of the bioassays and thus initial conditions, played a more significant role in coccolithophore (and diatom) community composition than trace metal additions, which supports the results from Chapter 2. The wide range of initial conditions of bioassays in this study across the GCB, specifically initial macronutrient availability as well as the composition of the starting

coccolithophore and diatom community, were good indicators of subsequent responses to trace metals. Relative proportions of coccolithophores and diatoms within the phytoplankton assemblage in addition to *in situ* macro- and micronutrient availability gave good insight into how the overall community would respond to trace metal addition.

Results in this chapter highlight the importance of examining the differential responses of the entire phytoplankton community, especially as different sized taxa respond differently to nutrient limitation. While these results suggest that +Fe addition, and to a lesser extent +Zn addition, stimulate both coccolithophore and diatom growth rates, based on the lack of significant differences between treatments' total chlorophyll *a* concentrations, small-celled phytoplankton do not respond to trace metal addition. Future studies need to incorporate both SEM and flow cytometry, as well as phytoplankton diagnostic pigments (High-Performance-Liquid-Chromatography) and/or size-fractionated chlorophyll *a* to determine the response of different components of the phytoplankton community. The results of this study also indicate that further research is needed to study how coccolithophores respond to Fe and Zn availability under different CO_2 concentrations, especially in the Southern Ocean where the effects of Ocean Acidification will be first felt.

Acknowledgements

Thanks go to the Master, the officers and crew and participating scientists aboard the *R/V Melville* in 2011 and *R/V Revelle* in 2012.

Work from this chapter was made possible through funding by the National Environmental Research Council (NERC) Postdoctoral Fellowship to Dr Alex J. Poulton, grant no. NE/F015054/1; UK Ocean Acidification funding (NERC, Defra, DECC), including an Added Value Award and tied studentship (H. Smith) to Dr Alex J. Poulton, grant no. NE/H017097/1; Great Belt cruises supported by National Science Foundation grants (OCE-0961660, OCE-0728582 to Dr W. M. Balch, Bigelow) and NASA (NNX11A) 72G, NNX11AL93G, NNX14AQ41G, NNX14AQ43A, NNX14AL92G, and NNX14AM77G to Dr W. M. Balch).

Chapter 4

Effect of iron addition and pCO_2 manipulations on phytoplankton communities in the Scotia Sea

Abstract

The Southern Ocean is an important region globally, playing a significant role in regulating the world's climate through the transport of heat, freshwater, nutrients and CO_2 (**?**). Rising atmospheric CO_2 causes a reduction in ocean pH (termed Ocean Acidification) as the oceans take up more atmospheric CO_2. Ocean Acidification is altering the balance of the ocean's carbonate chemistry and this process is accelerated in the Southern Ocean as CO_2 is more soluble at lower seawater temperatures. Coccolithophores, with their calcium carbonate shells, are likely to be sensitive to declining pH and there is conflicting evidence as to their response (**????**). As well as Ocean Acidification, dissolved iron (dFe) concentrations in the surface waters of the Southern Ocean are low (<0.1 nM) and limiting to phytoplankton growth and productivity (**?**), with various climate change scenarios predicting changes in the flux of dFe to the Southern Ocean, though the magnitude and direction of these changes are hard to quantify with so many factors affecting dust supply (**?**). Four iron (Fe) and carbonate chemistry manipulated bioassays were performed in the Scotia Sea region of the Southern Ocean in austral summer of 2013 in order to better understand how coccolithophores and phytoplankton respond to Fe and to future changes in pCO_2 conditions. Underway measurements of macro- and micronutrient concentrations, and underway counts of *Emiliania huxleyi* abundance were also used to complement the results of the bioassays as well as surface rates of primary production (PP) and calcite

production (CP) from CTD profiles along the cruise track. Significant increases in total phytoplankton biomass in response to +Fe addition occurred in three of the four Scotia Sea bioassays. Small ($< 10\mu$m) phytoplankton responded to Fe addition in terms of chlorophyll *a* in two bioassays (South Orkney Island (E2) and South Sandwich Island (E4)), with no change in the biomass of the large ($> 10\mu$m) phytoplankton size-fraction. However, a significant shift in phytoplankton dominance occurred in the South Georgia bioassay (E3), with +Fe amended treatments becoming overwhelmingly dominated by large ($> 10\mu$m) phytoplankton rather than small ($< 10\mu$m) phytoplankton such as coccolithophores. In fact, only this bioassay (E3) was found to have coccolithophores *(E. huxleyi)* present (mean (S.E) of $314.0 \pm 19.9\,\text{cells}\,\text{mL}^{-1}$ across all treatments and sampling time points), though there was no significant change in coccolithophore abundance in response to +Fe or elevated pCO_2 conditions. This bioassay (E3) had a N:Si of 1.24:1, potentially indicating that competition with diatoms for nitrate was potentially a factor once Fe-limitation was alleviated. Underway measurements of *E. huxleyi* abundance were strongly related with high N:Si and high *E. huxleyi* abundance was also associated with naturally Fe fertilised regions such as around South Georgia. Coccolithophores have a limited distribution in the Scotia Sea, which is possibly due to low seawater temperatures, while where coccolithophores were present, there was some evidence for enhanced abundances in association with increased Fe availability.

4.1 Introduction

Since the dawn of the industrial revolution, large quantities of carbon dioxide (CO_2) have been released into the atmosphere by humankind through a combination of increased fossil fuel use and deforestation (**?**). Less than half of this anthropogenic CO_2 now remains in the atmosphere, instead a large proportion (26%) has been taken up by the ocean (**?**) resulting in pH reductions from ~8.1 to as low as ~7.9 pH units and changes in carbonate chemistry, a process commonly termed 'Ocean Acidification'. The effects of Ocean Acidification will be detected earlier in polar oceans than elsewhere (**??**) as low seawater temperatures increase the solubility of CO_2. Calcifying organisms in the Southern Ocean are thought to be among the first that will be affected by ocean acidification as the increased solubility of CO_2 will result in changes to carbonate chemistry, whereby increased levels of pCO_2 will in turn lead to an increase in the solubility of calcium carbonate ($CaCO_3$) decreasing the $CaCO_3$ saturation state (**?**). Lowering of the $CaCO_3$ saturation state will have knock-on effects in the long term (centuries and longer) on the ocean's ability to absorb atmospheric CO_2 (**?**). With respect to calcifying organisms, $CaCO_3$ formation and dissolution rates vary with the saturation state (Ω), where the dissolution of $CaCO_3$ shells of coccolithophores (and other calcifying organisms) occurs when Ω is < 1.0. Saturation states vary with temperature and depth and are

lowest in the cold, high-latitude oceans such as the Southern Ocean (**?**). Thus, coccolithophores in the Southern Ocean could be at greater at risk of dissolution of their $CaCO_3$ shells by virtue of these low saturation states.

Many climate change scenarios have predicted that inputs of macro- and micronutrients (e.g. Fe) to the Southern Ocean will change through the alteration of aeolian fluxes and ice-melt (**??**), though the direction of change is difficult to quantify. Iron forms an integral part of many cellular and biogeochemical processes, for example Fe is required for the synthesis of photosynthetic pigments such as chlorophyll *a* and light-harvesting antenna. The Southern Ocean is largely Fe-limited as the major sources of Fe input are through aeolian dust deposition and continental sediments (**?**). Thus, changes in the supply of Fe are likely to have far reaching consequences for phytoplankton productivity and species composition in this region. The Southern Ocean is the largest high nutrient, low chlorophyll (HNLC) region in the world (**???**), although images of satellite derived surface chlorophyll (and particulate inorganic carbon) have revealed several areas of high phytoplankton (and coccolithophore) abundance (e.g. **??**). These areas are generally associated with island chains (e.g. Crozet, Kerguelen, South Georgia) and shallow topographic features (**???**) which are thought to provide sedimentary-sourced Fe to local phytoplankton communities. These areas of high phytoplankton biomass are maintained by natural Fe fertilization and play an important role in driving carbon export in the Southern Ocean (**?**).

Despite the majority of studies previously performed in the Southern Ocean focussing on diatoms, better access to scanning electron microscopes in the last 20 years as well as increased interest in nanoplankton has highlighted the importance of the coccolithophore *Emiliania huxleyi*, with a number of recent studies indicating that *E. huxleyi* is widespread in surface waters of the Antarctic Circumpolar Current (ACC) and north of the Polar Front (PF) (**?**) (see Figure **??**) in summer months (e.g. **??**). A four year study conducted by **?** in waters south of Australia reported high (up to $400\,\text{cells}\,\text{mL}^{-1}$) abundances of *E. huxleyi* between the PF (~ 55ºS) and the Southern ACC Front (SACCF) (~ 63ºS) during austral spring and summer. In Chapter 3, Fe availability was shown to have a strong influence on coccolithophore abundance across Great Calcite Belt in the Southern Ocean.

Ocean Acidification is generally expected to reduce calcification by marine organisms such as coccolithophores, which are the major pelagic producers of calcium carbonate ($CaCO_3$) in the world's oceans (**?**). The majority of studies exploring how coccolithophores respond to ocean acidification have been laboratory culture experiments, often using one strain and/or one species (often *E. huxleyi*). However, evidence as to how coccolithophores respond to decreased pH is conflicting, with some studies demonstrating a reduction in calcification in *Emiliania huxleyi* in response to increased atmospheric CO_2 (**???**) and other studies reporting increases in calcification in response to increasing CO_2 concentrations under light saturation (**?**). The effect of increased pCO_2/lower pH on *E. huxleyi* is

thought to be closely related to the morphotype studied (**??**).

A number of dFe response bioassays have been performed in the Southern Ocean, either looking at artificial Fe addition (e.g. EIFEX (**?**)) or natural Fe fertilization (e.g. KEOPS (**?**) and CROZE'X (**??**)). However, despite the importance of Fe availability for coccolithophores being highlighted by several recent studies (e.g. **??**; Chapters 2 and 3), none of these studies have focussed on the response of Southern Ocean coccolithophores. . Furthermore, recent literature (**?**) has also highlighted the potential expansion of coccolithophores into the polar oceans possibly linked to increased bicarbonate (HCO_3^-) availability for calcification due to Ocean Acidification, although another study has suggested that increased irradiance and stronger stratification may actually favour this biogeographical shift (**?**). A major restriction on the range expansion of coccolithophores is likely to be the availability of dFe, as well as competition with diatoms for dFe when dSi is relatively high (**?**).

The aims of this chapter are to: (1) examine the spatial distribution of coccolithophores in the context of dFe distribution and macronutrient (NO_x, dSi) concentrations, and (2) contrast responses of diatoms and coccolithophores (cell numbers and calcite production) to dFe enrichment and decreases in pH (increase in pCO_2). Four on-deck bioassays were performed during the cruise JR274 to the Scotia Sea in austral summer of 2013. Incubations were amended with ambient pCO_2 and Fe, Fe and elevated pCO_2 (+Fe, +750 µatm), and ambient Fe and increased $pCO_2$to $\sim$ 750 µatm, $\sim$ 1000 µatm and $\sim$ 2000 µatm. The hypotheses for this chapter are: (1) coccolithophores will respond positively to +Fe addition with increased growth rates and calcite production, under ambient pCO_2 conditions but negatively under elevated pCO_2 conditions; and (2) the general phytoplankton community will only respond positively to increased pCO_2 conditions when dFe is non-limiting.

4.2 Materials and Methods

4.2.1 Sampling

The data set was collected during a cruise to the Scotia Sea in the Southern Ocean (Figure **??**) in the austral summer of 2013 (11th of January to the 5th of February 2013) aboard the *RRS James Clarke Ross* (JR274). The cruise was part of the UK Ocean Acidification program (www.oceanacidification.org.uk). The data collected during the JR274 cruise includes: (1) underway measurements of macronutrient concentrations (NO_x and silicic acid), dFe concentrations and *E. huxleyi* abundance; (2) discrete measurements of primary production,$> 10\mu$m primary production and chlorophyll *a* concentration from CTD casts; and (3) four bioassays investigating the individual and combined effects of +Fe and pCO_2 manipulations.

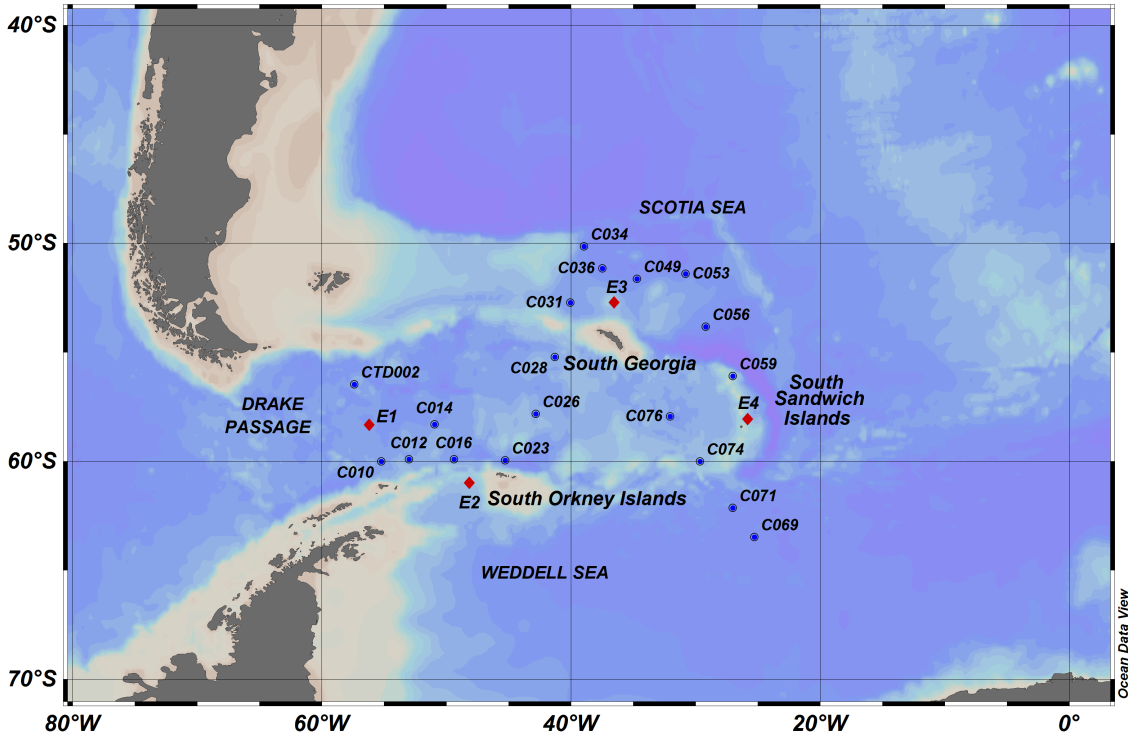

(a)

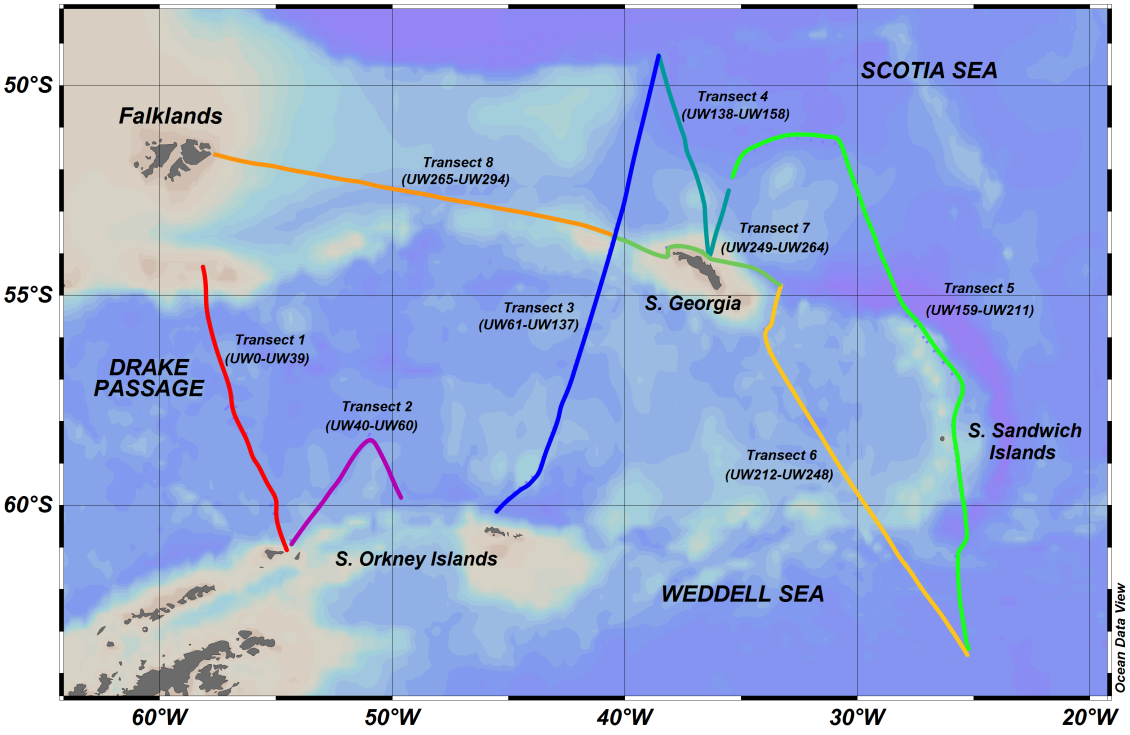

(b)

Figure 4.1: Map of the Scotia Sea, Southern Ocean showing a) the locations of CTDs (blue dots) and the four bioassays (red dots) and b) the cruise track with the different transects represented by different colours, underway station labels covered by each transect are provided in brackets (**?**).

4.2.2 Underway Data: Coccolithophore Counts, Macronutrients and Dissolved Iron

Underway data was collected from either the ship's underway seawater supply, a pipe supplying seawater directly to the ship's laboratories from an inlet approximately 6 m below the surface, or a trace metal-free fish (towed-body) with seawater pumped onboard using a Tangie centrifugal pump with a working pressure of 4 bar and a flow rate of $7.2\,m^{-3}$ per hour. This method of pumping water is relatively non-destructive and in a previous cruise (JR271), SEM samples from the underway supply showed no evidence of detrimental effects on the coccolithophore assemblage. Additionally, seawater was pumped through a large hole-size (~5 mm) mesh to prevent large particles from entering the underway supply. Samples were collected manually from the underway supply every two hours for the majority of the cruise, with the exception of around the South Orkney Islands to the north of South Georgia (Transect 3, Figure **??**), where sampling frequency was increased to once every hour. Samples were collected 24-hours a day, however the underway supply was switched off when there was a large concentration of floating ice. Seawater samples were collected for the following at each underway sampling point: 250mL of seawater for coccolithophore enumeration via light microscopy; 20mL for macronutrient concentrations (nitrite+nitrate and silicic acid). Macronutrient concentrations (nitrate+nitrite (NO_x) and dissolved silicic acid) were determined on-board using a Skalar San Plus autoanalyser following the methods of **?**.

Seawater samples for coccolithophore enumeration were gently filtered through 25 mm diameter, $0.8\,\mu$m pore-size Nuclepore cellulose nitrate filters and dried for approximately 2-4 hours at 40ºC. Filters were then stored in Petri-slides. Permanent slides of the filters were made on-board by mounting the filters using low viscosity Norland Optical Adhesive (NOA 74) onto glass microscope slides following methods in **?**. Coccolithophore cell counts and species identification were carried out under cross-polarising light using a Leitz Ortholux microscope ($\times$1000, oil immersion). Either 300 fields of view (FOV) or 300 individual cells (whichever came first) were counted per filter.

In addition to the samples from the ship's underway water supply, 94 surface seawater samples were also collected from an a towed fish which was deployed from the side of the ship to a depth of approximately 2 m every four hours in the open ocean and more frequently when approaching South Georgia. Samples were pumped into a clean sampling container using a Teflon pump and an acid-washed hose. Samples from the towed fish were analysed on-board for dissolved iron (dFe) using flow injection analysis (FIA) techniques (full methods in **?**). Seawater samples were acidified to pH ~1.9 using concentrated HCl (UpA grade) 24-hours before analysis and were spiked with 0.1% hydrogen peroxide one hour before analysis in order to convert any Fe(II) into Fe(III). Samples were pumped for 240 seconds through a column containing Toyopearl AF-Chelate-650M chelating resin (Sigma Aldrich). The column was rinsed for 30 seconds using MilliQ to remove residual salt. Iron was eluted using

0.4 M HCl (SpA). The eluate was then mixed along a 3 m long coiled tubing which was heated to 40ºC with 0.9 M ammonia solution (SpA Romil) and 0.3 M hydrogen peroxide (SpA, Romil) achieving a final pH of 9.4 ± 0.1. The solution was then passed through a photo-counter, with all dFe measurements in triplicate. Reference seawater (Geotraces-S) was measured to check the accuracy of the method. All sample handling and analytical work was done under the laminar flow hood in the clean container using clean trace metal techniques.

4.2.3 Conductivity Temperature Depth (CTD) Profiles: Coccolithophore Counts, Total Chlorophyll *a* Concentrations and Total and Size-fractionated Primary Production

Seawater samples were collected from the middle of the mixed layer (10-30 m) using a Conductivity Temperature Depth (CTD) rosette sampler. Seawater samples were drawn from Niskin bottles for coccolithophore enumeration via light microscopy (see subsection **??** for methodology), total chlorophyll *a* concentrations and measurements of total and $> 10\mu$m PP.

Replicate seawater samples for chlorophyll *a* measurements of 100mL were filtered onto 25 mm Whatman glass microfibre filters (Grade GF/F) or onto 10μm pore-size polycarbonate filters in order to yield a total chlorophyll *a* and a $> 10\mu$m size-fraction respectively (and therefore by difference a $< 10\mu$m size-fraction). Filters were then extracted in 90% acetone for 24-hours, and chlorophyll *a* was then measured using a Turner Designs Trilogy fluorometer calibrated using dilutions of a solution of pure chlorophyll *a* (sigma, UK) in 90% acetone and a solid fluorescence standard (**?**).

Daily rates (dawn-to-dawn, 24-hours) of total and size-fractionated ($< 10\mu$m) primary production (PP) (as well as calcite production (CP) for the bioassays) were measured following the methodology of **?**, see Figure **??** in Chapter 2. For total PP and CP, seawater samples (70mL, 3 light, 1 formalin-killed) were collected from Niskin bottles and spiked with $30-40\mu$Ci of 14C-labelled sodium bicarbonate and incubated on deck. Seawater samples were filtered through 25 mm 0.4μm Nuclepore polycarbonate filters and rinsed with fresh, filtered seawater to remove any residual 14C-sodium bicarbonate not incorporated during the incubation. Seawater samples for determination of size-fractionated PP, were spiked with $6-7\mu$Ci of 14C-labelled sodium bicarbonate and incubated on deck. Samples were then filtered through 25 mm 10μm Nuclepore polycarbonate filters and rinsed with fresh, filtered seawater as above. Filters were then placed into the bottom of glass vials and sealed with a gas-tight septum and small bucket containing a Whatman GFA filter soaked in phenylethylamine (PEA). The glass vials then had phosphoric acid (1mL, 1%) injected through the septum into the bottom of the vial to convert 14C-particulate inorganic carbon (calcite) into 14C-CO_2. This effectively allows one to differentiate organic carbon production by

photosynthesis from CP, which represents calcification. The GFA filters were then removed after approximately 24-hours and placed in a new glass vial, with 10-15mL liquid scintillation cocktail (Optima Gold, Perking Elmer) added to both. One vial contained the polycarbonate filter (non-acid labile; i.e. PP) and the other contained the GFA filter (acid-labile; i.e. CP). Activity on both filters was determined using a Tri-Carb 2100 Low Level Scintillation Counter and counts were converted to uptake rates using standard methodology (e.g. **??**).

4.2.4 Bioassays: Coccolithophore Counts, Primary Production, Calcite Production and Macronutrient Concentrations

Water for the bioassays was collected using trace metal clean Niskin bottles (24 $\times$ 10L) attached to a titanium framed CTD rosette sampler. In order to supply enough water for the large number of final measurements (see **?**), four successive CTD casts were required. CTDs were deployed at approximately 2-5 am local time and seawater was collected from the surface mixed layer (~20-30 m). Once on deck, bottles were immediately transferred to a class-100 filtered air environment within a trace metal clean container in order to avoid contamination. Unfiltered seawater was distributed into ~100 4.5L polycarbonate incubation bottles using acid-cleaned silicon tubing and sealed awaiting carbonate chemistry manipulation. The locations of the sampling for the bioassays are shown in Figure **??**.

Four bioassays were conducted to test the short-term response of phytoplankton to Fe addition and to artificial carbonate system manipulation. In bioassays E1 and E2, the effect of added Fe (+2 nM Fe), high pCO_2 (targeted at $\sim 750\,\mu$atm) as well as both added Fe and high pCO_2 ($750\,\mu$atm and $+2\,$nM Fe) were tested (Table **??**). In bioassays E3 and E4, having shown an +Fe response in bioassay E2, the treatments in the subsequent bioassays focussed on pCO_2 manipulation only, although further +Fe addition controls were also carried out. Individual bottles were manipulated in order to achieve three different pCO_2 levels (targeted at ~ 750, ~ 1000 and $\sim 2000\,\mu$atm) and this was achieved through the addition of $NaHCO_3^-$ and HCl ((**???**)). Initial carbonate chemistry was immediately measured to determine acid and base additions through total alkalinity (TA) and dissolved inorganic carbon (DIC) analyses. Time point measurements of carbonate chemistry were also included. Post dFe and/or pCO_2 manipulations, bottles were gas-tight sealed with septum lids, parafilm and incubated.

Incubation occurred within a purpose-built experimental laboratory container which allowed for precise temperature and light control (**?**). Temperature was maintained at the seawater temperature *in situ* at the time of water collection. Incubations were lit at an irradiance of approximately $100\,\mu Es^{-1}m^{-2}$ and bottles were exposed to 18-hours of light and 6-hours of darkness in order to ensure phytoplankton were not light limited during the

incubations. Bioassays were run for between 4- and 7-days, this included three collection time points at T0, T1 (2-, 3-, or 4-days) and T2 (4-, 6-, or 7-days). After the first bioassay showed that the response to treatments may be slowed by low ambient seawater temperatures, the remaining bioassays were run for a longer duration. Each experimental pCO_2 condition was run in triplicate.

Seawater samples of between 500 to 750mL, for enumeration of coccolithophore abundance using light microscopy (see subsection **??**), were collected from the four bioassays at three time points (T0, intermediate and T_{end}), from each bioassay three replicates samples were taken from each of the four treatments, resulting in 12 samples per time point. Seawater samples (70mL, 3 light, 1 formalin-killed) were collected from bioassays for determination of daily rates (dawn-to-dawn, 24-hours) of total and size-fractionated ($< 10\mu$m) PP and CP and incubated on deck. Methods for determination of total and size-fractionated PP and CP followed those in subsection **??**. Seawater samples of ~100mL were collected from bioassays for determination of total and $> 10\,\mu$m size-fractionated chlorophyll *a* (see subsection **??** for methodology), and macronutrient concentrations (nitrate+nitrite (NO_x) and silicic acid) (see subsection **??**).

4.2.5 Data Analysis

Statistical analysis of biotic and abiotic data was undertaken with one-way ANOVA tests used to determine if there were any significant differences between treatment responses in each bioassay experiment. Significant results obtained from ANOVA tests were further investigated using a Tukey HSD (Honestly Significantly Different) test ($p < 0.05$) for *post hoc* pair-wise multiple comparisons in order to determine which specific treatments were significantly different. ANOVAs were performed for total and size-fractionated chlorophyll *a* concentrations, NO_x, silicic acid concentrations, total and size-fractionated primary production and calcite production. Statistical tests were performed using R (**?**).

4.3 Results

4.3.1 Underway Results: Coccolithophore Counts, Macronutrients and Dissolved Iron

The cruise passed through a wide range of oceanographic regions across the Drake Passage, the western and eastern sections of the Scotia Sea and northerly parts of the Weddell Sea. Underway concentrations of NO_x were high ($> 10\mu$M) at the majority of the stations sampled, with the highest concentrations measured in the Drake Passage (Transect 1) ($20.43 \pm 0.25\,\mu$M) (Figure **??**). Low NO_x ($< 10\mu$M) concentrations were measured at a few locations,

Table 4.1: Table showing treatments applied, number of repetitions and sampling and sub-sampling of individual bioassays.*Bioassays E3 and E4 only had +Fe and +Fe+750µatm measurements taken for macronutrient and chlorophyll *a* concentrations and PP at T3 and T5 (respectively), whereas CP measurements were taken T6 and T7, respectively.

Bioassay	**Duration** (days)	**Treatments**	**Location**	**CTD #**
E1	4	Cont, +Fe (2 nM) , +Fe (2 nM) +750µatm, 750µatm	Mid Drake Passage	C005-C008
E2	6	Cont, +Fe (2 nM) , +Fe (2 nM) +750µatm, 750µatm	Ice-edge SW of South Orkneys	C018-C021
E3	3 and 6*	Cont, +Fe (2 nM), +Fe (2 nM) +750µatm, 750µatm,1000µatm, 2000µatm	North of South Georgia	C040-C043
E4	5 and 7*	Cont, +Fe (2 nM), +Fe (2 nM) +750µatm, 750µatm,1000µatm, 2000µatm	East of South Sandwich Islands	C062-C065

often in close proximity to islands in the Scotia Sea (South Georgia, South Sandwich Islands and the Falklands). The lowest NO_x concentrations (4.74μM) were measured towards the end of the cruise when approaching the Falkland Islands (UW293, Transect 8, Figure **??**). In contrast, silicic acid concentrations were highly variable and generally increased with latitude, ranging from 2.17μM (UW137, Transect 4) at the northern apex of the cruise to 77.62μM (UW223, T6) in the Scotia Sea approaching South Georgia (Figure **??**). The presence of *E. huxleyi* was restricted to regions with high N:Si; that is to say, the northern section of Transect 1, sections of Transects 3, 4, 5 and 6 (where silicic acid concentrations were low) and Transects 7 and 8 (Figure **??**). High *E. huxleyi* abundances were clustered around South Georgia with the highest abundances of *E. huxleyi* (1128.1 cells mL^{-1} and 843.1 cells mL^{-1}) recorded to the south-west of South Georgia (UW100 and UW84, respectively) (Figure **??**). Moderately high mean (S.E) *E. huxleyi* abundances were also recorded in the Drake Passage (175.8 ± 34.3 cells mL^{-1}) and approaching the Falkland Islands (Transect 8) (248.0 ± 20.5 cells mL^{-1}). Due to a combination of no samples being collected in the Drake Passage (Transect 1), during which bottles were being cleaned, and the ship passing through brash ice during the southern portion of Transect 2 (during which the towed fish could not be deployed), underway dFe measurements were patchy. However, there was a clear trend of elevated dFe concentrations (>2 nM) in the vicinity of South Georgia whereas concentrations remained <1 nM throughout the majority of the rest of the Scotia Sea (Figure **??**).

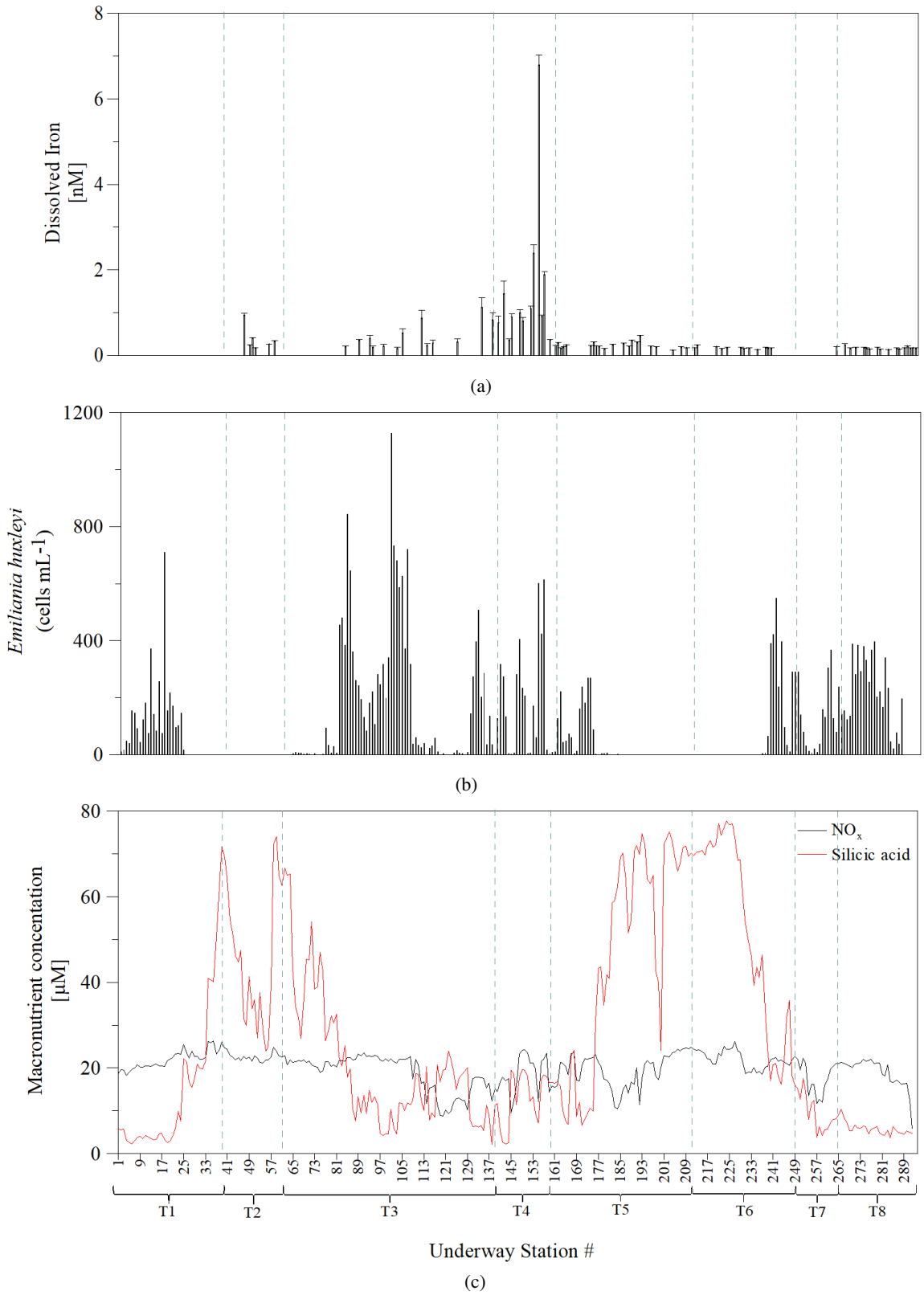

Figure 4.2: Underway measurements of a) dissolved iron (nM) (error bars indicate standard errors), b) *Emiliania huxleyi* abundance (cells mL^{-1}) and NO_x (nitrite+nitrate) and silicic acid (SiO_4) concentrations (μM) at each underway location along the cruise track. Dashed lines indicate the different transects of the cruise (i.e. Transect 1 labelled as T1, see Figure **??**). The black line represents NO_x concentrations and the red line represents silicic acid concentrations.

4.3.2 CTD Results: Total and Size-fractionated Primary Production and Total Chlorophyll a Concentrations

Total primary production (PP) (Figure **??**), $> 10\,\mu$m PP (Figure **??**) and total chlorophyll *a* concentrations (Figure **??**) were low ($< 1\,\mathrm{mmol\,C\,m^{-3}d^{-1}}$ for total PP and$< 1\,\mu\mathrm{g\,L^{-1}}$ for total chlorophyll *a*) at the majority of CTD stations with the exception of those sampled in the waters to the north of South Georgia ($> 2\,\mathrm{mmol\,C\,m^{-3}d^{-1}}$ for total PP and $> 2\,\mu\mathrm{g\,L^{-1}}$ for total chlorophyll *a*; C031, C036, C049, C056) and east of the South Sandwich Islands (C059) (Figure **??**). Station C031, which was sampled to the north-west of South Georgia exhibited the highest PP and total chlorophyll *a* concentrations ($14.90 \pm 5.23\,\mathrm{mmol\,C\,m^{-3}d^{-1}}$ and $14.11\,\mu\mathrm{g\,L^{-1}}$, respectively) encountered in the entire Scotia Sea. The proportion of the total PP composed of the $> 10\,\mu$m size-fraction ranged from as low as 4% (C09) in the Drake Passage, to as high as 86% (C28) to the south-west of South Georgia. CTD stations sampled from the Drake Passage and around the South Orkney Islands exhibited low total chlorophyll *a* concentrations and PP, with the majority of CTD locations dominated by small-celled phytoplankton (>75% of total PP composed of $< 10\,\mu$m size-fraction), with the exception of C002 which was dominated by $> 10\,\mu$m PP (59%). CTDs that exhibited elevated total PP ($> 3\,\mathrm{mmol\,C\,m^{-3}d^{-1}}$) and chlorophyll *a* concentrations ($> 4\,\mu\mathrm{g\,L^{-1}}$) had approximately 50% of their PP composed of $> 10\,\mu$m size-fraction. Station C36, sampled to the north of South Georgia, had high *E. huxleyi* abundance ($399.8\,\mathrm{cells\,mL^{-1}}$) and total PP was dominated by small phytoplankton (73% of total PP composed of $< 10\,\mu$m PP). However, the majority of CTD stations had no *E. huxleyi* present, while waters to the south and north-east of South Georgia (C28 and C31, C34, C36, respectively, see Figure **??**) exhibited low ($25.0\,\mathrm{cells\,mL^{-1}}$) to high ($399.8\,\mathrm{cells\,mL^{-1}}$) *E. huxleyi* abundance. Generally, *E. huxleyi* distribution in the Scotia Sea was limited to north of ~ 58ºS, and concentrated in close proximity to South Georgia.

Calcite production measured from CTD casts (Figure **??**) was highly variable ($0.01 \pm 0.60\,\mu\mathrm{mol\,C\,m^{-3}d^{-1}}$ (C74) to $51.44 \pm 6.60\,\mu\mathrm{mol\,C\,m^{-3}d^{-1}}$ (C53)), however, *E. huxleyi* cells were only detected at four CTD locations (in close proximity to South Georgia Island). Calcite production was lowest in the CTD locations sampled in the vicinity of the South Orkney Islands (C10 - C22) and also at the southern most CTD stations (C66-C74) in the Weddell Sea. High CP was measured in the central Scotia Sea (C26), south of South Georgia (C28) and at the northern most CTD stations to the North of South Georgia (C34-C36 and C44-C53 and C59) (Figure **??**). Cell-specific CP for CTDs 28 - 36 ranged from as low as $0.02\,\mathrm{pmol\,C\,cell^{-1}d^{-1}}$ (C31) where CP was low ($6.38 \pm 1.46\,\mu\mathrm{mol\,C\,m^{-3}d^{-1}}$) and *E. huxleyi* abundance was high ($399.9\,\mathrm{cells\,mL^{-1}}$), to a maximum of $1.70\,\mathrm{pmol\,C\,cell^{-1}d^{-1}}$ (C34) where CP was high ($42.38 \pm 2.24\,\mu\mathrm{mol\,C\,m^{-3}d^{-1}}$).

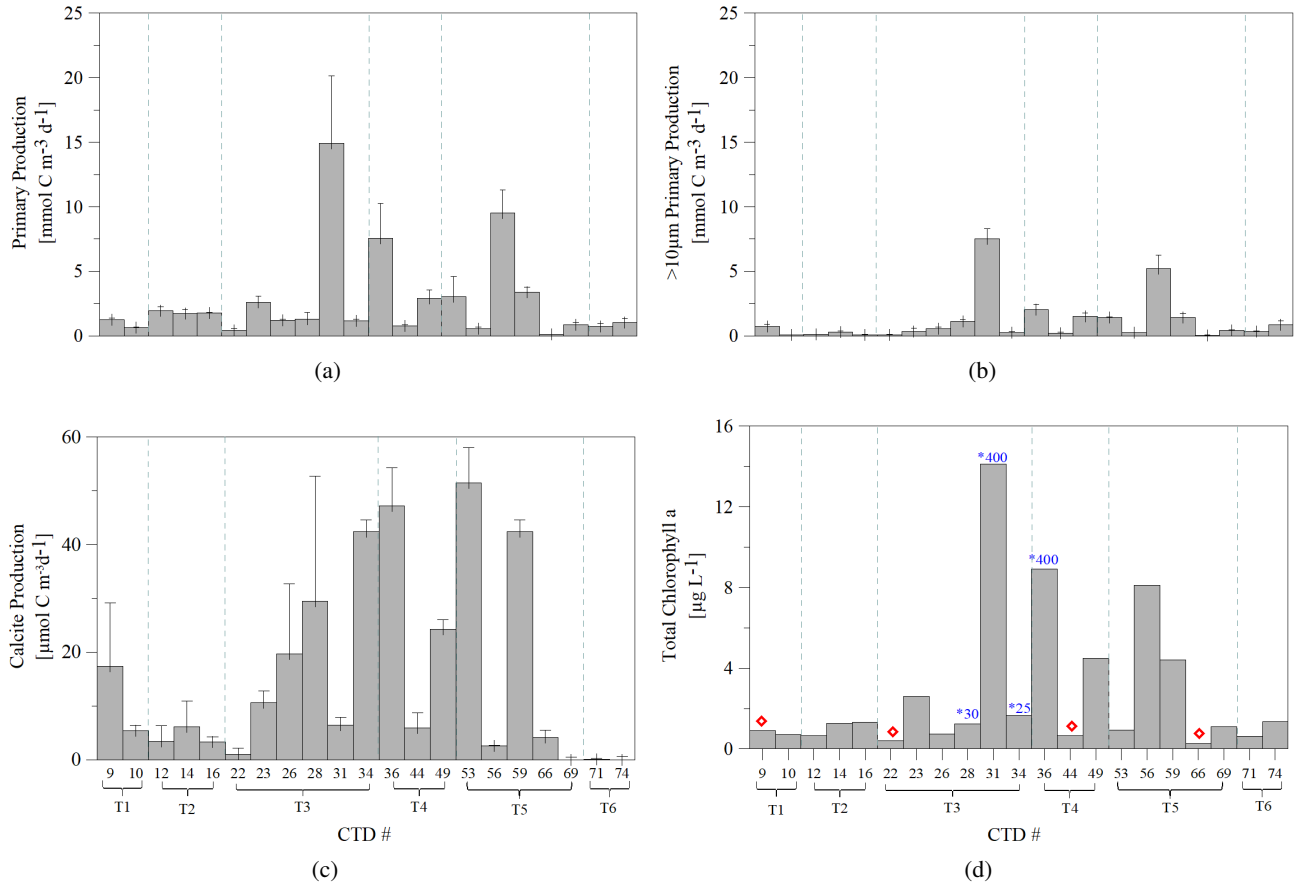

Figure 4.3: Bar graphs depicting a) total primary production ($\mathrm{mmol\,C\,m^{-3}d^{-1}}$), b) $>10\,\mu$m primary production ($\mathrm{mmol\,C\,m^{-3}d^{-1}}$), c) calcite production ($\mu\mathrm{mol\,C\,m^{-3}d^{-1}}$) and d) total chlorophyll *a* concentrations ($\mu\mathrm{g\,L^{-1}}$) collected from surface waters from select CTDs. Error bars indicate standard errors. Blue numbers indicate *Emiliania huxleyi* abundance ($\mathrm{cells\,mL^{-1}}$), only CTDs 28 - 36 had *E. huxleyi* cells present. Red diamonds indicate CTDs taken from the same location as bioassays E1-E4 (CTD9-CTD66, respectively).

4.3.3 Bioassay Results: Phytoplankton Responses to Fe and Elevated pCO_2

Sea surface temperatures (SST) at bioassay locations decreased with latitude, from 2.17ºC in bioassay E3 to -1.44ºC in bioassay E2 (Table **??**), while initial macronutrient concentrations were high throughout the bioassays (NO_x, $>18\,\mu$M and silicic acid, $>15\,\mu$M). Total chlorophyll *a* concentrations were also variable, with bioassays north and south of 58ºS characterised by low total chlorophyll *a* concentrations ($0.62\pm0.04\,\mu\mathrm{gL^{-1}}$ and $0.51\pm0.05\,\mu\mathrm{gL^{-1}}$, respectively), whereas bioassays sampled from the mid-Drake Passage and east of the South Sandwich Islands had comparatively higher initial chlorophyll *a* concentrations ($2.31\pm0.04\,\mu\mathrm{gL^{-1}}$ and $4.91\pm0.21\,\mu\mathrm{gL^{-1}}$, respectively) (Table **??**). The $>10\,\mu$m chlorophyll *a* size-fraction followed a similar pattern to that of total chlorophyll *a,* contributing between 35% (E3) and 100% (E1) to the total chlorophyll *a*. Total and size-fractionated PP was high in bioassays E1 and E4 ($\gtrsim 2.2\,\mathrm{mmol\,C\,m^{-3}d^{-1}}$ and $\gtrsim 1.5\,\mathrm{mmol\,C\,m^{-3}d^{-1}}$, respectively),

and comparatively low in bioassays E2 and E3 ($\lesssim 1\,\mathrm{mmol\,C\,m^{-3}d^{-1}}$) which equated to percentage contributions of 98% and 34% for E1 and E4, respectively, and 28% and 56% for E2 and E3, respectively (Table **??**). Initial CP, however, did not follow this pattern and CP was greatest in bioassay E1 ($60.33 \pm 18.24\,\mu\mathrm{mol\,C\,m^{-3}d^{-1}}$) and lowest in bioassay E4 ($4.78 \pm 0.65\,\mu\mathrm{mol\,C\,m^{-3}d^{-1}}$) (Table **??**).

Analysis of variance (ANOVA) ($p < 0.05$) indicated that in bioassays E2, E3 and E4, total chlorophyll *a* concentrations showed significant variations between treatments, however the $> 10\,\mu$m size-fractionated chlorophyll *a* concentrations only showed significant variations in E3 and E4. NO_x and silicic acid drawdown also showed significant variations among the treatments in all four bioassays. Measurements of total and $> 10\,\mu$m size-fractionated PP and CP in bioassay E1 were treated as unreliable and not included (A. Poulton, personal communication). There was no significant change ($p < 0.05$) in total ($F(3,8) = 2.17$) (Figure **??**) and $> 10\,\mu$m size-fractionated PP ($F(3,8) = 0.60$) (Figure **??**) in bioassay E2. However, bioassays E3 and E4, showed significant variation in both total ($F(5,12) = 5.92$ and 11.65, respectively) and $> 10\,\mu$m size-fractionated PP ($F(5,12) = 11.55$ and 5.65, respectively). Calcite production in all four bioassays showed no significant variation among treatment conditions ($F(3,8) = 1.15$ and 1.21 and $F(5,12) = 1.43$ and 1.36, respectively) (see full list of ANOVA and Tukey HSD results in Appendix **??**).

Bioassay E1 was run for 4-days (96-hours) and total chlorophyll *a* concentrations roughly doubled over the duration of the bioassay in all treatments (Figure **??**). In this bioassay, more than 90% of the total chlorophyll *a* biomass was composed of the $> 10\,\mu$m size-fraction in all treatments (Figure **??**). Tukey HSD tests showed that NO_x utilization increased significantly in the +Fe treatment ($4.02 \pm 0.14\,\mu$M) relative to both the 750 µatm ($2.73 \pm 0.07\,\mu$M) and +Fe +750 µatm ($2.62 \pm 0.19\,\mu$M) treatments ($p = 0.00$), though there was no change in NO_x drawdown between the control and +Fe treatment ($p = 1.00$). There was also no significant difference between the 750 µatm and +Fe +750 µatm treatments ($p = 0.93$) (Figure **??**). Silicic acid drawdown was highest in the control ($1.06 \pm 0.12\,\mu$M), and there was a significant difference in drawdown between all treatments with the exception of the 750 µatm and the +Fe +750 µatm treatments ($p = 0.10$). There was also a slight increase in silicic acid concentrations in the +Fe +750 µatm treatment (increase of $0.26 \pm 0.19\,\mu$M) (Figure **??**).

Table 4.2: Location (latitude and longitude) and initial conditions of bioassays including, sea surface temperature (SST), initial mean (±S.E) total chlorophyll *a*, $> 10\,\mu$m chlorophyll *a*, NO_x and silicic acid concentrations and initial mean (±S.E) total primary production (PP), $> 10\,\mu$m primary production and calcite production (CP).

Bioassay	**Lat** (ºN)	**Lon** (ºE)	**SST** (ºC)	**Total Chl a** (μgL^{-1})	**$> 10\,\mu$m Chl a** (μgL^{-1})	**NO_x** (μM)	**SiO_4** (μM)	**PP** (mmol C m^{-3} d^{-1})	**$> 10\,\mu$mPP** (mmol C m^{-3} d^{-1})	**CP** (μmol C m^{-3} d^{-1})
E1	-58.37	-56.25	1.94	2.31 ± 0.04	2.32 ± 0.14	22.01 ± 0.05	15.01 ± 0.06	2.27 ± 0.09	2.24 ± 0.38	60.33 ± 18.24
E2	-60.97	-48.13	-1.44	0.51 ± 0.05	0.34 ± 0.02	24.93 ± 0.11	63.58 ± 0.22	0.61 ± 0.03	0.17 ± 0.03	8.12 ± 5.29
E3	-52.69	-36.62	2.17	0.62 ± 0.04	0.22 ± 0.02	24.08 ± 0.15	19.39 ± 0.05	1.04 ± 0.02	0.58 ± 0.11	32.58 ± 26.10
E4	-58.09	-25.93	0.15	4.91 ± 0.21	2.39 ± 0.19	18.54 ± 0.60	71.31 ± 0.27	4.52 ± 0.31	1.54 ± 0.35	4.78 ± 0.65

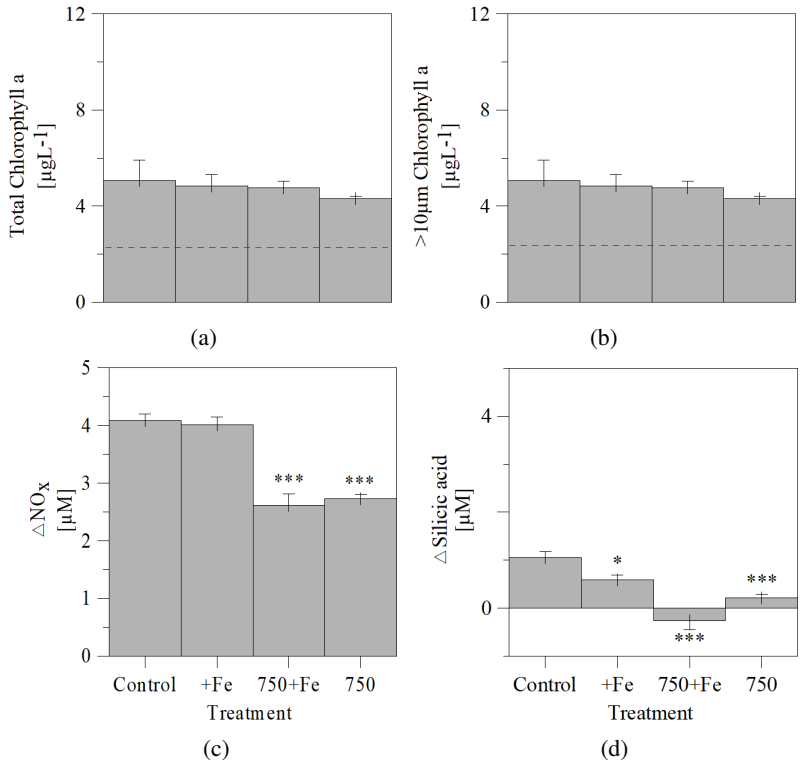

Figure 4.4: Bar graphs for bioassay E1 showing a) total chlorophyll *a* concentrations (μgL^{-1}), b) $>10\,\mu$m chlorophyll *a* concentrations (μgL^{-1}), c) the change in nitrate+nitrite (NO_x) concentrations (μM), and d) the change in silicic acid (SiO_4) concentrations (μM) over the course of the 96-hour bioassay. Error bars indicate standard errors. Dashed red lines indicate initial conditions. Asterisks indicate only significant results from Tukey HSD test for multiple pair-wise comparisons of significant ANOVA results between the control and treatments: * $p < 0.05$, ** $p < 0.01$, *** $p < 0.005$. n=3 for all bioassays.

Bioassay E2, which was run for 6-days (144-hours), had increased total chlorophyll *a* concentrations in all treatments. Pair-wise comparisons revealed that the +Fe treatment was significantly different from the control (p = 0.00), total chlorophyll *a* concentrations were also significantly higher in the +Fe treatment ($2.60 \pm 0.14\,\mu$gL^{-1}) compared with the 750 µatm treatment ($1.82 \pm 0.12\,\mu$gL^{-1}) (p = 0.00) and the +Fe+750 µatm treatment was significantly higher ($2.40 \pm 0.13\,\mu$gL^{-1}) than the 750 µatm treatment (p = 0.02) (Figure **??**). There was no significant difference between treatments with respect to the $>10\,\mu$m size-fractionated chlorophyll *a* concentrations, and this size-fraction dominated the total chlorophyll *a* concentrations in this bioassay, making up on average ~65% of the total (Figure **??**). The highest NO_x drawdown occurred in the +Fe treatment ($0.76 \pm 0.17\,\mu$M), which was significantly greater than the 750 µatm treatment (p = 0.00), although, there was no significant difference between any of the other treatments (Figure **??**). There was also a significant increase in silicic acid drawdown in the +Fe+750 µatm treatments relative to the control (p = 0.04) (Figure **??**).

There was no change in total or size-fractionated PP (Figure **??**) or CP in bioassay E2 (Figure **??**). Initially only

28% of the total PP was dominated by $> 10\mu$m PP and this proportion increased over the course of the bioassay, with the control exhibiting the greatest proportion of $> 10\mu$m PP (61%) and the treatments all exhibiting similar proportions of $> 10\mu$m PP (39% (750 µatm), 43% (+Fe) and 48% (+Fe+750 µatm)).

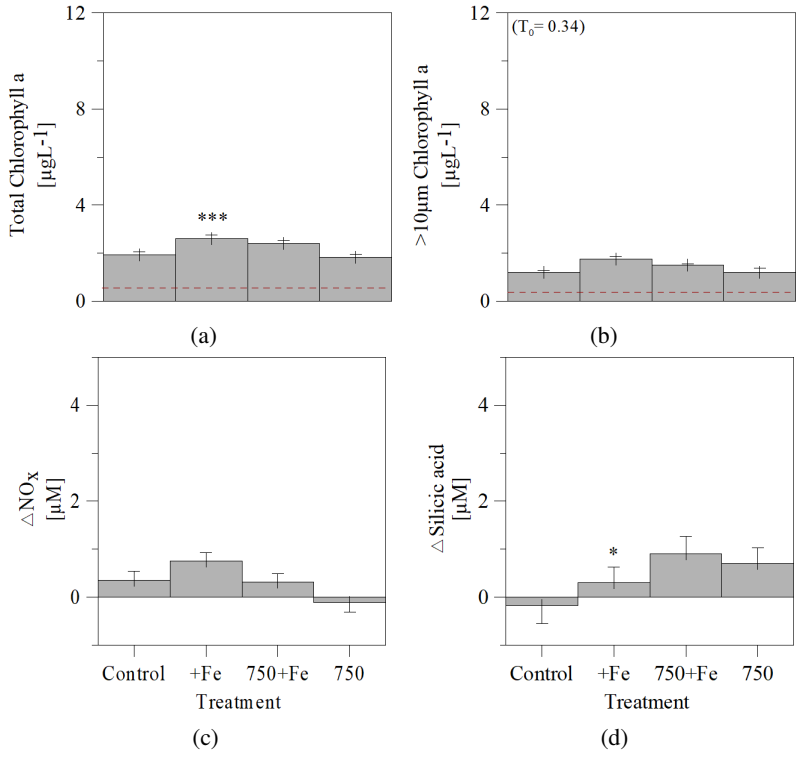

Figure 4.5: Bar graphs for bioassay E2 showing a) total chlorophyll *a* concentrations (μgL^{-1}), b)$> 10\mu$m chlorophyll *a* concentrations (μgL^{-1}), c) the change in nitrate+nitrite (NO_x) concentrations (μM), and d) the change in silicic acid (SiO_4) concentrations (μM) over the course of the 144-hour bioassay. Error bars indicate standard errors. Dashed red lines indicate initial conditions. Asterisks indicate only significant results from Tukey HSD test for multiple pair-wise comparisons of significant ANOVA results between the control and treatments: * $p < 0.05$, ** $p < 0.01$, *** $p < 0.005$. n=3 for all bioassays.

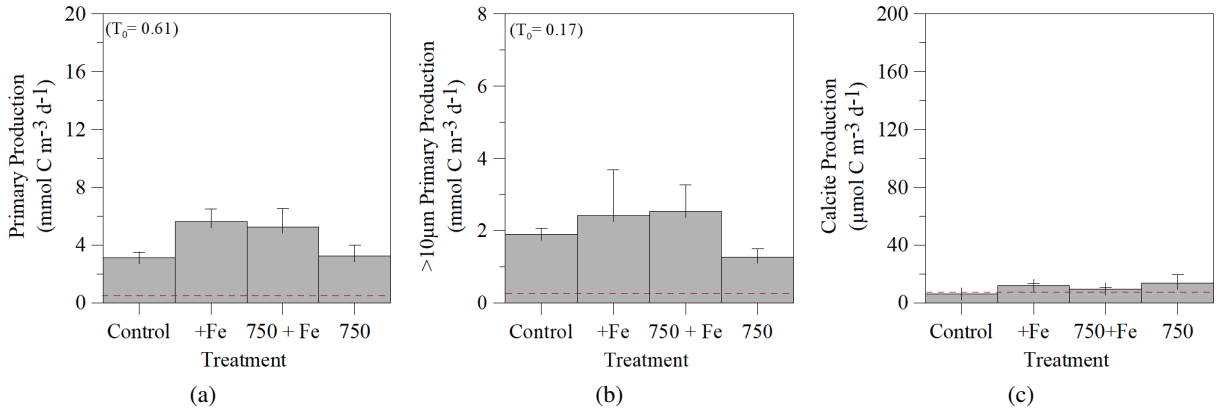

Figure 4.6: Bar graphs showing a) total and b)$> 10\,\mu$m size-fractionated primary production (mmol C m^{-3}d^{-1}) and c) calcite production (μmol C m^{-3}d^{-1}) in bioassay E2. Error bars indicate standard errors. Dashed red lines indicate initial conditions. Asterisks indicate only significant results from Tukey HSD test for multiple pair-wise comparisons of significant ANOVA results between the control and treatments: * $p < 0.05$, ** $p < 0.01$, *** $p < 0.005$. n=3 for all bioassays.

Bioassay E3 was run for a total of 6-days (144-hours), however Fe treatments (+Fe and +Fe+750 µatm) were sampled at 72-hours for macronutrient and chlorophyll *a* concentrations and at 144-hours for PP and CP. Total chlorophyll *a* concentrations in bioassay E3 (Figure **??**) were low overall ($< 1\,\mu$gL^{-1}), with the exception of the +Fe and +Fe +750 µatm treatments which exhibited significant increases ($p < 0.005$) in total chlorophyll *a* concentrations more than double those measured in the control and carbonate chemistry manipulated treatments. A similar pattern observed in the $> 10\,\mu$m chlorophyll *a* size-fraction. NO_x utilization was significantly increased in the +Fe, 750 µatm and 2000 µatm treatments relative to the control (p = 0.01, 0.00 and 0.00, respectively), whereas there was no change in NO_x drawdown between the control, +Fe +750 µatm and 1000 µatm treatments (p = 0.34 and 0.84, respectively) (Figure **??**). Silicic acid drawdown was significantly higher in the +Fe ($1.49 \pm 0.13\,\mu$gL^{-1}) and +Fe +750 µatm ($1.77 \pm 0.21\,\mu$gL^{-1}) treatments relative to the control (p = 0.00) and carbonate chemistry manipulations (p = 0.00) (Figure **??**). Additionally, silicic acid drawdown was significantly higher in the carbonate chemistry manipulated treatments than in the control (p = 0.01, 0.00 and 0.00, respectively). Only this bioassay (E3) had detectable *E. huxleyi* cells present. There were slight increases in abundance over time in the control (13%), +Fe (15%) and 2000 µatm (5%) treatments, with similar decreases in the Fe+750 µatm (-14%), 750 µatm (-20%) and 1000 µatm (-14%) treatments. However, these changes were not statistically significant ($F(5,12) = 2.62$, $p < 0.05$) (Figure **??**).

Tukey HSD tests on significant ANOVA results for bioassays E3 (Figure **??**) and E4 (Figure **??**) showed that PP in the Fe treatments (> 3.7 mmol C m^{-3}d^{-1}) were significantly greater than PP measured in the 2000 µatm treatment

(1.860.17 mmol C $m^{-3}d^{-1}$) (p = 0.02 and 0.00, respectively), and that total PP measured in all other treatments was similar. Iron treatments (+Fe and +Fe+750 µatm) in bioassay E3 (Figure **??**), had the highest $> 10\mu$m PP (2.86 ± 0.34 mmol C $m^{-3}d^{-1}$ and 1.98 ± 0.15 mmol C $m^{-3}d^{-1}$, respectively). $> 10\mu$m PP in the +Fe treatment was significantly greater than in the control (p = 0.00) or carbonate chemistry treatments (p = 0.00). Additionally, the 2000 µatm treatment had significantly lower $> 10\mu$m PP than in the +Fe +750 µatm treatment (p = 0.02). Bioassay E3 (Figure **??**), where CP was highest overall, had increases in CP in the control, +Fe and 750 µatm treatments.

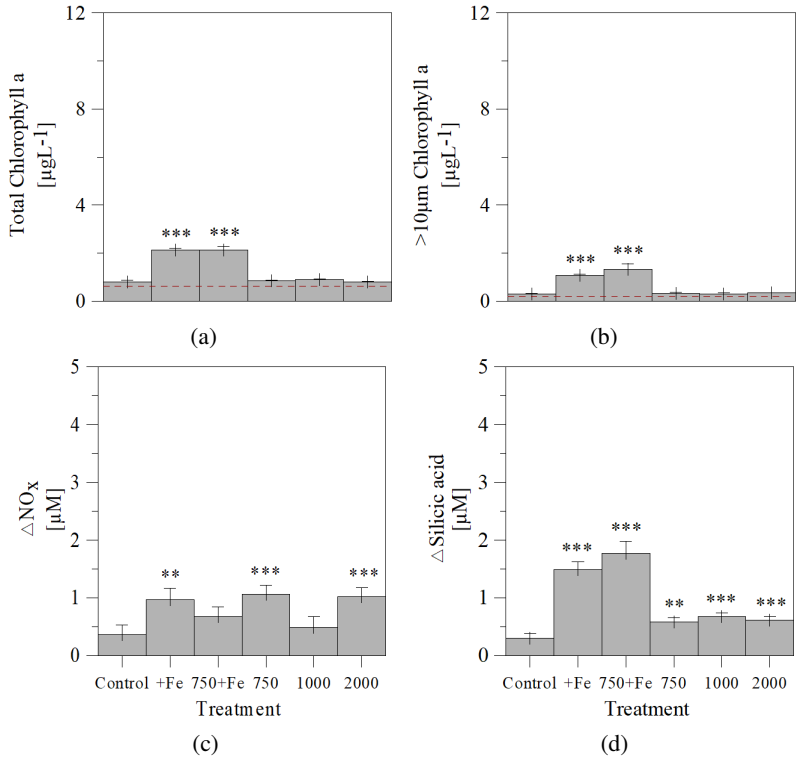

Figure 4.7: Bar graphs for bioassay E3 showing a) total chlorophyll *a* concentrations (μgL^{-1}), b) $> 10\mu$m chlorophyll *a* concentrations (μgL^{-1}), c) the change in nitrate+nitrite (NO_x) concentrations (μM), and d) the change in silicic acid (SiO_4) concentrations (μM) over the course of the 72-hour bioassay. Error bars indicate standard errors. Dashed red lines indicate initial conditions. Asterisks indicate only significant results from Tukey HSD test for multiple pair-wise comparisons of significant ANOVA results between the control and treatments: * p < 0.05, ** p < 0.01, *** p < 0.005. n=3 for all bioassays.

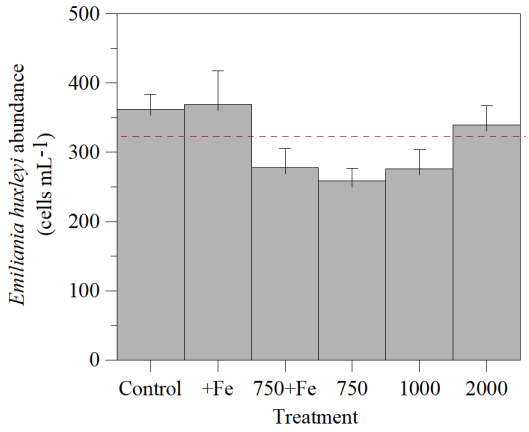

Figure 4.8: Bar graph showing *Emiliania huxleyi* cell abundance (cells mL^{-1}) in bioassay E3. Error bars indicate standard errors. Dashed red line indicates initial cell abundance.

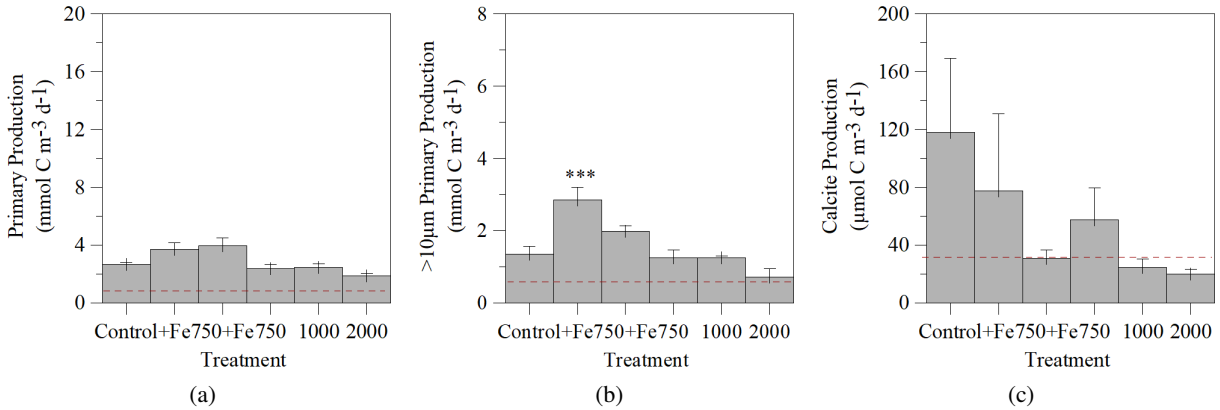

Figure 4.9: Bar graphs showing a) total and b)$> 10\,\mu$m size-fractionated primary production (mmol C $m^{-3}d^{-1}$) and c) calcite production (μmol C $m^{-3}d^{-1}$) in bioassay E3. Error bars indicate standard errors. Dashed red lines indicate initial conditions. *Shows results from T144. Asterisks indicate only significant results from Tukey HSD test for multiple pair-wise comparisons of significant ANOVA results between the control and treatments: * $p < 0.05$, ** $p < 0.01$, *** $p < 0.005$. n=3 for all bioassays.

Bioassay E4 was run for a total of 7-days (168-hours), however like bioassay E3, Fe treatments (+Fe and +Fe+750 µatm) were only sampled at 96-hours for macronutrient and chlorophyll *a* concentrations. Results for bioassay E4 were similar to those of bioassay E3.

Chlorophyll *a* and macronutrient concentrations in bioassay E4 were the highest of the four bioassays. Total chlorophyll *a* concentrations more than doubled in the +Fe ($9.85 \pm 0.77\,\mu$gL^{-1}) and +Fe +750 µatm ($9.70 \pm 0.81\,\mu$gL^{-1}) treatments and were significantly higher than the control ($6.05 \pm 0.60\,\mu$gL^{-1}) ($p < 0.05$) (Figure **??**). However, there was no significant difference in the $> 10\,\mu$m chlorophyll *a* size-fraction or in the NO_x or silicic acid drawdown ($p > 0.05$) between the Fe treatments and the control. Though, there were significant differences between the +Fe and the three carbonate chemistry manipulated treatments (p = 0.01, 0.05 and 0.01, respectively) (Figure **??**). There

was no statistically significant difference between treatments' NO_x utilization, with the exception of the two Fe treatments and the 2000 µatm treatment (p = 0.02). The +Fe and +Fe +750 µatm treatments were composed of a high proportion (74 - 100%) of small ($< 10\,\mu$m) phytoplankton, whereas the control and carbonate chemistry manipulated treatments were dominated by large ($> 10\,\mu$m) phytoplankton (76 - 100%).

The highest overall PP occurred in bioassay E4 (Figure **??**). Total PP in +Fe and +Fe +750 µatm treatments ($14.72 \pm 1.32\,\mathrm{mmol\,C\,m^{-3}d^{-1}}$ and $12.22 \pm 0.55\,\mathrm{mmol\,C\,m^{-3}d^{-1}}$, respectively) were significantly greater than PP in the control ($6.46 \pm 0.69\,\mathrm{mmol\,C\,m^{-3}d^{-1}}$) (p = 0.00 and 0.01, respectively) and that PP in the +Fe treatment was significantly greater than that in the three carbonate chemistry manipulated treatments (p = 0.00, 0.03 and 0.00, respectively). However, PP in the +Fe +750 µatm treatment was similar to total PP in the 750 µatm and 1000 µatm treatments (p = 0.06 and 0.47, respectively) and significantly higher than PP in the 2000 µatm treatment (p = 0.03). There was no difference between total PP in the carbonate chemistry treatments. Initially, only 34% of the total PP was composed of $> 10\,\mu$m PP (Figure **??**). The control had the highest proportion of $> 10\,\mu$m PP (72%) and the two Fe treatments (+Fe and +Fe+750 µatm) had the lowest, 39% and 44% respectively. Carbonate chemistry manipulated treatments had approximately 50% of the total PP composed of $> 10\,\mu$m PP. However, there was no difference in $> 10\,\mu$m PP between the majority of treatments, with the exception of the +Fe treatment which was significantly higher than the 750 µatm and 2000 µatm treatments (p = 0.05 and 0.01, respectively). Calcite production increased uniformly over the course of this bioassay, but did not change in response to Fe addition or elevated pCO_2 (Figure **??**).

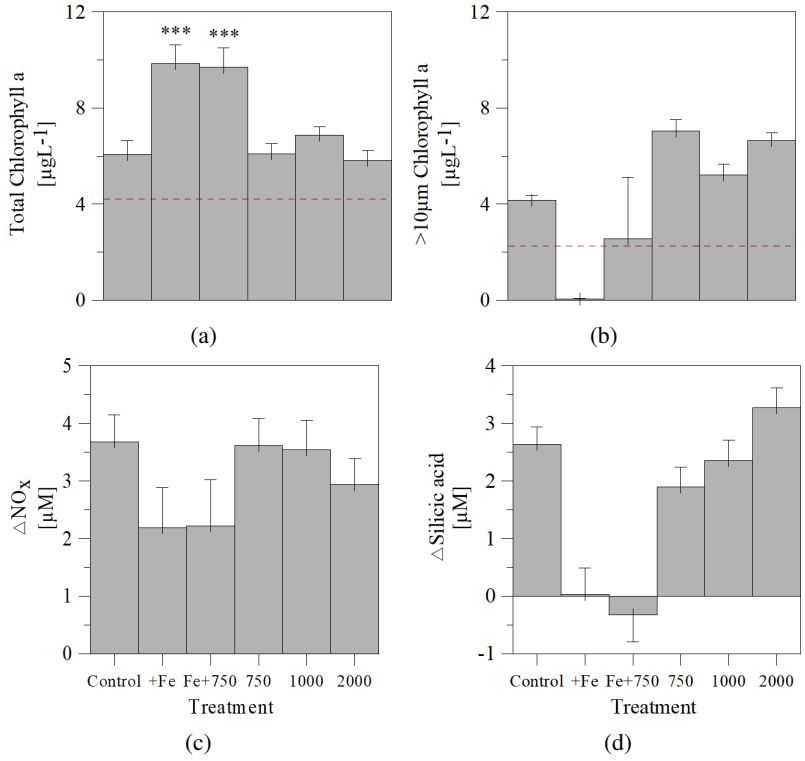

Figure 4.10: Bar graphs for bioassay E4 showing a) total chlorophyll *a* concentrations (μgL^{-1}), b) $>10\,\mu$m chlorophyll *a* concentrations (μgL^{-1}), c) the change in nitrate+nitrite (NO_x) concentrations (μM), and d) the change in silicic acid (SiO_4) concentrations (μM) over the course of the 96-hour bioassay. Error bars indicate standard errors. Dashed red lines indicate initial conditions. Asterisks indicate only significant results from Tukey HSD test for multiple pair-wise comparisons of significant ANOVA results between the control and treatments: * $p < 0.05$, ** $p < 0.01$, *** $p < 0.005$. n=3 for all bioassays.

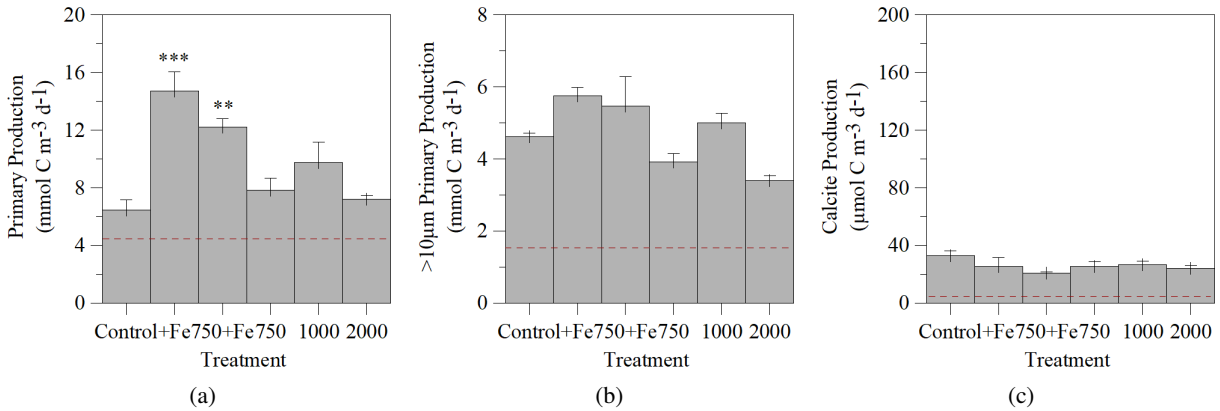

Figure 4.11: Bar graphs showing a) total and b)$>10\,\mu$m size-fractionated primary production (mmol C m^{-3}d^{-1}) and c) calcite production (μmol C m^{-3}d^{-1}) in bioassay E4. Error bars indicate standard errors. Dashed red lines indicate initial conditions. Asterisks indicate only significant results from Tukey HSD test for multiple pair-wise comparisons of significant ANOVA results between the control and treatments: * $p < 0.05$, ** $p < 0.01$, *** $p < 0.005$. n=3 for all bioassays.

4.4 Discussion

4.4.1 Coccolithophores in the Scotia Sea

Emiliania huxleyi cells were present at only a few locations across the Scotia sea (Figure **??**), with abundances ranging from as low as 1.7 cells mL^{-1} (southern portion of Transect 3, central Scotia Sea) to a maximum of 1128.1 cells mL^{-1} (south of South Georgia, Transect 3) (Figure **??**). Such low abundances in the central Scotia Sea were associated with relatively high silicic acid concentrations ($\sim 45\,\mu$M) and in general, high *E. huxleyi* abundance appeared to be related with low silicic acid concentrations ($< 2\,\mu$M) (Figure **??**). Specifically, the majority of *E. huxleyi* communities with abundances greater than ~ 50 cells mL^{-1} were found in waters with a N:Si ratio of >1. (Figure **??**). Previous studies in the Scotia Sea have found that silicic acid concentrations and sea surface temperatures are the two most influential factors in controlling *E. huxleyi* biogeography (**?**). In this study, high *E. huxleyi* abundance (> 200 cells mL^{-1}) was found at a range of dFe concentrations (0.13 nM to 1.89 nM) (Figure **??**), however high abundances of *E. huxleyi* were largely concentrated to the south-east and north of South Georgia (transects 3, 4 and 7, see Figures **??** and **??**). Moderately high abundances were found in the Drake Passage (Transect 1) and along the final leg approaching the Falkland Islands (Transect 8). The regions of elevated *E. huxleyi* abundance in this study, most notably around South Georgia, are areas traditionally associated with elevated dFe concentrations (with the exception of the Drake Passage) (**??**).

Despite *E. huxleyi* only being detected in four of the CTD locations (Figure **??**), again all in close proximity to South Georgia, calcification was measured in varying amounts in all of the CTD locations (Figure **??**). Cell-specific CP, calculated from CP and abundance, show that *E. huxleyi* cells were calcifying at between 0.02 pmol C $cell^{-1} d^{-1}$ and 1.70 pmol C $cell^{-1} d^{-1}$ in these locations. The calcification rate of *E. huxleyi* has been reported to range from 0.05 to 0.08 pmol C $cell^{-1} d^{-1}$ in the North Atlantic (**??**), so cell-specific calcification at these stations appears to be relatively high. Such high values of cell-specific CP may relate to other coccolithophore species being present, although differences between detection limits of *E. huxleyi* light microscope counts and CP measurements could also potentially explain this difference (i.e. *E. huxleyi* counts were on volumes of <10mL, whereas CP rate measurements were on ~100mL).

The data reported here on the latitudinal distribution of *E. huxleyi* in the Scotia Sea is in agreement with previous observations from the Southern Ocean (**?**). The southern-most extent of *E. huxleyi* surface distributions in this study was at $\sim$ 59.69ºS, to the north of the South Orkney Islands (Transect 2), where very low (~ 3 cells mL^{-1}) abundances of *E. huxleyi* were detected. In the Drake Passage in 2006 (**?**), the southern-most extent of *E. huxleyi*

was at 58.1ºS where moderate abundances of 266 cells mL^{-1} were observed, which agrees well with this study, where the southern-most extent of *E. huxleyi* in the Drake Passage was observed at $\sim$ 58.87ºS (16.67 cells mL^{-1}). The highest abundance recorded in the Drake Passage was 708.5 cells mL^{-1} at $\sim$ 57.04ºS, which roughly agrees with previous observations of maximum abundances (between $200-500$ cells mL^{-1}) in the Southern Ocean (**????**). The maximum abundance of *E. huxleyi* seen in this study, in association with South Georgia was 1128.1 cells mL^{-1}. **?** showed that the environmental variables that best correlated with coccolithophore distribution across the Drake Passage were sea surface temperature and mixed layer depth. However, abundance maximum may also be related to other factors at smaller spatial scales, such as increased increased Fe availability (**???**).

Elevated concentrations of nitrate relative to silicic acid are thought to provide non-silicious phytoplankton, such as coccolithophores, with a competitive advantage over diatoms (**?**). Certainly, *E. huxley*i distributions in the Scotia Sea were positively related with regions where silicic acid concentrations were low (Figure **??**). The Southern Ocean is known to be predominantly a HNLC region (**?**), with high concentrations of macronutrients (nitrate, dissolved silicic acid) and low phytoplankton productivity. However, there are also localised areas of high phytoplankton productivity sustained by natural Fe fertilization in association with Antarctic island chains (**??**). Underway dissolved Fe concentrations measured during this cruise were patchy due to the nature of dFe sampling (no samples were collected from the Drake Passage and sampling between the Drake Passage and South Orkney Islands was sporadic due to the ship encountering brash ice) (Figure **??**). However, it is clear that higher concentrations of dissolved Fe were found in the vicinity of islands (South Orkney, South Georgia and South Sandwich Islands). Similarly, the presence of *E. huxleyi* was patchy with higher abundances often found in the vicinity of known, natural Fe fertilised areas such as South Georgia. Based on underway measurements of dFe, macronutrients and coccolithophore abundance during this cruise, it is clear that while *E. huxleyi* is present in waters at a range of dFe concentrations, high abundances of *E. huxleyi* in the Scotia Sea were positively related with naturally Fe fertilised regions such as South Georgia (where the ratio of N:Si was also high) (Figure **??**). This is largely in agreement with other studies which found that silicic acid concentrations and sea surface temperature were influential variables in controlling nanoplankton biogeography (**?**), however, this study suggests that although *E. huxleyi* are known to have low Fe requirements, dFe availability is an important factor in controlling their abundance in the Scotia Sea. The availability of Fe, when nitrate is abundant relative to silicic acid, has also been suggested to be involved in the formation of the Patagonian Shelf coccolithophore bloom (**??**), where the source water for the bloom is from the Drake Passage and Scotia Sea.

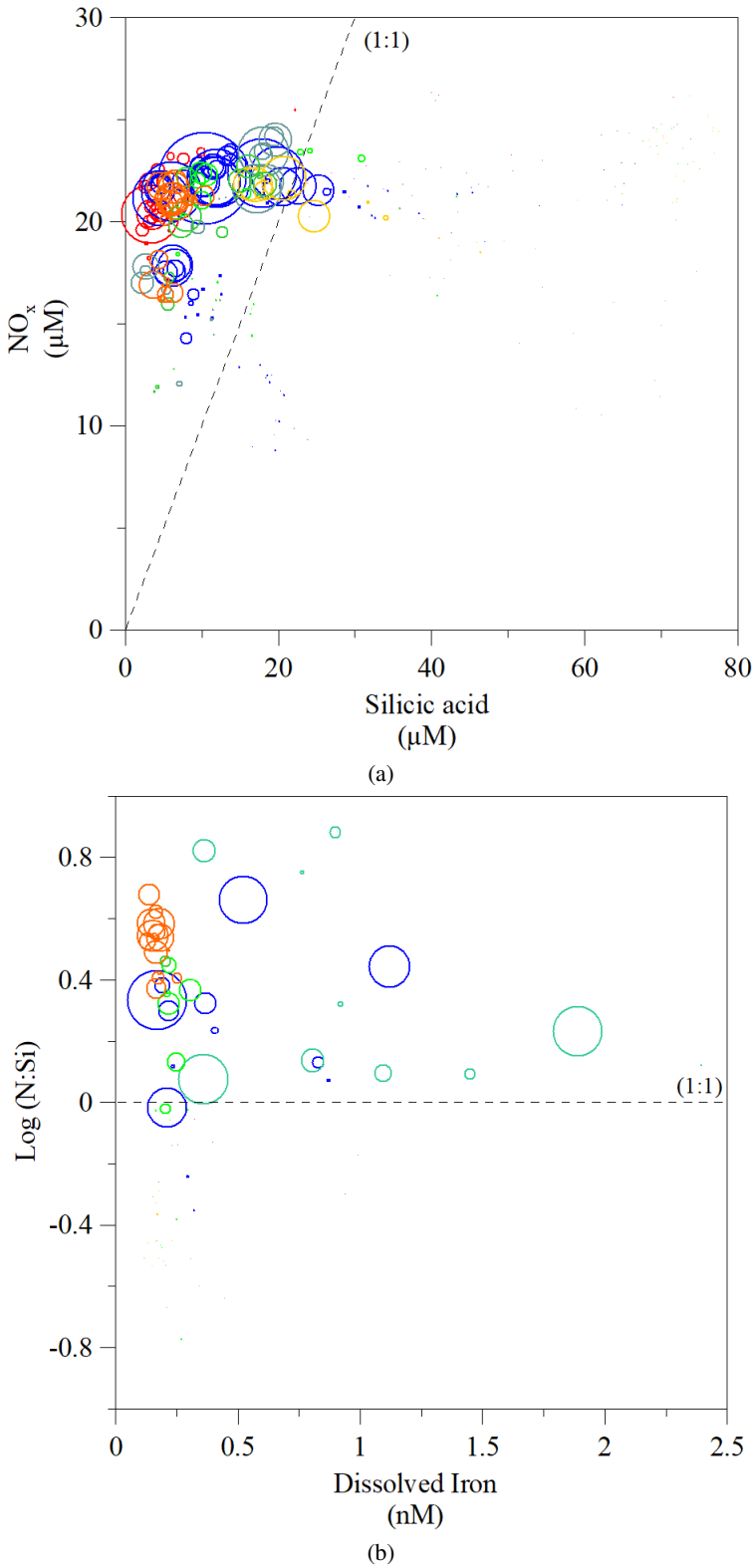

Figure 4.12: Bubble plots displaying the relationship between a) underway measurements of surface macronutrient concentrations (silicic acid and NO_x (μM)) to *E. huxleyi* abundance (cells mL^{-1}) and b) surface macro- and micronutrient concentrations (NO_x to silicic acid ratios and dissolved iron concentrations (nM)) and *Emiliania huxleyi* abundance. *E. huxleyi* abundance represented by bubbles with the smallest 1.67 cells mL^{-1} to largest 1128.13 cells mL^{-1}. The log of N:Si ratios was taken. Dashed lines indicate a ratio of N:Si of 1:1. Samples from the different transects of the cruise are colour coded (see Figure **??**).

4.4.2 Coccolithophore and Phytoplankton Responses to Iron

There was no significant response to either of the Fe treatments in bioassay E1 with respect to chlorophyll *a* concentrations (Figures **??** and **??**). The lack of response by the phytoplankton community in general to +Fe treatments, coupled with the relatively high levels of biomass (as inferred from total chlorophyll *a* concentrations) in this bioassay, suggests that this station was positioned within a non-Fe limited area such as a productive eddy. Moreover, the dominance by large phytoplankton (>90%), which typically have higher Fe requirements, is consistent with a conclusion that this community that was not suffering from *in situ* Fe limitation (**?**).

In contrast, there was a significant increase in total chlorophyll *a* biomass in bioassay E2 in response to +Fe, however there was no corresponding response in the large ($> 10\,\mu$m) size-fraction despite it making up >60% of the total phytoplankton community. This suggests that small, non-silicious phytoplankton (e.g. coccolithophores, dinoflagellates) were responding to +Fe in this location, which is further supported by the fact that there was no significant increase in silicic acid drawdown in the +Fe treatment (Figure **??**). However, there was no evidence of *E. huxleyi* cells being present in this bioassay from the light microscopy samples, and CP was also relatively low ($< 14\,\mu\text{mol}\,\text{C}\,\text{m}^{-3}\text{d}^{-1}$). Thus, *Phaeocystis* sp. or small dinoflagellates may be responding to Fe addition in this bioassay as both of these have been shown to respond to Fe in the Scotia Sea (**??**). The third bioassay was sampled from waters historically associated with the South Georgia phytoplankton bloom (**?**). However, total phytoplankton biomass was relatively low ($0.62 \pm 0.04\,\mu\text{g}\text{L}^{-1}$) and was initially dominated by small phytoplankton (65%) (Figures **??** and **??**). Despite these waters typically being associated with an Fe-replete environment (**?**), total and $> 10\,\mu$m size-fractionated chlorophyll *a* concentrations increased significantly in response to both the +Fe and to +Fe +750 µatm treatments. Previous blooms around South Georgia have been found to be heavily dominated by large phytoplankton and diatoms typically account for the majority of abundance (**?**). Large diatoms require higher concentrations of ambient dissolved Fe than smaller celled phytoplankton such as coccolithophores (**?**). This suggests that despite the bioassay location being traditionally associated with a naturally Fe fertilised bloom, it is likely that phytoplankton were Fe-limited in this bioassay. Hence, the bloom must have progressed to a point when Fe was becoming limiting again in terms of further nutrient utilization. Additionally, *E. huxleyi* abundance did not respond to +Fe treatment, whereas the proportion of large phytoplankton increased over the course of the bioassay with significant increases in $> 10\,\mu$m chlorophyll *a* Fe treatments relative to the control and carbonate chemistry treatments.

Large diatoms typically have higher Fe requirements (**?**) so that when Fe is not limiting, these species are able to outcompete and grow faster than the smaller diatoms and coccolithophores that are also more susceptible to

grazing pressure (**?**). In light of this, community response patterns in the fourth bioassay are particularly striking. Total chlorophyll *a* concentrations (Figure **??**) and PP (Figure **??**) increased significantly in the +Fe and +Fe +750µatm treatments. However, there was no corresponding response in the $> 10\mu$m size-fraction. Initially, the phytoplankton community was dominated by large phytoplankton (56%), while at the final time point the control remained dominated by large phytoplankton (69%), whereas in the two Fe treatments the proportion of small phytoplankton had increased dramatically (74-100% of the total chlorophyll *a*). There were also no changes in NO_x or silicic acid drawdown in the +Fe treatments. Few studies have reported shifts in dominance from large to small phytoplankton in response to Fe addition, which in this case is unexpected due to the high silicic acid concentrations ($> 68\mu$M) in this bioassay. One would expect that when macronutrient concentrations are high, and if Fe-limitation is alleviated the diatom population would flourish (**?**), whereas this does not happen in the fourth bioassay. Moreover, high silicic acid concentrations south of the Polar Frontal Zone (PFZ) (see Figure **??**) generally create favourable conditions for diatom growth (**??**), and Fe fertilization generally stimulates silicic acid depletion.

The location of bioassays where there were significant responses to Fe treatments were all in relatively close proximity to islands (South Orkney (E2), South Georgia (E3) and South Sandwich Islands (E4)) (Figure **??**), where one might expect the resident phytoplankton community to benefit from natural Fe fertilisation associated with the 'island mass effect' (**?**). However, significant increases in phytoplankton biomass observed in these three locations in response to Fe addition as well as non-limiting concentrations of both nitrate and silicic acid, suggest that phytoplankton were Fe limited. Within the different phytoplankton communities present and between the different bioassay locations the response to Fe was not uniform. Small ($< 10\mu$m) phytoplankton responded in E2 and E4, whereas in bioassay E3 it was the large size-fraction that responded to Fe addition. Moreover, bioassays E2 and E4 were both sampled from cold waters (-1.44 and 0.46ºC, respectively) with high silicic acid concentrations ($> 60\mu$M) relative to bioassay E3 where sea surface temperature was 2.18ºC and silicic acid concentrations were relatively low ($< 20\mu$M). It is possible that large phytoplankton in the two cold water bioassays (E1 and E4), were not as well adapted to the low seawater temperatures and were therefore unable to compete with the smaller size-fraction once Fe limitation was alleviated. Another possibility is that the large size-fraction was predated by large zooplankton allowing the small size-fraction to flourish. Such differences in bioassay response, linked to the initial conditions, highlights the importance of initial conditions in influencing phytoplankton community responses to alleviation of Fe limitation.

4.4.3 Phytoplankton Response to Elevated pCO_2

By the year 2100, pCO_2 levels in the ocean have been forecasted to have risen to approximately 700 ppm or higher (**?**). Rising CO_2 will effect marine plankton in various ways (**?**), and due to the inherent complexity of biological systems predicting the direction and magnitude of the change is difficult. In the results presented here, there were generally no changes in phytoplankton biomass or community composition in terms of total or size-fractionated chlorophyll *a* concentrations in response to elevated pCO_2 in all four bioassays. NO_x and silicic acid drawdown appeared to be the only measured parameters that were affected by elevated pCO_2 conditions, however, the response was not uniform across all bioassays. A similar response was observed in a natural phytoplankton assemblage in the Equatorial Pacific, where despite significant shifts in nutrient consumption (and taxonomic composition), total biomass and primary productivity did not change between low CO_2 (150 µatm) and high CO_2 (750 µatm) treatments (**?**). NO_x utilization in bioassay E1 (Figure **??**) decreased by ~33% in the 750 µatm and relative to the control silicic acid drawdown (Figure **??**) decreased by ~80%. Macronutrient drawdown in bioassay E3, however, showed significant increases in pCO_2 treatments relative to the control: NO_x utilization was ~180% and ~190% greater in the 2000 µatm and 750 µatm treatments respectively, and silicic acid drawdown was significantly greater in all three pCO_2 treatments compared with the control (between 90 and 120%). *E. huxleyi* growth rates and CP were not affected by elevated pCO_2 in bioassay E3 (Figure **??**), which contradicts evidence that PP and CP by this coccolithophore species is significantly increased by high pCO_2 (**?**). In the two bioassays where NO_x and silicic acid drawdown responded significantly to elevated pCO_2 (E1 and E3) the N:Si ratio was >1, whereas in bioassays E2 and E4 where phytoplankton did not appear to be impacted by elevated pCO_2 the ratios of NO_x:Si was much lower (<0.40). This implies that diatoms are favoured in waters with N:Si ratios of less than 1, whereas other phytoplankton would be favoured in waters with a high N:Si (**??**). Changes in nutrient utilisation at low CO_2 levels (150 µatm) have been observed by **?**, where higher ratios of nitrate:silicate consumption by phytoplankton occurred. Differences between bioassays were perhaps related to group specific differences in CO_2 sensitivity (**?**). The carbon fixation rate in all diatom species (tested so far) indicate that they are at or close to CO_2-saturation already (**?**), whereas coccolithophores (such as *E. huxleyi* and *Gephyrocapsa oceanica*) are well below saturation at current CO_2 levels (**??**), therefore coccolithophores may have a competitive advantage over diatoms at elevated CO_2 levels. Differences in carbon acquisition mechanisms between diatoms and coccolithophores might also explain why coccolithophore abundance and calcification did not respond to elevated pCO_2.

In three of the four bioassays, the response of phytoplankton to +Fe and +Fe +750 µatm was similar, suggesting that elevated pCO_2 did not negatively affect the phytoplankton response to +Fe addition. In bioassay E3 the

macronutrient drawdown was elevated in the 750 µatm and 2000 µatm treatments relative to the control, although silicic acid drawdown in the pCO_2 treatments was less than in the +Fe treatments while NO_x drawdown in the 750 µatm and 2000 µatm treatments was similar to the drawdown observed in the +Fe treatment. It is possible that these differing responses are due to shifts in community composition such that contrasting biochemical mechanisms and use of carbon-concentrating mechanisms (CCMs) by different diatom species leads to changes in macronutrient utilization (**?**).

4.5 Conclusions and Wider Implications

Our results highlight the importance of regional influences and initial conditions in predicting phytoplankton responses to changing conditions. Observations from the underway sampling and CTD profile sampling showed positive linkage between coccolithophores (cell numbers, calcite production) and iron availability where silicic acid was low and likely limiting to diatoms. In contrast, coccolithophores were only found in one bioassay from around South Georgia and did not respond to Fe addition, possibly due to the high silicic acid here and hence the strong potential for diatoms to outcompete them for macronutrients. Coccolithophores have low Fe requirements relative to diatoms and Fe availability has been shown to limit phytoplankton productivity in the HNLC Southern Ocean. As the future flux of Fe (and other trace metals) are predicted to change in response to climate change and human driven changes in land use, it is important to study the response of the different groups of phytoplankton (with different Fe and trace metal requirements) to Fe and to elevated pCO_2. While the higher pCO_2 levels (1000 µatm and 2000 µatm) used in this study, are unrealistic, with the lowest (750 µatm) approximately triple pre-industrial levels, following a lack of response at the lower pCO_2 levels, it was decided to use higher pCO_2 concentrations to try and to find a correlation which would allow predictions of responses along the slope. A similar method was utilised by **?**.

In terms of pCO_2, bioassay experiments identified a wide range of phytoplankton responses to elevated pCO_2, which may have been influenced by a wide range of variables, including the ratio of NO_x to silicic acid in surface waters, SST and *in situ* Fe limitation. Climate change predications suggest that by the end of this century, CO_2 concentrations in the surface waters of the oceans will have risen nearly threefold relative to pre-industrial times (**??**). This will lead to changes in the ratio of $[HCO^-]$:$[CO_2]$ accompanied by a lowering of seawater pH by 0.35 units. These changes will affect phytoplankton in a variety of ways which may be dependent on individual taxa and species' sensitivity to CO_2. Coccolithophores, such as *E. huxleyi* are sensitive to fluctuations in CO_2 and may benefit from future changes in CO_2 compared with diatoms and *Phaeocystis* (**?**).

With climate models predicting that organisms in the Southern Ocean will feel the effects of ocean acidification first (**??**). It is important to quantify the response of different phytoplankton groups in the Southern Ocean to changing pCO_2 conditions and it is therefore recommended that future studies in this region use a combination of light microscopy and/or scanning electron microscopy (SEM) to identify and enumerate the mineralising nanoplankton component of the community, flow cytometry to determine the contribution of small phytoplankton to total biomass and size-fractionated primary production and chlorophyll a measurements which will allow scientists to better understand outcomes of bioassays. While climate change and Ocean Acidification may lead to future decreases in dFe, which may negatively affect coccolithophore abundance, it is also possible that other changes associated with climate change such as increasing sea surface temperatures and higher irradiances, could lead to a further expansion of coccolithophore biogeography in the Southern Ocean (**?**).

Acknowledgements

Thanks go to the Master, the officers and crew and participating scientists aboard the *RRS James Clark Ross*.

Work from this chapter was made possible through funding by the National Environmental Research Council (NERC) Ocean Acidification funding (NERC, Defra, DECC) to Dr Alex J Poulton UK , grant no. NE/H017097/1.

Chapter 5

General Synthesis

The work presented in this thesis investigated the response of coccolithophores and other phytoplankton groups (diatoms, microplankton, *Synechococcus*, picoeukaryotes) to iron (Fe) and other trace metals (zinc (Zn) and cobalt (Co)) in the North Atlantic (Iceland and Irminger Basins) and in the Southern Ocean (Great Calcite Belt, Scotia Sea). In addition, the effect of elevated pCO_2 conditions on phytoplankton in the Scotia Sea was also investigated. The main aims of the thesis were:

1. To investigate the effect of Fe availability on coccolithophores in the North Atlantic Ocean and contrast this response with that of other phytoplankton (diatoms, *Synechococcus*, picoeukaryotes) groups (Chapter 2);

2. To investigate the effect of trace metal availability (i.e. Fe, Zn and Co) on coccolithophores across the Great Calcite Belt (GCB, Southern Ocean) and to contrast this response with that of the diatom community (Chapter 3);

3. To determine the effects of Fe addition and elevated pCO_2 on the summer phytoplankton community in the Scotia Sea (Chapter 4).

This final synthesis chapter provides an overall summary of the findings of the three results chapters, and includes a comparison of the response of coccolithophores in the northern and southern hemispheres to Fe, as well as the wider implications of the main findings; including whether other trace metals (such as Zn and Co) could be influencing coccolithophore and phytoplankton communities. Finally, the limitations of this study and possible future directions are discussed.

5.1 Overview of Key Findings

The major findings of this thesis were:

1. Iron addition positively enhances coccolithophore growth rates (Chapters 2 and 3) and calcite production (CP) (Chapter 2);

2. The response of both coccolithophores and diatoms is strongly influenced by initial conditions (i.e. macronutrient availability, phytoplankton composition and *in situ* Fe availability) (Chapters 2 and 3);

3. Coccolithophore (and diatom) species composition do not radically change in response to dFe addition (Chapters 2 and 3):

4. Coccolithophore community composition is more diverse in the North Atlantic than in the Southern Ocean (Chapters 2, 3 and 4);

5. Zinc addition also positively enhanced growth rates of coccolithophores (and diatoms) in some of the bioassays across the GCB (Chapter 3);

6. Elevated pCO_2 appeared to have little or no effect on phytoplankton biomass (i.e. total chlorophyll *a* concentrations) but did influence NO_x and silicic acid uptake in some of the bioassays from the Scotia Sea (Chapter 4).

5.1.1 Synopsis of Each Results Chapter

Chapter 2: During the summer 2010 cruise to the North Atlantic, the main differences in the coccolithophore and diatom community responses to +Fe addition were largely related to the location (Iceland or Irminger Basin) of the sampling for the bioassays and hence the initial conditions (macro- and micronutrient availability and initial phytoplankton community composition and abundance) for each of the bioassays. Bioassays sampled from the Iceland Basin, which were characterised by low initial concentrations of nitrate and silicic acid (<0.70 and $< 0.84\,\mu$M, respectively), showed significant responses to +FeN and +N addition indicating that the *in situ* phytoplankton communities were co-limited by both Fe and nitrate (and likely also by silicic acid). In contrast, Irminger Basin bioassays only responded strongly to +Fe addition, with initial Fe concentrations ranging from <0.01 nM to 0.28 nM and hence the phytoplankton communities here were limited by Fe availability. Coccolithophore abundance in the Irminger basin increased relative to the control in all +Fe amended treatments with a similar pattern observed in

the Iceland Basin, though coccolithophore abundance also increased in the +FeN amended bioassays. This study is the first to focus on the response of coccolithophores to Fe addition in the North Atlantic Ocean and shows strong evidence that Fe availability is an important factor influencing both growth and calcification of coccolithophores in the Iceland and Irminger basins.

Chapter 3: Observations from two cruises across the GCB, specifically the South Atlantic (2011) and South Indian (2012) sectors, showed further evidence of positive coccolithophore responses to Fe, as well as to Zn addition. Coccolithophore abundance increased in four of the six bioassays in response to Fe, and in three of the six bioassays in response to Zn addition. Similarly, diatom abundance also increased in five of the six bioassays in response to Fe. Fe addition stimulated increased chlorophyll *a* biomass as well as increased NO_x utilization, whereas total chlorophyll *a* biomass showed significant decreases in two of the bioassays with Zn treatments and NO_x utilisation was significantly increased in another two Zn bioassays. This study is one of the first to demonstrate a significant response of coccolithophores (*E. huxleyi*) to Zn addition in the Southern Ocean and provided further evidence that coccolithophores respond positively to Fe availability.

Chapter 4: The 2013 cruise to the Scotia Sea sampled a wide variety of biogeographic regions, with three of the four bioassays showing strong evidence of a significant increase in phytoplankton biomass in response to Fe. This cruise sampled the southern limit of coccolithophore distribution and as a result, coccolithophores were only detectable in one of the bioassays (near South Georgia island) and in this bioassay they did not respond to Fe addition. Underway sampling of coccolithophores (*E. huxleyi*) suggested that their abundance was related to the N:Si ratio (and to dFe availability), with moderate to high *E. huxleyi* abundance associated with areas of relatively elevated N:Si ratios. Additionally, it appears that there was some tendency towards higher E. huxleyi abundance a elevated dFe concentrations, however this relationship is not clear and it is important to note that other factors such as grazing pressure or light could be controlling cell numbers. In two of the bioassays, the small ($< 10\mu$m) size-fraction responded to Fe addition in terms of chlorophyll a biomass, whereas a bioassay near South Georgia island, which was initially dominated by small phytoplankton, underwent a significant shift in community structure with large phytoplankton becoming dominant upon Fe addition. The response of Scotia Sea phytoplankton to elevated pCO_2 was more complex: there were no significant changes in biomass, however, elevated pCO_2 appeared to affect the utilisation of the macronutrients NO_x and silicic acid.

5.2 Coccolithophore Responses to Iron Availability

This study presents strong evidence that coccolithophores are limited by Fe availability in both the northern and southern hemispheres. Coccolithophore growth rates showed consistent evidence of being positively stimulated by +Fe addition (Tables **??** and **??**). The coccolithophore community in the North Atlantic was comparatively more diverse than in the GCB and Scotia Sea, where coccolithophore assemblages were predominantly composed of *E. huxleyi*. However, it is also apparent that coccolithophore community structure did not show any significant variation in response to Fe (Tables **??** and **??**), rather that +Fe addition stimulated the growth of the initial coccolithophore community uniformly. Additionally, calcite production showed dramatic increases in +Fe treatments in Chapter 2 (Table **??**) and results highlighted the impact that rare, large and heavily calcified species such as *Coccolithus pelagicus*, can have on total calcite concentrations and production (**??**). It is possible that, as happens in diatom populations, different sized coccolithophores will have different responses to +Fe addition through differential nutrient requirements. One might expect small cells like *E. huxleyi* and *Syracosphaera* spp. to outcompete large coccolithophores like *C. pelagicus* at low dFe concentrations. This could be an important factor influencing the biogeography of coccolithophores in the Southern Ocean where Fe is perennially limiting and the small coccolithophore *E. huxleyi* is dominant.

Growth rates of coccolithophores in +Fe treatments were generally higher overall in the North Atlantic than in the GCB, with Fe treatment growth rates ranging from $-0.19\,\mathrm{d}^{-1}$ to $1.44\,\mathrm{d}^{-1}$ (Figure **??**), in contrast in +Fe treatments in the GCB bioassays' growth rates ranged more widely from $-2.34\,\mathrm{d}^{-1}$ to $1.95\,\mathrm{d}^{-1}$ (Figure **??**). Differences in overall growth rate responses may be linked to the initial dFe concentration, where the average concentration (S.E) of dFe in the Irminger and Iceland Basins was $0.08 \pm 0.24\,\mathrm{nM}$ and $0.06 \pm 0.06\,\mathrm{nM}$ (**?**), respectively. In contrast, South Atlantic Ocean bioassays had comparatively higher initial dFe concentrations ($0.74 \pm 0.01\,\mathrm{nM}$) and the average dFe concentrations in the South Indian Ocean were $0.25 \pm 0.05\,\mathrm{nM}$. Thus, although both the North Atlantic and GCB bioassays were sampled from Fe limited waters, North Atlantic bioassays were comparatively more Fe limited at the start of the experiments and responded more strongly to subsequent +Fe addition, with the same trend evident in the GCB between the South Atlantic and South Indian Ocean bioassays. This suggests (unsurprisingly) that the actual initial concentration of dFe may be an important indicator of the magnitude of coccolithophore response and hence, it is of paramount importance to obtain accurate initial dFe measurements.

5.3 Comparison of Coccolithophore and Diatom Responses to Iron

A comparison of bioassay responses to Fe in the North Atlantic and in the Southern Ocean, two regions with seemingly contrasting macro- and micronutrient stoichiometries, reveals some surprising trends in phytoplankton responses. Iron inventories are highest in the North Atlantic and lowest in the Southern Ocean and traditionally, have had matching expected trends in Fe-limitation (**?**). Analysis of the coccolithophore and diatom communities in the North Atlantic and across the GCB in the Southern Ocean revealed differences in community structure, relative abundances and diversity between the two hemispheres. However, an analysis of similarities test (ANOSIM) indicated that the coccolithophore community responded to Fe addition similarly in the North Atlantic and Southern Ocean. There were significant differences ($p = 0.001$) in coccolithophore community structure between bioassays, but notably, there were no significant changes in community composition between treatments ($p = 0.089$ and 0.989, respectively). Despite there being no shift in coccolithophore species composition, coccolithophore growth rates showed dramatic increases in response to Fe addition in a number of bioassays (Figure **??**), even in bioassays where coccolithophore abundance decreased over time, it appeared that Fe had an ameliorating effect on the rate of decrease, such that despite overall decreases in abundance across the entire bioassay, coccolithophore abundance in +Fe treatments did not decrease as much as coccolithophore abundance in the control. Additionally, there were also significant differences between the coccolithophore community in the Iceland Basin and the Irminger Basin ($p = 0.001$), which was largely due to an increased abundance of *Syracosphaera* spp. in the Irminger Basin. In contrast, no difference in coccolithophore species composition was observed between the South Atlantic and South Indian Ocean bioassays ($p = 0.431$). A similar response was observed in the diatom community, with significant differences ($p = 0.001$) between bioassays and locations in both the North Atlantic and GCB.

Table 5.1: Summary of coccolithophore responses to iron addition in the North Atlantic and Great Calcite Belt. Coccolithophore abundance (cells mL^{-1}), % increase or decrease in abundance over the course of the bioassay and dominant coccolithophore taxa (contribution to total coccolithophore abundance in brackets). Stars (*) indicate that while abundance decreased in the Fe treatment, the decrease was less dramatic than the control, suggesting a positive affect of Fe addition on abundance despite an overall decrease. Iron treatments where abundance increased by >100% are in bold.

North Atlantic				Great Calcite Belt			
Bioassay	**Abundance**	**% change T0**	**Dominant Species**	**Bioassay**	**Abundance**	**% change T0**	**Dominant Species**
	(cells mL^{-1})				(cells mL^{-1})		
Iceland Basin				**South Atlantic**			
IE5.1 Cont	21	-58	*E. huxleyi* (88%)	MV3 Cont	983	-38	*E. huxleyi* (99%)
IE5.1 Fe	34	-32*	*E. huxleyi* (61%)	MV3 Fe	747	-53	*E. huxleyi* (100%)
IE5.2 Cont	26	333	*E. huxleyi* (100%)	MV4 Cont	50	5582	*Syracosphaera* (76%)
IE5.2 Fe	**37**	**517**	*E. huxleyi* (95%)	**MV4 Fe**	**80**	**8991**	*Syracosphaera* (50%)
IE5.7 Cont	8	700	*E. huxleyi* (89%)				
IE5.7 Fe	**82**	**8100**	*Syracosphaera* (49%)				
Irminger Basin				**South Indian**			
IE5.3 Cont	27	-95	*Rhabdosphaera* (67%)	RV1 Cont	136	43	*E. huxleyi* (64%)
IE5.3 Fe	229	-59*	*Syracosphaera* (81%)	**RV1 Fe**	**374**	**294**	*E. huxleyi* (86%)
IE5.4 Cont	375	4	*Syracosphaera* (76%)	RV2 Cont	689	89	*E. huxleyi* (100%)
IE5.4 Fe	**502**	**39**	*Syracosphaera* (71%)	RV2 Fe	660	81*	*E. huxleyi* (94%)
IE5.5 Cont	26	57	*C. pelagicus* (47%)	RV3 Cont	21	2000	*E. huxleyi* (100%)
IE5.5 Fe	79	30	*E. huxleyi* (47%)	**RV3 Fe**	**47**	**4600**	*E. huxleyi* (100%)
IE5.6 Cont	4	20	*E. huxleyi* (53%)	RV4 Cont	362	90	*E. huxleyi* (78%)
IE5.6 Fe	**77**	**1440**	*E. huxleyi* (57%)	RV4 Fe	<1.74	-99	-

Table 5.2: Summary of diatom responses to iron addition in the North Atlantic and Great Calcite Belt. Diatom abundance (cells mL^{-1}), % increase or decrease in abundance over the course of the bioassay and dominant diatom taxa (contribution to total coccolithophore abundance in brackets). Stars (*) indicate that while abundance decreased in the Fe treatment, the decrease was less dramatic than the control, suggesting a positive affect of Fe addition on abundance despite an overall decrease. Iron treatments where abundance increased by >100% are in bold.

North Atlantic				Great Calcite Belt			
Bioassay	**Abundance**	**% change T0**	**Dominant Taxa**	**Bioassay**	**Abundance**	**% change T0**	**Dominant Taxa**
	(cells mL^{-1})				(cells mL^{-1})		
Iceland Basin				**South Atlantic**			
IE5.1 Cont	314	-44	*Pseudonitzschia* (41%)	MV3 Cont	356	42	*Fragilariopsis* (sml) (60%)
IE5.1 Fe	421	-25*	*Pseudonitzschia* (28%)	MV3 Fe	209	-16	*Fragilariopsis* (sml) (62%)
IE5.2 Cont	472	63	*Fragilariopsis* (sml) (24%)	MV4 Cont	1407	221	*Fragilariopsis* (sml) (65%)
IE5.2 Fe	**760**	**163**	*Pseudonitzschia* (29%)	**MV4 Fe**	**1874**	**328**	*Pseudonitzschia* (44%)
IE5.7 Cont	189	117	*Fragilariopsis* (sml) (58%)	RV1 Cont	9	200	*Fragilariopsis* (sml) (60%)
IE5.7 Fe	**3685**	**4136**	*Pseudonitzschia* (70%)	**RV1 Fe**	**154**	**5033**	*Pseudonitzschia* (40%)
Irminger Basin				**South Indian**			
IE5.3 Cont	522	-16	*Pseudonitzschia* (42%)	RV2 Cont	714	458	*Chaetoceros* (med) (42%)
IE5.3 Fe	**3334**	**435**	*Pseudonitzschia* (55%)	**RV2 Fe**	**968**	**656**	*Pseudonitzschia* (51%)
IE5.4 Cont	2466	63	*Fragilariopsis* (sml) (77%)	RV3 Cont	2256	38	*Fragilariopsis* (sml) (57%)
IE5.4 Fe	**3812**	**152**	*Fragilariopsis* (sml) (48%)	**RV3 Fe**	**2597**	**59**	*Fragilariopsis* (sml) (53%)
IE5.5 Cont	2500	156	*Pseudonitzschia* (72%)	RV4 Cont	418	181	*Pseudonitzschia* (73%)
IE5.5 Fe	**3944**	**304**	*Pseudonitzschia* (73%)	**RV4 Fe**	**855**	**474**	*Pseudonitzschia* (74%)
IE5.6 Cont	1030	68	*Fragilariopsis* (sml) (43%)				
IE5.6 Fe	**4576**	**648**	*Nitzschia* (51%)				

Factors influencing community responses to dFe appear to be strongly linked to the *in situ*/initial conditions, specifically in terms of nutrient availability. Macro- and micronutrient (NO_x, silicic acid and Fe) concentrations in addition to the initial phytoplankton community composition and abundance should all be taken into account when assessing phytoplankton responses to Fe. It is well established that when silicic acid is limiting, diatoms which require silica to form their frustules are out-competed by non-silicious species (**???**). Moreover, simulation models have suggested that when silicic acid concentrations dip below a critical level, coccolithophores can become dominant (**?**). Coccolithophores were rarely present in high abundances in bioassays where silicic acid was abundant and higher abundances most often were associated with areas where silicic acid was low (Figure **??**).

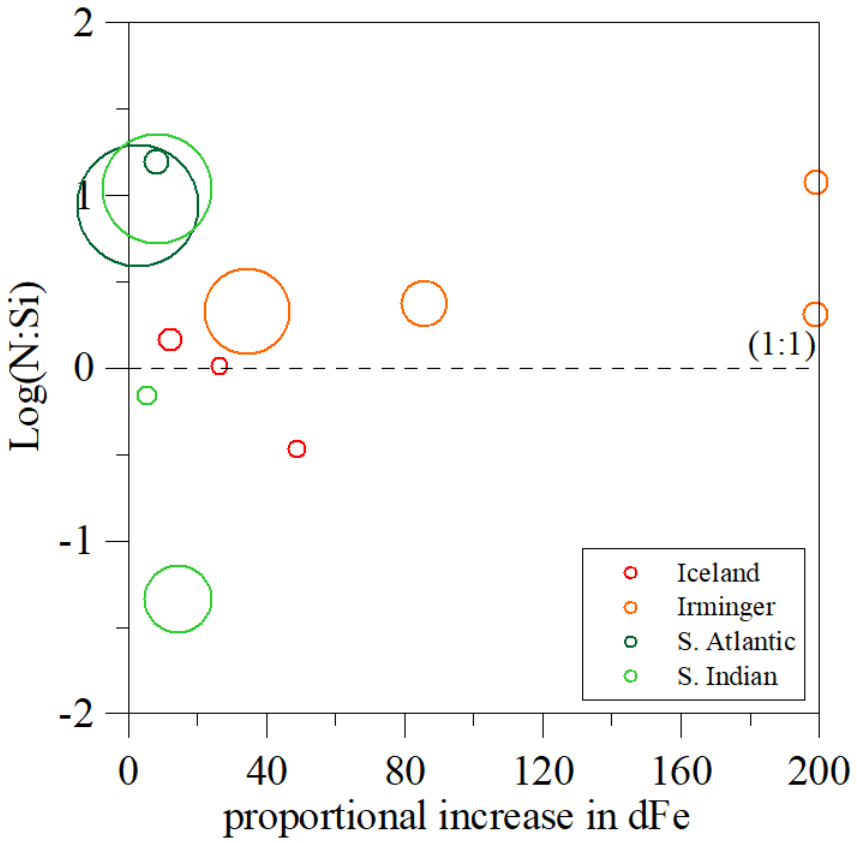

Figure 5.1: Bubble plot displaying the relationship between surface macronutrient concentrations (NO_x and silicic acid) and the proportional change in dFe concentrations (proportional increase from initial dFe to final dFe (initial dFe + 2 nM) and coccolithophore abundance in the +Fe treatments of bioassays in the North Atlantic (Iceland (red circles) and Irminger (orange circles) Basins) and Great Calcite Belt (South Atlantic (dark green circles) and South Indian (light green circles). Coccolithophore abundance ranged from $< 1.74\,\text{cells}\,\text{mL}^{-1}$ to $757\,\text{cells}\,\text{mL}^{-1}$. Dashed line indicates a ratio of N:Si of 1:1. The log of N:Si ratios was taken.

5.4 Potential for Zinc Limitation

The results from this study (Chapter 4) are among the limited observations that support the potential for Zn availability to have a strong control on coccolithophore growth and calcite production. **?** found evidence of Zn positively affecting the abundance of small diatoms and coccolithophores in the north-eastern subarctic Pacific Ocean. Concentrations of dZn in the Southern ocean are relatively high (>2 nM, **?**), thus Zn limitation is thought to be less likely in the Southern Ocean than in other HNLC regions. Initial dZn in bioassays ranged from as low as 0.28 nM to a maximum of 29.75 nM, with limiting concentrations (<2 nM) measured at the majority of bioassay locations (Figure **??**). Typically values of dZn concentrations in surface waters of the Southern Ocean range between 1.1 to 8.0 nM (**?**), thus concentrations in our study were lower (with the exception of one bioassay) than average. There was strong evidence of Zn limitation in a number of bioassays across the GCB, with dramatic increases in coccol-

ithophore abundance in three bioassays and increases in NO_x utilization in both South Atlantic Ocean bioassays and one South Indian Ocean bioassay. Bioassays that exhibited enhanced coccolithophore growth rates in Zn treatments had initial dZn concentrations of <1.5 nM, however, Zn concentrations are lowest in the North Atlantic and highest in the Southern Ocean (**?**). However, evidence of Zn limitation in the Southern Ocean highlights the need to further investigate the role of Zn in limiting coccolithophore (and diatom) growth in the North Atlantic.

Zinc limitation, in contrast to Fe limitation, has not been as well considered before as there is limited information on Zn concentrations in the ocean, especially on chemical speciation and organic complexation. Zinc plays an important role in a number of biological and structural functions most notably with regards to carbon and phosphate uptake. With respect to its role in limiting coccolithophore growth, Zn plays a role as a co-factor in carbonic anhydrase (CA), which enhances the rate of dehydration of bicarbonate ions (HCO_3^-) to free CO_2 (**?**). However, coccolithophores are thought to primarily use CO_2 formed from HCO_3^- during internal calcification and would in theory have no use for Zn as a co-factor in carbonic anhydrase (**?**). Thus, it is likely that the role of Zn in promoting coccolithophore growth is not linked to carbonic anhydrase, but rather to the enzyme alkaline phosphatase. Evidence that coccolithophore growth is co-limited by the availability of Zn and phosphate and that incubations where Zn was high exhibited higher phosphatase activity (**?**). Moreover, there is evidence that the demand for Zn (or Co, or both) increases under low pCO_2 conditions, thus in light of the positive response by coccolithophores in the Southern Ocean, where low seawater temperatures increase the solubility of CO_2, further Zn addition experiments under differing pCO_2 and phosphate (inorganic and organic) conditions would be useful in trying to understand the role of Zn in coccolithophores.

5.5 Limitations and Future Directions

This study has primarily utilised on-deck bioassay incubations to assess the effect of trace metals and elevated pCO_2 on *in situ* phytoplankton communities. This approach to studying phytoplankton in their 'natural environment' has many merits: for example, initial phytoplankton populations are diverse and adapted to the *in situ* environment, a distinct advantage over laboratory culture experiments. Thus, it allows a more realistic view of how phytoplankton might respond to changing conditions in different oceanic regions and provides insights into how factors such as natural variations in macro- and micronutrient availability might influence response patterns in different parts of the world's ocean.

However, there are limitations in this approach. Bioassays are incubated at 'optimal' and steady light conditions and as such, phytoplankton growth responses may be inflated compared to the natural environment where

light conditions fluctuate as cells are mixed through the upper mixed layer. Another weakness lies in methods of water collection, where large volumes of water are collected from Niskin bottles from CTDs or the underway system for use in bioassays and there is the potential for large inter-sample bottle variability. For example, if a coccolithophore population was largely dominated by small, weakly calcifying coccolithophore species such as *E. huxleyi* or *Syracosphaera* spp. but had low abundances of large, heavily calcified species such as *C. pelagicus*; even small differences in the relative proportions of these coccolithophores between bottles could introduce a lot of noise into the calcification results. This would lead to high variation within treatments and between treatments and severely limit the power of statistical tests to determine significant responses. Similarly, inclusion of one or a few mesozooplankton would act in the same way by exerting non-uniform grazing on treatment replicates. It is recommended that more targeted studies on smaller scale - or the opposite - much larger studies (e.g. mesocosms) be conducted.

In Chapters 2 and 3, the duration of the bioassays was found to be a significant factor affecting community structure. In future studies, it is recommended that incubation lengths be adjusted to account for the length of time it will take a community to respond, thus a fast growing community could respond within 48-hours whereas slower growing communities might take days. Thus, a series of sub-sampling points could be used in order to determine the optimal time to sample, however this method has its own limitations which include introducing potential contamination and needing larger volumes of sample water.

The drawback of bioassays is that results are complicated by the complex ecological interactions at play and thus in order to best interpret the outcomes of these studies it is important to have a good understanding of the composition of the plankton community, as well as on interactions occurring within the community such as growth and grazing. The findings presented in this thesis also highlight the importance of a thorough understanding of the phytoplankton community structure. A combination of methods which would allow a more complete view of the phytoplankton community in bioassays is useful. Scanning electron microscopy (SEM) is an extremely useful and important tool in identifying and enumerating mineralising nanoplankton groups (such as coccolithophores) which are broken down in traditional acidic Lugols solution. Additional tools are needed, such as flow cytometry to successfully enumerate the picoplankton and nanoplankton size-fractions (**?**). However, this approach has its own limitations in detecting groups which are in relatively low cell abundances (e.g. coccolithophores $< 50\,\text{cells}\,\text{mL}^{-1}$; A. Poulton, personal communication). Indirect measurements such as size-fractionated chlorophyll *a* and primary production or phytoplankton diagnostic pigments (**?**) are also useful tools for interpreting the complex responses of phytoplankton communities. The interpretation of bioassay outcomes in Chapter 4 were complicated by the lack

of species data, instead inferences from total and size-fractionated chlorophyll *a* biomass and primary production and calcite production measurements were used, however a breakdown of species composition would have been useful in further understanding the size-fractionated response.

The findings presented in this thesis highlight the need for further studies investigating the impacts of Fe and Zn on coccolithophores in a range of different environments. Bioassays investigating the effect of Fe addition and Zn addition could be complemented by adding additional treatments such as nitrate+silicate. A combination of scanning electron microscopy (SEM), flow cytometry and calcite production measurements over a wider range of time points would enable a more thorough understanding of the effect(s) of macro- and micronutrient availability on coccolithophores. Furthermore, a full suite of measurements describing initial conditions of the bioassays (e.g. SST, mixed layer depth, dFe, dZn, macronutrient concentrations, primary productivity, calcite production, chlorophyll *a* concentrations as well as a full breakdown of initial species composition) would allow more robust and insightful results. Lastly, incorporating data from additional time points would allow a better understanding of how the duration of bioassays influences the responses. The response of coccolithophores to Fe and Zn has important implications for the global carbon cycle and this thesis has highlighted the importance of gaining a better understanding of the complex interactions that are involved.

Appendix A

Supplementary Data for Chapter 2: Statistical Results

Table A.1: Results of one-way ANOVA on total and size-fractionated chlorophyll *a* and macronutrient concentrations for Iceland Basin Bioassays. Significance codes: 0 '***' 0.001 '**' 0.01 '*' 0.05

Bioassay	**Duration**		**Chl a**		**SF Chl a**		**NO_x**		**SiO_4**	
	(hrs)	**df**	**F-value**	**p-value**	**F-value**	**p-value**	**F-value**	**p-value**	**F-value**	**p-value**
IE5.1	48	3	19.02	0.000***	4.31	0.040*	450.80	0.000***	3.71	0.061
IE5.2	48	3	98.48	0.000***	62.60	0.000***	104.80	0.000***	1.35	0.330
IE5.7	72	3	65.87	0.000***	55.29	0.000***	25.02	0.000***	0.87	0.495

Table A.2: Tukey HSD test results for multiple pair-wise comparisons of significant ANOVA results for Iceland basin bioassays. Significant results are in bold.

Bioassay	**Pairs**	**Chl a**				**SF Chl a**				**NO_x**			
		diff	**p-value**	**lwr**	**upr**	**diff**	**p-value**	**lwr**	**upr**	**diff**	**p-value**	**lwr**	**upr**
IE5.1	Cont-Fe	0.153	0.533	-0.198	0.504	-0.070	0.280	-0.185	0.045	0.000	1.000	-0.169	0.169
	Cont-FeN	0.773	**0.000**	0.422	1.124	0.057	0.439	-0.058	0.171	1.180	**0.000**	1.011	1.349
	Cont-N	0.210	0.294	-0.141	0.561	0.013	0.981	-0.101	0.128	1.523	**0.000**	1.354	1.692
	Fe-FeN	0 .620	**0.002**	0.269	0.971	0.127	**0.031**	0.012	0.241	1.180	**0.000**	1.011	1.349
	Fe-N	0.057	0.953	-0.294	0.408	0.083	0.171	-0.031	0.198	1.523	**0.000**	1.354	1.692
	FeN-N	-0.563	**0.004**	-0.914	-0.212	0.043	0.638	-0.158	0.071	0.043	**0.000**	0.174	0.512
IE5.2	Cont-Fe	0.057	0.848	-0.167	0.281	0.053	0.564	-0.074	0.181	0.000	1.000	-0.228	0.228
	Cont-FeN	1.060	**0.000**	0.836	1.284	0.493	**0.000**	0.366	0.621	0.707	**0.000**	0.479	0.934
	Cont-N	0.247	**0.032**	0.023	0.471	0.137	**0.036**	0.009	0.264	1.020	**0.000**	0.792	1.248
	Fe-FeN	1.003	**0.000**	0.779	1.227	0.440	**0.000**	0.313	0.567	0.707	**0.000**	0.479	0.934
	Fe-N	0.190	0.099	-0.034	0.414	0.083	0.232	-0.044	0.211	1.020	**0.000**	0.792	1.248
	FeN-N	-0.813	**0.000**	-1.037	-0.589	-0.357	**0.000**	-0.484	-0.229	0.313	**0.010**	0.086	0.541
IE5.7	Cont-Fe	0.488	**0.001**	0.241	0.735	0.131	**0.024**	0.019	0.244	-0.253	0.865	-1.304	0.797
	Cont-FeN	0.955	**0.000**	0.708	1.202	0.405	**0.000**	0.292	0.517	1.850	**0.002**	0.799	2.901
	Cont-N	0.062	0.853	-0.185	0.309	0.025	0.885	-0.087	0.138	1.900	**0.002**	0.849	2.951
	Fe-FeN	0.467	**0.001**	0.220	0.714	0.273	**0.000**	0.161	0.386	2.103	**0.001**	1.053	3.154
	Fe-N	-0.427	**0.002**	-0.674	-0.180	-0.106	0.066	-0.219	0.007	2.153	**0.001**	1.103	3.204
	FeN-N	-0.893	**0.000**	-1.140	-0.646	-0.379	**0.000**	-0.492	-0.266	0.050	0.999	-1.001	1.101

Table A.3: Results of one-way ANOVA on total and size-fractionated chlorophyll *a* and macronutrient concentrations in Irminger Basin bioassays. Significance codes: 0 '***' 0.001 '**' 0.01 '*' 0.05

Bioassay	**Duration**	**Chl a**			**SF Chl a**		**NO_x**		**SiO_4**	
	(hrs)	**df**	**F-value**	**p-value**	**F-value**	**p-value**	**F-value**	**p-value**	**F-value**	**p-value**
IE5.3	120	1	12.34	0.008**	10.87	0.011*	62.60	0.000***	3.17	0.113
IE5.4	120	1	1615.00	0.000***	319.70	0.000***	698.30	0.000***	258.10	0.000***
IE5.5	72	3	140.20	0.000***	28.48	0.000***	379.50	0.000***	78.39	0.000***
IE5.6	120	1	791.40	0.000***	714.50	0.000***	101.00	0.000***	16.52	0.004***

Table A.4: Tukey HSD test results for multiple pair-wise comparisons of significant ANOVA results for Irminger basin bioassay IE5.5. Significant results are in bold.

Pairs	**Chl a**				**SF Chl a**				**NO_x**				**SiO_4**			
	diff	**p-value**	**lwr**	**upr**	**diff**	**p-value**	**lwr**	**upr**	**diff**	**p-value**	**lwr**	**upr**	**diff**	**p-value**	**lwr**	**upr**
Cont-Fe	1.905	**0.000**	1.580	2.230	1.347	**0.000**	0.845	1.848	-1.023	**0.000**	-1.366	-0.681	-0.327	**0.000**	-0.424	-0.229
Cont-FeN	1.650	**0.000**	1.258	2.042	0.022	1.000	-0.583	0.627	1.363	**0.000**	1.021	1.706	-0.317	**0.000**	-0.414	-0.219
Cont-N	0.015	0.999	-0.377	0.407	1.098	**0.001**	0.493	1.703	2.317	**0.000**	1.974	2.659	0.017	0.945	-0.081	0.114
Fe-FeN	-0.255	0.248	-0.634	0.125	-1.325	**0.000**	-1.910	-0.739	2.387	**0.000**	2.044	2.729	0.010	0.987	-0.088	0.108
Fe-N	-1.890	**0.000**	-2.269	-1.510	-0.249	0.609	-0.835	0.337	3.340	**0.000**	2.998	3.682	0.343	**0.000**	0.246	0.441
FeN-N	-1.635	**0.000**	-2.073	-1.197	1.076	**0.002**	0.400	1.752	0.953	**0.000**	0.611	1.296	0.333	**0.000**	0.236	0.431

Table A.5: Results of one-way ANOVA on primary production and calcite production. Significance codes: 0 '***' 0.001 '**' 0.01 '*' 0.05

Bioassay	**Duration**		**PP**		**CP**	
	(hrs)	**df**	**F-value**	**p-value**	**F-value**	**p-value**
IE5.1	48	3	2.31	0.22	2.77	0.18
IE5.4	120	1	43.14	0.00**	9.03	0.04*
IE5.6	120	1	158.30	0.00***	33.34	0.00**

Appendix B

Supplementary Data for Chapter 3: Statistical Results

Table B.1: Results of one-way ANOVA on total chlorophyll *a* and macronutrient concentrations from South Atlantic bioassays. Significance codes: 0 '***' 0.001 '**' 0.01 '*' 0.05

Bioassay	**Duration**	**df**	**Chl**		**NO_x**		**SiO_4**	
	(hrs)		**F-value**	**p-value**	**F-value**	**p-value**	**F-value**	**p-value**
MV3	102	3	0.845	0.507	1185.000	0.000***	2.800	0.109
MV4	73	3	1.410	0.309	73.340	0.000***	4.458	0.040*

Table B.2: Tukey HSD test results for multiple pair-wise comparisons of significant ANOVA results for South Atlantic bioassay MV3. Significant results are in bold.

Bioassay	**Duration**	**Pairs**	**NO_x**			
			diff	**p-value**	**lwr**	**upr**
MV3	102	Cont-Fe	3.280	**0.000**	3.029	3.531
		Cont-Zn	4.067	**0.000**	3.816	4.317
		Cont-Co	-0.997	**0.000**	-1.247	-0.746
		Fe-Zn	0.787	**0.000**	0.536	1.037
		Fe-Co	2.283	**0.000**	2.033	2.534
		Zn-Co	3.070	**0.000**	2.819	3.321

Table B.3: Tukey HSD test results for multiple pair-wise comparisons of significant ANOVA results for South Atlantic bioassay MV4. Significant results are in bold.

Bioassay	**Duration**	**Pairs**	**NO_x**				**SiO_4**			
			diff	**p-value**	**lwr**	**upr**	**diff**	**p-value**	**lwr**	**upr**
MV4	73	Cont-Fe	0.683	**0.000**	0.465	0.902	-0.100	0.480	-0.313	0.113
		Cont-Zn	0.790	**0.000**	0.571	1.009	-0.167	0.134	-0.380	0.047
		Cont-Co	-0.050	0.882	-0.269	0.169	0.233	**0.033**	0.020	0.447
		Fe-Zn	0.107	0.449	-0.112	0.325	-0.067	0.754	-0.280	0.147
		Fe-Co	0.633	**0.000**	0.415	0.852	0.133	0.264	-0.080	0.347
		Zn-Co	0.740	**0.000**	0.521	0.959	0.067	0.754	-0.147	0.280

Table B.4: Results of one-way ANOVA on total chlorophyll *a* and macronutrient concentrations for South Indian bioassays. Significance codes: 0 '***' 0.001 '**' 0.01 '*' 0.05

Bioassay	**Duration**	**df**	**Chl**		**NO_x**		**SiO_4**	
	(hrs)		**F-value**	**p-value**	**F-value**	**p-value**	**F-value**	**p-value**
RV1	121	3	0.779	0.538	0.200	0.889	0.667	0.596
RV2	160	3	250.900	0.000***	85.300	0.000***	2.867	0.104
RV3	147	3	27.420	0.000***	10.580	0.004***	3.012	0.094
RV4	141	3	40.070	0.000	0.200	0.889	1.960	0.209

Table B.5: Tukey HSD test results for multiple pair-wise comparisons of significant ANOVA results for South Indian bioassay RV2. Significant results are in bold.

Bioassay	**Duration**	**Pairs**	**Chl**				**NO_x**			
			diff	**p-value**	**lwr**	**upr**	**diff**	**p-value**	**lwr**	**upr**
RV2	160	Cont-Fe	0.955	**0.000**	0.800	1.111	-0.877	**0.000**	-1.129	-0.625
		Cont-Zn	-0.171	**0.032**	-0.327	-0.016	0.237	0.066	-0.015	0.489
		Cont-Co	0.185	**0.021**	0.030	0.341	-0.160	0.253	-0.412	0.092
		Fe-Zn	-1.127	**0.000**	-1.282	-0.971	1.113	**0.000**	0.861	1.365
		Fe-Co	1.140	**0.000**	0.985	1.296	-1.037	**0.000**	-1.289	-0.785
		Zn-Co	0.014	0.991	-0.142	0.169	0.077	0.768	-0.175	0.329

Table B.6: Tukey HSD test results for multiple pair-wise comparisons of significant ANOVA results for South Indian bioassay RV3. Significant results are in bold.

Bioassay	**Duration**	**Pairs**	**Chl**				**NO_x**			
			diff	**p-value**	**lwr**	**upr**	**diff**	**p-value**	**lwr**	**upr**
RV3	147	Cont-Fe	0.306	**0.001**	0.167	0.445	-0.250	0.150	-0.580	0.080
		Cont-Zn	0.126	0.075	-0.013	0.265	0.153	0.487	-0.177	0.484
		Cont-Co	0.071	0.476	-0.084	0.227	-0.307	0.069	-0.637	0.024
		Fe-Zn	-0.180	**0.015**	-0.319	-0.041	0.403	**0.019**	0.073	0.734
		Fe-Co	0.377	**0.000**	0.222	0.532	-0.557	**0.003**	-0.887	-0.226
		Zn-Co	0.197	**0.017**	0.042	0.352	-0.153	0.487	-0.484	0.177

Table B.7: Tukey HSD test results for multiple pair-wise comparisons of significant ANOVA results for South Indian bioassay RV4. Significant results are in bold.

Bioassay	**Duration**	**Pairs**	**Chl**				**NO_x**			
			diff	**p-value**	**lwr**	**upr**	**diff**	**p-value**	**lwr**	**upr**
RV4	141	Cont-Fe	0.487	**0.001**	0.255	0.719	-0.960	**0.000**	-1.154	-0.766
		Cont-Zn	-0.270	**0.024**	-0.502	-0.038	0.457	**0.000**	0.263	0.651
		Cont-Co	0.095	0.584	-0.137	0.327	-0.123	0.252	-0.317	0.071
		Fe-Zn	-0.757	**0.000**	-0.989	-0.525	1.417	**0.000**	1.223	1.611
		Fe-Co	0.582	**0.000**	0.350	0.814	-1.083	**0.000**	-1.277	-0.889
		Zn-Co	-0.176	0.149	-0.408	0.056	0.333	**0.003**	0.139	0.527

Appendix C

Supplementary Data for Chapter 4: Statistical Results

Table C.1: Results of one-way ANOVA on total and size-fractionated chlorophyll *a* and macronutrient concentrations. Significance codes: 0 '***' 0.001 '**' 0.01 '*' 0.05

Bioassay	**Duration**		**Chl a**		**SF Chl a**		**NO_x**		**SiO_4**	
	(hrs)	**df**	**F-value**	**p-value**	**F-value**	**p-value**	**F-value**	**p-value**	**F-value**	**p-value**
E1	96	3	0.416	0.743	0.541	0.668	40.380	0.000***	24.910	0.000***
E2	144	3	8.459	0.000***	1.937	0.202	6.526	0.001**	3.202	0.036*
E3	72	5	89.780	0.000***	20.230	0.000***	13.020	0.000***	55.710	0.000***
E4	96	5	7.539	0.000***	5.941	0.005**	3.647	0.009**	5.735	0.001***

Table C.2: Tukey HSD test results for multiple pair-wise comparisons of significant ANOVA results for bioassay E1 (96-hours). Significant results are in bold.

Pairs	**NO_x**				**SiO_4**			
	diff	**p-value**	**lwr**	**upr**	**diff**	**p-value**	**lwr**	**upr**
Cont-Fe	0.070	0.979	-0.411	0.551	0.464	**0.030**	0.035	0.894
Cont-Fe750	1.468	**0.000**	0.987	1.949	1.317	**0.000**	0.887	1.746
Cont-750	-1.359	**0.000**	-1.840	-0.878	-0.842	**0.000**	-1.272	-0.413
Fe-750	-1.289	**0.000**	-1.770	-0.808	-0.378	0.101	-0.807	0.052
Fe-Fe750	1.398	**0.000**	0.917	1.879	0.852	**0.000**	0.423	1.282
Fe750-750	0.109	0.927	-0.372	0.590	0.474	**0.026**	0.045	0.904

Table C.3: Tukey HSD test results for multiple pair-wise comparisons of significant ANOVA results for bioassay E2 (144-hours). Significant results are in bold.

Pairs	**Chl**				**NO_x**				**SiO_4**			
	diff	**p-value**	**lwr**	**upr**	**diff**	**p-value**	**lwr**	**upr**	**diff**	**p-value**	**lwr**	**upr**
Cont-Fe	0.664	**0.004**	0.176	1.153	-0.402	0.196	-0.937	0.133	-0.478	0.591	-1.501	0.545
Cont-Fe750	0.468	0.064	-0.685	0.957	0.041	0.997	-0.494	0.576	-1.080	**0.035**	-2.103	-0.057
Cont-750	0.112	0.924	-0.376	0.601	-0.470	0.101	-1.005	0.065	0.882	0.111	-0.141	1.905
Fe-750	0.777	**0.001**	0.288	1.265	-0.872	**0.001**	-1.407	-0.337	0.404	0.709	-0.618	1.427
Fe-Fe750	-0.196	0.699	-0.021	0.292	0.443	0.133	-0.091	0.978	-0.602	0.396	-1.625	0.421
Fe750-750	0.580	**0.015**	0.092	1.069	-0.429	0.153	-0.964	0.106	-0.198	0.953	-1.221	0.825

Table C.6: Results of one-way ANOVA on total and size-fractionated primary production and calcite production. Significance codes: 0 '***' 0.001 '**' 0.01 '*' 0.05

Bioassay	**Duration**	**df**	**PP**		**SF PP**		**CP**	
	(hrs)		**F-value**	**p-value**	**F-value**	**p-value**	**F-value**	**p-value**
E1	96	3	0.282	0.837	0.414	0.748	1.152	0.386
E2	144	3	2.171	0.169	0.597	0.635	1.211	0.366
E3	144	5	5.922	0.006**	11.550	0.000***	1.428	0.283
E4	96	5	11.650	0.000***	5.646	0.007**	1.364	0.304

Table C.4: Tukey HSD test results for multiple pair-wise comparisons of significant ANOVA results for bioassay E3 (72-hours). Significant results are in bold.

Pairs	**Chl**				**SF Chl**				**NO_x**				**SiO_4**			
	diff	**p-value**	**lwr**	**upr**	**diff**	**p-value**	**lwr**	**upr**	**diff**	**p-value**	**lwr**	**upr**	**diff**	**p-value**	**lwr**	**upr**
Cont-Fe	1.332	**0.000**	1.052	1.613	0.769	**0.002**	0.285	1.252	-0.607	**0.006**	-1.080	-0.134	-1.186	**0.000**	-1.502	-0.869
Cont-Fe750	1.332	**0.000**	1.052	1.613	1.001	**0.000**	0.517	1.485	-0.320	0.344	-0.793	0.153	-1.472	**0.000**	-1.789	-1.155
Cont-750	-0.040	0.990	-0.238	0.158	-0.018	1.000	-0.502	0.466	0.697	**0.000**	0.362	1.031	0.282	**0.007**	0.058	0.506
Cont-1000	-0.086	0.784	-0.284	0.113	0.001	1.000	-0.483	0.485	0.131	0.844	-0.203	0.466	0.367	**0.000**	0.143	0.591
Cont-2000	0.008	1.000	-0.191	0.206	-0.021	1.000	-0.505	0.463	0.659	**0.000**	0.324	0.993	0.309	**0.002**	0.085	0.533
Fe-Fe750	0.000	1.000	-0.344	0.344	0.232	0.605	-0.251	0.716	0.287	0.674	-0.293	0.866	-0.287	0.253	-0.675	0.101
Fe-750	1.292	**0.000**	1.012	1.573	0.750	**0.002**	0.267	1.234	0.090	0.992	-0.383	0.563	-0.903	**0.000**	-1.220	-0.587
Fe-1000	1.247	**0.000**	0.966	1.527	0.770	**0.002**	0.286	1.253	-0.476	0.048	-0.949	-0.002	-0.819	**0.000**	-1.136	-0.502
Fe-2000	1.340	**0.000**	1.060	1.620	0.747	**0.002**	0.264	1.231	0.052	0.999	-0.421	0.525	-0.877	**0.000**	-1.193	-0.560
Fe750-750	1.292	**0.000**	1.012	1.573	0.983	**0.000**	0.499	1.467	0.377	0.185	-0.096	0.850	-1.190	**0.000**	-1.507	-0.873
Fe750-1000	1.247	**0.000**	0.966	1.527	1.002	**0.000**	0.518	1.486	-0.189	0.833	-0.662	0.284	-1.106	**0.000**	-1.422	-0.789
Fe750-2000	1.340	**0.000**	1.060	1.620	0.980	**0.000**	0.496	1.464	0.339	0.283	-0.134	0.812	-1.163	**0.000**	-1.480	-0.847
750-1000	-0.046	0.982	-0.244	0.153	0.019	1.000	-0.465	0.503	-0.566	**0.000**	-0.900	-0.231	0.084	0.864	-0.140	0.308
750-2000	0.048	0.978	-0.151	0.246	-0.003	1.000	-0.487	0.481	-0.038	0.999	-0.372	0.297	0.027	0.999	-0.197	0.251
1000-2000	-0.093	0.717	-0.292	0.105	0.022	1.000	-0.461	0.506	-0.528	**0.000**	-0.862	-0.193	0.058	0.970	-0.166	0.282

Table C.5: Tukey HSD test results for multiple pair-wise comparisons of significant ANOVA results for bioassay E4 (96-hours). Significant results are in bold.

Pairs	**Chl**				**SF Chl**				**NO_x**				**SiO_4**			
	diff	**p-value**	**lwr**	**upr**	**diff**	**p-value**	**lwr**	**upr**	**diff**	**p-value**	**lwr**	**upr**	**diff**	**p-value**	**lwr**	**upr**
Cont-Fe	3.800	**0.003**	1.043	6.557	-4.102	0.153	-9.263	1.058	-1.434	0.275	-3.420	0.551	-0.676	0.580	-1.916	0.565
Cont-Fe750	3.648	**0.004**	0.891	6.405	-1.584	0.898	-6.745	3.576	-1.464	0.254	-3.450	0.521	-0.319	0.970	-1.560	0.922
Cont-750	-0.038	1.000	-1.988	1.911	-2.904	0.451	-8.065	2.257	-0.072	1.000	-1.476	1.332	-0.734	0.145	-1.612	0.143
Cont-1000	-0.822	0.800	-2.772	1.127	-1.070	0.979	-6.231	4.091	-0.136	1.000	-1.539	1.268	-0.278	0.930	-1.155	0.599
Cont-2000	0.236	0.999	-1.713	2.185	-2.499	0.598	-7.660	2.661	-0.749	0.601	-2.153	0.655	0.646	0.257	-0.232	1.523
Fe-Fe750	-0.152	1.000	-3.528	3.224	2.518	0.591	-2.643	7.678	-0.030	1.000	-2.462	2.402	0.357	0.980	-1.163	1.876
Fe-750	3.762	**0.003**	1.005	6.518	-7.006	**0.007**	-12.167	-1.845	-1.507	0.227	-3.492	0.479	-1.410	**0.018**	-2.651	-0.169
Fe-1000	2.978	**0.028**	0.221	5.735	-5.172	**0.049**	-10.333	-0.011	-1.570	0.191	-3.555	0.415	-0.953	0.216	-2.194	0.287
Fe-2000	4.036	**0.001**	1.279	6.793	-6.602	**0.010**	-11.762	-1.441	-2.183	**0.024**	-4.169	-0.198	-0.030	1.000	-1.271	1.211
Fe750-750	3.610	**0.004**	0.853	6.366	-4.488	0.103	-9.649	0.672	-1.537	0.209	-3.522	0.449	-1.053	0.135	-2.294	0.187
Fe750-1000	2.826	**0.042**	0.069	5.583	-2.654	0.541	-7.815	2.506	-1.600	0.175	-3.585	0.385	-0.597	0.699	-1.837	0.644
Fe750-2000	3.884	**0.002**	1.127	6.641	-4.084	0.156	-9.244	1.077	-2.213	**0.021**	-4.199	-0.228	0.327	0.967	-0.914	1.567
750-1000	-0.784	0.829	-2.733	1.165	1.834	0.832	-3.327	6.995	-0.063	1.000	-1.467	1.341	0.457	0.625	-0.421	1.334
750-2000	0.274	0.998	-1.675	2.224	0.404	1.000	-4.756	5.565	-0.677	0.697	-2.081	0.727	1.380	**0.000**	0.503	2.257
1000-2000	-1.058	0.583	-3.008	0.891	1.430	0.931	-3.731	6.590	0.613	0.775	-0.791	2.017	-0.923	**0.034**	-1.801	-0.046

Table C.7: Tukey HSD test results for multiple pair-wise comparisons of significant ANOVA results for total and size-fractionated primary production in bioassay E3 (144-hours). Significant results are in bold.

Pairs	**PP**				**SF PP**			
	diff	**p-value**	**lwr**	**upr**	**diff**	**p-value**	**lwr**	**upr**
Cont-Fe	1.049	0.313	-0.567	2.666	1.512	**0.004**	0.466	2.557
Cont-Fe750	1.302	0.145	-0.314	2.919	0.634	0.377	-0.411	1.680
Cont-750	0.313	0.984	-1.303	1.930	0.095	1.000	-0.950	1.141
Cont-1000	0.229	0.996	-1.388	1.845	0.100	0.999	-0.946	1.145
Cont-2000	0.805	0.572	-0.811	2.421	0.621	0.397	-0.424	1.667
Fe-Fe750	0.253	0.994	-1.363	1.869	-0.878	0.121	-1.923	0.168
Fe-750	1.363	0.119	-0.253	2.979	1.607	**0.002**	0.562	2.653
Fe-1000	1.278	0.157	-0.338	2.894	1.612	**0.002**	0.566	2.657
Fe-2000	1.854	**0.022**	0.238	3.471	2.133	**0.000**	1.088	3.179
Fe750-750	1.616	0.050	0.000	3.232	0.730	0.249	-0.316	1.775
Fe750-1000	1.531	0.067	-0.085	3.147	0.734	0.245	-0.312	1.779
Fe750-2000	2.107	**0.009**	0.491	3.724	1.256	**0.016**	0.210	2.301
750-1000	-0.085	1.000	-1.701	1.531	0.004	1.000	-1.041	1.050
750-2000	0.492	0.902	-1.125	2.108	0.526	0.562	-0.520	1.571
1000-2000	-0.576	0.830	-2.193	1.040	-0.522	0.570	-1.567	0.524

Table C.8: Tukey HSD test results for multiple pair-wise comparisons of significant ANOVA results for total and size-fractionated primary production in bioassay E4 (96-hours). Significant results are in bold.

Pairs	**PP**				**SF PP**			
	diff	**p-value**	**lwr**	**upr**	**diff**	**p-value**	**lwr**	**upr**
Cont-Fe	8.264	**0.001**	3.781	12.747	1.120	0.357	-0.688	2.928
Cont-Fe750	5.763	**0.010**	1.281	10.246	0.848	0.627	-0.960	2.656
Cont-750	-1.361	0.903	-5.843	3.122	0.709	0.771	-1.099	2.517
Cont-1000	-3.278	0.212	-7.760	1.205	-0.374	0.979	-2.181	1.434
Cont-2000	-0.742	0.992	-5.225	3.740	1.225	0.275	-0.583	3.032
Fe-Fe750	-2.501	0.460	-6.983	1.982	-0.272	0.995	-2.080	1.536
Fe-750	6.903	**0.002**	2.421	11.386	1.829	**0.047**	0.022	3.637
Fe-1000	4.986	**0.026**	0.504	9.469	0.747	0.734	-1.061	2.554
Fe-2000	7.522	**0.001**	3.039	12.004	2.345	**0.009**	0.537	4.153
Fe750-750	4.403	0.055	-0.080	8.885	1.557	0.108	-0.251	3.365
Fe750-1000	2.486	0.466	-1.997	6.968	0.474	0.944	-1.333	2.282
Fe750-2000	5.021	**0.025**	0.539	9.504	2.073	**0.022**	0.265	3.880
750-1000	-1.917	0.707	-6.400	2.566	-1.083	0.390	-2.890	0.725
750-2000	0.618	0.997	-3.864	5.101	0.516	0.923	-1.292	2.323
1000-2000	-2.535	0.446	-7.018	1.947	-1.598	0.095	-3.406	0.210